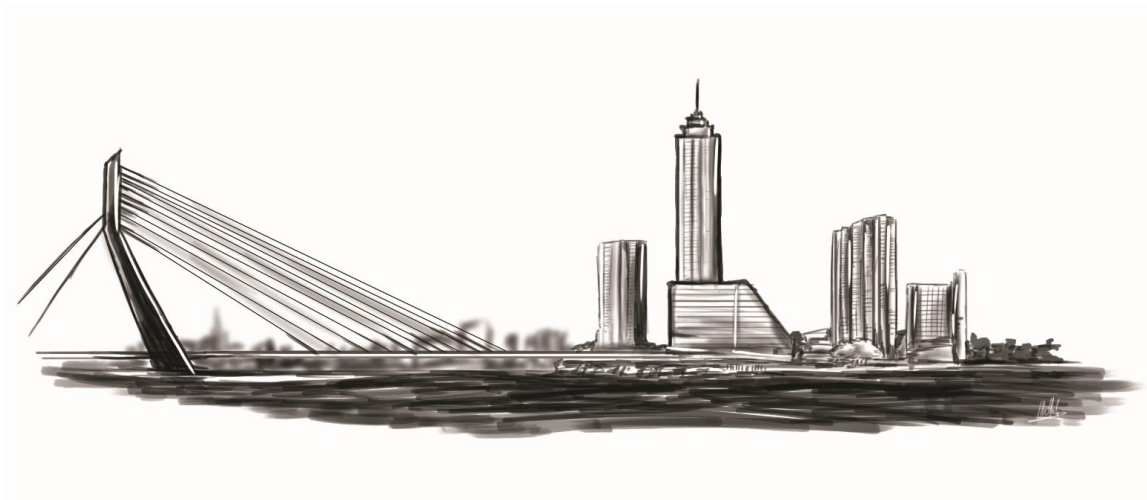


The Zalmhaven tower

An investigation on the feasibility of precast concrete in a high-rise building in the Netherlands



Research report

Sven ten Hagen

November 2012

The Zalmhaven tower

An investigation on the feasibility of precast concrete in a high-rise building in the Netherlands

MSc graduation thesis

Delft University of Technology
Faculty of Civil Engineering and Geosciences

Author:

Sven ten Hagen
Student number: 1364049
Sventenhagen@gmail.com

Graduation committee:

Prof.ir. R. Nijse
Prof.ir. A.Q.C. van der Horst
Dr.ir.drs. C.R. Braam
Ing. H.J Hoorn
Ir. D.C. van Keulen

ABT/ Delft University of Technology, chairman
BAM Infraconsult/ Delft University of Technology
Delft University of Technology
Zonneveld ingenieurs
Ingenieursstudio DCK/ Delft University of Technology

Preface

After thirteen months, I proudly present the results of my graduation research in this master thesis report. With this thesis I will conclude my study Civil Engineering at the University of Technology in Delft, the Netherlands. The main subject of this thesis is the structural and logistical feasibility of a precast high-rise building in the Netherlands. This topic corresponds with my specialisation Structural Design, which is part of the master program Building Engineering.

Within this thesis many aspects related to precast high-rise buildings have been examined, discussed and compared. Aside from the structural and logistical feasibility, this thesis also contains an underlying goal: provide an overview of the properties which characterise a precast high-rise building with respect to an identical cast in situ building. By providing this overview it's attempted to create more awareness which aspects should be considered when a precast high-rise building is designed. The Netherlands may not be leading with regard to the building height, but when it comes to prefabrication we define the standard. To maintain this position, innovation is required. It may be stated that innovations aren't born, they have to be made.

Many people have contributed to my graduation process and by their support I was able to obtain the results which are combined in this thesis report. First of all, I would like to thank prof.ir. R. Nijse, prof.ir. A.Q.C. van der Horst, dr.ir.drs. C.R. Braam, ing. H.J. Hoorn and ir. D.C. van Keulen for their time, guidance, knowledge and enthusiasm. I would like to highlight two of the graduation committee members: ing. H.J. Hoorn and ir. D.C. van Keulen. Ing. H.J. Hoorn was my daily supervisor at Zonneveld ingenieurs and despite of his very busy schedule, there was always room for one of my many questions. Ir. D.C. van Keulen took the role as second daily supervisor and assisted considerably regarding the use of a FEM program and understanding precast concrete.

Zonneveld ingenieurs offered me a work place in their office and I really enjoyed the past thirteen months. The office environment provided perfect conditions to stay focused during this considerable time span and I felt as one of them: the only difference between me and my colleagues was the project number and the student working hours. I would like to sincerely thank all my colleagues for their time, assistance, interest and relaxing lunch breaks.

I'm also very thankful of the support of ing. R. Vonken and ing. G. Baggermans from Hurks precom+. They supported my thesis with much required insight and knowledge on precast elements, the execution process and global design. I'm amazed by ing. R. Vonken and ing. G. Baggermans, who supported a student graduating at a different company without any compensation. Also ing. R. Rekers from Technosoft BV deserves a grateful notification for providing me a full license of AxisVM.

Last but not least, I would like to thank my family and friends for their support, interest, feedback and editorial comments. I would like to highlight several friends for their abundant support and involvement: ing. B. van Aken, S.A. Flierman MSc, H.R Herfst BSc, ing. R.J. van Lindenberg and D. Tahery BSc. It can be stated that without them, the people mentioned in the previous paragraphs and everyone else, how short and small their help might have been, this thesis would have been considerably different. Thank you very much!

Sven ten Hagen

Rotterdam, November 2012

Table of contents

ABSTRACT	10
1 INTRODUCTION	14
1.1 PROBLEM DESCRIPTION	14
1.2 OBJECTIVE	15
1.3 BOUNDARY CONDITIONS.....	15
1.4 OUTLINE OF THE REPORT.....	15
2 MOST IMPORTANT ASPECTS FROM THE LITERATURE STUDY.....	18
2.1 WIND LOAD	18
2.2 CONNECTIONS	18
2.3 ELEMENT CONFIGURATION	19
2.4 MATERIAL PROPERTIES	19
2.5 PROGRESSIVE COLLAPSE.....	19
3 DESCRIPTION OF THE ZALMHAVEN TOWER.....	22
4 DESIGN	26
4.1 STRUCTURAL CONCEPTS.....	26
4.2 ANALYSIS OF THE CONCEPTS AND DETERMINATION FINAL CONCEPT.....	30
4.3 OPTIMAL ELEMENT CONFIGURATION OF CONCEPT 1	32
4.4 SEVERAL DESIGN ASPECTS OF CONCEPT 1	38
4.5 DESIGN OF THE CONSTRUCTION METHODOLOGY	40
4.6 CONCLUSION.....	56
5 LOADS ON THE STRUCTURE.....	58
5.1 CONSEQUENCE CLASS, REFERENCE PERIOD AND ENVIRONMENTAL EXPOSURE CLASS	58
5.2 VERTICAL LOAD.....	58
5.3 HORIZONTAL LOAD	62
5.4 ACCIDENTAL LOADS	64
5.5 LOAD CASES AND LOAD COMBINATIONS	64
6 SELECTION OF THE FEM PROGRAM	66
6.1 SCIA ENGINEER.....	66
6.2 AXISVM.....	66
6.3 FINAL PROGRAM CHOICE.....	66
6.4 CONCLUSION.....	68
7 MODELLING IN AXISVM.....	70
7.1 MODEL SCHEME.....	70
7.2 MODEL DESCRIPTION OVERVIEW	71
7.3 ELEMENT SCHEMATISATION.....	72
7.4 MATERIAL PROPERTIES	73
7.5 DOMAIN.....	75
7.6 MESH SIZE	76
7.7 SCHEMATISATION OF THE CONNECTIONS.....	77
7.8 DETERMINING THE CONNECTION STIFFNESS	78
7.9 INFLUENCE OF THE FLOOR	84
7.10 APPLICATION OF THE LOADS	84
7.11 SCHEMATISATION OF THE FOUNDATION	85

8	THE INFLUENCE OF CONNECTION AND ELEMENT PROPERTIES	86
8.1	THE INFLUENCE OF THE SHEAR STIFFNESS OF THE HORIZONTAL CONNECTION	86
8.2	THE INFLUENCE OF THE VERTICAL OPEN JOINT	89
8.3	THE INFLUENCE OF THE ELEMENTS ON THE CYCLE TIMES	91
8.4	CONCLUSION	96
9	RESULTS OF THE FEM ANALYSIS	98
9.1	DISTRIBUTION OF FORCES.....	98
9.2	FORCES IN THE STRUCTURE	100
9.3	DEFORMATIONS.....	109
9.4	SECOND ORDER EFFECTS	117
9.5	SHEAR LAG.....	119
9.6	STRUCTURAL FACTOR AND ACCELERATION OF THE BUILDING.....	126
9.7	REINFORCEMENT DESIGN	130
9.8	VERIFICATION OF THE YOUNG’S MODULUS	142
9.9	EVALUATION CONCEPT 3.....	145
9.10	CONCLUSION	146
10	DIMENSIONAL CONTROL	148
10.1	DIMENSIONAL CONTROL	148
10.2	DIMENSIONAL ACCURACY IN THE STANDARDS.....	152
10.3	DIMENSIONAL TOLERANCES AND DEVIATIONS IN A PRECAST HIGH-RISE BUILDING	159
10.4	CONCLUSION	172
11	PROJECT REALISATION	174
11.1	CYCLE TIME	174
11.2	PRECAST BUILDING TIME	185
11.3	COSTS.....	186
11.4	CONCLUSION	187
12	CONCLUSION	188
13	RECOMMENDATIONS	190
14	EVALUATION AND LEVEL OF ACCURACY	192
	BIBLIOGRAPHY	193
	APPENDIX A: ELEMENT CONFIGURATION	196
	APPENDIX B: LOADS ON THE STRUCTURE.....	200
B.1	VERTICAL LOADS	200
B.2	HORIZONTAL LOADS.....	203
	APPENDIX C: MODELLING IN AXISVM.....	208
C.1	THE INFLUENCE OF THE DOMAINS	208
C.2	MESH SIZE	213
C.3	DETERMINING THE CONNECTION STIFFNESS	221
	APPENDIX D: INFLUENCE OF THE CONNECTION PROPERTIES	228
D.1	THE INFLUENCE OF THE SHEAR STIFFNESS OF THE HORIZONTAL CONNECTION	228
D.2	THE INFLUENCE OF THE VERTICAL OPEN JOINT	232
	APPENDIX E: RESULTS OF THE FEM ANALYSIS	238
E.1	DISTRIBUTION OF FORCES.....	238

E.2	CALCULATION SHEETS OF THE NATURAL FREQUENCY, STRUCTURAL FACTOR, ACCELERATION AND REINFORCEMENT	274
APPENDIX F:	DIMENSIONAL CONTROL	276
APPENDIX G:	CYCLE TIME	280
APPENDIX H:	CONSTRUCTION TIME	284
APPENDIX I:	FEASIBILITY CHECK OF THE HOISTING SHED.....	288

Abstract

The number of high-rise buildings and their corresponding height are increasing in the world. This also holds for the Netherlands although the maximum heights are considerably lower. However, compared to the world an interesting phenomenon occurs in the Netherlands: a clear increase of precast concrete high-rise buildings can be observed. The popularity of this building method is created by our prosperity, increasing the building requirements, working conditions but also the cost of labour. However, the highest building in the world with a load bearing precast structure is only 132m high (Het Strijkijzer in The Hague). Is this the maximum height of precast concrete or can we achieve greater heights with this building method? And how do the transport systems cope with the increased height of a precast structure? With these possibilities and questions in mind the following objective was formulated:

Is it structurally and logistically feasible to construct a 202.25 meter precast tower in Rotterdam, the Netherlands?

The Zalmhaven tower, with an original height of 190m and which should have been constructed in the previous decade, will be used as a reference project. To limit the scope of the subject, precast concrete elements in a masonry configuration and open vertical joints¹ are applied. To compare the results, the Zalmhaven tower is also modelled as a monolithic structure (for example created with a tunnel system). For the transport system at the construction site a hoisting shed will be used for the precast structure. The elements are transported to the building site via the road with Just in Time (JiT) delivery. These decisions are based on a preliminary research performed before the literature study.

With the objective and boundary conditions, the following division is made: the thesis starts with the results of the literature study and a description of the reference project. Subsequently the design is made, the loads are determined and the modelling properties are defined. In combination with the influence of the connections and element properties, the results of the Finite Element Method (FEM) analysis are obtained. With the dimensional control and project realisation this thesis comes to an end.

From the risk analysis made during the literature study it can be stated that the connections are the strength and weakness of precast concrete. The connections weaken the structure because the stiffness, strength and coherency are lower. However by dividing the structure in sections, it becomes possible to prefabricate the elements in a controlled environment and assemble them at the construction site. With this characteristic property and the boundary conditions concerning the wind load, connections, element configuration and material properties an optimal element configuration is designed for the Zalmhaven tower. Subsequently a design is made for the transport system, incorporating a hoisting shed and JiT delivery of elements via the road.

With the loads on the structure, the choice of FEM program and several modelling techniques, the influence of the connections on the structure is considered. The examination shows that introducing connections will always influence the behaviour of the structure. When the shear stiffness of the horizontal connection is varied, it can be stated that a low or high stiffness has only a small influence on the results. Using monolithic properties for the horizontal connections will result in non-realistic values and this method should not be applied. If the open vertical joint of the masonry configuration would be used structurally, the global effects are limited while considerably more difficult connections have to be made. Locally the results are more present and the shear force in

¹ An open vertical joint doesn't contain any structural connection between the elements. Therefore this open joint is unable to transfer any forces.

the centre of the elements is reduced. The amount of connections also influences the transport system and the corresponding cycle times. The examination has shown that there is a non-linear relation between the mass and transport speed: a 50% reduction of the mass only results in a 30% faster transport speed. Furthermore, two elements require twice as much time for the crane related actions. These aspects ensure that the cycle time of two 15 ton elements is almost twice as long as one 30 ton element.

Aside from the influence of the connection properties, the distribution of forces within the structure is also of significant importance. Therefore eight different models have been examined with precast and monolithic properties. The models show that the distribution of normal and shear force is comparable on a global scale (the entire structure). When the local scale is examined (per element), the normal force remains more or less comparable. Due to the open vertical joint, the distribution of shear force changes significantly. The lack of structural properties of the open joint require that the shear force is transported to the over and underlying elements, reducing the structural area with 50%. As a result of this mechanism, 18% more shear reinforcement has to be applied in the centre of the over and underlying dowel elements to absorb the higher forces.

Besides the distribution of shear force, the stiffness may also be considered as a characteristic property. This property determines the design of high-rise structures and is decisive for the viability of a precast high-rise building. According to the analysis, the stiffness reduction of the precast configuration is smaller than 4% when compared to an identical cast in situ variant. This difference is considerably small because large precast concrete elements in a masonry configuration, a high concrete strength class and a large building slenderness are combined in the design of the Zalmhaven tower.

During the FEM analysis more aspects have been considered, for example the second order effects, shear lag, structural factor $c_s c_d$, building acceleration and the verification of the Young's modulus. Since these aspects don't provide characteristic differences between the precast and cast in situ building method, they have only been determined for the precast design. The analysis of the building acceleration provides an interesting result: the requirements are easily met. This is unexpected at a high-rise building, but can be explained by the high stiffness of the sub- and superstructure and the considerably large mass of the design.

When the dimensional control is examined, it can be stated that the current standards are outdated and large reduction factors (up to 50%) may be applied at the allocation of measurement points, adjustment and manufacturing of the elements. With these standards the Zalmhaven tower is constructed on paper, resulting in an exceeded tolerance every tenth floor. Therefore it should be possible to place every wall element level and relative to the previous element and only absorb the deviations every tenth level in the connection. However this method isn't applied in practise and the deviations are normally controlled in the wet connection and screed layer at every level. The main reason for this standard method are the large risks of only correcting every tenth level and the marginal benefits of the one in ten method.

During the project realisation the cycle time of a precast structure is compared to that of a cast in situ structure. While the precast cycle time may only be 10 to 25% shorter, the construction time per floor is reduced by 50%. This difference is created by the large lead time² of casting concrete and the resulting inability to accelerate. Due to the significant influence of the cycle time on the total construction time at high-rise buildings, the building may be operated at an earlier stage when precast concrete is applied. The economical viability of precast concrete isn't examined because it's subjective to several assumptions and only represents the current market value. Therefore it's very difficult to

² The time before the next action can be performed.

connect any conclusions to this aspect. Since the costs are a significant aspect of the viability of a project, boundary conditions with respect to the structure are provided. For example the amount of floor and wall elements or the amount of diaphragm walls.

From this thesis it may be concluded that it's structurally and logistically feasible to construct a 202.25m tower in the Netherlands. Compared to a cast in situ structure the stiffness is hardly influenced and the building can be completed at an earlier stage. An economical feasibility study has to show which building method is preferred for the Zalmhaven tower.

1 Introduction

High-rise buildings nowadays determine the skyline of a city. Started as a symbol of status in the growing economy of America, the Home Insurance Building in Chicago from 1885 can be considered as the first skyscraper in the world [Wikipedia 2012]. Today, the Middle East and Far East house the tallest buildings in the world.

Because of the growing world population and economic pressure, the urban areas increase in their size. At the end of the twentieth century around 46% of the world population lived in urban areas. It's predicted that this number will grow [Hayden, 2009:10-29]. High-rise buildings are the current solution for the lack of space: large areas with a small footprint. The Netherlands is not considered as a participant on the high-rise market, but the Dutch skyscrapers are slender compared to buildings in other countries. This high slenderness is the result of the Dutch building code on the amount of light entering the building and the lack of extraordinary loads, such as earthquakes and hurricanes.

With the increasing heights of the current skyscrapers a question arises: what is the most suitable material for a high-rise building? Steel and concrete are the two most applied solution. Steel made tall buildings possible but nowadays most high-rise buildings are made out of concrete. Concrete is very suitable for these buildings because of its high mass, large damping factor and lateral stiffness. Concrete buildings are more stable and its occupants are less able to perceive building motion. When one chooses for concrete, there is a second question to be answered: precast or cast in situ? Cast in situ is very common, but precast is becoming more and more important in the Netherlands. The reason for this increase is our prosperity, building requirements and working conditions, but also the cost of labour. The Prinsenhof³, Het Strijkijzer, Waterstadtoeren and the Erasmus MC tower are a few examples of this trend.

1.1 Problem description

The demand for high-rise buildings is growing. Furthermore, they become more and more slender with growing heights. Building costs and time are under large pressure and experienced construction workers are hard to find. In the recent years, most industries have optimized their process. Research of ING [ING, 2010] has shown that this optimisation has not occurred in the construction sector (there is optimisation to a certain level, but this is not radical enough). To survive the financial crisis a change of mind is needed. Precast in combination with an integrated transport process could be part of this change of mind.

Zonneveld ingenieurs is interested in the possibilities of precast concrete at one of their high-rise projects: the Zalmhaven tower in Rotterdam. The Zalmhaven tower, with a original height of 189.1m, was designed with cast in situ concrete. To cast the building on site, a tunnel system would be used with tower cranes. Nevertheless, this tower has potential to be built in precast concrete. The following aspects explain why:

- The building is rectangular, has 61 floors and consists out of regular floor plans. These regular floor plans and the amount of floors are beneficial for the repetition factor.
- The building site is located in the centre of Rotterdam. The site is rather small and it is surrounded by dwellings.
- The current construction time of the cast in situ building method is rather long: 30 months. By using a precast construction method, the building only has to be assembled on the construction site, reducing the total building time.

³ The Prinsenhof project consists out of 8 towers. Only the 4 office towers are made out of precast concrete.

- The market for dwellings is currently under large pressure. The financial crisis is responsible for the fact that this building isn't constructed yet. Reducing the construction time results in apartments that are easier to sell. For example, a dwelling that is finished within fifteen months is more attractive than a dwelling that is finished in thirty months.
- Reducing the construction time could also result in more revenues at an earlier stage. Looking at the current market for dwellings, this will probably be the main argument to use precast concrete instead of cast in situ concrete.
- The construction process is shifted from building site to factory: construction becomes assembling. The conditions in the factory are better and this part of the building process becomes independent of the weather. Furthermore, at the factory the building process is more centralized: the transport of material and equipment is reduced. The material arriving at the building site mainly consists out of finished prefabricated elements and this results in a cleaner building site where less area and personnel are required.

However a 202.25m precast building⁴ has never been built before. And the current transport systems for precast buildings have been used for a maximum height of 132m (Het Strijkijzer in The Hague). Why is the largest precast building only 132m high (approximately 1/6th of the tallest building on earth, the Burj Khalifa) and are tower cranes used at Het Strijkijzer or a hoisting shed of the Erasmus MC tower sufficient or is a new system required?

1.2 Objective

On the basis of the previous questions of the problem description, a research question can be formulated for this thesis:

Is it structurally and logistically feasible to construct a 202.25 meter precast tower in Rotterdam, the Netherlands?

The objective of this thesis is to make a structural and logistical design for the Zalmhaven tower in precast concrete and examine if it's feasible. A sub-goal of this thesis is to provide an overview of the characteristic properties of a precast building with respect to an identical cast in situ variant.

1.3 Boundary conditions

The research question and objective contain many aspects. To limit the scope of this thesis, this research is limited to the structural and logistical feasibility. The economical feasibility will not be considered. Furthermore, the Zalmhaven tower will be used as reference project and the Eurocode (European Building Standards) with the Dutch National Annex will be used as legislation.

1.4 Outline of the report

During the literature study many interesting aspects have been examined. This thesis will start with a short enumeration of these aspects in chapter 2. Chapter 3 will continue with a description of the Zalmhaven tower, providing essential information for the structural and construction methodology design.

⁴ The building height has been increased to pass the 200m limit. This will be explained in more in chapter 3.

In chapter 4 the design of the load bearing structure and the construction methodology is incorporated. After the conceptual design, the loads on the structure are determined in chapter 5. The final loads can only be determined after the design is finished because the structural wind load factor $c_s c_{dr}$, the second order effect and the dead load depend on the structure. Before any structural results can be obtained, the Finite Element Method (FEM) program should be determined in combination with the modelling aspects. Two FEM programs are compared and a final program chosen in chapter 6. Chapter 7 continues with the modelling techniques required to obtain accurate and valid results. The material properties, mesh size, connection schematisation and application of the load are a few aspects which are examined.

Chapter 8 is the first chapter with structural and construction methodology results. In the structural part, the influence of the horizontal and vertical connections are determined. The construction methodology in this chapter is represented by the relation between the mass and cycle times. In chapter 9 the results of the FEM analysis are provided. The distribution of forces, deformations, accelerations and the reinforcement design are a few of the aspects which are analysed. The construction methodology continues with the dimensional design in chapter 10 and the project realisation is described in chapter 11.

In chapter 12 a conclusion is provided which is accompanied by several recommendations in chapter 13. This thesis ends with an evaluation of the obtained results in chapter 14.

2 Most important aspects from the literature study

During the literature study many interesting aspects have been examined. In this chapter a brief summary will be given of the most important aspects.

2.1 Wind load

Wind can be considered as a dynamic and complex load. The magnitude and direction of the wind velocity is time varying and changes over the building height and width. Therefore the wind properties can only be described statistically.

In the literature study insight is provided on how the phenomenon wind is described in the Eurocode and what has to be calculated to obtain the wind load. Also several other aspects have been examined. For example: the acceleration due to cyclic wind loading, vortex shedding and the difference between NEN-EN 1991-1-4 and NEN 6702. From the analysis several important conclusions can be made:

- Compared with NEN 6702, the Eurocode gives higher values for the basic wind velocity, reference height and wind friction. This results in higher loads for taller buildings. Nevertheless, the peak velocity pressures ($q_p(z)$) are lower in area 2 and 3 compared to NEN 6702. This is the result of more accurate (and complex) methods that are used by the Eurocode. By introducing a higher form factor the differences are reduced between the codes.
- When the height of a building increases, the comfort of the occupants becomes decisive. Because a 200m tower has never been constructed in the Netherlands before, the comfort levels of the building become a point of interest. With the Eurocode also a new calculation method becomes available that has more possibilities to accurately calculate the accelerations of the building. With the abundance of options (that make the calculation rather complex and difficult to understand) it's possible to achieve results that are comparable to the results obtained by a FEM analysis.

2.2 Connections

A precast building can be schematised as a large building kit which is assembled at the construction site. The connections play a critical role during the entire construction process. They should be simple and fast to ensure a swift assembly process, containing enough adjustment properties to prevent delays and still be strong enough to resist the large forces of a high-rise building. Therefore multiple connections have been examined to determine which connection provides the best results:

- For the vertical connection between wall elements the masonry configuration with an open vertical joint provides the most benefits (an open vertical joint contains no connection between the elements and holds therefore no structural stiffness). This configuration results in a higher stiffness than for example a traditional layout with a reinforced mortar connection. Besides the higher stiffness, the amount of work is reduced considerably due to the open vertical joint.
- The traditional starter bar connection with mortar is preferred for the horizontal connection between parallel elements. It's also possible to use a dry connection (often used at quay walls or steel structures), but several problems arise: reduced stiffness, difficult to execute, possible element splitting and a high level of accuracy is required). With pump grouting (onderpompen in Dutch) it's possible to achieve a 97% degree of filling.

- For the connection between the wall and floor a system used at Het Strijkijzer provides many benefits. The massive floor elements are supported by four internal steel tubes with bearing plates. Since the diaphragm reinforcement and all the ducts are already installed in the factory, only a small screed layer is required during the finishing stage. This method results in a considerable time reduction.
- The last connection is the vertical connection between perpendicular walls. This connection plays an important role in the cooperation between the walls in x and y-direction. The interlocking halfway connection and staggered connection are two good solutions of which the interlocking halfway connection provides the highest stiffness. The staggered connection is preferred when it comes to constructability due to the less strict tolerances and accessibility of the connection.

The two words “joint” and “connection” often result in confusion and therefore a word definition is used: a connection is the material connecting the two adjoining parts of the precast concrete elements, for example a reinforced mortar connection. A joint is the space (area) between the two elements where they meet each other, for example an open vertical joint.

2.3 Element configuration

There are many element configurations possible, each with their own structural properties. During the literature study several configurations have been examined, for example a vertical masonry configuration or a traditional configuration with a continuous vertical connection. Based on the research of Keulen [Keulen, 2012], a horizontal element configuration is preferred over a vertical configuration. The size of the elements also influence the structural properties: the wall elements should preferably be as large as possible.

2.4 Material properties

The application of higher strength concrete becomes more and more custom. The use of Ultra High Strength Concrete (UHSC) is currently reserved for prestige projects and a price reduction is necessary before it's widely introduced in the building industry. High Strength Concrete (HSC) is a more common concrete mixture and often results in better performing structures. Compared with Ordinary Concrete (OC), it may be possible to achieve a reduction of costs when the benefits of High strength Concrete are utilised. For example, the increased Young's modulus could counteract the reduced stiffness of a precast structure. Moreover, the structural dimensions can be limited due to the increased compression strength.

2.5 Progressive collapse

Progressive collapse is an important aspect of the structural design. Several structures have collapsed due to (un)foreseen situations and the resulting extraordinary loads. Depending on the consequence class, different measures have to be taken. For a Consequence Class 1 (CC1) structure no extraordinary loads have to be considered and for a CC3 structure a systematic risk analysis is obligatory. The reason for this enhanced level of security is not that these structures are less predictable than CC1 and CC2 structures, but because the consequences of a collapse are far greater.

Although there was no precast structural design during the risk analyses, several interesting conclusions could be made:

- The shear walls in combination with the facade columns and the floors contain the highest relative risk. To prevent disproportional collapse, measures should be taken to mitigate the relative risk level. A second load bearing system is a good example that will reduce the severity of the resulting damage. To reduce the severity of initial failure, the extraordinary loads have to be prevented or reduced.
- The foundation contains the lowest relative risk level and non-structural measures in combination with a high robustness will reduce this relative risk to an acceptable level.

Performing a risk analysis provides insight in how the structure performs and reacts. Failure paths are discovered and progressive collapse is prevented. On the other hand, it should be noted that the risk analysis is not able to identify all relevant risks. It's likely that events or relations between events and failures are overlooked and as a result (important) failure modes may be forgotten.

The previous results hold on a global scale for a precast structure. When the structure is compared with a cast in situ variant, the global risks remain comparable. On a local scale an important distinction can be made: the connections. The connections are the strength and weakness of precast concrete and the division and properties should be an important aspect during the upcoming structural design. The connections are a weak link because they are subject to more errors and commonly have a lower reinforcement ratio than the surrounding elements. Due to this lower reinforcement ratio and other connection properties (smooth concrete surface), they have a lower resistance than the surrounding concrete. By introducing connections also opportunities are created: it's now possible to prefabricate the elements and assemble them on the construction site.

bearing facade. A 1m thick foundation slab ensures a proper coherence of the foundation. In the literature study more information is provided on the foundation and the considered alternatives.

The Zalmhaven tower is located near the Hoge Heren towers (both with a height of 103m) and the Hoge Erasmus tower (h=93m), as can be seen in Figure 4.

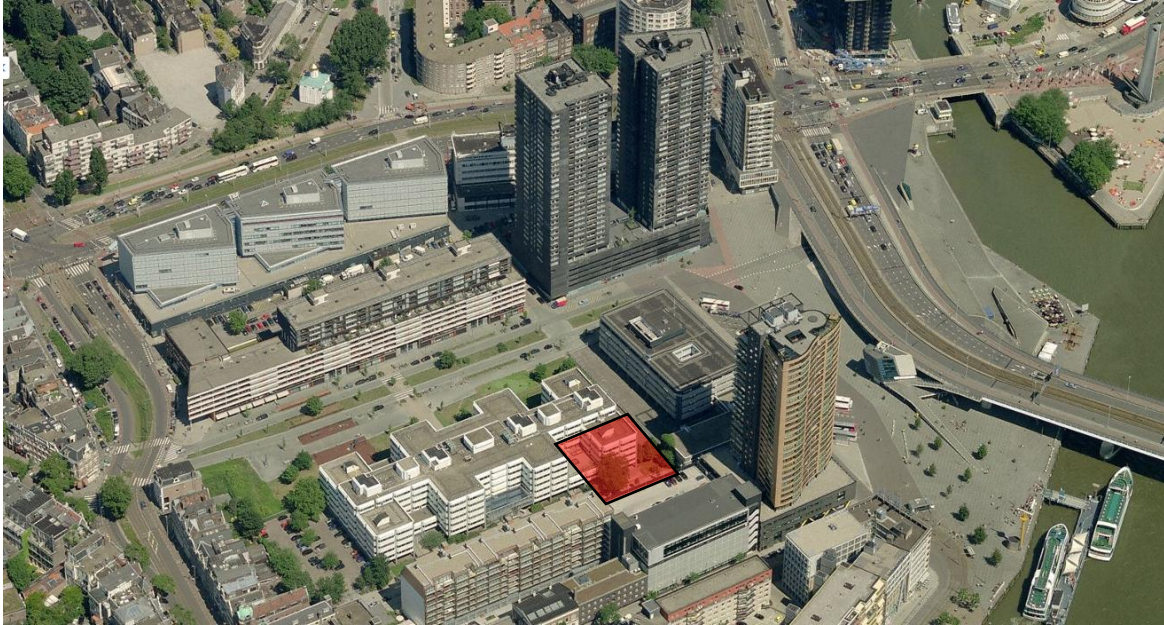


Figure 4 Aerial view from the south [Bing maps, 2012]

Figure 5 and Figure 6 give an artist impression of the entire project. The height difference between the Zalmhaven and the surroundings is clearly visible.



Figure 5 Artist impression of the Zalmhaven tower and low rise [Top100.nl, 2012]



Figure 6 Artist impression of the Zalmhaven tower and the surroundings [Zalmhaven, 2012]

Between 2004 and 2011, Zonneveld has made three structural designs with many different heights. The first cast in situ concrete design was based on two bays (two walls in x and y-direction). In the second concrete design an extra wall was added in the y-direction to reduce the floor span and to increase the stiffness. Because of this additional wall, the wall thickness is reduced from 500 to 400mm in the y-direction. The third design was based on a composite structure with steel and concrete. Due to the building acceleration a concrete core with two outriggers wasn't sufficient and a mega structure was required. By reducing the amount of concrete a considerably cheaper foundation could be applied. The mega structure design also resulted in construction time reduction of 50%. Though the composite mega structure design contained many benefits, the second concrete design was used as final design. A precast design was never examined.

More information on the original tunnel system design by Zonneveld ingenieurs can be found in report 2 of the literature study.

A facade tube was never applied because it's physically impossible to construct a facade tube with a tunnel system. With precast concrete this problem isn't present. The question that remains is if it's desirable to use a load bearing facade for dwellings: facade tubes are more efficient since they utilize the perimeter of the structure, but the window sizes are reduced. It's possible to place small windows at the bottom and large windows at the top (this was done in an early design of the Erasmus MC tower), but it is likely that the Building Aesthetics Committee will not approve. At Het Strijkijzer they applied a facade tube and constant window openings. Despite the structural system, the size of the window openings is still acceptable. In Figure 8 and Figure 9 the window size can be seen from the inside and in Figure 9 an opening in the structural wall is visible (all the internal walls have an opening to provide more flexibility for the future).



Figure 8 Window size of Het Strijkijzer [Het Strijkijzer, 2012]



Figure 9 Structural wall and window size of Het Strijkijzer [Het Strijkijzer, 2012]

Besides maintaining the current structural layout or replacing it by a facade tube, there are two more structural possibilities: combine a facade tube with the current structural

layout or create an I-profile layout. The four concepts will be elaborated in the following sections.

4.1.1 Concept 1: maintaining current structural system

As already discussed in the previous sections, this configuration utilizes the separation walls as structural walls and a maximum floor span of 7.8m is obtained. Compared to the facade tube there are several benefits:

- no additional separation walls have to be placed,
- no additional columns and beams are needed to support the floors,
- large facade openings from the floor to the ceiling provide more value,
- small shear lag effects, because the walls are close to each other.

Besides the benefits there are also two important disadvantages. The current monolithic design is already loaded at its maximum capacity. By replacing the walls by prefabricated elements, the stiffness is reduced. A higher concrete quality in combination with thicker walls may not be sufficient. The second disadvantage is the reduced flexibility. The structural walls prevent future changes to the layout.

4.1.2 Concept 2: facade tube

To overcome the stiffness reduction, a more efficient stability system could be used. Facade tubes belong to this category and provide a high stability with a small structural area. By removing the internal walls, the layout becomes very flexible. Unfortunately, concept 2 has several disadvantages compared to concept 1:

- additional separation walls have to be placed,
- additional columns and beams are needed to support the floors,
- the facade openings are reduced,
- shear lag is increased, because the walls are only connected at the corners.

To prevent these disadvantages, a third concept was made that combines all the positive aspects of concept 1 and 2.

4.1.3 Concept 3: facade tube with internal walls

By adding internal walls to the facade tube, most of the disadvantages of concept 2 are removed. Because the two systems work together, the stiffness of the facade tube can be reduced and the size of the window openings can increase. Also extra openings can be added to the internal walls, to increase the flexibility of the apartments. This technique was also applied at Het Strijkijzer, as can be seen in Figure 10 and Figure 11.

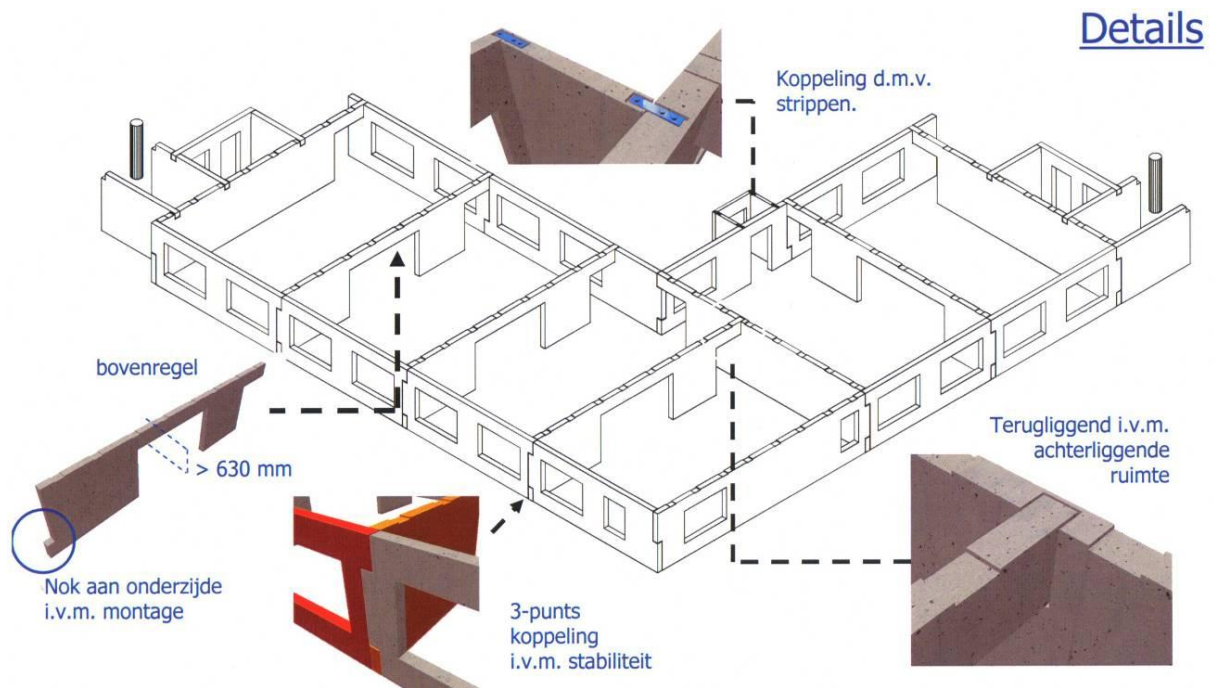


Figure 10 Structural system of Het Strijkijzer [Corsmit PowerPoint, 2012]



Figure 11 Interior of Het Strijkijzer [Corsmit PowerPoint, 2012]

4.1.4 Concept 4: I-profile layout

Concept 2 and 3 have a large influence on the design of the building. Since concept 1 may not provide enough stiffness, a fourth concept was designed: the I-profile layout, see Figure 12. With these flanges it's still possible to apply windows from the floor to the ceiling and the transparency is only slightly diminished.

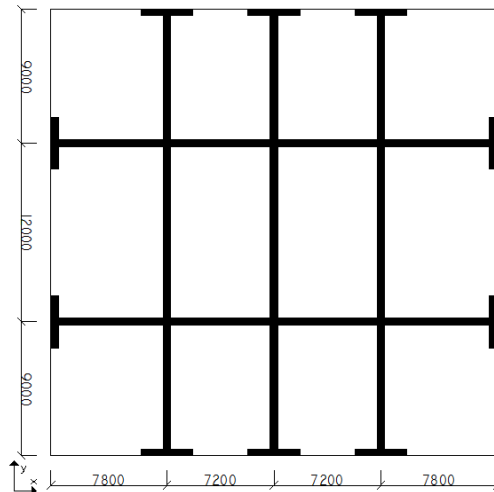


Figure 12 Layout concept 4

Concept 4 contains all the benefits of concept 1 and incorporates this with a higher stiffness.

4.1.5 Foundation

The layout of the foundation depends on the structural concept. For example, a facade tube requires more support at the perimeter of the structure while the original concept requires more support underneath the internal structural walls. During the literature study several variants have been examined for the original layout and diaphragm walls were the best solution. These diaphragm walls can also be used for concept 2 and 3, but different configurations of the walls should be examined (especially for concept 2).

4.2 Analysis of the concepts and determination final concept

Now that the four structural concepts are known, a preliminary design is made and analysed. Because concept 1 and 4 share several similarities, concept 4 will only be examined if the stiffness of concept 1 is insufficient. Of course walls with a thickness of 600mm can be applied at concept 1, but the current thickness of 500mm in the x-direction is already enormous.

4.2.1 Analysis of concept 1

Concept 1 (the original layout) was already analysed by Zonneveld ingenieurs as a cast in situ design (see Report 2 of the research study). As a result three walls with a thickness of 400mm are placed in the x-direction and two walls with a thickness of 500mm in the y-direction. To reduce the costs and dead load of the 500mm walls, the thickness is reduced to 400mm from the 27th floor. With the current design, the structure is already near its maximum capacity. By replacing the cast in situ walls with precast elements, the literature study has shown that a stiffness reduction up to 10% may be expected. To overcome this stiffness reduction without increasing the wall thickness, the

stiffness of the concrete should increase. Zonneveld ingenieurs applied C53/60 at the lower levels, but with precast concrete strength classes up to C90/105 can be used.

With the precast design, the floors have also changed. Due to new requirements for contact sound insulation, floors should have a minimal mass of 800kg/m^2 . Floors with a lower mass may be used, but then the top screed layer has to be acoustic decoupled to achieve the same acoustic insulation values. Applying a decoupled floor is often very complex and could result in delays during the finishing phase. To prevent any delays, massive 320mm thick floors with integrated ducts are applied. By integrating the ducts in the precast floor, an extra action is removed from the finishing phase. Compared to the original design, the floor thickness has increased with 30mm from 290mm to 320mm. Besides the differences between a cast in situ and a precast design, there are also differences between the calculations. Zonneveld ingenieurs calculated the design according to the NEN standard, but in this thesis the design will be calculated according to the Eurocode. In the literature study it was already noted that there are several differences between these standards (for example the consequence classes, $c_s c_d$ and the peak velocity pressure). These differences will also affect the outcome of the calculations. Because of these differences and the larger mass of the floors, a new analysis of concept 1 is made.

Several interesting aspects can be concluded from the analysis:

- The dead load on the foundation has increased from 805MN to 964MN. This increase of 159MN is due to the five additional floors and the increased floor mass. The live load has increased to 53MN (approximately 10MN more) because of installations and the additional floors.
- In the Eurocode C_{dim} and ϕ_1 are replaced by $c_s c_d$. Due to a new calculation method the results have changed: from $C_{dim} * \phi_1 = 0.87 * 1.25 = 1.09$ to $c_s c_d = 1.11$. This is an increase of 2%.
- The Eurocode has also introduced a new calculation method for the peak velocity pressure, resulting in lower peak velocity pressure values compared to the NEN (only in area 2 and 3). Because of the higher structural factor and the large force coefficient, the difference is minimal. Because of the increased height the moment has increased at the foundation compared to the original design: from 1479MN to 1664MN (12.5% higher). When the values of both designs are examined at 190m, the new Eurocode design has a 3% smaller wind moment.
- Despite the lower wind load, the Excel calculation still predicts tensile stresses at the foundation at load combination ULS2. This might be the result of the increased partial factors for consequence class 3. The calculation is too inaccurate to base any hard conclusions, but it's useful for comparison with the other two concepts.

4.2.2 Analysis of concept 2

The analysis of concept 2 is comparable with concept 1, but the structural properties differ from each other. Since the internal walls are removed, columns and beams have to be placed to support the floor. The stability is now provided by a facade tube with a thickness of 400mm and 30% window openings. The central core is maintained for vertical load bearing properties and the wall thickness is reduced to 300mm. When concept 2 is compared with concept 1, several remarks can be made:

- Concept 2 has a dead load at the foundation of 869MN. This is 95MN less than concept 1 because the mass of the walls has been reduced. This reduction can be achieved because the facade tube is more efficient than concept 1. The live load has not changed.

- Since there are no internal walls, only a part of the flanges may be taken into account for moment of inertia. Based on a preliminary calculation shear lag will reduce the moment of inertia with 19%.
- Despite the reduction of mass, the moment of inertia has increased with 25% compared to concept 1. Due to this increase in stiffness, $c_s c_d$ and the second order effects have been reduced. Since these factors are a part of the wind load calculation, the moment at the foundation decreases with 7%.
- Because of the higher moment of inertia and the lower load, there are no tensile stresses at the foundation. From all the load combinations ULS2 has still the smallest compression stress: 4.5N/mm^2 .

4.2.3 Analysis of concept 3

Concept 3 combines the best aspects of concept 1 and 2. When using the bundled tube structural system, internal walls of 300mm and a facade of 300mm thick are required. The stiffness of the internal walls is reduced to accommodate extra openings and the facade has approximately 30% openings. When concept 3 is compared with concept 2, one important remark can be made:

The dead load of concept 3 is 15MN lower than concept 2 because of the lower mass of the structural facade. Despite of the thinner facade walls and the less efficient internal walls, the moment of inertia is almost equal to the one in concept 2. This is because the shear lag is reduced by 50% due to the presence of the internal walls.

When concept 3 is compared with concept 1, the dead load is reduced by 110MN. The moment at the foundation has also decreased with 8% and ULS2 has the smallest compression stress of 4.9N/mm^2 .

4.2.4 Conclusion and determination final concept

When the three concepts are compared with each other, it can be concluded that concept 3 has the most favourable properties: the lowest structural weight with the highest moment of inertia. It should be noted that concept 3 is still not considered light when compared with a steel structure. This high mass has a positive influence on the dynamic effects of the structure and the analysis confirms this assumption: concept 3 has an acceleration of 0.076m/s^2 . This value is still within the limit of 0.18m/s^2 from NEN-EN 1991-1-4 and NTA Hoogbouw (03-A Wind).

When concept 2 is considered, the only aspect that stands out compared to the other concepts is the freedom of the layout. Though concept 3 comes close, the open internal walls do not provide the same amount of freedom. Despite this disadvantage of concept 2, the additional columns, beams, walls and increased shear lag provide too many disadvantages compared with concept 3. Therefore concept 2 is the first concept which is eliminated. Now only concept 1 and 3 remain. At first it was decided to design and elaborate both concepts. Concept 1 was examined first because the structural layout was easier to model: concept 3 contains fourteen additional and difficult to model connections between the structural walls and the facade or between the facades at the corners. Due to the elaborate examination of concept 1 and the many other aspects of the construction methodology which have been analysed, the remaining available time was insufficient to completely model and design concept 3. Therefore concept 3 will be evaluated at the end of the structural results in section 9.9.

4.3 Optimal element configuration of concept 1

With an estimated wall thickness for concept 1 of 500mm in the x-direction and 400mm in the y-direction, the precast element configuration can be designed. But first several assumptions are made to be able to design a suitable configuration.

4.3.1 Element configuration assumptions

With concept 1 the five internal walls intersect. At the monolithic cast in situ design this was no problem. For the precast design a smart solution should be applied that is able to activate the perpendicular walls. In the literature study several connections have been examined. Two solutions with a high stiffness are the Interlocking Halfway Connection (IHC) and the Staggered Connection (SC), shown in Figure 13.

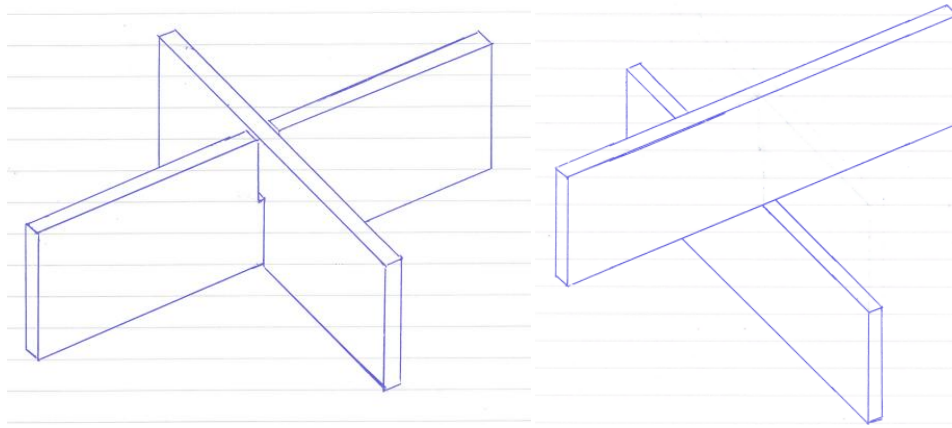


Figure 13 IHC (left) and SC (right)

When the structural properties of these connections are compared, it can be concluded that the smeared stiffness of the IHC is twice as large as the smeared stiffness of the SC [Tolsma, 2010]. The reduced stiffness of the SC will result in a larger lateral deflection of the structure. Unfortunately, the IHC connection requires smaller tolerances and it is more difficult to assemble on the building site. Besides these two important aspects, this connection is also difficult to model in a finite element program. The SC may have a lower stiffness, but the connection is more practical and less difficult to model. Because of these aspects, the SC is used as connection between perpendicular wall elements

The next aspects that determine the element configuration are the maximum mass and size of the elements. The Gross Vehicle Weight (GVW) is limited at 50 ton in the Netherlands. This means that the entire truck with trailer, cargo and driver may not weigh more than 50 ton. With an estimated weight of 14 ton for a truck with trailer, the elements are limited at a mass of 36 ton. The maximum length of this truck with trailer is 16.5m, resulting in a maximum element length of 13.5m. If one of these properties is exceeded, an exemption permit has to be acquired. Obtaining a permit for almost all the elements will lead to additional unwanted costs. Elements with a length up to 12m are near the maximum element length that can be easily produced at the factory and handled at the building site.

The last aspect which should be taken into account is the minimal overlap between the elements. To obtain a proper structural coherence, the element overlap should be at least $1/4^{\text{th}}$ of the element length [Falger, 2003].

With these four boundary conditions the element configuration of concept 1 can be designed.

4.3.2 Optimal element configuration

According to the literature study (see also section 2.3), the best structural properties are obtained when the elements are one storey high and as large as possible. With a maximum mass of 36 ton (see the previous section) the following dimensions are obtained for the 400 and 500mm walls:

$$l_{\max,500} = \frac{m \cdot g}{h \cdot t \cdot \rho_{\text{concrete}}} = \frac{36 \cdot 9.81}{3.05 \cdot 0.5 \cdot 25} = 9.3 \text{ [m]}$$

$$l_{\max,400} = \frac{m \cdot g}{h \cdot t \cdot \rho_{\text{concrete}}} = \frac{36 \cdot 9.81}{3.05 \cdot 0.4 \cdot 25} = 11.6 \text{ [m]}$$

These values are without door openings. With a door width of 1.25m, these values could be increased by 1m (there is still a lintel above the openings). Therefore the wall elements should have a maximum length of 10.3m for the 500mm walls or 12.6m for the 400mm walls. Because of the production process, the maximum element length of the 400mm wall is reduced to 12m.

The following step is to take the walls of the Zalmhaven tower into account. Per structural wall, the layout of the openings is different and therefore first a designation of the walls will be given in Figure 14. The three walls in the y-direction are given the number 1, 2 and 3 and the two walls in the x-direction are given the number 4 and 5.

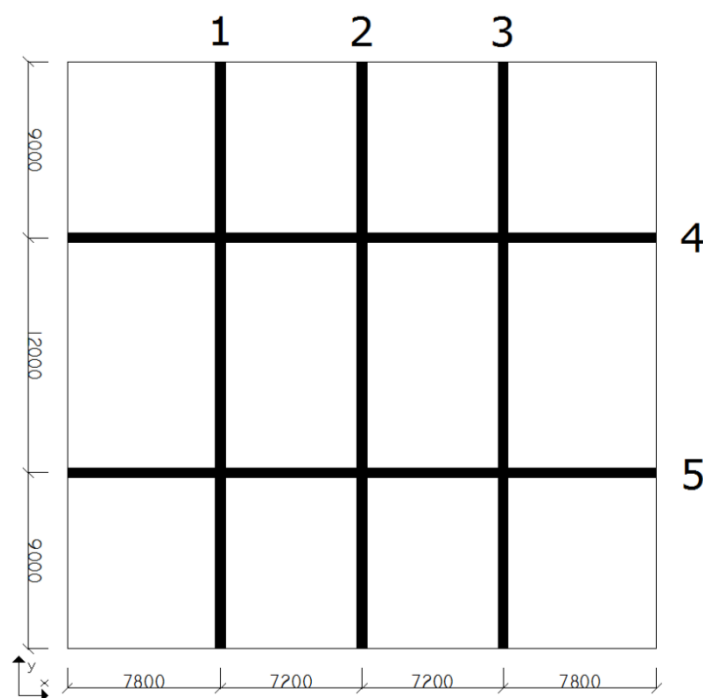


Figure 14 Designation structural layout

The entire overview of the wall openings can be found in appendix A. With the obtained boundary conditions, it's possible to create an optimal layout. First the configuration of wall 1, 2 and 3 will be determined.

Element configuration wall 1, 2 and 3

Over the height the amount of door openings will vary, depending on the configuration of the apartments. The location of the doors, if present, will always remain identical as shown in Figure 15. In this figure also the location of the Staggered Connection on the even floors is shown. With a maximum element length of 12m, the configuration on the even floors is already determined: two elements with a length of 9m and one element with a length of 12m. Now only the uneven floors remain. Due to the minimal overlap of 1/4th of the element length (2.25 or 3m), the amount of freedom is limited. Figure 16 shows two hatched areas where no vertical connection may be located due to this overlap. Therefore three locations remain where the vertical connection can be created. With only one vertical connection in the centre of the uneven floor two elements would be created with a length of 15m. This exceeds the limit of 12m and two small elements are required at the corners. In conjunction with wall 4 and 5 a corner element with a

length of 3m is chosen (to increase the amount of repetition). The final element configuration is shown in Figure 17.

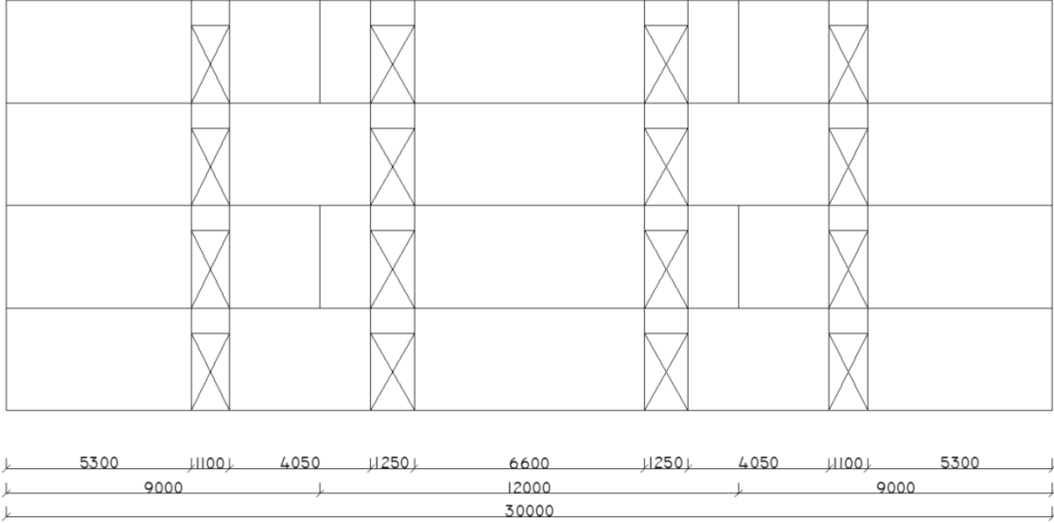


Figure 15 Location of the openings and SC in wall 1, 2 and 3⁶

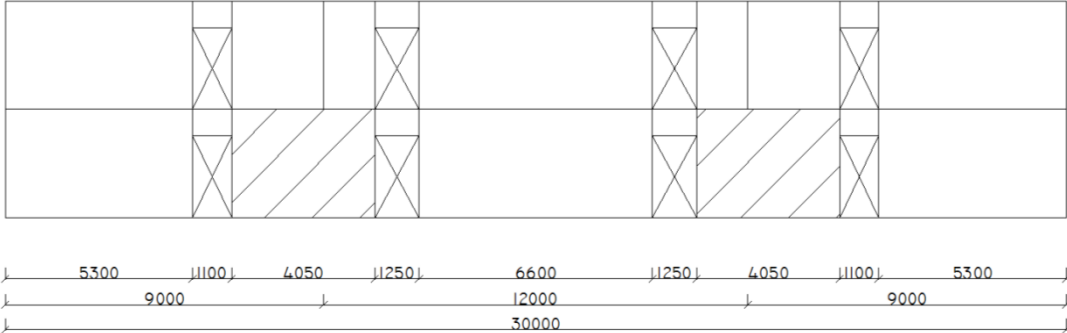


Figure 16 Restricted areas due to overlap at wall 1, 2 and 3

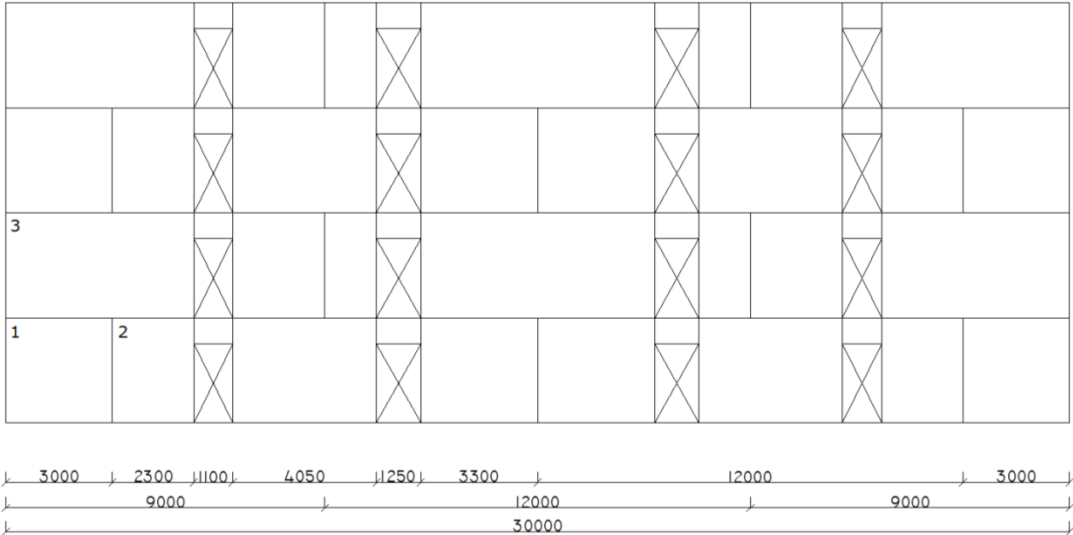


Figure 17 Final element configuration of wall 1, 2 and 3

⁶ The lintels above the doors may appear as separate elements, but these two lines are required for the calculation program (different Young’s modulus, see section 7.5).

In conclusion, wall 1, 2 and 3 are constructed out of three different elements. The weight of the elements may vary since not every element contains a door opening. Therefore the outline of the formwork will remain identical, but a special mold will be placed inside the formwork depending on the element. In Table 2 the area and mass of the different elements is shown.

Table 1 Area and mass of the elements of wall 1, 2 and 3

Element number	Area	Mass
[-]	[m ²]	[ton]
1	9.15	9.33
2	31.20-34.07	31.80-34.73
3	24.92-27.45	25.40-27.98

Element configuration wall 4 and 5

At wall 4 and 5, the wall openings are limited to the four shown locations in Figure 18. Furthermore, the location of the Staggered Connection is shown on the uneven floors. Due to the maximum length of 10.3m for wall 4 and 5, the element configuration at the uneven floors is already determined by the SC: two elements of 7.2m and two elements of 7.8m. Now only the even floors remain. Due to the minimal overlap of 1/4th of the element length (1.8 or 1.95m), the amount of freedom is limited considerably. Figure 19 shows three hatched areas where no vertical connection may be located due to this overlap. Therefore four locations remain where the vertical connection can be created. The exact location within these four remaining areas is chosen in conjunction with wall 1, 2 and 3 to create the highest amount of repetition. The final element configuration is shown in Figure 20.

At the 27th floor level, the wall thickness is reduced to 400mm, and therefore element 3 isn't required anymore from level (element 3 was required because the load was higher than 36 ton).

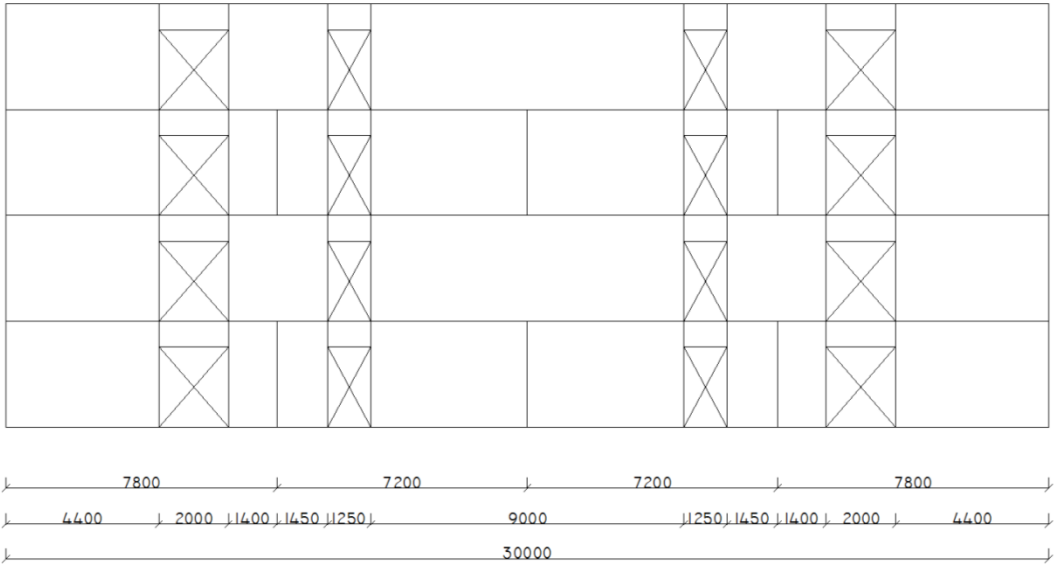


Figure 18 Location of the openings and SC in wall 4 and 5

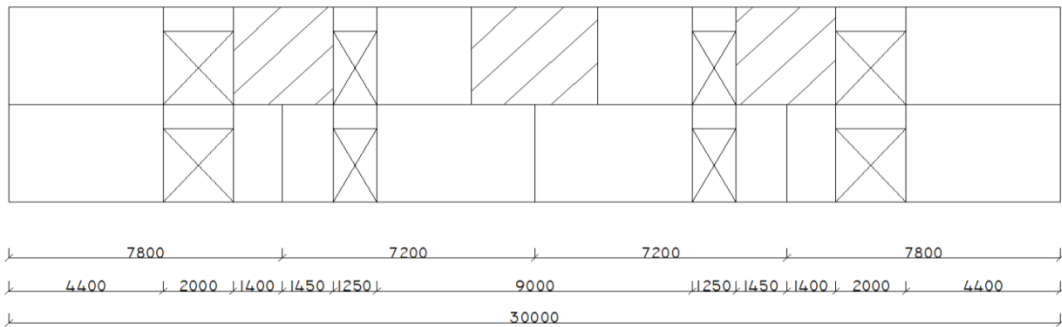


Figure 19 Restricted areas due to overlap at wall 4 and 5

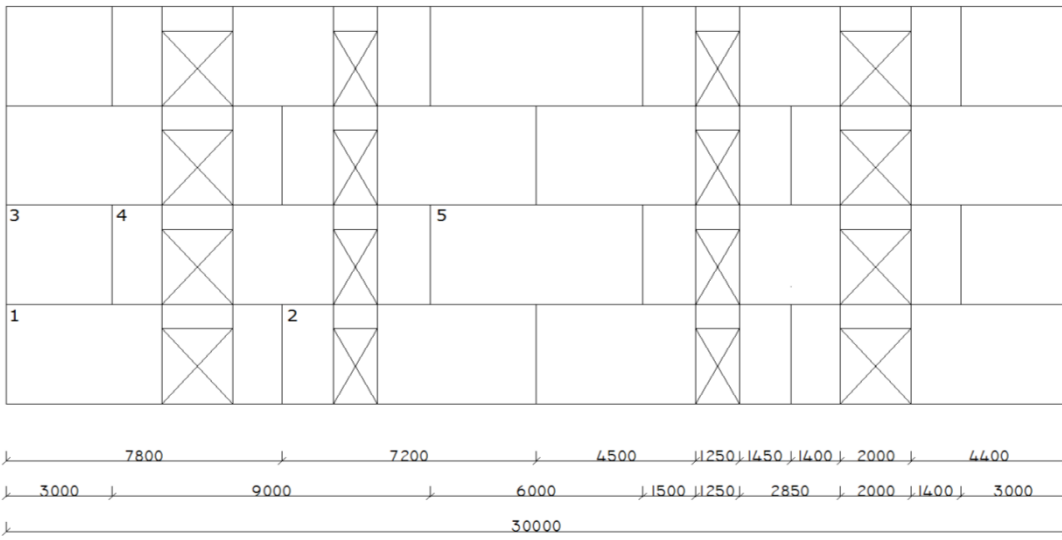


Figure 20 Final element configuration of wall 4 and 5

In conclusion, wall 4 and 5 are constructed out of five different elements. Just as the elements of wall 1, 2 and 3, the weight of the elements may vary due to the door openings. In Table 2 the area and mass of the different elements is shown.

Table 2 Area and mass of the elements of wall 4 and 5

Element number [-]	Area [m ²]	Mass [ton]
1	19.19-23.79	24.45-30.31
2	19.09-21.96	24.32-27.98
3	9.15	11.66
4	19.98-24.58	25.46-31.32
5	18.3	23.32

Relation element mass, risks and cycle time

As can be seen in Table 2, elements with a considerable size and mass are applied at the Zalmhaven tower. Does the size influence the risks and cycle time? This question can be replied by yes for both aspects: due to the larger size, the impact when something goes wrong increases (the consequences increase together with the element size). For example if the element is damaged irreparable, it's more difficult to replace the element. Besides this disadvantageous, larger elements reduce the amount of actions (less transport or vertical connections), making the process more efficient. Furthermore the large elements also positively influence the structural properties. Since the cycle time is leading in a high-rise design (an important difference between low and high-rise designs), the relation between the element mass and cycle time is determined on a quantitative level in section 8.3.

Conclusion

As a result of the door openings and the Staggered Connection, the amount of freedom for the element configuration is limited considerably. Only several small areas remain in which the vertical connection can be placed. The area increases when smaller elements are chosen, but according to the literature study (see also section 2.3) and the relation between mass and the cycle time (see section 8.3), the elements should be as large as possible. The current location of the vertical connections within the small available area could be changed, but this will have a negative influence on the amount of repetition between the three walls in the y-direction and two walls in the x-direction.

The three walls in the y-direction are composed out of three different elements. The two walls in the x-direction are composed out of five different elements. Due to similarities, the entire structure is only composed out of six different elements. It should be noted that the two elements of 3 and 9m long don't have the same thickness (400mm versus 500mm) and therefore cannot use the same formwork. The height off the formwork determines the thickness of the element and casting a 400mm element in a 500mm formwork provides difficulties. Nevertheless, utilizing the same perimeter will benefit the construction of the formwork.

The element configuration at the first five levels hasn't been discussed yet. In appendix A, the configuration is already visible and the choices behind this layout will be discussed in section 4.5.7 of the construction methodology.

4.4 Several design aspects of concept 1

Besides the element configuration, several other design aspects have to be discussed. For example the applied massive floors, the plug&play bathroom units and the balconies.

Already discussed at the analysis of concept 1, massive floor slabs with a thickness of 320mm will be applied at the Zalmhaven tower. These floors meet the requirements regarding contact sounds by using mass (at least 800kg/m²). Furthermore, these floors include a reinforcement net for the diaphragm action of the entire level. To ensure a coherent diaphragm action, the floor elements have to be connected at the corners by coupling reinforcement, shown in Figure 21. This figure also clearly shows the steel angles on which the floors are supported. To protect the angles during a fire and to absorb deviations, a thin screed layer is required. Because all the ducts are included in the floor, a screed layer of 50mm is sufficient.



Figure 21 Massive concrete floor slabs [Hurks group, 2012]

By incorporating all the ducts in the floor, the amount of actions during the construction and finishing stage are reduced considerably. Another aspect which requires a large amount of time during the finishing stage are the bathrooms (multiple disciplines are required in a small area). To reduce the required time for the finishing stage, plug&play bathroom units will be applied (see Figure 22).

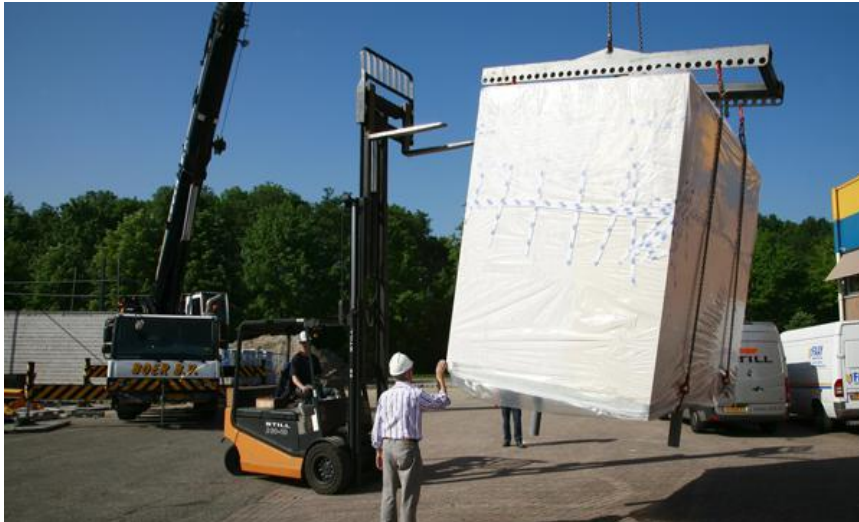


Figure 22 Plug&play bathroom unit [Faay, 2012]

These units are completely finished and only have to be connected to the ducts in the floor. By locally reducing the floor thickness (20 to 50mm according to the model), there will be no height difference between the unit and apartment floor. Because the bathroom units have a production time of four weeks, the design of the bathroom can be changed until the last moment by owner of the apartment. The flexibility is increased even more by making it possible to place the unit at multiple locations within the apartment.

These bathroom units are placed in the apartments during the construction phases (ruwbouw in Dutch). After the ducts and wires are connected, the screed layer can be poured. This action can already take place when they are still constructing this level (for example when the floor elements are placed on top of the level. Now only several actions remain in the apartment during the finishing stage (afbouwfase in Dutch): placing the internal separation walls (metal stud), finishing the electrical works (most ducts and wires are already incorporated in the walls and floors) and finishing the walls and ceiling. These remaining actions can be executed very quickly after the construction stage since the sandwich elements in combination with a hoisting shed provide a weather proof environment. It's estimated that the finishing stage is completed six layers behind the construction phase⁷.

At the beginning of this chapter, a structural layout was shown of the Zalmhaven tower, see Figure 7. In this figure several balconies are clearly visible. These balconies, originally made out of precast elements, do not contribute to the difference between precast and cast in situ high-rise design. Therefore these balconies are not part of the thesis. Because of the structural design, these balconies can always be added to the design. If concept 3 would have been elaborated, problems might occur with adding the balconies (the facade tube is intersected by a floor to ceiling high door opening).

The last remaining aspect of concept 1 that should be considered is the foundation. As discussed in section 4.1.5, the layout of the original foundation may be used since the

⁷ This aspect has been discussed with Gerard Baggermans and Ron Vonken from Hurks beton. Hurks beton is one of the leading companies utilizing new techniques to speed up the finishing stage.

structural configuration hasn't changed. Therefore 1.5m thick, 3.3m wide and 63.2m long diaphragm wall elements will be used, with a layout shown in Figure 23. Between the diaphragm and structural walls, a 1m thick foundation slab ensures a proper coherence and load distribution of the foundation.

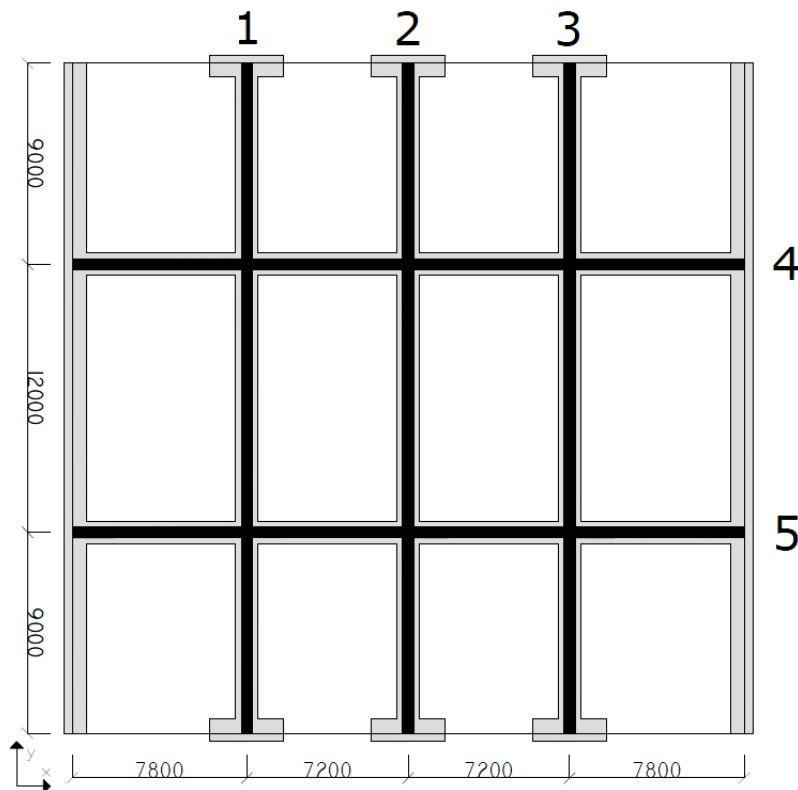


Figure 23 Layout foundation

4.5 Design of the construction methodology

In the literature study, the construction methodology was already discussed. It may be concluded that the construction methodology is an important aspect of a project since it determines the construction speed, building method, element size and many other aspects. This is because the construction methodology includes the entire process from the production of the elements at the factory till the placement of the elements at their final location.

Since the time of this thesis is limited, only a transport system will be designed for the construction site. During the literature study the building method, transport system between the factory and the building site and the transport system on the building site were already examined and will this be shortly recapitulated first.

4.5.1 Recapitulation of the literature study, building method

In this thesis a precast design is made for the Zalmhaven tower. The following benefits of precast support this decision:

- The construction time is reduced considerably since all the elements only have to be assembled on the building site. Simple and fast connections in combination with a high amount of repetition ensure a swift and efficient construction process.
- By reducing the construction time, the financial risk is minimized. This is because revenues are created in an earlier stage and because the short construction time results in a smaller interest loss. Since the precast elements are often not created

by the contractor, more work is outsourced to a controlled environment, creating an even smaller financial risk.

- The construction process is shifted from building site to factory. The conditions in the factory are weather independent, resulting in a higher quality and less delays. Furthermore, at the factory the building process is more centralized, reducing the transport of material and equipment.
- Because the construction is replaced with an assembly process, less personnel and space is required. This is beneficial for urban construction projects.

Though precast concrete has many benefits, the advantageous of cast in situ should not be underestimated. The following four aspects are considered to be the most important benefits of cast in situ structures:

- Cast in situ buildings are jointless and a monolithic structure is created. This has a positive effect on the interaction (second load bearing system) and the flow of forces.
- The designer has a large amount of freedom. The formwork is the only limiting factor. Floor spans in two directions are common and the integration of ducts and pipes are no problem.
- Because there is no prefabrication, the final designs can be made at a later stage. This reduces initial cost, interest loss and increases freedom.
- Liquid concrete has a small transport volume compared to precast elements and the amount of transport can be reduced.

With the precast building method, also an element configuration is required. The element configuration is discussed in section 4.3.

4.5.2 Recapitulation of the literature study, horizontal transport system

The next step in the construction methodology is the transport from the factory to the building site. Often transport by road is applied. Due to the location of the Zalmhaven tower, it's also possible to transport the elements via the river Nieuwe Maas. By applying transport over the river, several benefits are obtained:

- The ship has a very large capacity with almost no restrictions for the prefab elements. The final size of the elements will be limited by the factory and the building site (mainly by the vertical transport system).
- Due to the large capacity of a ship, a floating storage area is created. The storage area on site can be reduced
- By using transport over the water instead of using the road, the busy centre of Rotterdam is relieved of additional transport.

Unfortunately this method also contains several disadvantages. The distance between the river Nieuwe Maas and the Zalmhaven tower is 200m and the elements have to be lifted out of the ship onto a transport vehicle. Furthermore, the transport time between the factory and building site will increase noticeable with a ship. Since elements up to 36 ton can be transported via the road, which stretches the limit of a vertical transport system, the nearly unlimited capacity of the ship hasn't any additional benefits. Therefore it's decided to maintain the traditional transport system via the road.

As mentioned before, an element transported via the road is limited at 36 ton. According to the same legislation, elements up to a length of approximately 13.5m and a height of 3.5m can be transported without a permit. To prevent delays due to traffic, Just in Time (JiT) delivery may be applied. This method also reduces the required storage on site.

The JiT principle suggested in the literature study is based on a nearby vacant plot which will be used as waiting and storage area. At the Maashaven Noordzijde (marked with an A in Figure 24) or the Rijnhaven Zuidzijde approximately 10 000m² is available per plot. This is more than enough for temporary storage and several waiting spots for trucks. The storage depots are approximately 2.5km or 10 minutes away from the Zalmhaven tower.

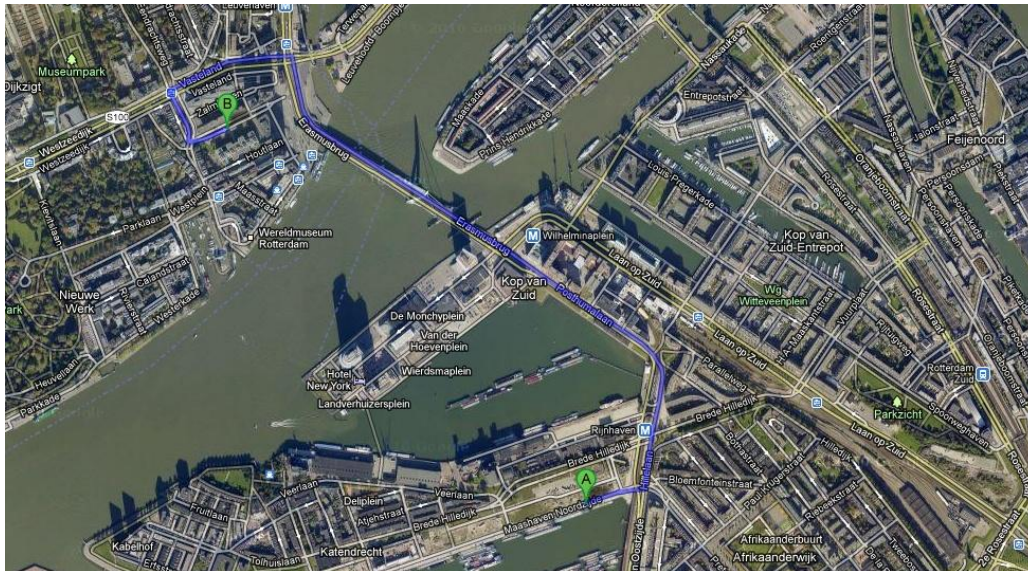


Figure 24 JiT truck waiting area [Google, 2012]

With this storage depot, a construction site ticket in combination with a logistic operator can be applied (used for the first time at JuBi, The Hague). Every delivery has to be registered in advance at the logistical operator, in order to organise the transport and storage of all the materials. This application is done via the building site ticket and the supplier has to indicate when and where it will be delivered (basement or fifth floor for example), how long it will take and which resources are required (forklift, gantry crane or nothing at all). Based on the schedules, the logistical operator will then assess if it's possible to unload the delivery. With an approved building site ticket, the truck has to report at the storage depot. At this location it's verified if the correct materials or elements are delivered, if they are on time and if they are damaged. Consequently, the logistic foreman at the building site is informed. He determines whether the transport may drive to the building site or if it has to wait (for example when there is a delay). When the transport is approved, the truck may drive to the building site and deliver its cargo. By applying the construction site ticket, a very efficient and organised transport system is obtained. These benefits also occurred at the JuBi project and no delays were encountered due to the horizontal transport system [Herwijnen, 2011].

Since the literature study no new insights have been obtained, providing a better solution for the horizontal transport between the factory and the building site. Therefore the JiT principle in combination with the building site ticket and storage depot will also be applied at the Zalmhaven tower.

4.5.3 Recapitulation of the literature study, vertical transport system

The second stage of the transport system describes the vertical and horizontal transport on the building site. During the literature study tower cranes and a hoisting shed were examined. Eventually the hoisting shed was chosen as transport system for the Zalmhaven tower because of the following advantageous:

- A hoisting shed has a low weather dependency since all the construction activities take place inside. Because of these controlled conditions, the quality of the

construction process increases. For example, the concrete isn't affected by low temperatures and an excess of rain water. Also the working conditions will become better, satisfying the higher requirements of today. To reduce the weather dependency of the vertical transport, a guided system should be applied.

- With taller buildings, the hoisting cables increase as well. Due to this longer length, the sway of the element as a result of the wind will increase, possibly damaging the finished facade. Therefore the vertical transport has to be interrupted during strong winds, providing delays. A guided transport system, which is only possible at a hoisting shed, will prevent most of the delays and reduce the drop safety zone. This latter is especially beneficial for projects with a small construction site. Aside from the drop safety zone, a construction shed reduces the required area even more because the construction area is moved from the ground to the top floor.
- The hoisting shed encloses the entire top floor, providing a working platform at the outside of the facade. Therefore the joints of the sandwich elements can easily be controlled on leaks (high-rise buildings often struggle with the water tightness at higher levels). Placing lightning conductors and cleaning the windows are several other tasks that can easily be executed from this platform.
- The hoisting shed also provides enough room for a lunch shack, toilet and equipment container. Consequently, the construction workers don't have to travel during their break, reducing the vertical transport. It may not be very obvious, but the vertical transport of personnel will become substantial at a high building level.
- By applying two gantry cranes, the hoisting shed is able to separate the transport flows. This results in cycle times that are independent of the height⁸, creating a better efficiency at a higher level. Furthermore, the gantry cranes often provide a higher load capacity than the standard available tower cranes in the Netherlands. Worldwide there are tower cranes available with a higher capacity and transport speed, but the availability of these cranes provides risks. These risks aren't encountered at a project specific hoisting shed.

Though, applying a hoisting shed also induces several problems:

- Until now, the two hoisting sheds used in the Netherlands (at the Delftse Poort and the Erasmus MC tower) were project specific. This resulted in relatively high investment costs and the inability to reuse the hoisting shed. Since there is no standard system available yet, upcoming hoisting sheds might suffer from the same difficulties.
- In contrast to the hoisting sheds applied in Japan which were used as hat truss, the hoisting shed will often be dismantled at the top floor. At the Erasmus MC tower with a height of 120m this was just possible with a heavy load crawler crane LR 1600/2 from Mammoet. This crane was so special, it was never used in Europe before and had to be shipped in especially for this project. Unfortunately, with a maximum height of 184m, this heavy load crane is insufficient for the Zalmhaven tower and another method has to be applied. A tower crane is a possible solution or it's possible to utilise the window cleaning system of the top floor, but before a 450 ton hoisting shed is dismantled will take a considerable time. Therefore a better solution has to be designed to dismantle the hoisting shed. Figure 25 depicts the dismantling process of the Erasmus hoisting shed.
- The two hoisting sheds applied in the Netherlands used the facade as support. Consequently, the facade has to stay open for a certain time period. At the Delftse Poort this was no problem since the facade was placed in a different building phase. At the Erasmus MC, the hoisting shed was supported by four window openings, resulting in a large concentration of forces. After the building shed

⁸ When the transport system is designed properly, the horizontal cycle will always be leading. At the last few floors this may change due to the high required capacity.

moved to the floor above, the truss beams were removed and the windows installed.



Figure 25 Dismantling of the Erasmus hoisting shed [Topaas, 2011]

To overcome the previous problems several hoisting sheds from abroad have been analysed. In Japan two promising systems have been applied in the previous century: Big Canopy from Obayashi Corporation and the SMART system from Shimizu. Both systems are elaborated in the literature study. By utilising techniques applied at these two systems, several disadvantageous are overcome.

4.5.4 Design of transport system on the building site (hoisting shed)

With the advantageous, disadvantageous and reference projects in mind, three hoisting sheds have been designed:

- Design 1, based on the Erasmus MC tower.
- Design 2, based on the design of the SMART system of Shimizu.
- Design 3, based on the Delftse Poort.

Hoisting shed design 1

Hoisting shed design 1 is nearly identical to the system applied at the Erasmus MC tower, but the dimensions have changed. To incorporate the steel truss on which the hoisting shed is supported, openings have to be created in the structural walls. At the Erasmus tower, the truss was supported by the load bearing facade, shown Figure 26 and Figure 27. At these four corner locations all the vertical and horizontal forces were transmitted.



Figure 26 Supporting truss of the Erasmus MC tower



Figure 27 Hoisting shed at the Erasmus MC tower

The Zalmhaven tower also contains a load bearing facade at two sides, but they do not provide any stability. Therefore the horizontal forces from the hoisting shed have to be transported via the floors to the structural walls. This has consequences for the detailing of the facade and the floor. In Figure 28 a render is shown of the hoisting shed. At the location of the truss beam, the window has to be temporarily removed.

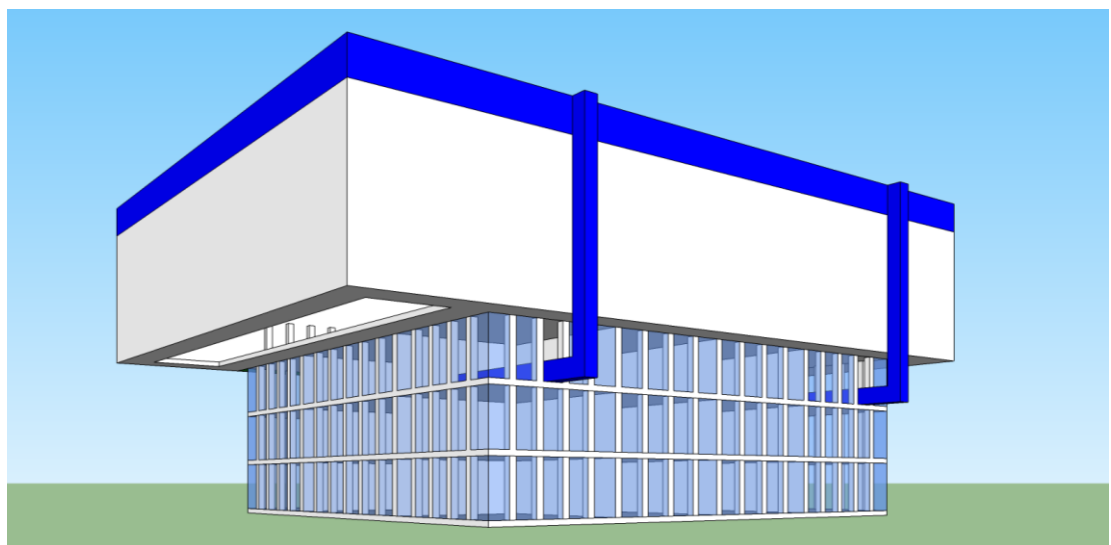


Figure 28 Hoisting shed design 1

Figure 29 provides a top view of the hoisting shed. The two orange gantry cranes are clearly visible.

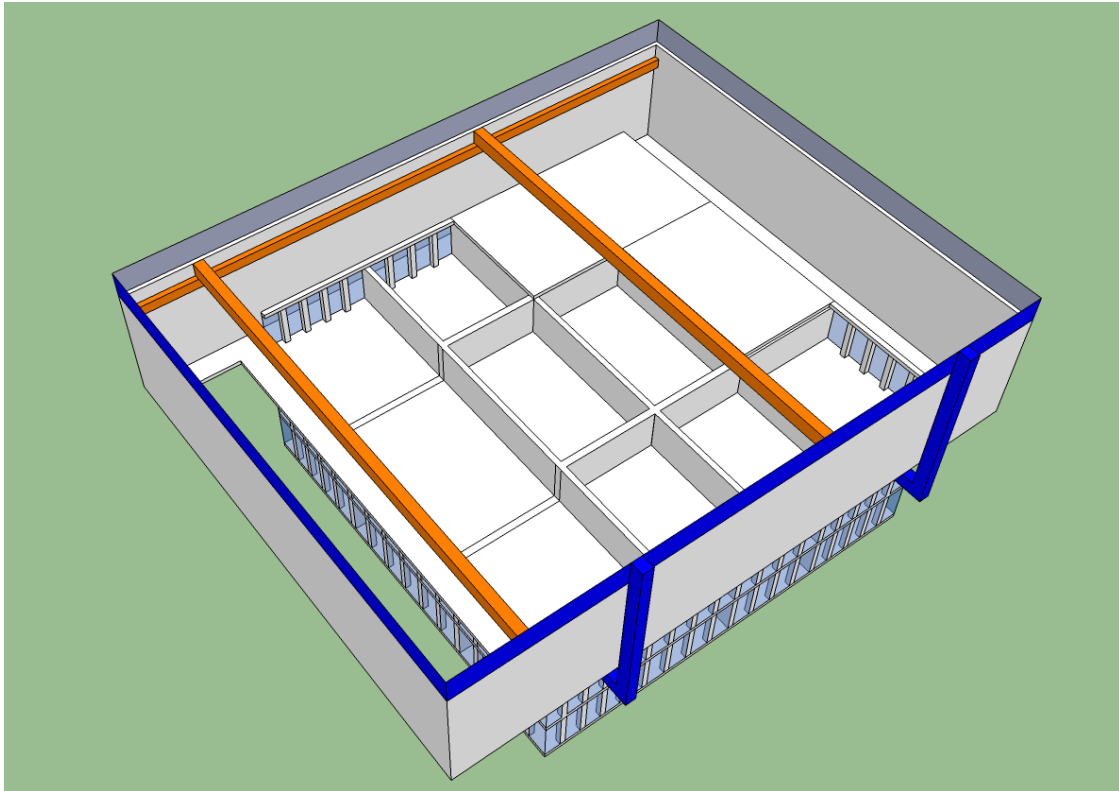


Figure 29 Top view of the hoisting shed design 1

The Erasmus design is simple and straight forward, but contains several disadvantageous:

- openings have to be created for truss beams in the structural walls,
- special detailing has to be applied to direct the forces from the hoisting shed to the structural walls,
- at the structural truss, the facade cannot be closed,
- the climbing system can be used to climb back after the top floor is constructed, but problems occur. For example: the windows have to be removed and the openings in the structural walls still have to be open.

Hoisting shed design 2

Design 2 applies the same supporting structure as the system of Shimizu: internal columns. By applying internal columns, the facade isn't interrupted by the supporting structure. Unfortunately this also creates a problem: the finished facade can't be used to climb back down. In Figure 30 the SMART hoisting shed is shown.

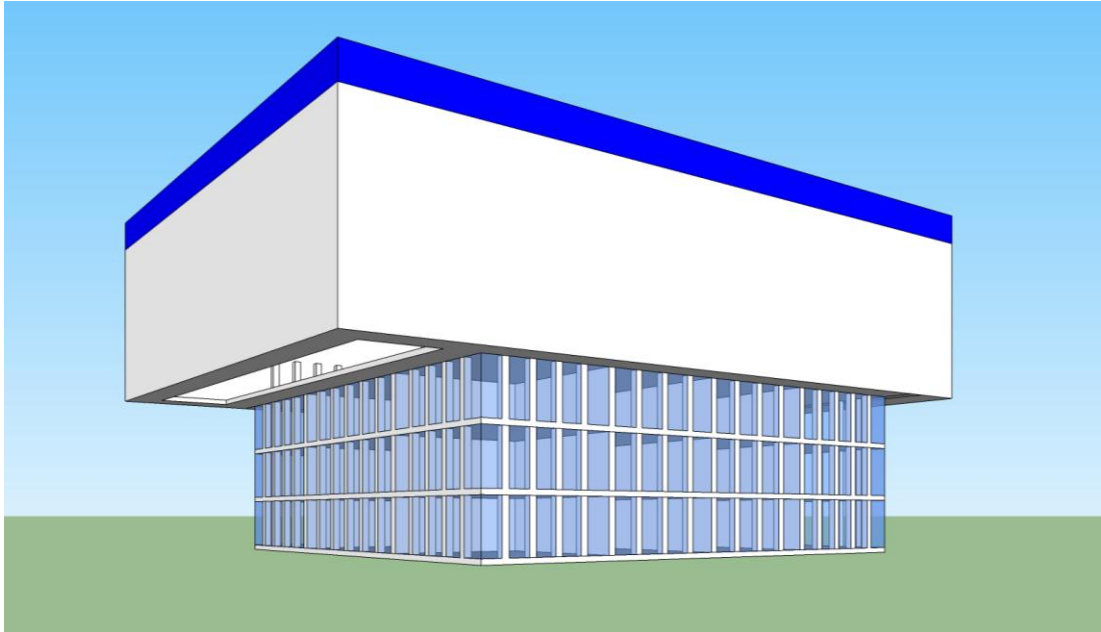


Figure 30 Hoisting shed design SMART

In Figure 31 a top view is depicted of the SMART system. The structure above the columns is clearly visible, supporting the entire hoisting shed. Due to these columns at least four gantry cranes are required to reach all the locations. However, utilizing multiple gantry cranes ensure that more elements can be placed at once. The four supporting points are connected to the structural walls by anchors. To provide enough stability, the length of the supporting columns has to stretch over several floors. Therefore openings have to be provided in the floors.

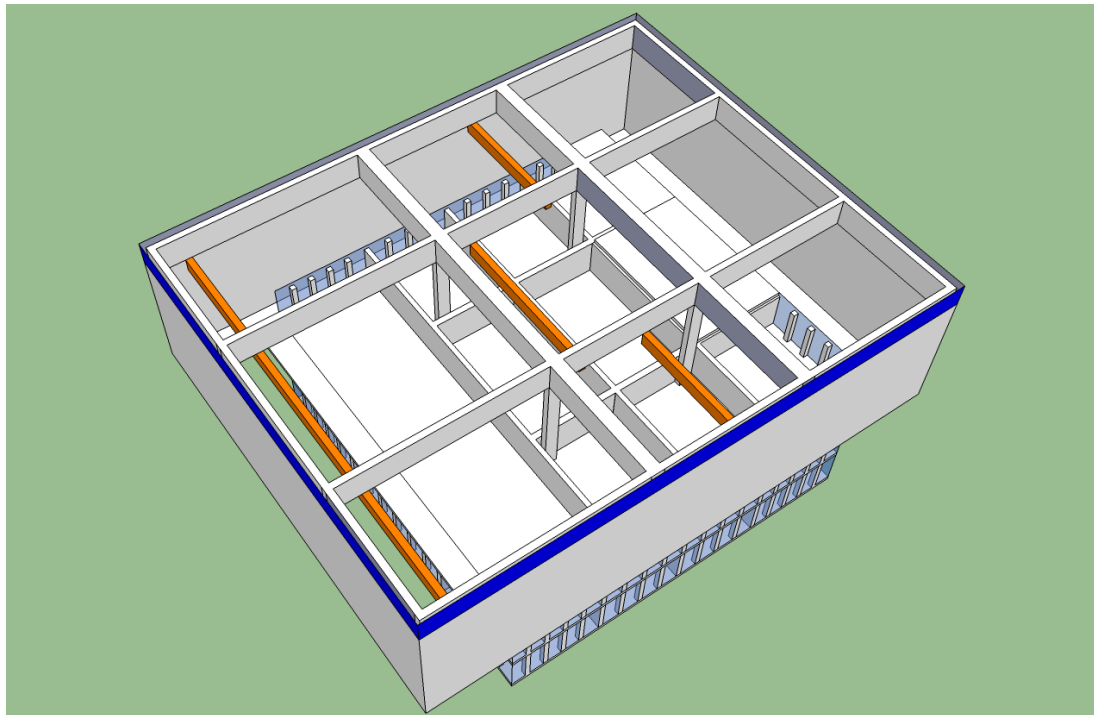


Figure 31 Top view of the hoisting shed design SMART

PERI GmbH is one of the companies providing self climbing systems. In Figure 32 two anchor plates are shown. Figure 33 shows the anchor plate, column and jacking system.

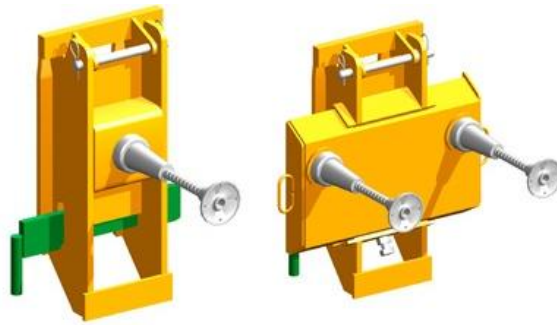


Figure 32 Anchors for the self climbing system [Peri, 2012]



Figure 33 Jacking system for the self climbing system [Peri, 2012]

It should be noted that the anchors have a maximum capacity of 100 kN or 10 ton. With a hoisting shed load of 300 to 450 ton (depending on the hoisting shed design and excluding the wind load), multiple anchors have to be used per support. This requires a high amount of accuracy because if one of the anchors is located slightly lower than designed, it will not bear any load. Hydraulic systems with multiple anchors have already been applied at precast buildings (for example the Delftse Poort hoisting shed), but it should be a point of interest. Furthermore, a powerful jacking system has to be applied to lift the hoisting shed. The small hydraulic cart shown in Figure 33 will be insufficient.

Besides Peri GmbH, Doka Group also provides many solutions for heavy automatic climbing systems. An example is the automatic climbing SKE system.

When all the aspects are considered, the following advantageous can be summed:

- by applying internal columns, the facade isn't interrupted,
- multiple transport cycles can be applied since there are more gantry cranes,
- by applying an existing system, the costs of the hoisting shed can be reduced.

Unfortunately, this system also contains several disadvantages:

- due to the internal columns, the structure can't climb back,
- openings have to be created in the floor for the supporting columns,
- walls near the supporting columns are difficult to place.

Hoisting shed design 3

The hoisting shed of the Delftse Poort was supported at four corners by multiple anchors in one load bearing concrete facade element (see chapter 3.4 of the literature study). Each support was capable of bearing 100kN (50kN dead load and 50kN wind load). With hydraulic jacks, the hoisting shed travelled to the next floor within one day. This technique came from sliding formwork systems and since the facade was placed in a different stage, it could also be applied at the Zalmhaven tower. The Zalmhaven tower has no large load bearing facade elements which provide stability, but the end faces of the structural walls could be utilised. Figure 34 shows the structural layout of the Zalmhaven tower and the ten supporting end faces are clearly visible.

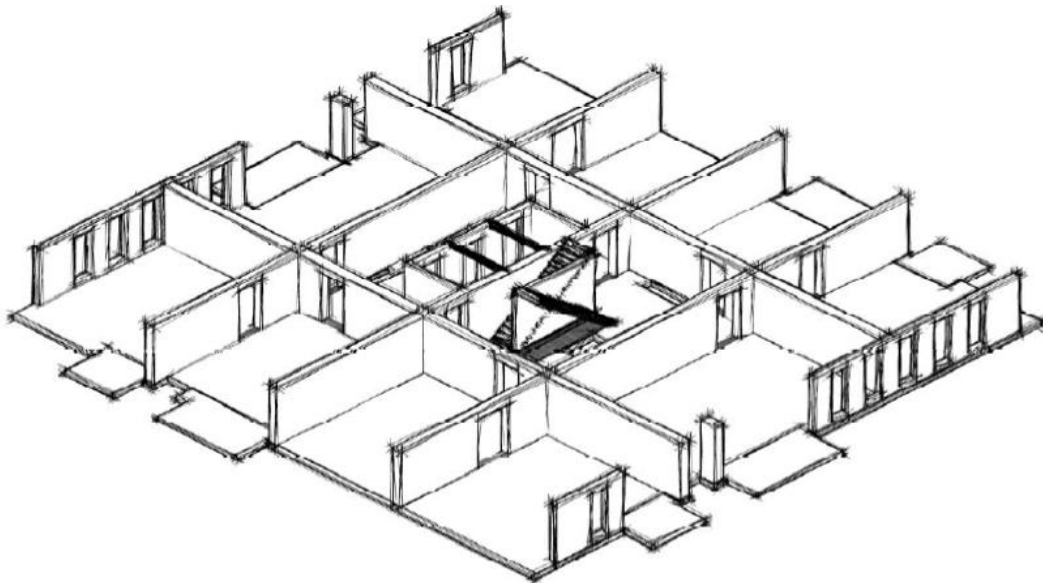


Figure 34 Structural layout of the Zalmhaven tower [Zonneveld ingenieurs, 2012]

Just as with the hoisting shed design 2 of the previous section, an automatic climbing system can be applied. With 10 support locations, the load per support varies between 30 and 45 ton, which is lower than the load of the Delftse poort. Figure 35 depicts the hoisting shed system based on the Delftse Poort.

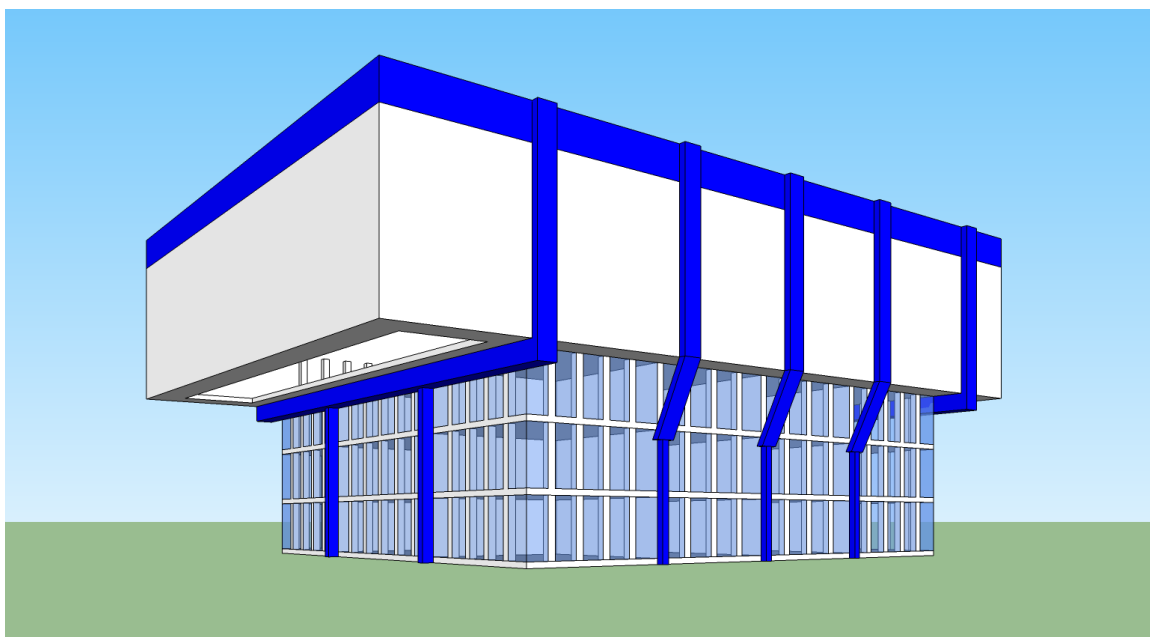


Figure 35 Hoisting shed design Delftse Poort

By utilising the end faces of the structural wall, this system is able to climb back after the top floor is constructed⁹. A point of attention is the connection between the jacking system and the end faces: the facade has to be locally removed in order to provide room for the anchors. This connection should provide no problems as long as the opening in the facade is waterproof (water leakage will endanger the finishing stage). By utilising external support, only two gantry cranes are required and there are no internal obstacles, as shown in Figure 36.

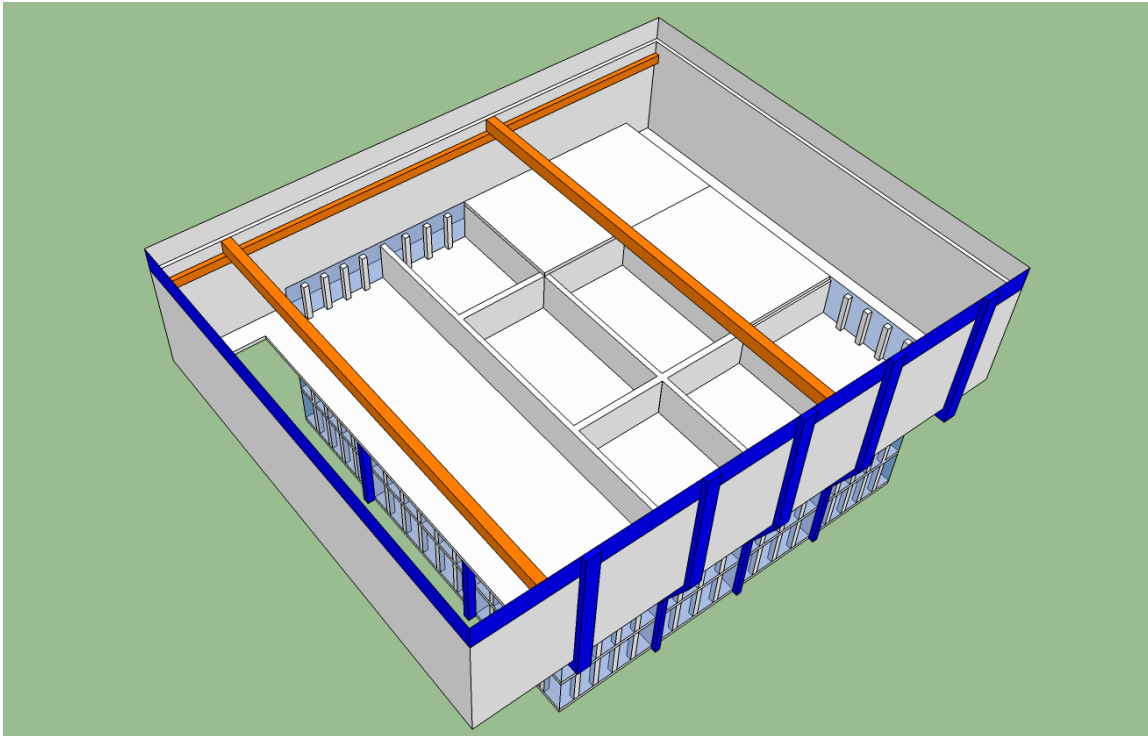


Figure 36 Top view of the hoisting shed design Delftse Poort

Compared to the other two systems, hoisting shed design 3 contains several important benefits:

- by applying an existing system, the costs of the hoisting shed can be reduced,
- the hoisting shed is able to climb back after constructing the top floor,
- there are no internal obstacles,
- no openings have to be created in the floors or structural walls.

The only point of attention for this design is the connection between the jacking system and end faces of the structural walls. When this detail is correctly engineered, this should provide no problems.

4.5.5 Determination final transport system

In the previous section three designs have been discussed for a hoisting shed. The largest disadvantage of a hoisting shed at a building of 202.25m are the costs and how the hoisting shed is dismantled after the top floor is constructed. The three designs are based on existing hoist sheds, reducing the amount of required innovation. A second method to reduce the costs is to reuse the hoisting shed after the Zalmhaven tower is completed. For example, the hoisting shed could be used as a construction building and

⁹ In order to climb back, the roof has to be removed and may therefore provide no structural stability to the hoisting shed.

only a new foundation is required¹⁰. Since the hoisting shed contains a high amount of steel trusses, it may be more efficient to construct the hoisting shed out of modular elements and reuse it at another construction project as a hoisting shed or as automatic climbing formwork platform. In Figure 37 an example is shown of an automatic climbing formwork platform of Doka Group in Basel, Switzerland (Messturm Basel).



Figure 37 Automatic climbing formwork platform from Doka Group [Doka, 2012]

This system has many similarities with the hoisting shed design 3 and by applying modular elements, the hoisting shed system may become interchangeable.

The only obstacle that remains is the ability to disassemble the hoisting shed after the top floor is finished. From the three designs, design 3 (based on the Delftse Poort) is able to climb down very easily; only the roof has to be removed. At the ground, the disassembly should provide no problems and the required disassembly time will be shorter than at a height of 202.25m. While the hoisting shed climbs down, the final facade elements can be placed over the anchor elements.

Because of this aspect and the similarities between the hoisting shed and automatic climbing platforms from Peri and Doka, design 3 is chosen as final design for the Zalmhaven tower. Since the water tightness of the openings in the facade are an important aspect in this design, an engineering detail was created, shown in Figure 38.

¹⁰ This was also eventually done with the hoisting shed of the Erasmus MC tower.

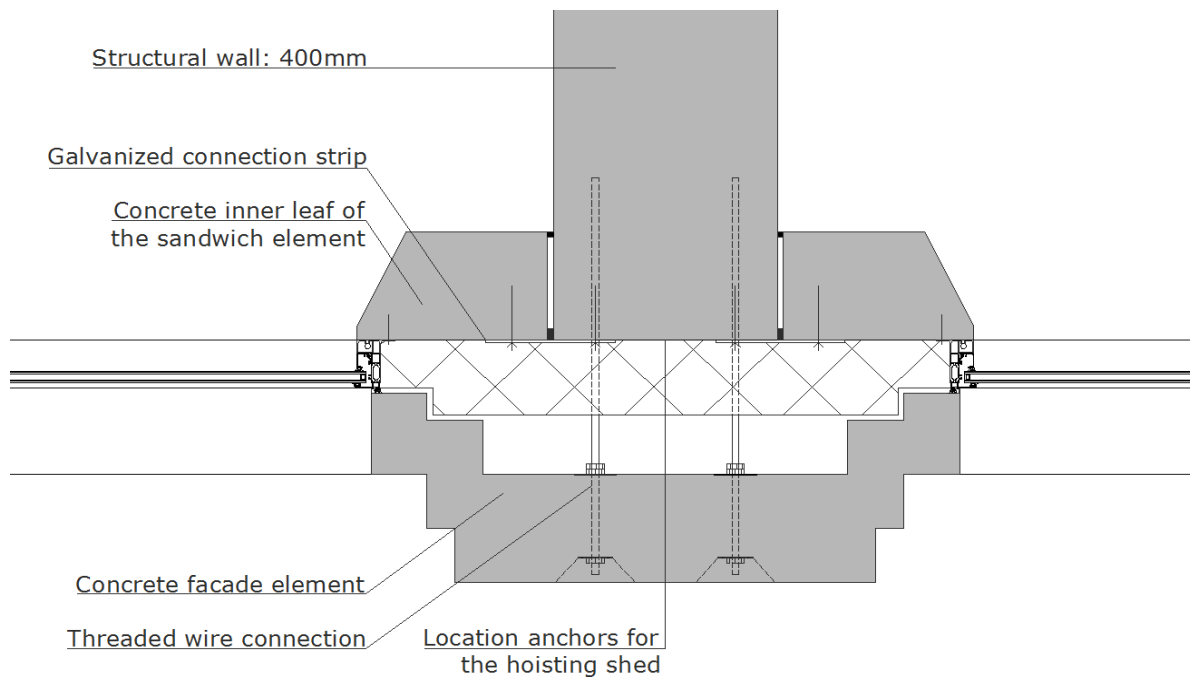


Figure 38 Detail of the facade

The sandwich elements are connected to the structural walls with galvanized strips. Between the sandwich element and the structural wall, an elastic strip provides a watertight connection. No kit is applied since it's difficult to apply the kit behind the galvanized strips. A kit will be used on the inside, to provide a smooth finishing and a secondary water barrier. When the hoisting shed climbs back, the insulation, steel corbels and threaded wires will be placed. Because all the provisions (for example DEMU anchors) are already incorporated in the structural wall, the placement of the insulation and supporting system of the facade should be very swift. After the two corbels and threaded wires are connected, the facade element can be placed. The final adjustment of the facade element is slightly more complicated since a top-down method is applied (it's impossible to reach the nuts behind the element). Therefore the nuts have to be adjusted, the element placed and if it isn't level, the element has to be removed and the nuts have to be readjusted. To reduce the amount of required labour, the concrete facade element may be replaced by a composite element with a similar appearance. Due to the reduced weight, a clicking system is able to fulfil the structural properties, resulting in a shorter connection time.

4.5.6 Design aspects of the final hoisting shed design

In the previous section hoisting shed design 3 was chosen as final design because of its ability to climb down and the similarities with existing systems. In order to calculate with this design (for example the cycle times), several design aspects have to be considered:

- How is the weather dependency of the hoisting shed decreased?
- What is the load capacity of the gantry cranes?
- What the transport speed of the gantry cranes?

With a hoisting shed and sandwich facade elements a very low weather dependency is obtained, resulting in a robust system. By applying a guided vertical transport system, the weather dependency is reduced even more. The following aspects show why the vertical transport system dependency is reduced by a guided system [Mei, 2012]:

- The occurrence of weather delays and the wind sensitivity increases with a higher building height. A guided system is hardly affected by these aspects (there is hardly any sway of the element).
- A guided transport system has a low minimum required area (for example the drop zone), which is beneficial in an urban areas.
- The entire construction process is influenced by the availability of the transport system. A large possibility of delays will endanger the entire construction process.

Figure 39 shows a possible solution for the guided vertical transport system. The orange guidance rails shown in Figure 39 can be attached to the anchors which are also used for the jacking system of the hoisting shed.

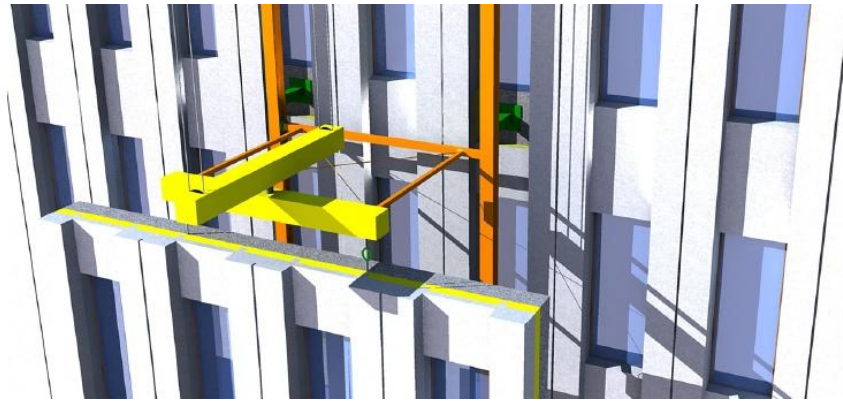


Figure 39 Guided vertical transport system [Meij, 2012]

The next design aspect is the load capacity of the gantry cranes. The maximum element mass is 36 ton. This load is increased by the weight of the stabiliser (evenaar in Dutch), guidance system and steel cables. This results in the following loads:

- the maximum element load is 36 ton,
- for the stabiliser, the same double system as applied at the Erasmus MC tower will be used. This system has a load of 3.6 ton [Meij, 2012], see Figure 40,
- the guidance system has a load of approximately 3 ton [Meij, 2012],
- for the vertical transport four Bridon Endurance 50DB cables will be used with a total load of 0.3 ton/100m [Kwint, 2012].

With these loads, a minimum gantry crane capacity of 43.2 ton is required. The hoisting shed of the Erasmus MC tower contained two beams per gantry crane, reducing the load per beam and increasing the stability, see Figure 40.

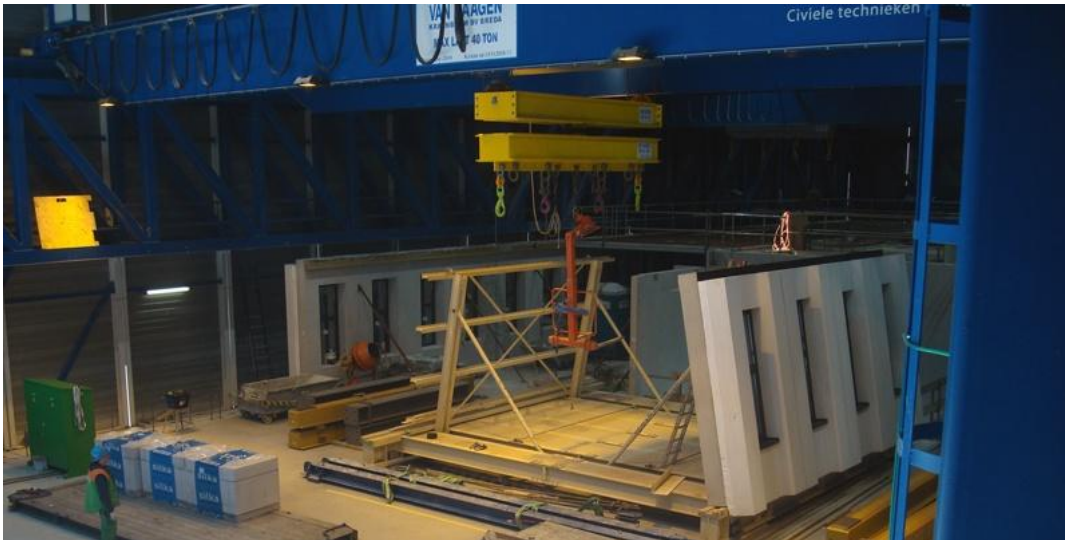


Figure 40 Gantry cranes and double stabiliser

The final design aspect is the transport speed of the vertical transport system. With increasing height, the transport time will increase considerably. Since the Erasmus MC tower has a maximum height of 120m, the capacity of this system will probably be insufficient for the Zalmhaven tower. According to the cycle time calculations of section 11.1.1, the transport capacity applied at the Erasmus MC tower satisfies the requirements of the Zalmhaven tower, which is unexpected. The fact that the vertical transport system at the Erasmus MC tower had a low utilisation ratio at the top floor (80%) and because the vertical transport wasn't optimised (the average mass per movement was too low) explains why the requirements are satisfied at the Zalmhaven tower.

In Figure 41 the vertical transport speed of the Erasmus MC is shown in dark blue. The gearless drive unit has an estimated power of 110kW, based on the other values.

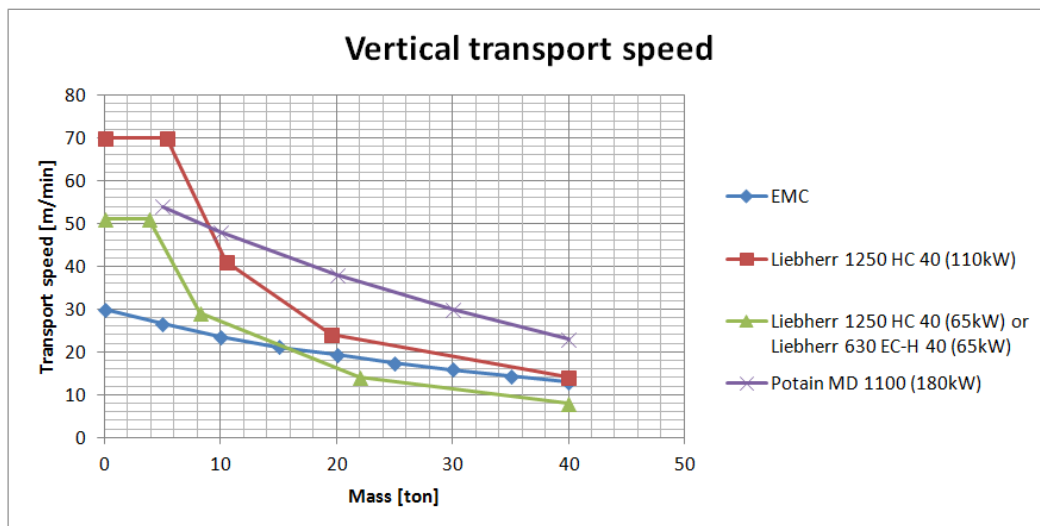


Figure 41 Vertical transport speed

4.5.7 Start-up of the hoisting shed

In the previous sections multiple aspects of the hoisting shed have been discussed, but there is still one important aspect remaining: the start-up of the hoisting shed. Due to the plinth and a minimal support length for the jacking system (three floor levels), the

hoisting shed can't start at the ground floor. Therefore the fifth floor will be the starting level of the hoisting shed and the sixth floor will be the first level constructed by the hoisting shed. To construct the hoisting shed at the fifth floor, a Demag Terex CC2500-1 crawler crane will be used (identical to the crane used to construct the Erasmus MC tower hoisting shed). This crane has an enormous load capacity and is able to place elements up to 44 ton at a distance of 32m. Because of this large load capacity, larger elements can be applied at the first five floors, resulting in better structural properties of the Zalmhaven tower. For example: elements with a length up to 15m and a mass of 43.7 ton will be applied, see appendix A. Due to this high load and longer length, an exemption is required for the horizontal transport. In Figure 42 the Demag crawler crane is shown at the construction of the Erasmus MC tower. This crane will also be utilised to disassemble the hoisting shed when the building is finished.



Figure 42 Demag Terex CC2500-1 [d9t, 2010]

4.5.8 Conclusion

During the literature study many interesting aspects for the design and construction of the Zalmhaven tower have been examined. Besides examining the possibilities, several decisions were made in the literature study to speed up the design process. For example: precast concrete was chosen over cast in situ concrete as building method. For the horizontal transport system, trucks in combination with the JiT principle were preferred. A hoisting shed would be applied as vertical transport system since it had many benefits compared with traditional tower cranes. Because only the methods were discussed in the literature study, a design still had to be made for the hoisting shed. From the three different designs, design 3 based on the Delftse Poort was chosen as final vertical transport system. The other two designs were less suitable since they were more difficult to disassemble. In order to incorporate this hoisting shed in the calculations, several design aspects had to be considered. For example a vertical guidance system was applied to reduce the weather dependency and to minimise the drop safety zone. In order to transport the 35 ton elements to a height of 202.25m, the gantry cranes are designed with a load capacity of 43.2 ton and a drive unit¹¹ of 110kW (identical to the Erasmus MC tower). The crane which is required to construct the hoisting shed can also be utilised for the first five floors. As a result of the high load capacity, larger elements can be applied at the first five floors.

¹¹ The horizontal gantry crane may be equipped with a less powerful drive unit due to the small vertical transport distance.

4.6 Conclusion

In this chapter the design of the structure and construction methodology is determined. Based on these designs, the feasibility of a 202.25m precast tower can be examined. First of all several structural concepts were designed and analysed. Concept 3 based on a facade tube with internal walls provided the best structural properties and was therefore considered in combination with the original layout (concept 1). Due to the limited amount of time only the original layout will be considered in this thesis and based on the results concept 3 will be evaluated.

With the structural layout and several boundary conditions from the transport system, an optimal element configuration has been determined. Within these boundary conditions, the elements should be as large as possible. As a result, elements with a mass varying between 9.33 and 34.73 ton are created. Besides the element configuration several other aspects had to be considered. For example the floor type, foundation layout and the possibility of using prefabricated bathroom units.

The construction methodology, containing the entire process from the production of the elements at the factory till the placement of the elements at their final location, was the last aspect of this chapter. Based on the literature study, several possibilities have been examined for the horizontal and vertical transport and it could be concluded that transporting elements via the road with JiT in combination with a hoisting shed provided the most benefits. By utilising the end faces of the structural walls, a modular system based on automated climbing systems was obtained. Since it's supported by anchors in the end faces, this hoisting shed is also able to climb back. The weather dependency of a hoisting shed is relatively low and by utilising a guided vertical transport system this dependency is reduced even more. The crawler crane required to construct the hoisting shed is also employed to construct the first five levels. By using the crawler crane, larger elements up 15m and 43.7 ton can be applied, improving the structural properties at the bottom section.

5 Loads on the structure

As any other object on earth, the Zalmhaven tower is subjected to loads. The loads can be placed in two categories: dead and live load or horizontal and vertical load. The latter category will be chosen in this thesis. Aside from the categories, what is the magnitude of the wind load which is acting on a 200m high tower? And what are the values of the vertical load?

The goal of this chapter is to determine the extent of all the loads acting on the Zalmhaven tower. Besides these values, the consequence class, reference period and load combinations also play an important role in determining the loads.

The consequence class, reference period and environmental exposure class will be examined first in section 5.1. Consequently the vertical and horizontal load will be discussed in section 5.2 and 5.3. Section 5.4 continues with the accidental loads. This chapter ends with the load cases and combinations in section 5.5.

5.1 Consequence class, reference period and environmental exposure class

The Zalmhaven tower is categorised as a consequence class 3 structure since it has a large consequence regarding the loss of life, and a significant economic and social effect on the environment. Furthermore, the Zalmhaven tower exceeds the maximum amount of storeys of consequence class 2a and 2b (see table A.1 of NEN-EN 1991-1-7).

The reference period is 50 years, which is the standard value for a large non-temporary building.

The super-structure is categorised as XC-3 because the concrete is located inside the building with a moderate humidity or it's located outside, but protected from the rain. The sub-structure contains one basement layer and the surface level of the soil is located at 3.20m+NAP. The water table is approximately 1.5m lower than the surface level [Rotterdam, 2012] and the basement walls will be wet and dry. Therefore the sub-structure is categorised as XC-4.

Below a short recapitulation is given:

- consequence class: 3,
- reference period: 50 years,
- environmental exposure class super-structure: XC-3,
- environmental exposure class sub-structure: XC-4.

5.2 Vertical load

The vertical load consists of dead and live load. In Figure 43 an overview of the structural layout is depicted. Three different load categories can be distinguished: floors, walls and the facade. The dead and live load will be discussed per category.

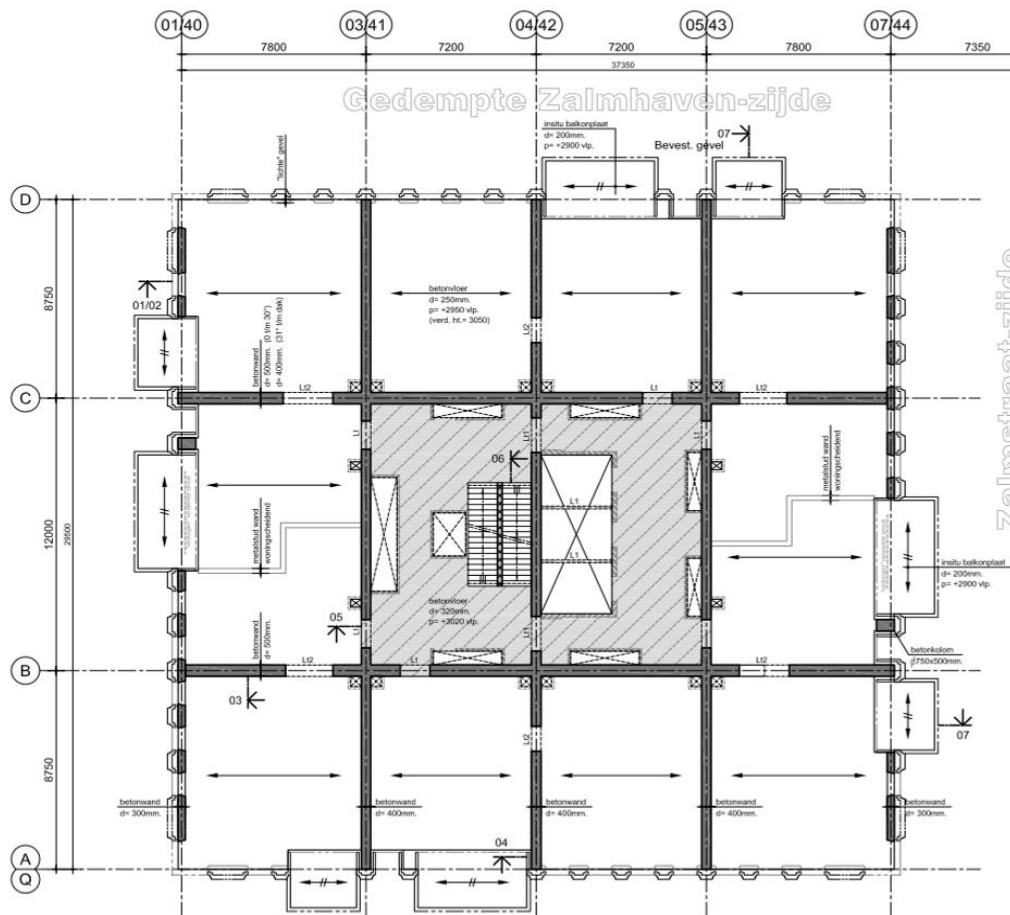


Figure 43 Structural layout of the Zalmhaven tower

5.2.1 Vertical load from the floor

Dead load

The Zalmhaven tower has 65 floors. Because of sound regulations in the National Building Code 2012, a 320mm thick massive concrete slab will be used for all the floors. This heavy concrete floor, with a weight of more than 800kg/m^2 , satisfies the regulations with regard to contact sounds. By using mass instead of other techniques (for example a floating screed layer), time and costs are reduced. Furthermore, the mass solution is very unsusceptible to errors, reducing time and costs even more. Besides the massive floors, a thin screed layer of 50mm to level and finish the floors is still required. The pipes are already incorporated in the floor.

The massive floor and screed layer result in a dead load of 9.25kN/m^2 . This load is present in every load case ($\Psi=1.0$).

On the ground floor a massive slab of 1m thick is used to spread the forces over the foundation. This floor is casted in situ (just as the foundation) and has a dead load of 25kN/m^2 , present in every load case ($\Psi=1.0$).

Besides the load of the floors, there's an additional (live) load added to the dead load: the separation walls. This distributed wall load is based on a Gyproc SoundBloc metal stud wall with an average sound insulation of 61dB and a fire resistance of 120 minutes [Gyproc, 2012]. The metal stud wall has a dead load of 32.2kg/m^2 , resulting in a line load of 0.86kN/m^1 (floor to ceiling height is 2.68m). According to section 6.3.1.2 of NEN-EN 1991-1-1 this line load may be replaced by a distributed live load of $q_k=0.5\text{kN/m}^2$. In this thesis, the distributed wall load is added to the dead load of the structure since this

is allowed at dwellings. For an office building it's possible that a new tenant remodels the entire (or a large part of the) building and (temporarily) removes all the internal walls. In a dwelling building there are multiple tenants and it's highly unlikely that all the internal walls will be removed and remain absent. Therefore the live distributed wall load is incorporated in the dead load.

Live load

The Zalmhaven tower only houses dwellings. According to NEN-EN 1991-1-1, table NB.1-6.2 (National Annex), dwellings are subjected to a live load of 1.75kN/m^2 . When this load is combined with another live load (for example wind), it may be reduced by 60% ($\Psi=0.4$ in table NB.2-A1.1 of NEN-EN 1990).

Due to the function of the ground floor (lobby area), a live load of 5.0kN/m^2 is assumed. A reduction factor of $\Psi=0.6$ may be applied when combined with other live loads. A reduction factor of 0.6 is applied instead of 0.4 because this area will be used as an escape route during emergencies.

The first two floors will be used for storage and installations, which results in a live load of 5kN/m^2 . Due to the nature of this load, no reduction factor may be applied ($\Psi=1.0$).

The panorama floor on 65th floor is subjected to a live load of 5kN/m^2 . In contrast to the ground floor this area isn't used as an escape route and a reduction factor of 0.4 may be applied in combination with other live loads ($\Psi=0.4$).

The previous aspects have been shortly summarized:

<u>Dwelling floor</u>		
Floor slab (d=320mm)	<u>G</u>	<u>Q</u>
Screed layer (50mm)	8.00kN/m ²	
Distributed wall load	1.25kN/m ²	
Live load ($\Psi_0=0.4$)	0.50kN/m ²	1.75kN/m ²
Total	<hr/> 9.75kN/m ²	<hr/> 1.75kN/m ²
<u>Lobby floor (ground floor)</u>		
Floor slab (d=1000mm)	<u>G</u>	<u>Q</u>
Live load ($\Psi_0=0.6$)	25.0kN/m ²	5.00kN/m ²
Total	<hr/> 25.0kN/m ²	<hr/> 5.00kN/m ²
<u>Installation/storage floor</u>		
Floor slab (d=320mm)	<u>G</u>	<u>Q</u>
Screed layer (50mm)	8.00kN/m ²	
Distributed wall load	1.25kN/m ²	
Live load ($\Psi_0=1.0$)	0.50kN/m ²	5.00kN/m ²
Total	<hr/> 9.75kN/m ²	<hr/> 5.00kN/m ²
<u>Panorama floor</u>		
Floor slab (d=320mm)	<u>G</u>	<u>Q</u>
Screed layer (50mm)	8.00kN/m ²	
Distributed wall load	1.25kN/m ²	
Live load ($\Psi_0=0.4$)	0.50kN/m ²	5.00kN/m ²
Total	<hr/> 9.75kN/m ²	<hr/> 5.00kN/m ²

Resulting load on the walls

With the previous obtained loads it's possible to calculate the distributed line loads. The floors span in the y-direction and depending on the bay, they span 7.20 or 7.80m.

The two walls on line 3 and 5 in Figure 43 bear a floor area with a width of 7.50m. This results in the following values:

- Dead load floors: $9.75\text{kN/m}^2 \cdot 7.50\text{m} = 73.13\text{kN/m}$ ($\Psi_0 = 1.0$)
- Live load ground floor: $5.00\text{kN/m}^2 \cdot 7.50\text{m} = 37.50\text{kN/m}$ ($\Psi_0 = 0.6$)
- Live load install/storage: $5.00\text{kN/m}^2 \cdot 7.50\text{m} = 37.50\text{kN/m}$ ($\Psi_0 = 1.0$)
- Live load dwellings: $1.75\text{kN/m}^2 \cdot 7.50\text{m} = 13.13\text{kN/m}$ ($\Psi_0 = 0.4$)
- Live load panorama: $5.00\text{kN/m}^2 \cdot 7.50\text{m} = 37.50\text{kN/m}$ ($\Psi_0 = 0.4$)

The wall on line 4 of Figure 43 has a smaller floor width of 7.20m. This results in the following line load values:

- Dead load floors: $9.75\text{kN/m}^2 \cdot 7.20\text{m} = 70.20\text{kN/m}$ ($\Psi_0 = 1.0$)
- Live load ground floor: $5.00\text{kN/m}^2 \cdot 7.20\text{m} = 36.00\text{kN/m}$ ($\Psi_0 = 0.6$)
- Live load install/storage: $5.00\text{kN/m}^2 \cdot 7.20\text{m} = 36.00\text{kN/m}$ ($\Psi_0 = 1.0$)
- Live load dwellings: $1.75\text{kN/m}^2 \cdot 7.20\text{m} = 12.60\text{kN/m}$ ($\Psi_0 = 0.4$)
- Live load panorama: $5.00\text{kN/m}^2 \cdot 7.20\text{m} = 36.00\text{kN/m}$ ($\Psi_0 = 0.4$)

Wall B and C of Figure 43 do not support any floors. Due to the connection between the walls in x and y-direction, most of the vertical force is eventually taken up by these two walls. The larger stiffness (500mm versus 400mm) is the main cause of this phenomenon (see section 9.1).

5.2.2 Vertical load from the walls

The stability walls only provide a dead load and this load is calculated by AxisVM itself. For the excel calculations, the line loads are still determined. Depending on the direction, the walls have a thickness of 400 or 500mm. With a volumetric mass of 25kN/m^3 and a height of 3.05m, this results in a line load of 30.50kN/m (400mm) or 38.13kN/m (500mm). Due to the openings in the walls, the load can be multiplied with a reduction factor of 0.9:

- Dead load 400mm wall: $30.50\text{kN/m} \cdot 0.90 = 27.45\text{kN/m}$ ($\Psi_0 = 1.0$)
- Dead load 500mm wall: $38.13\text{kN/m} \cdot 0.90 = 34.31\text{kN/m}$ ($\Psi_0 = 1.0$)

5.2.3 Vertical load from the facade

In the left and right facade of Figure 43 (line 1 and 7), load bearing columns provide support for the floors and the facade. These columns do not contribute to the stability and are therefore not incorporated in the model. The top and bottom facade (line A and D) are supported by the floor and the floor transports the load to the walls.

Based on the current design of Zonneveld ingenieurs, the load bearing facade has a dead load of 5.00kN/m^2 . When this is multiplied by the floor to floor height of 3.05m, a line load of $5.00\text{kN/m}^2 \cdot 3.05\text{m} = 15.25\text{kN/m}$ is obtained.

The non-load bearing facade has a dead load of 3.00kN/m^2 , resulting in a line load of $3.00\text{kN/m}^2 \cdot 3.05\text{m} = 9.15\text{kN/m}$. Through the floor, this load is transferred to the walls and load bearing facade. The line load will slightly spread, but for simplicity the load on the walls and load bearing facade will be assumed as a point load. The two walls on line 3 and 7 in Figure 43 obtain a point load of $9.15\text{kN/m} \cdot 7.50\text{m} = 68.63\text{kN}$. The wall on line 5 obtains a point load of $9.15\text{kN/m} \cdot 7.20\text{m} = 65.88\text{kN}$.

5.3 Horizontal load

Due to the wind, the structure is horizontally loaded. In the literature study a Maple file was created to calculate the exact extreme wind pressure depending on the height and the acceleration due to cyclic wind loading. With a calculation sheet made by TNO for Zonneveld ingenieurs and the extreme pressure table of NEN-EN 1991-1-4 (table NB.4), the Maple file was validated.

To calculate the wind load on the structure, the following equation is used from section 5.3 of NEN-EN 1991-1-4:

$$F_w = c_s c_d * c_f * q_p(z_e) * A_{ref} * n$$

in which:

- $c_s c_d$ is the structural factor for taking into account the effect of wind actions from the non-simultaneous occurrence of peak wind pressures on the surface (c_s) together with the effect of the vibrations of the structure due to turbulence (c_d).
- c_f is the force coefficient for the structure or a structural element.
- $q_p(z_e)$ is the peak velocity pressure at the reference height.
- A_{ref} is the reference area of the surface.
- n is the second order effect of the structure. This is incorporated in the wind load to prevent a non-linear calculation during the first three stages of the design. The estimated second order should be validated at the end with a non-linear calculation.

In appendix B.2 the wind load is calculated for the Zalmhaven tower. With these values, the wind load over the building height can be plotted, see Figure 44. Although the wind load is constructed out of multiple boxes, the logarithmic wind profile is clearly visible.

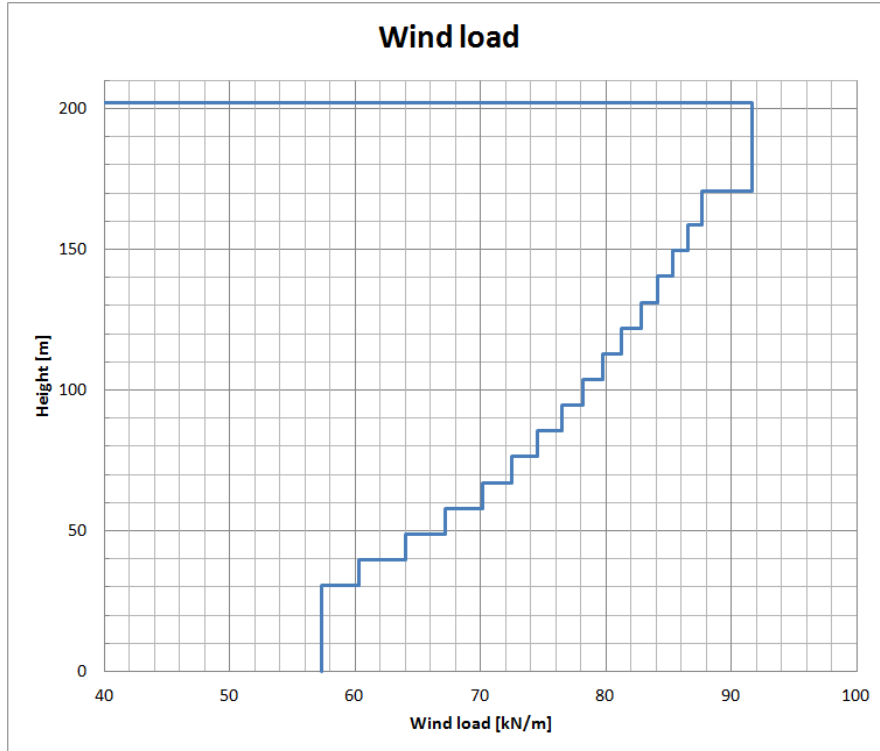


Figure 44 Wind load over the building height

Figure 44 is consistent with Figure 45 from section 7.2.2 from NEN-EN 1991-1-4. For z_{strip} a height of 9.15m (3 storeys) is maintained.

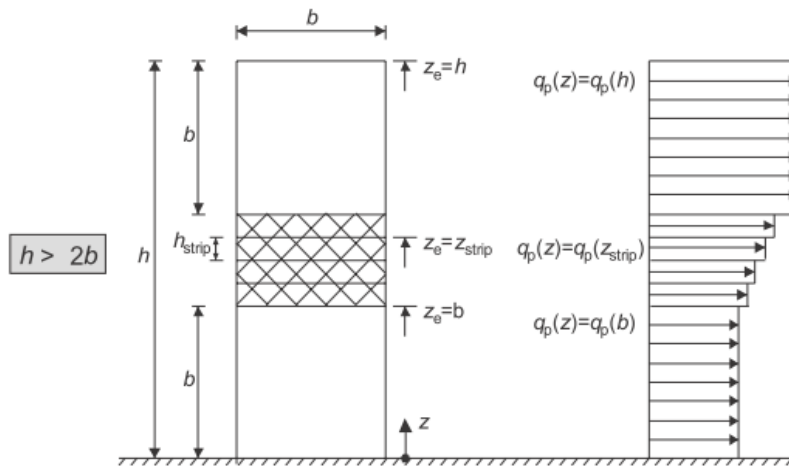


Figure 45 Reference height z_e [NEN-EN, 2011]

In Table 3 the line loads per wall are provided. To calculate the line load from the force per meter height, the following formula is used:

$$q_{\text{wind, line load}} = \frac{F \cdot h_{\text{floor}}}{n \cdot d_{\text{building}}}$$

in which:

- $q_{\text{wind, line load}}$ is the wind line load per wall,
- F is the force per meter height,
- n is the amount of walls in the considered direction,
- d_{building} is the building depth (30m).

Table 3 Wind line load per wall

Area	Height	Force per meter height	Line load x-direction per wall	Line load y-direction per wall
	[m]	[kN/m]	[kN/m]	[kN/m]
1	0-30.5	57.29	2.91	1.94
2	30.5-39.65	60.29	3.06	2.04
3	39.65-48.80	64.01	3.25	2.17
4	48.80-57.95	67.15	3.41	2.28
5	57.95-67.10	70.11	3.56	2.38
6	67.10-76.25	72.44	3.68	2.45
7	76.25-85.40	74.54	3.79	2.53
8	85.40-94.55	76.44	3.89	2.59
9	94.55-103.70	78.16	3.97	2.65
10	103.70-112.85	79.78	4.06	2.70
11	112.85-122.00	81.26	4.13	2.75
12	122.00-131.15	82.78	4.21	2.81
13	131.15-140.30	84.12	4.28	2.85
14	140.30-149.45	85.36	4.34	2.89
15	149.45-158.60	86.50	4.40	2.93
16	158.60-170.80	87.64	4.46	2.97
17	170.80-202.25	91.65	4.66	3.11

5.4 Accidental loads

Preventing accidental loads is far more effective than designing the structure to resist the load. During the literature study many solutions have been examined while performing a risk analyses. Because of the location of the load bearing walls and district heating, collisions and explosions are unlikely to occur. The possibility of an earthquake is also considerably small. Therefore no accidental loads will be taken into account.

5.5 Load cases and load combinations

The previous mentioned loads were discussed separately, but during the lifetime of a building they can be present in combination with other loads. Therefore several load cases and combinations have been designed.

5.5.1 Load cases

The following load cases can be distinguished:

- LC1= Dead load of the structure,
- LC2= Live wind load,
- LC3= Live floor load.

5.5.2 Load combinations

With these three load cases several load combinations can be constructed. In NEN-EN 1990 National Annex the partial factors are provided, shown in Table 4 and Table 5.

Table 4 Partial factors for consequence class 1 and 3 group B [NEN-EN, 2011]

CC	Blijvende en tijdelijke ontwerpsituaties	Blijvende belastingen		Overheersende veranderlijke belasting	Veranderlijke belastingen gelijktijdig met de overheersende	
		Ongunstig	Gunstig		Belangrijkste (indien aanwezig)	Andere
1	(Vgl. 6.10a)	1,2 $G_{k,j,sup}^a$	0,9 $G_{k,j,inf}$		1,35 $\psi_{0,1} Q_{k,1}$	1,35 $\psi_{0,i} Q_{k,i} (i > 1)$
	(Vgl. 6.10b)	1,1 $G_{k,j,sup}^b$	0,9 $G_{k,j,inf}$	1,35 $Q_{k,1}$		1,35 $\psi_{0,i} Q_{k,i} (i > 1)$
3	(Vgl. 6.10a)	1,5 $G_{k,j,sup}^a$	0,9 $G_{k,j,inf}$		1,65 $\psi_{0,1} Q_{k,1}$	1,65 $\psi_{0,i} Q_{k,i} (i > 1)$
	(Vgl. 6.10b)	1,3 $G_{k,j,sup}^b$	0,9 $G_{k,j,inf}$	1,65 $Q_{k,1}$		1,65 $\psi_{0,i} Q_{k,i} (i > 1)$

Table 5 ψ -values for building structures [NEN-EN, 2011]

Belasting	ψ_0	ψ_1	ψ_2
Voorgeschreven belastingen in gebouwen, categorie			
Categorie A: woon- en verblijfsruimtes	0,4	0,5	0,3
Categorie B: kantoorruimtes	0,5	0,5	0,3
Categorie C: bijeenkomstruimtes	0,6/0,4 ^a	0,7	0,6
Categorie D: winkelruimtes	0,4	0,7	0,6
Categorie E: opslagruimtes	1,0	0,9	0,8
Categorie F: verkeersruimte, voertuiggewicht ≤ 30 kN	0,7	0,7	0,6
Categorie G: verkeersruimte ^b , $30 \text{ kN} < \text{voertuiggewicht} \leq 160$ kN	0,7	0,5	0,3
Categorie H: daken	0	0	0
Sneeuwbelasting	0	0,2	0
Belasting door regenwater	0	0	0
Windbelasting	0	0,2	0
Temperatuur (geen brand)	0	0,5	0
^a De waarde 0,6 geldt voor delen van het gebouw die in geval van een calamiteit zwaar kunnen worden belast door een mensenmenigte (vluchtroutes, trappen enz.); de waarde 0,4 geldt in overige gevallen. ^b Met verkeersruimte wordt in dit geval een ruimte bedoeld waar voertuigen kunnen rijden, bijvoorbeeld parkeergarages.			

The following load combinations can be distinguished:

- $SLS1^{12} = 1.0 \cdot G + 1.0 \cdot Q_{k,1} + 1.0 \cdot Q_{k,j} = 1.0 \cdot LC1 + 1.0 \cdot LC2 + 1.0 \cdot LC3$,
- $ULS1^{13} = 1.3 \cdot G + 1.65 \cdot Q_{k,1} + 1.65 \cdot \psi_{0,j} \cdot Q_{k,j} = 1.3 \cdot LC1 + 1.65 \cdot LC2 + 1.65 \cdot \psi_{0,2} \cdot LC3$,
- $ULS2 = 0.9 \cdot G + 1.65 \cdot Q_{k,1} = 0.9 \cdot LC1 + 1.65 \cdot LC2$,
- $ULS3 = 1.5 \cdot G + 0.0 \cdot Q_{k,1} + 1.65 \cdot \psi_{0,1} \cdot Q_{k,1} = 1.5 \cdot LC1 + 0.0 \cdot LC2 + 1.65 \cdot \psi_{0,1} \cdot LC3$.

¹² Serviceability Limit State

¹³ Ultimate Limit State

6 Selection of the FEM program

There are many Finite Element Method (FEM) programs available today that can perform calculations on concrete reinforced structure. But which program is most suited to calculate a 200m prefabricated concrete tower?

The goal of this chapter is to answer the previous question by examining two FEM programs: Scia Engineer and AxisVM. Based on a small experiment, both programs will be examined and one program will be chosen.

This chapter will start with a small description of the FEM programs in section 6.1 and 6.2. Based on a small test, the final program choice will be elaborated in section 6.3. Section 6.4 will end with a conclusion of this chapter.

6.1 Scia Engineer

Scia Engineer is a well-known FEM program in the engineering practice and Zonneveld ingenieurs is one of the companies that use the program. Scia Engineer is capable of calculating steel, timber and concrete structures. The menus are organised and the program is easy to use. Because of this simplicity, advanced possibilities are hidden and several options cannot be changed. For example, the Young's modulus is equal in all three directions and the stiffness of a connection (for example a foundation pile) is equal for tension and compression. If a connection is loaded in tension, the stiffness has to be manually changed. This last shortcoming is very important for prefabricated structures because loading in tension or compression has a very large influence on the stiffness of a joint.

6.2 AxisVM

The second program is AxisVM from Technosoft. This program is less well known in the Netherlands, but this does not reflect the possibilities of the program. Compared to Scia Engineer, the user friendliness is equal, but the program contains more advanced options. With AxisVM it is possible to change the connection to a non-linear connection.

6.3 Final program choice

Only Scia Engineer and AxisVM were taken into account because these two programs are used by one or more supervisors of this thesis. Therefore time was saved during first stages of the modelling process. With both programs a wall was modelled, to compare the results. Model 1 is a monolithic wall and model 2 is a prefabricated wall with an open vertical joint. The results can be seen in Figure 46 and Figure 47.

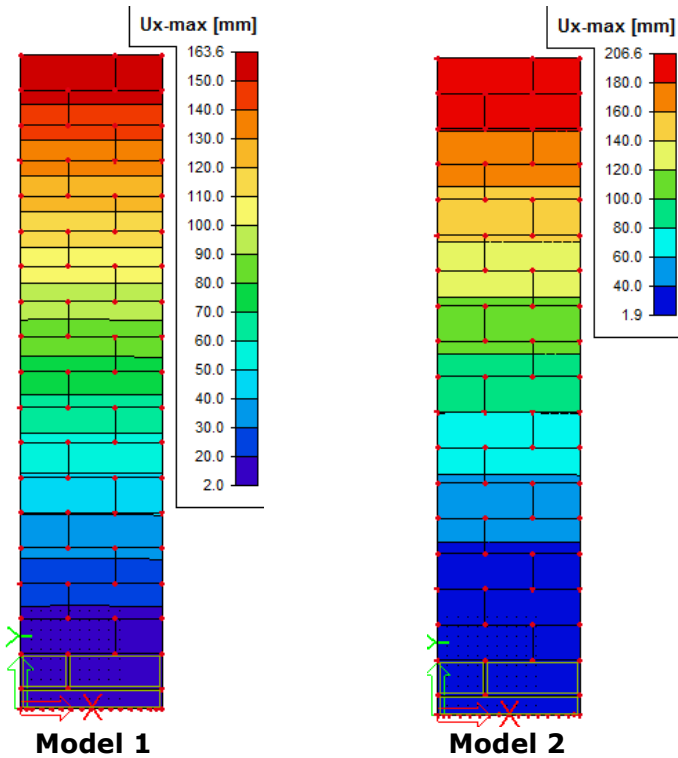


Figure 46 Concrete wall in Scia Engineer

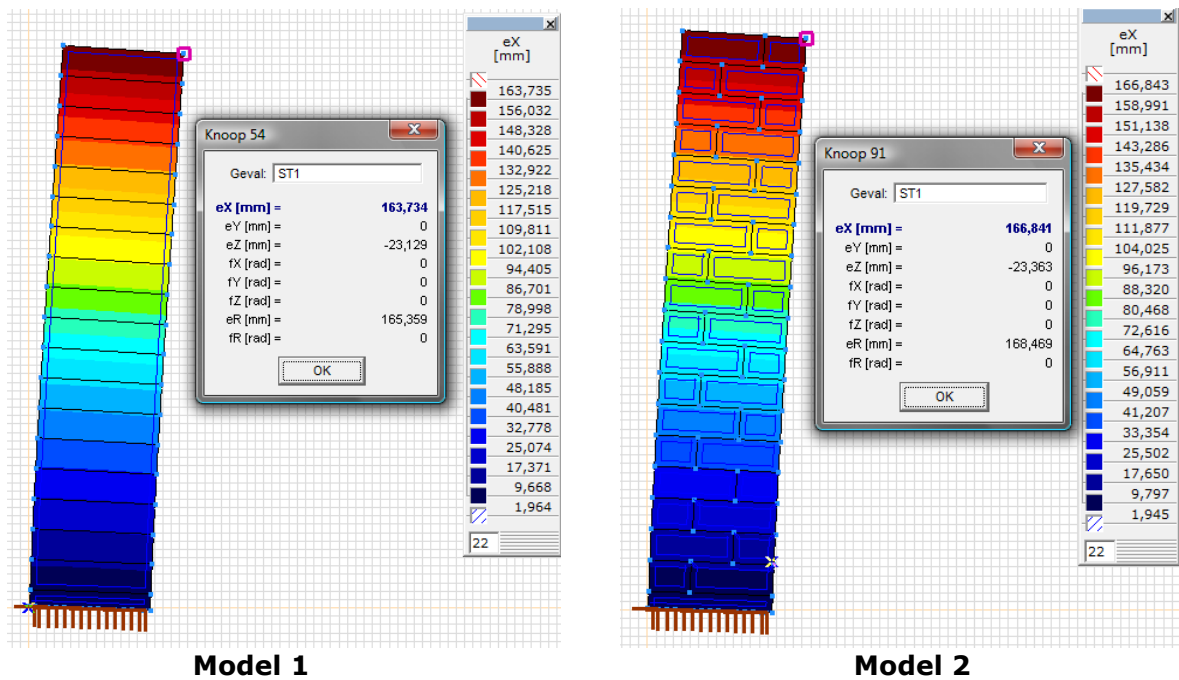


Figure 47 Concrete walls in AxisVM

The difference between the monolithic and precast wall in Scia Engineer is more than 26%. The difference in AxisVM is only 2%. The displacements of the monolithic walls are very close to each other, but the displacements of the precast walls show a large difference. The exact cause of this large difference is unknown. It is likely that the model created in Scia Engineer still contains one or several errors since the values of the AxisVM model are within 0.5% of the reference model (this reference model was created by one of the supervisors of the graduation committee in AxisVM). This 0.5% is likely caused by the difference in mesh size (the mesh size was not given in the calculation example). The likely errors in the Scia Engineer model combined with the higher amount

of freedom in AxisVM (more advanced options) resulted in AxisVM to be the final FEM program.

6.4 Conclusion

AxisVM is chosen as the definitive FEM program because it has more advanced options and it's likely that the Scia Engineer model still contains one or several errors. How the Zalmhaven tower will be modelled in AxisVM will be explained in the next chapter.

7 Modelling in AxisVM

A FEM analysis can be quite cumbersome. Due to all the aspects that have to be entered, the complexity of a three dimensional model increases quickly and mistakes are easily made. Identifying these errors may be rather time consuming due to the black box nature of a FEM analysis.

The goal of this chapter is to obtain a transparent modelling process which is easy to understand and prevents mistakes. To achieve this goal, a model scheme will be introduced. Furthermore a modelling description will be given of how the Zalmhaven tower is schematised in AxisVM.

This chapter will start with the model scheme in section 7.1. A short overview of the model description is provided in section 7.2. In section 7.3 the model description starts with the elements that are used by AxisVM. Section 7.4 and 7.5 continue with the elements properties and the domains. The mesh size is described in section 7.6. How the connections are schematised and the determination of the stiffness is discussed respectively in section 7.7 and 7.8. Consequentially the influence of the floor is discussed in section 7.9. This chapter ends with the application of the loads in section 7.10 and the schematisation of the foundation in section 7.11.

7.1 Model scheme

In order to calculate the deflection, shear forces and many other aspects of a prefabricated high-rise tower, a FEM program has to be used. By immediately entering all the values in a three dimensional (3D) model, it will become difficult to understand the reactions of the structure. Furthermore, errors are difficult to observe since the reactions are unknown. Therefore a model scheme was created to prevent complex models in an early stage. This scheme is shown in Figure 48.

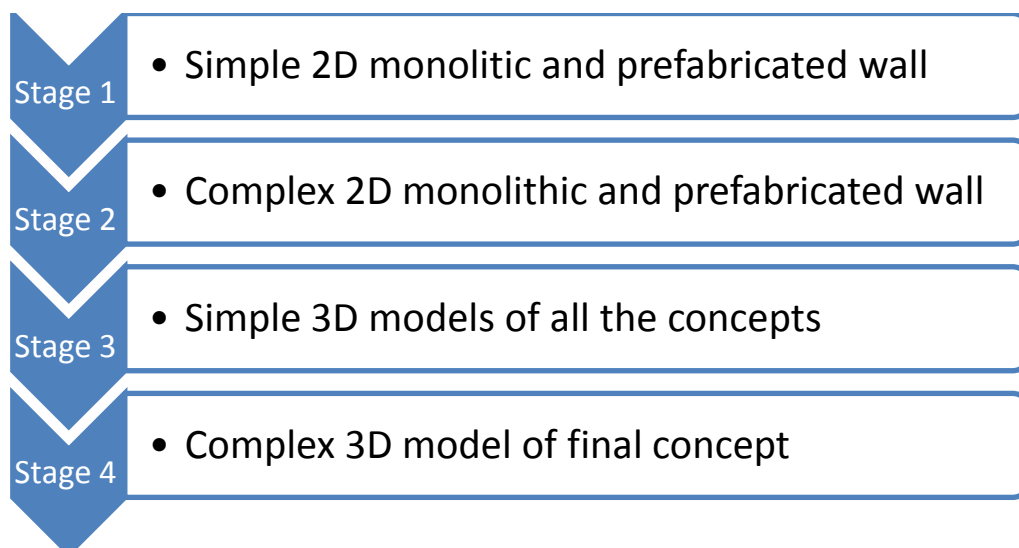


Figure 48 Layout model scheme

During stage 1 two simple 2D models are created: one of a prefabricated wall and the other of a monolithic wall. These models are kept simple to make the reactions and flow of forces evident. The monolithic model is used to compare the differences between the two building methods. There is a gradual transition between stage 1 and stage 2, because the complexity of both models is slowly extended. Door openings, connections for perpendicular wall elements (for example the Staggered Connection, see section 4.3.1) and the foundation are a few aspects that can be applied one at a time. It would become impossible to understand which aspect has the largest effect if all the aspects

are applied at once. Now the behaviour of a prefabricated wall is known, simple 3D models can be made of the structural concepts. By creating a simple 3D model of every concept, it's possible to study the different behaviour of the concepts. After the final concept is chosen, the complexity of this model can gradually be increased. The final 3D model can be used to calculate the total deflection, forces in the elements, the first natural frequency and many other aspects. This final model should accurately approximate the actual behaviour of the Zalmhaven tower.

7.2 Model description overview

In this section a short overview will be given of how the Zalmhaven tower is schematised in AxisVM. Between the parentheses the sections are stated in which a more detailed description is given.

- The models will be calculated with a first order linear analysis. In stage 4 it's possible to use a geometrical non-linear analysis. This non-linear analysis is able to take the second order effects into account and the second order magnification factor used in the previous stages can be checked. During the first three stages the second order effect will be taken into account by multiplying the wind load by a magnification factor.
- The structure will be schematized in stage 1 and 2 with membrane elements in a two-dimensional plane. During stage 3 and 4, shell elements are used in a three-dimensional plane (§7.3).
- For all the walls a concrete quality C90/105 will be used. C90/105 has the following properties: $f_{ck}=90\text{N/mm}^2$, $f_{ctm}=5.0\text{N/mm}^2$, $E_{cm}=44000\text{N/mm}^2$, $E_{cd,uncracked}=29333\text{N/mm}^2$, $\rho=25\text{kN/m}^3$ and $\nu=0.2$. The lintels endure large forces and are likely to be cracked. The cracks reduce the stiffness and therefore $1/3^{\text{rd}}$ of the original stiffness is used: $E_{cd,cracked}=14667\text{N/mm}^2$ (§7.4).
- The lintels have a lower Young's modulus compared to the other parts of the wall element. Therefore it's not possible to use one domain for the entire wall element with lintel. Furthermore, stiffer lintels attract forces. It must be prevented that the forces in the lintel are so large that there is not enough space for the required reinforcement (§7.5).
- The mesh will be automatically generated by AxisVM as triangles. During all the stages, the effect of the mesh size has to be examined. A finer mesh will give more accurate values, but the calculation time will increase (§7.6).
- The connection between the elements will be defined as an edge hinge. The horizontal connection will have a normal and shear stiffness. The normal stiffness is equal to the surrounding concrete and the shear stiffness is determined by the normal force. For the vertical connection, an open joint is used and therefore the connection has no stiffness (§7.7 and §7.8).
- The dowel action of the floors will not be taken into account because the dowels aren't present at the structure (§7.9).
- To calculate the realistic forces in the load bearing walls, the floors have to be removed in the 3D models. Because of the large thickness, the floors have a stiffness that is comparable to the wall elements. The FEM program will distribute the forces over the floors and walls (large effective width), but in reality, the floors do not contribute. To prevent the walls from buckling, struts or sliding hinges can be used were the floor used to be (§7.9).
- The horizontal load is divided over the structural walls as a line load per floor. This distribution is due to the load introduction of the floor slabs (diaphragm action). The vertical load is also divided over the entire stability structure as a line load per floor (§7.10).
- Due to simplifications, only the foundation under the load bearing walls is modelled (§7.11).

7.3 Element schematisation

In AxisVM four different surface elements can be modelled:

- membrane with plane stress,
- membrane with plane strain,
- plate,
- shell.

For all the elements it's estimated that the displacements are small. The variation of internal forces within an element can be regarded as linear.

7.3.1 Membrane elements

Membrane elements are used to model 2D structures that are dominated by in-plane membrane forces and out of plane bending moments are discarded. To achieve this, finite Serendipity elements with eight nodes are used. The internal membrane forces are given by: n_x , n_y , n_{xy} , n_1 , n_2 and q_n .

AxisVM is based on triangular finite elements (see section 7.6.1) and the 2D 8-node Serendipity elements are commonly used in FEM programs to represent the 2D quadrangle shapes. To resolve this difference, the Serendipity elements have been adjusted. In a few programs it's possible to use a 2D 9-node Lagrange element (for example DIANA). In Figure 49 the Lagrangian and Serendipity element schematisations are shown. As long as the mesh elements remain square or rectangular, the Serendipity and Lagrangian elements can exactly determine linear or quadratic displacement fields. If they only have an angular distortion, a difference will occur between the two elements. The 9-node Lagrangian can still exactly represent a quadratic displacement field, while the 8-node Serendipity element cannot (only the linear displacement field remains exact). If the mesh elements are distorted beyond just angular distortion (curved sides for example) neither of them can exactly represent quadratic displacements. As long as the mesh elements aren't curved, it appears that the Lagrangian schematisation is the best solution. Unfortunately the additional 9th node results in a considerable increase of equations and calculation time.

Since the membrane forces are dominated by in-plane membrane forces and out of plane bending moments are discarded, the curvature of the mesh element can be neglected. Although the rotations are considered to be small in AxisVM, the Serendipity element may not provide accurate results for quadratic polynomials (a mathematical expression of variables with a finite length). Because the 2D triangular mesh elements result in a linear displacement field, the Serendipity element configurations was chosen because of its reduced calculation time.

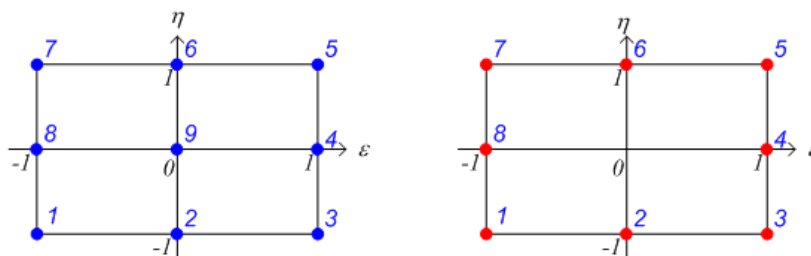


Figure 49 Lagrangian (left) and Serendipity (right) element schematisation [Knight, 2012]

7.3.2 Plate elements

Plate elements may be used to model 2D structures whose behaviour is dominated by flexural effects. The plate elements incorporate flexural (plate) behaviour only; the in-plane behaviour is not taken into account. This behaviour is obtained by a 9-node Heterosis finite element which is based on the Mindlin-Reissner plate theory (this allows for transverse shear deformation effects). The plate element is suitable for modelling thin and thick plates. The internal plate forces are given by: m_x , m_y , m_{xy} , v_x , v_y , m_1 , m_2 and q_m .

Instead of the 9-node Heterosis element, also the 8-node Serendipity and 9-node Lagrangian element could be used to model a plate. However, a plate element is dominated by flexural effects and they are both unable to present exact results in this case. The Heterosis element, based on the Mindlin-Reissner plate theory, is capable of presenting exact results.

Besides the Mindlin-Reissner plate theory, many FEM programs also provide the Kirchhoff plate theory. The Kirchhoff theory is designed for thin plates and incorporates deformations due to moments. Deformations due to shear force are neglected. Due to the introduction of computers, the more complicated Mindlin-Reissner plate theory for thick plates became applicable. This theory does incorporate deformations due to shear force besides the bending moment deformations. Aside from thick plates, the theory also holds for thin plates.

7.3.3 Shell elements

Shell elements can be used to model structures with behaviour that is dependent upon both in-plane (membrane) and flexural (plate) effects. The shell element consists of a superimposed membrane and plate element to incorporate the combined behaviour. Therefore the element can be loaded in-plane or perpendicular to its plane. The internal membrane forces are given by: n_x , n_y , n_{xy} , n_1 , n_2 and q_n . The internal plate forces are given by: m_x , m_y , m_{xy} , v_x , v_y , m_1 , m_2 and q_m .

7.3.4 Linear and non-linear calculations

The linear calculation method in AxisVM is based on the assumption that the displacements occurring are very small and that the equilibrium may be formulated using the undeformed system as an approximation.

The non-linear calculations are based on the Newton-Raphson theory. This theory is very efficient (quadratic convergence) and can be applied when there are large second order effects.

7.3.5 Applied elements

During stage 1 and 2 of the model scheme membranes with plane stress will be used for the 2D walls. Since all the out of plane forces are discarded by the membrane elements, a shell element will be used for the 3d models (stage 3 and 5 of the model scheme). In stage 1, 2 and 3 a linear calculations will be used. In stage 4 it's possible to apply a non-linear calculation.

7.4 Material properties

In the original design by Zonneveld ingenieurs a concrete strength class of C53/65 was used with a Young's modulus of $E_{cm}=38000\text{N/mm}^2$. The design was eventually calculated with a smeared Young's modulus of 20000N/mm^2 . The transition of cast in situ concrete

to precast concrete in this thesis results in a lower stiffness of the structure. By applying High Strength Concrete this reduction of stiffness may be counteracted and the literature study has shown that it's possible to achieve a cost reduction when applied properly. Therefore the concrete class C90/105 will be applied at the Zalmhaven tower. The concrete class C90/105 has the following properties:

$$f_{ck}=90\text{N/mm}^2, f_{ctm}=5.0\text{N/mm}^2, E_{cm}=44000\text{N/mm}^2, \rho=25\text{kN/m}^3 \text{ and } \nu=0.2.$$

Due to creep and shrinkage the full Young's modulus may not be used for uncracked concrete. Calculating the actual Young's modulus is very complex due to the dependency on other aspects and the interrelations. To prevent complex and time consuming calculations, a well proven rule of thumb is used in practice¹⁴:

$$E_{cd,uncracked}=E_{cm}/1.5$$

$$E_{cd,cracked}=E_{cm}/3$$

The Young's modulus of uncracked concrete is divided by 1.5 to take creep into account. The cracked concrete is divided by 3 since cracking reduces the stiffness of the concrete.

Due to the high dead load of the structure, the walls will always be under compression. On the other hand, the lintels will likely crack as a result of the large bending moments that occur near the wall openings. After the first structural calculations are completed, it should be examined if the applied cracked Young's modulus of 14667N/mm^2 still remains feasible. This is an important monitoring step since a lintel with a higher Young's modulus will attract more forces requiring more reinforcement. But the thin lintel has only a limited capacity for reinforcement bars. In Table 6 an overview of the used concrete classes in combination with the Young's modulus are depicted.

Table 6 Concrete classes used in the structure

Element	Concrete class	Uncracked Young's modulus	Cracked Young's modulus
	[-]	[N/mm ²]	[N/mm ²]
Floors	C53/65	25333	12667
Walls X-direction	C90/105	29333	14667
Walls Y-direction	C90/105	29333	14667
Load bearing columns	C90/105	29333	14667
Diaphragm walls (cast in situ)	C35/45	20000 ¹⁵	20000 ²
Foundation slab (cast in situ)	C35/45	20000 ²	20000 ²

For the reinforcing steel B500B will be used with a Young's modulus of 200000N/mm^2 and a yield strength of $f_{yd}=500/1.15=435\text{N/mm}^2$.

Several techniques can be used to optimise the cost of the structural walls. An example is to reduce the width of the walls at a certain height (this is also applied at the current design of Zonneveld ingenieurs). Due to repetition two other methods are more preferred: reducing the reinforcement ratio and using a lower concrete strength class. During the design, these optimisations will not be taken into account. After the design, there may be room for optimisation.

¹⁴ This method is also used by the book CB2 (Constructieer Gewapend Beton), based on Eurocode 2.

¹⁵ This Young's modulus value is a smeared value and it's assumed that there is no difference between cracked and uncracked concrete.

7.5 Domain

When a structure is modelled in a FEM program, domains are used for separate structural elements. For example, a single floor slab, wall element or column may be represented by one domain. With the help of a domain, several properties can be allocated to the element. For example the surface element type (membrane, plate or shell), the material properties (C50/60 or C90/105) and thickness.

If a monolithic structure is modelled, the entire structure should be made with one domain since there are no joints or connections¹⁶. Because of practical reasons (constructing the model), it may be more convenient to use multiple domains in a monolithic model. But do the multiple domains influence the structural properties? To answer this question, three structures are modelled in appendix C.1. The first structure contains a domain for every wall element and between these elements interface elements are applied. The second structure is also modelled with a domain for every wall element, but there are no interface elements. Without the interface elements, AxisVM automatically connects the domains to each other. The third structure is composed out of one domain element, representing a wall that was casted in a continues process.

When the results are compared it can be concluded that there is a difference between a monolithic structure composed out of one domain and a monolithic structure with multiple domains (with or without interface elements). Since the differences are relatively small, it's acceptable to use multiple domains or multiple domains with interface elements for a monolithic structure. To obtain monolithic results with interface elements, a stiffness equal or larger than $k_x=k_y=1*10^{10}$ kN/m/m is required. By using a high stiffness, the interface elements become very stiff. This high stiffness makes the interface elements obsolete and values are obtained which are comparable to model 2 (no interface element, resulting in an infinite stiffness between the two elements). When the actual normal stiffness and a very high shear stiffness are entered in the first model ($k_y=7.33*10^8$ kN/m/m and $k_x=1*10^{10}$ kN/m/m), the differences become larger between model 1 and model 2 and 3. This is unexpected because the normal stiffness is based on the stiffness of the surrounding concrete (see section 7.8) and this should provide monolithic values. It can be concluded that the lower stiffness in combination with the interface elements provide too much deformation in the connections. Because these differences are smaller than 0.5% (660% larger than the largest difference calculated with $k_x=k_y=1*10^{10}$ kN/m/m, see Table 32), this less stiff behaviour is neglected.

Due to the large moments near the openings in the walls, the lintels are likely cracked. Therefore the stiffness has to be reduced. In one domain it's impossible to specify multiple strength properties and as a result three domains have to be used to model one wall section. This is illustrated in Figure 50. Since the three domains are connected without interface elements, the connection will behave monolithic; as if there was no connection.

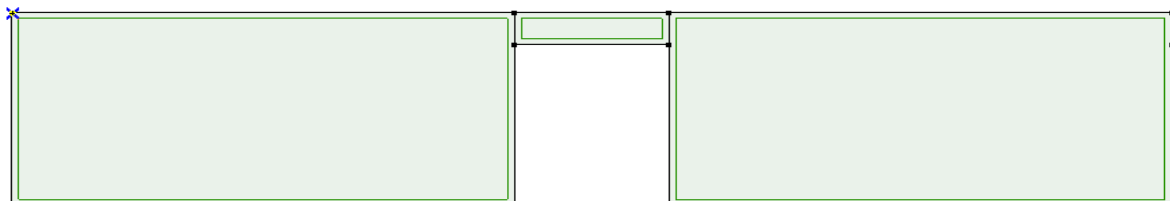


Figure 50 Three domains

¹⁶ There may be connections visible in the concrete due to the casting sequence, but these connections have a strength that approximates the surrounding concrete and are therefore not considered as a real connection.

7.6 Mesh size

The mesh size is one of the important factors that determine the accuracy of the calculations. A large mesh size will result in a short calculation time but it may not provide accurate calculation results. On the other hand, a small mesh size will provide more accurate results, but this is accompanied by a long calculation time. Therefore it's of great importance to know what mesh size will result in an optimum between these two extremes. This optimum has to be determined for a 2D and 3D model.

7.6.1 Mesh generation

The mesh is automatically generated by AxisVM 10 and only consists out of triangles. In AxisVM 11 it's also possible to use quadrangle or a combination of triangle and quadrangle mesh elements, but this does not affect the results. When a 3D model is meshed, the triangle (2D) mesh elements remain. This is because the elements in the 3D model don't have a physical thickness; the 3D model consists out of flat elements. To incorporate the 3D behaviour, the amount of DOF's (degrees of freedom) in the mesh nodes are increased. This assures that mesh elements at a perpendicular connection interact. As a result of the increased amount of DOF's, the mesh generation and calculation time will also increase considerably.

7.6.2 Size of the mesh

To determine which mesh size provides the best results, a mesh analysis with four parts will be performed. In part 1 till 3, three different methods are examined to mesh a 2D structure. First a uniform mesh size will be used for the entire structure. The size of the mesh is the only variable and will be reduced in several steps. In the second part, the mesh size will be reduced locally (only the lintels) and in the third part of this analysis, the mesh size will have a different size according to the height. Based on these results, an optimal mesh size will be determined for a 3D structure in part 4.

In appendix C.2 the results are displayed of the previous four parts. It can be concluded that a mesh size according to the height provides the most accurate results in a 2D structure. Unfortunately, the program has a limited memory capacity and the smallest mesh size that can be analysed is 250mm for the bottom ($1/3^{\text{rd}}$ of the total height) and 500mm for the top (the remaining $2/3^{\text{rd}}$ of the total height). When a mesh size of 250mm at the bottom and 750mm at the top is used, the calculation time is reduced by 34% while the results only differ 0.1%.

A mesh size of 250mm at the bottom and 750mm at the top are too small for a 3D model. The smallest mesh size that can be applied is 750mm at the bottom ($1/4^{\text{th}}$ of the building height) and 1500mm at the top ($3/4^{\text{th}}$ of the building height). But this mesh size is too large to provide accurate local results. Therefore the mesh size will be reduced to 250mm around the considered element. This method is applicable since the local distribution of forces is highly dependent on the mesh size while the global distribution of forces is only slightly dependant.

An entire structural wall was used for this analysis and the smallest mesh size which was examined was 250mm. A smaller mesh size couldn't be analysed because this resulted in a memory problem. Therefore it's unknown if the results converge even more at lower mesh values. Therefore it's recommended to perform the mesh analysis only on a section of the entire model. With these result, the optimal mesh size can be determined without any memory problems.

7.7 Schematisation of the connections

The connections are a considerable aspect of precast structures: they are the difference between a nearly monolithic structure and several individual structures. Defining the properties and schematising the connections is therefore an important aspect of this thesis. In this section it will be elaborated how the connections are entered in AxisVM. In section 7.8, the stiffness of the connections will be determined.

The connections in AxisVM are modelled by interface elements (called "edge hinge" in the program). By placing an interface element between two different domains, the monolithic connection automatically created by AxisVM is prevented. By using an interface element, six different properties can be specified: the stiffness and rotation stiffness in the local x, y and z-direction: k_x represents the shear stiffness, k_y represents the normal stiffness and k_z is the out of plane shear stiffness (only required in a 3D structure). The rotation stiffness of the connection isn't used in this thesis (k_{xx} , k_{yy} , k_{zz}). The unit of the shear and normal stiffness is kN/m/m, a stiffness per meter of connection. In Figure 51, an example is given of a connection between two precast elements.

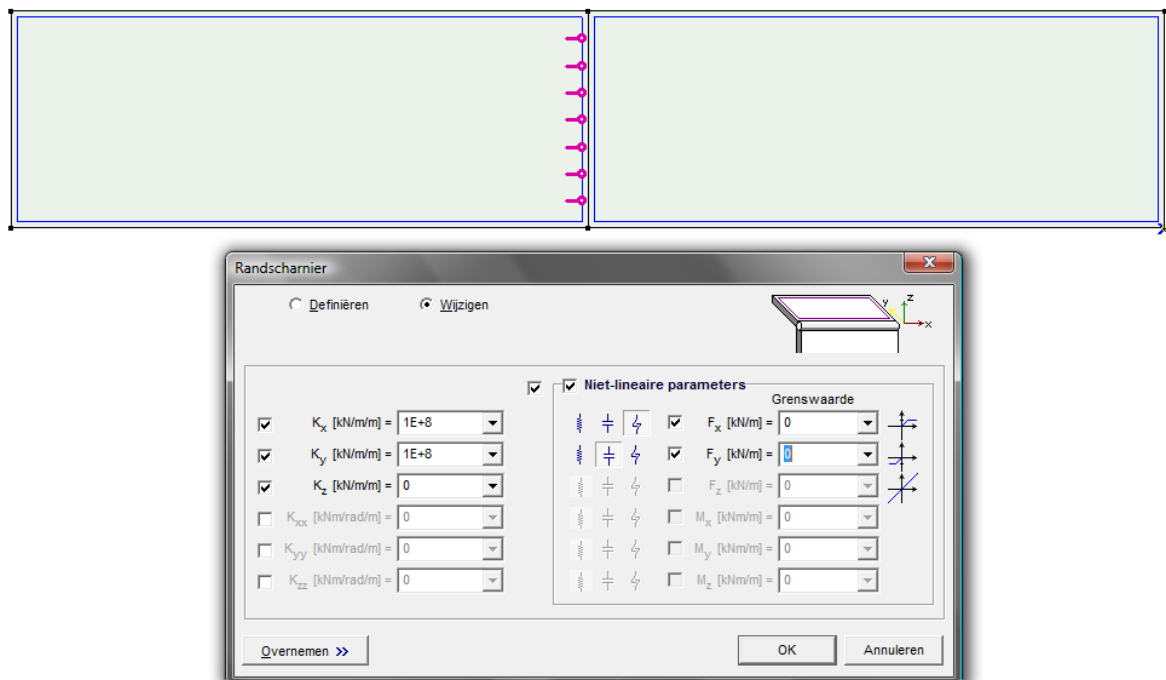


Figure 51 Connection between two domains

In Figure 51, it's clearly visible how the interface element is located at the left domain. The interface element can also be placed in the right domain and unfortunately the location of the interface element has a small influence on the results. This influence will be encountered in section 9.1. Besides this, it can also be noted that the connection has no physical thickness in the model. An important aspect of the connection is the behaviour under tension and compression. Besides the stiffness, non-linear parameters can be defined. For example: the stiffness is equal for compression and tension. When the second box is chosen, the stiffness only holds for compression and when the entered resistance is exceeded, the resistance reduces to 0kN/m/m. The third box is identical, but than for tension. Unfortunately it's impossible to specify a different reduced resistance than 0kN/m/m.

In section 2.2 four different connections were mentioned. The open vertical joint and the grouted starter bar connection can be modelled with the previous mentioned edge hinges. In section 7.9 it will be explained why the floors aren't incorporated in the model.

For the fourth connection (Interlocking Halfway Connection (IHC) or Staggered Connection (SC)), the modelling properties of the edge hinge are insufficient. In Figure 52 it can be observed that both connections have a small area where the two crossing walls connect. The IHC has two of these areas and the SC only one. To model this connection, a spring with a stiffness in three directions is used. To prevent large peak forces around this spring, two stiff bars are added. In Figure 53 an example is depicted of this connection.

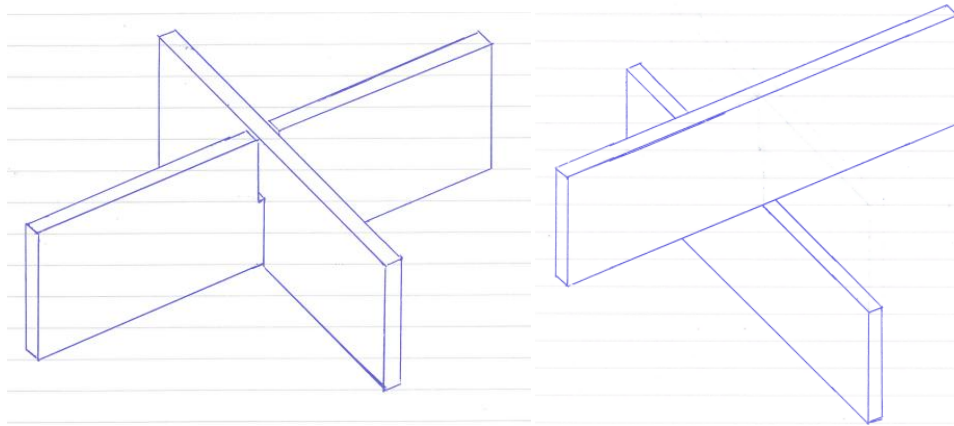


Figure 52 IHC (left) and SC (right)

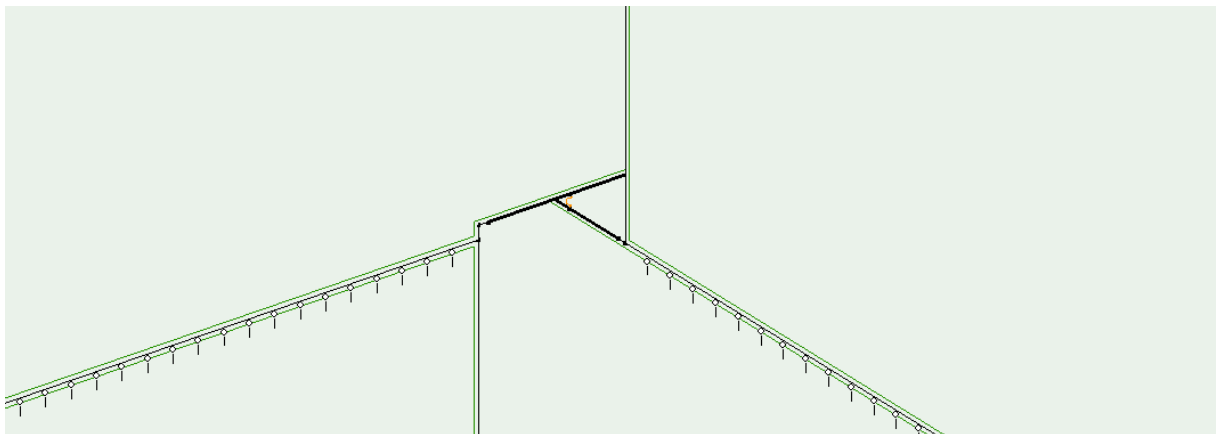


Figure 53 3D connection between the walls

7.8 Determining the connection stiffness

The stiffness of a precast connection depends on the location and orientation. Within a single connection, there are also large differences between the normal and shear stiffness. In this section it will be explained how the different stiffness are determined.

7.8.1 Monolithic structures

As mentioned in section 7.5, there are three different methods to model a monolithic structure: use a domain for every element with interface elements, use a domain for every element without interface elements or use one domain for the entire structure. With the last two methods no stiffness is required. To obtain monolithic results with the interface elements, a stiffness of $k_x=k_y=k_z=1 \cdot 10^{10}$ kN/m/m is required.

7.8.2 Normal stiffness of a horizontal precast connection (k_y)

During the literature study two variants have been analysed for the horizontal connection: a wet reinforced connection and dry connection. The dry connection is uncommon in buildings industry due to the reduced stiffness, possible element splitting and the high level of accuracy that is required. The grouted starter bar connection is far more common and is capable of transporting tensile forces. Several factors determine the strength of this wet connection [Falger, 2004]:

- strength of the mortar,
- degree of filling,
- thickness of the connection,
- reinforcement ratio,
- strength of the surrounding concrete,
- location of the connection (confined or not).

In a parametric study performed by BFBN [Bennenk, chapter 8] it's concluded that the compression capacity mainly depends on the degree of filling and the strength class of the surrounding concrete. The strength class of the mortar is less important. For tension, the reinforcement ratio is the only important factor since there is no adhesion.

When the connection is created with a thixotropic k90 mortar and the previous aspects are taken into consideration, a compression stiffness equal to the surrounding concrete may be assumed. This assumption is based on the following equation (the entire derivation of this assumption is provided in appendix C.3.2):

$$k = \frac{A \cdot E}{L} \text{ [N/mm]}$$

in which:

- k is the stiffness of the connection
- A is the considered area
- E is the Young's modulus of the mortar
- L is the thickness of the connection.

When the stiffness is determined for a certain area and a connection thickness of 1mm is taken into account the equation can be rewritten to:

$$k = \frac{A \cdot E}{L} = \frac{A \cdot E}{A \cdot 1} = E \text{ [N/mm}^3\text{]}$$

When the actual connection thickness (20mm) is taken into consideration, the stiffness value will be reduced, but with the serial spring equation it can be proven that the stiffness of the connection will remain identical to the wall. For this example an area of $A=500 \cdot 1000\text{mm}^2$, a Young's modulus of $E=2933\text{N/mm}^2$, a connection thickness of 20mm and a wall height of 3030mm will be used (total height is 3050mm).

The equation for serial springs is given by:

$$\frac{1}{k} = \frac{1}{k_1} + \frac{1}{k_2}$$

The three different values for the stiffness are:

$$k_1 = \frac{E \cdot A}{L} = \frac{29333 \cdot 500 \cdot 1000}{20} = 7.33 \cdot 10^8 \text{ [kN/m/m]}$$

$$k_2 = \frac{E \cdot A}{L} = \frac{29333 \cdot 500 \cdot 1000}{3030} = 4.84 \cdot 10^6 \text{ [kN/m/m]}$$

$$k_3 = \frac{E \cdot A}{L} = \frac{29333 \cdot 500 \cdot 1000}{3050} = 4.81 \cdot 10^6 \text{ [kN/m/m]}$$

$$k_{\text{actual}} = \frac{1}{\frac{1}{k_1} + \frac{1}{k_2}} = \frac{1}{\frac{1}{7.33 \cdot 10^8} + \frac{1}{4.84 \cdot 10^6}} = 4.81 \cdot 10^6 \text{ [kN/m/m]}$$

k_{actual} is identical to k_3 , ensuring that the connection stiffness is identical to the surrounding concrete. The entire derivation of the normal stiffness can be found in appendix C.3.2.

Under tension, the stiffness of the connection reduces considerably since the lack of adhesion prevents the mortar to transfer any tensile forces. Due to the high dead load of the concrete tower, no tensile stresses occur in the connections. Therefore no tensile stiffness is required for the horizontal connection. In Table 7 and Table 8 an overview is given of the stiffness values of the connections.

7.8.3 Shear stiffness of a horizontal precast connection (k_x)

Aside from a normal force, the horizontal connection also endures a shear force. Compared to traditional precast structure, the masonry configuration results in local higher shear forces because the open vertical joint cannot transfer any normal force. This aspect will be examined in more detail in section 9.1. The resistance of the connection depends on five mechanisms:

1. Adhesion between the mortar and prefab element
2. Friction between the mortar and prefab element
3. Dowel action of the starter bars
4. Pull out of the starter bars
5. Normal force in the connection.

In contrast to the compression stiffness of the horizontal connection the shear resistance will be lower than the surrounding concrete. The smooth surface of the precast elements is the main cause of this reduction: there is little or no adhesion and mechanism 1 is removed. When the connection is loaded in tension, also mechanism 2 will be equal to zero.

To determine the shear resistance, Eurocode NEN-EN 1992-1-1, section 6.2.5 can be used:

$$V_{Rdi} = c f_{ctd} + \mu \sigma_n + \rho f_{yd} (\mu \sin(\alpha) + \cos(\alpha)) \leq 0,5 v f_{cd}$$

In which:

V_{Rdi}	is the design shear resistance at the interface
c and μ	are factors depending on the interface (for smooth: $c=0,2$ and $\mu=0,6$)
f_{ctd}	is the design tensile strength of the concrete
σ_n	is the normal stress in the joint that can coincide with shear force, positive for pressure, whereby $\sigma_n < 0,6 f_{cd}$ and negative for tension. It's advised to use $c f_{ctd} = 0$ when σ_n is in tension.
ρ	is the area of the protruding bars divided by the connection area: A_s/A_i
α	is the angle of the reinforcement (see Figure 54)
v	is the stiffness reduction factor:

$$v = 0,6 \left[1 - \frac{f_{ck}}{250} \right]$$

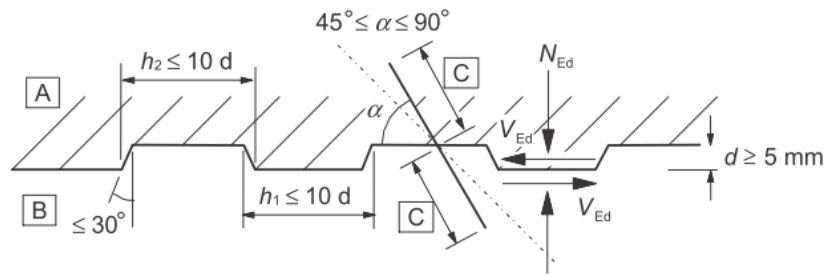


Figure 54 Shear resistance of a horizontal connection [NEN-EN, 2011]

The first part of the shear resistance formula takes the adhesion into account. Because the concrete elements have a smooth surface, $c \cdot f_{ctd}$ becomes equal to zero. The second part is responsible for the normal stress. In case the connection is loaded in tension, this value also becomes equal to zero. The third part is the contribution of the reinforcement (mechanism 3 and 4).

When a connection is loaded in compression and contains starter bars ($\alpha=90^\circ$), the formula can be rewritten as:

$$V_{Rdi} = \mu \sigma_n + \mu \rho f_{yd} \leq 0,5 v f_{cd}$$

Besides the reduced resistance, the shear resistance is also more difficult to determine as it depends on the normal stress in the connection (σ_n): v_{Rdi} will change over the height and the width of the structure. Therefore an iterative calculation is required to determine the resistance exactly. First an estimated resistance has to be used to determine the stiffness. Based on the results, the normal force distribution can be determined. According to this distribution, the new shear resistance can be determined, resulting in a new stiffness. This process has to be continued until there is no perceptible difference. In section 8.1 this aspect will be discussed in more detail.

With the obtained shear resistance, the shear stiffness can be determined. Research of Straman [Straman, 1988] has shown that there is a linear relation between the shear resistance and the deformation:

$$k_u = \frac{V_{Rdi}}{\delta_u} \text{ [N/mm}^3\text{]}$$

in which:

- k_u is the shear stiffness
- V_{Rdi} is the shear resistance
- δ is the deformation, also known as slip.

Although this research was performed on vertical connections, the mechanism remains equal. Tests done in this research show that the connection will fail at a deformation of approximately 1mm. But according to Figure 55 the relation shouldn't be linear but bi-linear. At first, the mortar and concrete are still connected to each other and the stiffness is relatively high. At a certain deformation the connection is lost and the stiffness is reduced.

In consultation with two of the supervisors (dr.ir.drs. C.R. Braam and ir. D.C. van Keulen) this certain deformation is placed at $\delta_{u,1}=0.4\text{mm}$. At the moment there is no literature available that supports this assumption, but preliminary research shows that this assumption is reasonable.

An important question remains, when is the deformation of 0.4mm exceeded? In this thesis it will be assumed that during the SLS the deformations are within this boundary (the third diagram of Figure 55). In the ULS, this value is likely exceeded and a deformation of 1.0mm will be used to determine the shear stiffness (the second diagram of Figure 55). The difference in behaviour is clearly visible in Figure 55: in the SLS a considerable larger k_x may be applied.

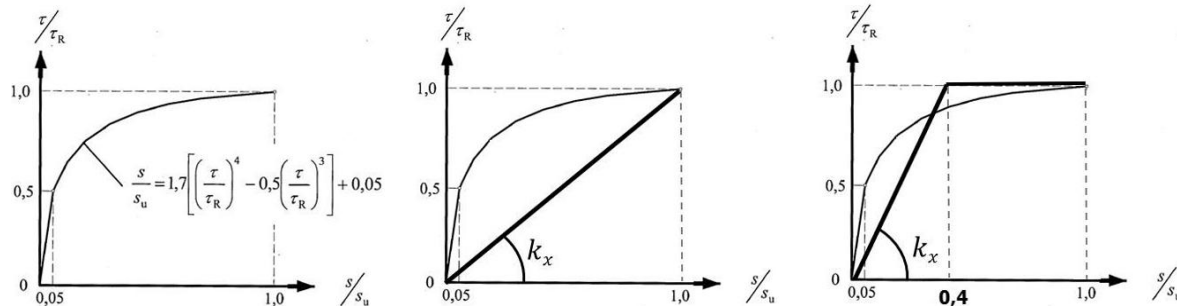


Figure 55 Relation between shear resistance and deformation [Keulen, 2012]

Using a deformation of 0.4mm results in a considerable higher shear stiffness in SLS, but due to the high stiffness of the surrounding concrete elements this will only have a small influence (see section 8.1). It's possible to incorporate the bi-linear behaviour in AxisVM (see section 6.2), but the calculation time will increase considerably. Therefore the values will be manually adapted in SLS.

The shear stiffness calculation can be found in appendix C.3.3. In Table 7 the shear stiffness values are depicted.

7.8.4 Normal and shear stiffness of the vertical connection (k_y and k_x)

For the vertical connection between parallel walls the masonry configuration with an open vertical joint provides the most benefits. The open joint doesn't fulfil any structural properties and the forces that would normally be present in this connection have to be transported via a different mechanism. This mechanism is provided by the masonry configuration: the vertical shear force is transported to the over or underlying elements by a minimal overlap of the elements. The normal force that was present in the vertical connection is now transported as shear by the horizontal connection.

In AxisVM it's possible to enter a stiffness of 0kN/m/m for the connection. As a result, the connection will behave as an open vertical joint. The physical opening of 20 or 30mm isn't present in the model. Eventually the open vertical joint will be closed with a non-structural material because of the building physics and fire hazards.

7.8.5 Normal and shear stiffness of the connection between perpendicular walls

The staggered or interlocking halfway connection (see section 4.3.1) between perpendicular walls has a stiffness equal to the surrounding concrete when loaded with compression. The same method as with the horizontal connection between parallel walls of section 7.8.2 is used. The results are depicted in Table 9. Due to the behaviour of this connection, tension forces also occur. These tension forces are only encountered at the top of the structure due to the low dead load. Unfortunately, under tension the normal stiffness of the connection is reduced considerably. This is because the forces are now only transferred by the reinforcement (there's no adhesion between the mortar and the precast element). As a result, the steel elongates. If an elongation length equal to the connection thickness is assumed, a very high stiffness is obtained. But in reality, the elongation length will be larger than just the connection thickness. To calculate the actual

stiffness under tension, fib Bulletin number 43 is used. The results of this calculation are shown in Table 10.

The calculation of the shear stiffness is almost identical to section 7.8.3. The only difference is that the stiffness is not calculated per meter but for the connection area. Just as the normal stiffness, shear stiffness is also reduced by tension. From formula (5.5), only the reinforcement term remains. Due to the high reinforcement ratio, the reduction is relatively small (11%).

The calculation of the normal and shear stiffness between perpendicular walls can be found in appendix C.3.4 and C.3.5.

7.8.6 Stiffness values applied in this thesis

In Table 7 until Table 10 the stiffness values applied in this thesis are depicted. In appendix C.3 the underlying calculation values are provided.

Table 7 Stiffness parameters horizontal connection

Wall thickness	Normal comp. stiffness $k_{y,c}$	Normal tension stiffness $k_{y,t}$	Shear comp. stiffness (s=1) $k_{x,c}$	Shear comp. stiffness (s=0.4) $k_{x,c}$	Shear tension stiffness $k_{x,t}$
[mm]	[kN/m/m]	[kN/m/m]	[kN/m/m]	[kN/m/m]	[kN/m/m]
400	$5.87 \cdot 10^8$	Not applicable	$4.61 \cdot 10^6$	$1.15 \cdot 10^7$	Not applicable
500	$7.33 \cdot 10^8$	Not applicable	$5.76 \cdot 10^6$	$1.44 \cdot 10^7$	Not applicable

Table 8 Shear stiffness base on different normal stress values, $\delta=1.0\text{mm}$ and $t=500\text{mm}$

Average normal stress σ_{aver}	Calculation value normal stress σ_{calc}	Shear stiffness k_x
[N/mm ²]	[N/mm ²]	[N/mm ²]
0-5	2.5	$1.39 \cdot 10^6$
>5-10	7.5	$2.89 \cdot 10^6$
>10-20	15	$5.14 \cdot 10^6$
>20-30	25*	$5.76 \cdot 10^{6**}$

* This value is limited at 17.1N/mm^2 due to a shear limit, see section 8.1.3.

** Maximum shear stiffness due to shear limit at 17.1N/mm^2 .

Table 9 Normal stiffness of connection between perpendicular walls

Wall thickness	Compression normal stiffness $k_{v,s,c}$	Tension normal stiffness $k_{v,s,t}$
[mm]	[kN/m]	[kN/m]
400	$2.93 \cdot 10^8$	$4.01 \cdot 10^6$
500	$2.93 \cdot 10^8$	$4.01 \cdot 10^6$

Table 10 Shear stiffness of connection between perpendicular walls $k_{x,s}$

Wall thickness	Compression shear stiffness $k_{x,s,c}$ (s=1)	Compression shear stiffness $k_{x,s,c}$ (s=0.4)	Tension shear stiffness $k_{x,s,t}$ (s=1)	Tension shear stiffness $k_{x,s,t}$ (s=0.4)
[mm]	[kN/m]	[kN/m]	[kN/m]	[kN/m]
400	$2.30 \cdot 10^6$	$5.76 \cdot 10^6$	$2.05 \cdot 10^6$	$5.20 \cdot 10^6$
500	$2.30 \cdot 10^6$	$5.76 \cdot 10^6$	$2.05 \cdot 10^6$	$5.10 \cdot 10^6$

7.9 Influence of the floor

Besides the walls, the floors also play an important role in the distribution of forces. The diaphragm action ensures that the wind load is transported to the structural walls. Because of this property, the wind load is placed as a line load at every floor. In section 7.10 the application of forces will be discussed in more detail. Aside from the diaphragm action, the floors will also behave as dowels. The tension ties are commonly placed around the precast floors and the area is filled up with fluid mortar. As a result, an edge beam is created that connects the single precast wall elements. The size of the edge beam determines the amount of the dowel action (see Figure 56).

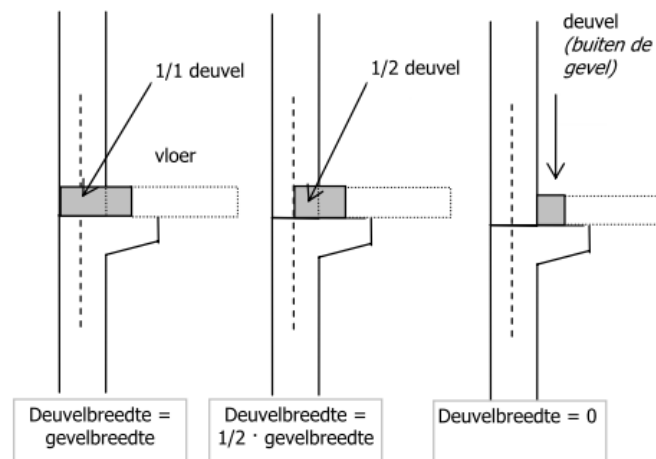


Figure 56 Dowel action of the edge beam [Pieterse, 2007]

The effect of the dowel action is considerably reduced due to the masonry configuration: the overlying element has a stiffness far greater than the dowel, reducing the effectiveness of the dowel. Furthermore, the floor slabs used in this thesis are supported by four steel angles in the corner and the tension ties are incorporated in the floor elements (see section 2.2). As a result, the dowel mentioned previously isn't present in this structure and will not be taken into consideration in the models.

Based on how the floors are modelled in AxisVM, it might be possible that the floors also increase the effective area off the wall. Due to this increased area, the FEM model might allow forces to flow through the floor that in reality flow through the wall. As a result, the distribution of forces might be disturbed in the model. To avoid any problems, the floor will be removed from the model. To prevent stability problems, beams or sliding hinges will be used on several locations where the floors used to be.

7.10 Application of the loads

The forces that are acting on the structure have to be modelled correctly to represent the actual behaviour. In this section it will be discussed how the loads are applied. The determination of the loads is provided in chapter 8.

7.10.1 Vertical load

The dead load of the concrete walls can be automatically calculated by AxisVM and is placed as an area load on the walls. It's also possible to calculate the dead load by hand and place it as a line load on the walls, but this method requires more steps as the wall openings change regularly.

The floors are supported by four steel angles at the corners and a small and concentrated line load should be applied to approach the actual behaviour. For simplicity, the load from

the floor is smeared over the entire wall length as a line load. This line load is applied at the top of every element, as depicted in Figure 57.

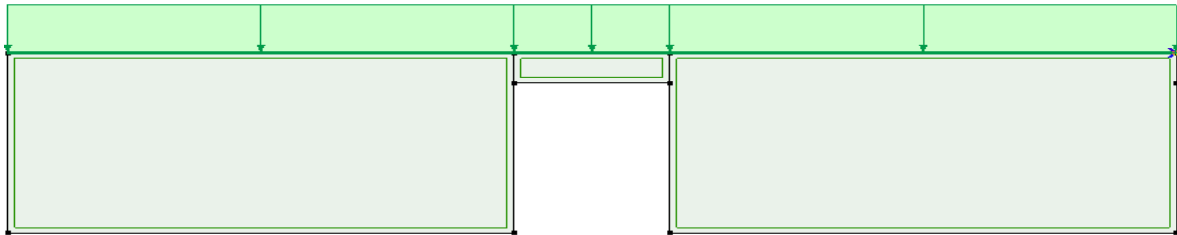


Figure 57 Application of vertical load

7.10.2 Horizontal load

The wind load is transported via the facade through the floors to the structural walls and is eventually dissipated in the foundation. The diaphragm action of the floors ensures the transition from facade to the structural walls. Since the floors aren't included in the structural model (see section 7.9), the wind load is placed as a horizontal line load on the walls. In Figure 58 an example is given.

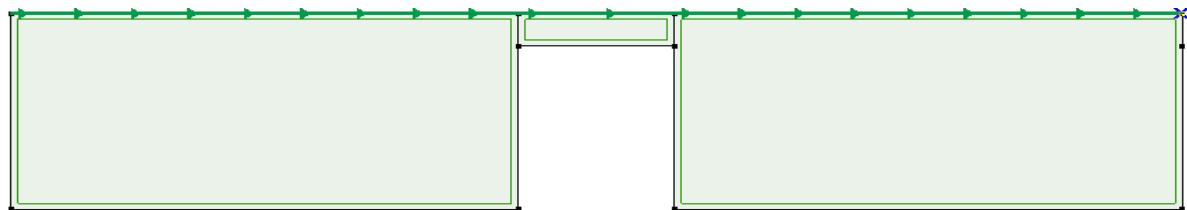


Figure 58 Application of horizontal load

In appendix D.2 a reference model is created with floors and the behaviour of this model is nearly identical to the line wind load assumed in this section. A small difference occurs due to the finite stiffness of the floors (the line load of Figure 58 should be slightly parabolic, with the largest load at the edges) and because of the force coefficient of the wind load (the wind pressure at the front facade is larger than the wind suction at the rear facade).

7.11 Schematisation of the foundation

In chapter 3 and section 4.4 the layout of the foundation is shown. The diaphragm walls are located under the structural walls and underneath the two load bearing facades. Thanks to the 1m thick foundation slab, the diaphragm walls at the circumference are also activated for the stiffness. To reduce the complexity of the model, the floors, load bearing facade and foundation slab haven't been modelled. Therefore the diaphragm walls around the circumference are ineffective and aren't modelled either. As a result the actual stiffness of the foundation will be higher than calculated with this model, creating smaller deflections than calculated in chapter 9.3. The stiffness of the diaphragm walls is shown in Table 11. In the literature study a more detailed overview of the calculations made by MOS grondmechanica is shown.

Table 11 Diaphragm stiffness [Zonneveld ingenieurs, 2004]

Panel level	Panel size	Stiffness
	[m ²]	[kN/m]
60m-NAP	0.8x3.3	517355
	1.0x3.3	575555
	1.2x3.3	627225
	1.5x3.3	697190

8 The influence of connection and element properties

In the previous chapter it has been discussed how the walls and connections should be schematised to obtain accurate results. But the shear stiffness of the horizontal connection should be analysed in more detail because this aspect is influenced by the normal stress and varies over the entire structure. Furthermore, it may be beneficial to utilise the open vertical joint structurally in the lower region of the building, increasing the strength and stiffness. Aside from the structural effect of the connections, the elements also influence the construction methodology. How do the cycle times relate to the size of the elements?

The main goal of this chapter is to determine how the connections and elements influence the total design. By analysing the effects, conclusions can be made with respect to the variable shear stiffness, the influence of the vertical open joints and the relation between the element size and cycle times.

Section 8.1 will start with the shear stiffness of the horizontal connection. The vertical connection will be discussed in section 8.2. The dependency of the cycle times to the element size is examined in section 8.3. This chapter ends with a conclusion in section 8.4.

8.1 The influence of the shear stiffness of the horizontal connection

The walls of the Zalmhaven tower contain large concrete elements in a masonry configuration. This configuration makes a vertical structural connection obsolete and this reduces costs and construction time. The horizontal connection remains and determines the stiffness of the entire structure. The normal stiffness of the horizontal connection (k_y) is only affected by the concrete strength class and doesn't deviate over the building height (see section 7.8.2). The shear stiffness is influenced by the concrete strength class, reinforcement ratio and normal stress (see section 7.8.3). The first two aspects are considered constant over the building height, but the normal stress deviates over the building height and width. To incorporate this dependency, AxisVM should contain a module that calculates the stiffness based on the normal stress, but unfortunately this is not present at AxisVM 10 and 11 (and most other FEM programs). The only solution is a manual iterative calculation, where first a stiffness for every connection is estimated. Then the normal stress is calculated by AxisVM and a new shear stiffness is manually calculated and entered in the model. This process should be continued until the values converge. Since the normal stress deviates over the building height and width, this is a very labour intensive process. Aside from the question whether or not this iterative method should be applied it should also be examined what the influence is of a low or high stiffness on top deflection and distribution of shear and normal forces.

The complete overview of the analysis can be found in appendix D.1. In the following sections a short overview of the model schemes, results and conclusions will be provided.

8.1.1 Model scheme of the investigation part 1

The investigation starts with modelling five walls with a different constant shear stiffness value for the entire structure. By varying the stiffness, the influence of the stiffness can be determined on the deflection and distribution of forces: does a slender precast building require a very stiff horizontal connection or are the requirements also satisfied with a low stiffness? Because the stiffness depends on the normal stress, the stiffness is varied between 0 and 20N/mm². The stiffness values of the different walls are combined

in Table 12. Because research of Falger [Falger, 2003] has shown that changing the stiffness results in larger differences when the stiffness is relatively low, a medium low stiffness value with a normal stress of 5N/mm^2 is added (an additional step).

Table 12 Parameters for the shear stiffness investigation

Wall number	Shear stiffness [kN/m/m]	Normal stiffness [kN/m/m]	Representative normal stress [N/mm ²]
1 (low)	$6.41 \cdot 10^5$	$7.33 \cdot 10^8$	0
2 (medium low)	$2.14 \cdot 10^6$	$7.33 \cdot 10^8$	5
3 (medium high)	$3.64 \cdot 10^6$	$7.33 \cdot 10^8$	10
4 (high)	$5.76 \cdot 10^6$	$7.33 \cdot 10^8$	20*
5 (monolithic)	-	-	-

* This value is limited at 17N/mm^2 due to a shear limit.

For this investigation wall 4 is used with openings (see section 4.3.1) and the structure is loaded by dead load and a non-uniform wind load. To compare the influence of the different stiffness values, local and global aspects are compared. For example the top deflection, moment in the lintel or the shear stress in the horizontal connection. All the remaining model properties (mesh size, foundation stiffness, location of the sections or applied Young's modulus) can be found in appendix D.1.

8.1.2 Results of part 1

From the results it can be noticed that the largest differences in top deflection and distribution of forces occur between wall 1 and 2 (low and medium low stiffness). As the shear stiffness becomes higher, the results converge. This phenomenon was also observed by Falger during his research on different connections [Falger, 2003, p86].

The results also show that a lower shear stiffness leads to larger normal stress values at the corners and smaller shear stress values along the connection.

When all the values are observed, it can be noticed that there is a large difference between a precast wall with a high shear stiffness and a monolithic wall. The largest deviations can be found at the top deflection, around the lintels and at the shear stress in the horizontal connection.

Now that the walls have been modelled with a constant shear stiffness, the question remains: what happens when the shear stiffness deviates over the building height and width?

8.1.3 Model scheme of the investigation part 2

To answer the question of the previous section, the model scheme of section 1 is extended with a sixth wall with a shear stiffness related to the normal stress. To achieve this relation between normal stress and stiffness, the connection will be placed in a class depending on the normal stress. Per wall element the average normal stress is determined and consequently placed in the associated class. The different normal stress classes can be found in Table 13. The interval between 0 and 10N/mm^2 is divided into two classes because the results change faster at low shear stiffness values.

Table 13 Normal classes for part 2

Average normal stress σ_{aver} [N/mm ²]	Calculation value normal stress σ_{calc} [N/mm ²]	Shear stiffness k_x [N/mm ²]
0-5	2.5	$1.39 \cdot 10^6$
>5-10	7.5	$2.89 \cdot 10^6$
>10-20	15	$5.14 \cdot 10^6$
>20-30	25*	$5.76 \cdot 10^{6**}$

* This value is limited at 17N/mm² due to a shear limit.

** Maximum shear stiffness due to shear limit at 17N/mm².

8.1.4 Results of part 2

When the results of the second analysis are observed in detail it can be noted that the values of wall 6, with a stiffness that depends on the normal stress, are nearly equal to wall 3 and 4 of the previous section. Based on these results, the iterative method would be pointless since it doesn't create more accurate results. However a side note should be placed at the results: these values are obtained at the bottom (6th level) where the stiffness of wall 6 is nearly identical to wall 3 and 4. Therefore the values have also been compared on the 26th level since the shear stiffness of wall 6 is reduced over the height (lower normal stress). According to the new results, almost all the differences between wall 3, 4 and 6 have been reduced: the higher level has a positive influence on the differences. This phenomenon can be explained by the fact that the tension and compression stresses are larger near the bottom of the structure. A Large difference between tension and compression results in more different load classes, making it more susceptible to differences.

From all the results of part 2 of the analysis, wall 4 with the high stiffness approximates the actual distribution most accurately. Since the differences are acceptably small, a constant high stiffness may be applied at all the connections if one does not want to use the iterative method.

8.1.5 Conclusion

By examining the results of the six different walls, several interesting conclusions can be made with respect to the shear stiffness. For example, when the shear stiffness of the horizontal connections increases, the results (top deflection, shear and normal stress) start to converge. Therefore it may be concluded that increasing the shear stiffness of the horizontal connection has more effect when the current shear stiffness is relatively low.

When the shear stiffness of the horizontal connection is reduced, the distribution between shear and bending changes. To maintain a stable structure, more forces will be transferred by bending, resulting in larger normal forces at the outer fibre of the structure.

When a monolithic structure is considered, the shear stiffness of the connection is considerably larger than that of a precast structure. Therefore using a monolithic schematisation of the connections to design a staggered precast wall with open vertical joints will result in non-realistic values: the top deflection will be underestimated and the shear stresses are overestimated. Furthermore, as a result of the precast load distribution the lintels obtain a higher bending moment and shear force. Using a monolithic model to design a precast structure will therefore underestimate these values.

The results also show that the actual shear stiffness values obtained by the iterative method are nearly identical to a high constant shear stiffness: the maximum differences are acceptably low. Furthermore, the difference isn't influenced by the height. It may be

concluded that the elaborated and iterative method to calculate the actual shear stiffness is not required and the entire structure may be modelled with a high shear stiffness of $5.76 \cdot 10^6 \text{ kN/m/m}$.

8.2 The influence of the vertical open joint

The vertical connection plays an important role in the stiffness of traditional precast buildings. The masonry configuration circumvents this relation by using dowel elements and the vertical connection¹⁷ may be left open (structurally). The two elements above and below the vertical joint are considered to be the dowel elements and they transfer the shear force which would normally flow through the vertical connection. Since the vertical open joint doesn't contain any stiffness, the dowel elements locally obtain higher forces. Although the dowel elements transfer the shear force, it's unknown how the top deflection or the distribution of shear forces reacts when the vertical open joints are used structurally.

To resolve this unknown aspect, multiple models will be analysed. First three closed 2D walls will be examined to understand the distribution of forces:

1. a closed 2D wall with an open vertical joint,
2. a closed 2D wall containing a vertical connection with a high stiffness,
3. a closed 2D monolithic wall.

Consequently, the openings will be added to the three walls. Based on the results, it will be determined whether or not it's beneficial use the open vertical joint structurally. The complete overview of the analysis can be found in appendix D.2. In the following sections a short overview of the model scheme, results and conclusions will be provided.

8.2.1 Model scheme

For the first three models wall 4 is used without any openings (see section 4.3.1). By removing the openings, disruptions created by the openings are prevented, resulting in the actual behaviour of the vertical open joint. For the last three models also wall 4 is chosen and the openings are maintained to obtain the actual behaviour.

To compare the models, local and global results will be examined. The top deflection and shear distribution provide the global results while the moment, shear and normal force of several critical sections will provide the local results. The remaining model scheme aspect can be found in appendix D.2.

8.2.2 Results of the closed 2D walls

When the three closed walls are considered, it can be observed that a vertical connection with a high stiffness (model 2) has almost no influence on the top deflection, normal force and the moment distribution. The results remain more or less comparable to the results of the model with an open vertical joint (model 1). When one considers the high stiffness of the over and underlying dowel elements, it becomes clear why the vertical connection has nearly no influence on the stiffness and global moment and shear distribution. Nevertheless, the shear force in the elements is influenced considerably. This difference can be explained by the shear force distribution: the shear force has to be transported around the open vertical joint into the dowel elements. Because of the open

¹⁷ The two words "joint" and "connection" are overlapping and therefore a word definition is used: a connection is the total physical link including the adjoining parts of the precast concrete elements and a joint is the space (area) between the two elements where they meet each other.

vertical joint the structural area is locally reduced by 50% and the dowel elements absorb up to 25% more shear force.

An interesting aspect is the difference in top deflection between the three models without openings: the precast wall with open vertical joint only deflects 2.5% more than the monolithic wall. When the deflections of the wall with openings are considered, it can be observed that the deflection increases to 13%. This difference in deflection between the closed wall and wall with openings can be explained by the behaviour of the wall on the openings. By adding openings, the distribution between shear and bending and also the internal flow of forces changes (see section 9.1).

The results of the monolithic wall differ considerably from that of the two other models due to the monolithic properties. It can be stated that the monolithic schematisation will result in non-realistic results when used for a precast structure.

8.2.3 Results of the 2D walls with openings

When the openings are added, the differences between model with an open vertical joint and the model containing a vertical connection with a high stiffness increase slightly. These slightly larger differences are created by the adapted distribution of forces: there is less area available to transfer the forces to the dowel elements. Nevertheless, the differences with respect to the top deflection, normal force and the moment distribution remain small.

8.2.4 Conclusion

The previous two analysis have shown that the vertical connection has nearly no influence on the stiffness of the structure, normal force and moments of the wall elements. Despite the lack of influence on the stiffness, which is an important aspect in high-rise buildings, the vertical connection does influence the distribution of shear force. As a result of the open vertical joint, the shear force has to be transported by the over and underlying dowel elements, also increasing the moment and shear force in the lintel. In the 202.25m high Zalmhaven tower this results in considerable large shear forces at the bottom of structure, which exceed the resistance of unreinforced concrete. Since the shear forces are lower in a structure where the vertical connection is utilised, a new question arises: do the structural benefits outweigh the additional required labour? To answer this question, several aspects have to be considered:

- How much additional labour is required?
- Is this additional labour easy to execute?
- Does this additional labour provide results as expected?
- What is the resistance of a concrete element with an economical reinforcement ratio?

When the vertical connection is structurally utilised, 25% more connections have to be made per floor. Besides the 25% more labour, the vertical connection is also more difficult to construct: placing horizontal and vertical reinforcement, adding formwork, casting and removing the formwork. Since the shear stiffness of the vertical connection has nearly no added value, it possible to construct an unreinforced connection which can only take up compression force. But this connection requires special engineered details to maintain its properties (for example a tension tie at the bottom of the elements). Without these details the vertical unreinforced connection may open up (you can literally put a piece of paper between the cracks) and fail due to the tension forces. Because of these aspects, it's preferred in practise to leave the vertical joint structurally open. The only aspect which remains is the required resistance of the element and the increased amount of vertical reinforcement. Due to the open vertical joint, the over and underlying dowel

elements obtain a larger shear force in the centre (see section 9.1). According to the calculations of section 9.7, the required vertical reinforcement increases with 18%¹⁸ in the central area of the element. The effect on the horizontal and moment reinforcement is negligible. The additional cost of 18% more vertical reinforcement in the centre and the coinciding additional labour outweigh the disadvantages of using the vertical connection structurally. Therefore it may be concluded that the masonry configuration in combination with a vertical open joint is a better solution than the identical masonry configuration in combination with structurally vertical connections.

8.3 The influence of the elements on the cycle times

The cycle time includes the sum of activities that are required to complete a building layer. By summing the required time per floor, the total construction time can be calculated. During the literature study the cycle time in relation to the transport system and building height was already studied. In this section the relation between the element size and cycle time will be analysed, combined with the building height. This is an interesting aspect since very heavy precast elements are applied at the Zalmhaven tower. These heavy and large elements are beneficial for the structural properties, but how does this influence the cycle time?

Before the element size and cycle times are considered, a recapitulation will be provided of the literature study, regarding the cycle time of the transport system¹⁹.

8.3.1 Recapitulation of the literature study: cycle time versus transport system

As mentioned in the introduction, the cycle time includes the sum of activities that are required to complete a building layer. To determine the cycle time of a building layer, the following three questions have to be answered:

1. Which activities have to be executed to complete the layer?
2. How much time does this activity requires?
3. Which activities can be executed parallel?

When the cycle time of a floor is determined, it can be optimized. The following four aspects can be considered during the optimisation:

1. reduce the required time per activity,
2. reduce the amount of activities in the critical path,
3. reduce the transport time,
4. reduce the amount of elements that have to be transported.

Reducing the required time per activity (for example placing a floor element in 20 minutes instead of 30 minutes) has only a small relation with the transport system (the gantry crane is able to return quicker to the starting point for the next element) and is therefore not discussed in more detail. The activity "vertical transport" is affected by the building height, but this will be examined in step 3. Furthermore, reducing the time per activity should be considered with care since a very short time may induce errors.

¹⁸ This difference is between a precast wall with open vertical joints and a monolithic wall with no joints. When the difference between a precast wall with open vertical joints and a precast wall with structural vertical connections is considered, the difference will be smaller, but in the same order of magnitude.

¹⁹ The analysis made in the literature study is based on a master thesis report of van der Meij [Meij 2012].

The amount of activities has a large influence on the cycle time. These activities can be separated into two categories: crane related and crane unrelated activities. The crane related actions in the critical path of a separated (hoisting shed) and non-separated (tower crane) are shown in Table 14.

Table 14 Critical path activities of a separated and non-separated transport system

Separated transport		Non-separated transport	
Vertical transport	Horizontal transport	Vertical transport	Horizontal transport
1. Attaching of the element		1. Attaching of the element	
2. Element orientation for transport		2. Element orientation for transport	
3. Vertical transport of the element		3. Vertical transport of the element	
4. Element orientation for storage			4. Horizontal transport of the element
5. Detaching of the element			5. Element orientation and adjustment
6. Returning vertical (unloaded)	7. Attaching of the element		6. Detaching of the element
	8. Element orientation for transport		7. Returning horizontal (unloaded)
	9. Horizontal transport of the element	8. Returning vertical (unloaded)	
	10. Element orientation and adjustment		
	11. Detaching of the element		
	12. Returning horizontal (unloaded)		

The elements which are discussed in Table 14 are for example:

- structural wall elements,
- facade elements,
- floor elements,
- scissor stairs,
- concrete aerated blocks for several internal walls,
- bathroom units.

The amount of actions, 12 for a separated system and 8 for a non-separated system determine the cycle time to a significant extend. It should be noted that while the separated system contains more actions, the actions per system are less (6 versus 8).

The crane unrelated actions do not require the presence of the crane and can therefore be executed parallel with the crane related actions. For a precast element several actions can be enumerated:

- determining the correct location of the element (in x, y and z relative to a reference point),
- cleaning the connection,
- creating the connection (with or without formwork),
- removing the braces.

In order to execute these actions simultaneously with the crane related actions, enough personnel should be available on the construction floor. If this requirement is satisfied, the crane unrelated actions have no influence on the cycle time.

The transport time and the amount of elements that have to be transported are the two last aspects which influence the cycle time. Just as the amount of actions, the amount of elements also significantly influences the cycle time: less elements results in less transport time, less actions and consequently the cycle time is reduced. Before the transport time can be examined, the following aspects have to be discussed: the utilization ratio of the (gantry) crane and the norm time.

The utilization ratio is the percentage of time which the transport system is utilised. For example, the maximum utilisation ratio of a tower crane is 80%. This implies that minimal 20% of the cycle time the tower crane is inactive, waiting to transport a new element. This boundary is set at 80% to increase the robustness of the system and schedule. As a result, breaks (not included in the schedule), short delays and human errors won't affect the schedule. At a hoisting shed, the maximum utilisation ratio is set at 90% since a hoisting shed has a higher robustness (less susceptible to weather delays). If the utilisation ratio is too high, multiple transport systems can be applied, the amount elements that have to be transported can be reduced or the transport speed can be increased.

The scheduled time which one element utilises the transport system is called the norm time. This norm time includes the transport time and the required time for the crane related actions (for example attaching, adjusting and detaching of the element). In other words, the norm time is the total time between the moment of attaching the element to the crane and the moment the crane returns for the second element (step 1 to 6, 7 to 12 or 1 to 8 in Table 14). In practise, often a constant value is used for the crane related actions, based on the size accuracy, accessibility and visibility of the actions.

The last aspect which remains is the transport time. Unlike the crane related actions, the transport time increases over the building height. When a hoisting shed is considered with a separated transport system, Figure 59 is obtained.

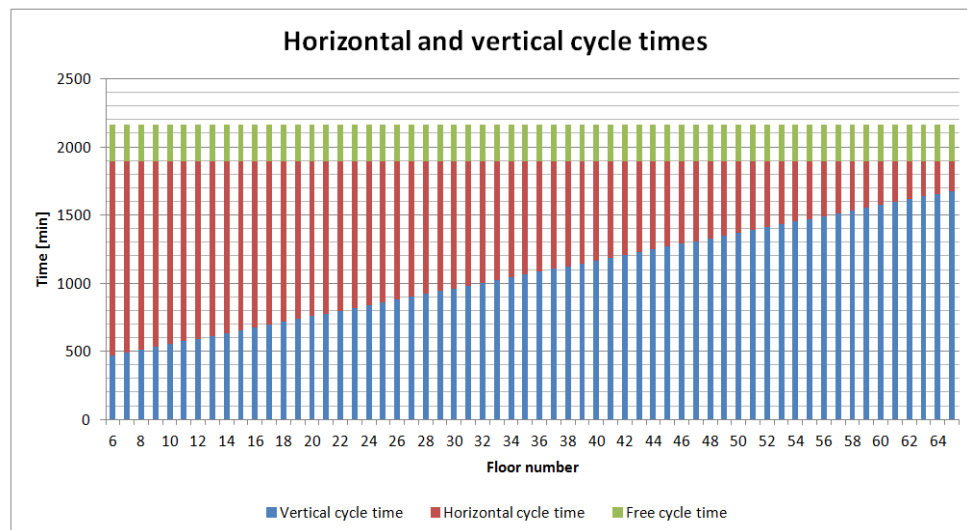


Figure 59 Horizontal and vertical cycle times of a separated system

The blue lines represent the vertical cycle times. Due to the increasing height, the cycle times increase. The red lines represent the horizontal cycle times. Since the horizontal transport isn't affected by the height²⁰, the cycle times remain constant. The green lines are the remaining unused cycle time (at least 10% at a hoisting shed). At the sixth floor the total height is only 18.30m, resulting in a very short vertical transport time. Since

²⁰ The horizontal distance and the amount of crane related actions remains identical at all the floors (optimisations not included). At Figure 59 it might seem that the horizontal cycle time decreases over the building height, but the base of the red lines extends behind the blue lines.

the horizontal time remains constant, the vertical transport system is only utilised very little (less than 25% of the total available cycle time). Since the efficiency is very low at the start of a project (the construction workers aren't familiar yet with the process), the vertical gantry crane may be utilised as second horizontal transport system. This additional second horizontal system should be planned very carefully since the two gantry cranes may obstruct each other.

At the 65th floor, the vertical transport time has increased considerably and the horizontal and vertical cycle time are nearly identical. It should be prevented that the vertical transport cycle becomes larger than the horizontal cycle since this ensures a stagnation of the work on the construction floor (the construction workers have to wait for the new elements). When this requirement is fulfilled, a separated transport system isn't affected by the building height and constant cycle times can be maintained. At a non-separated system, the height affects the cycle time (see Table 14) and it's nearly impossible to acquire a constant cycle time. It's possible, but then very large buffers have to be included in the process, making the cycle time very inefficient at the bottom of the tower. Furthermore, when they are near the top floor, the construction workers have to wait for the elements, making also the top of the construction inefficient.

So in conclusion, the cycle time includes the sum of activities that are required to complete a building layer. Per activity, there is a certain norm time, which contains the crane related actions and transport time. When a separated system is applied, the horizontal cycle time should be leading which isn't affected by the height. As a result, constant cycle times are obtained over the height, ensuring an optimal and efficient construction process.

8.3.2 The influence of the mass on the cycle time

Now that all the aspects required for the cycle time and the relation between the cycle time and height have been examined, the influence of the mass will be analysed in more detail. The mass itself only influences the transport speed: a low mass results in a high transport speed and vice versa. But indirectly the mass also influences the amount of elements and actions: by applying very large elements (large mass), less elements and crane related actions are required per floor. The question that follows: is the lower transport speed of a heavy element compensated by fewer elements and actions?

To answer this question, first the relation between the transport speed and mass is analysed. In Figure 60 the vertical transport speed of the Erasmus MC hoisting shed is shown.

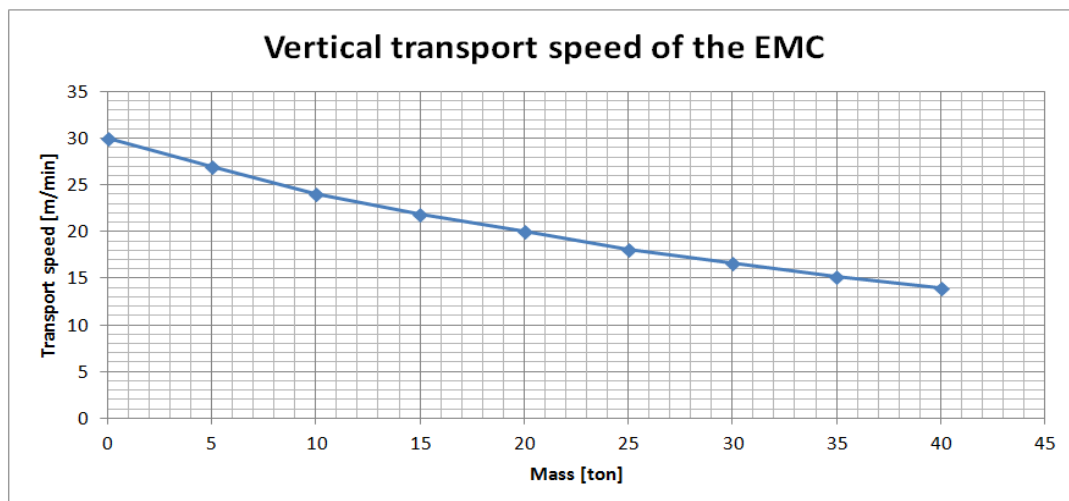


Figure 60 Transport speed of different systems

When a trend line is added in the Excel sheet, the following equation is obtained:

$$y = 29,476e^{-0.019x}$$

This is a non-linear relation: at 30 ton this results in a transport speed of 16.7m/min and at 15 ton a speed of 22.2m/min is obtained. At half the mass, the speed has only increased with 33%. When the system is unloaded (returning) a speed of 30m/min is reached. When a building of 200m is considered in combination with 6 minutes of cranes related actions per element, the following comparison can be made:

One element of 30 ton has a total of 6 minutes of crane related actions. The total vertical transport time is:

$$T_{30} = \frac{h}{v_{\text{loaded}}} + \frac{h}{v_{\text{unloaded}}} = \frac{200}{16.7} + \frac{200}{30} = 18.6 \text{ minutes}$$

$$T_{\text{total},30} = 18.6 + 6 = 24.6 \text{ minutes}$$

The vertical norm time of one 30 ton element is 24.6 minutes.

Two elements of 15 ton have a total of 12 minutes of crane related actions²¹. The total vertical transport time is:

$$T_{15} = 2 \cdot \left(\frac{h}{v_{\text{loaded}}} + \frac{h}{v_{\text{unloaded}}} \right) = 2 \cdot \left(\frac{200}{22.2} + \frac{200}{30} \right) = 31.4 \text{ minutes}$$

$$T_{\text{total},30} = 31.4 + 12 = 43.3 \text{ minutes}$$

The vertical norm time of two 15 ton elements is 43.3 minutes. This is almost twice as large as the vertical norm time of one 30 ton element. This difference is so large since the two 15 ton elements require more actions and because the relation between mass and transport speed isn't linear. It can be concluded that at every vertical transport movement, the maximum allowable mass should be transported.

When the horizontal transport cycle is considered, two important aspects should be taken into account: the transport time isn't affected by the height and the transport speed is constant for all the loads. Attaching or detaching a 15 or 30 ton elements requires the same amount of time since both elements are connected at two points. Placing and positioning a 30 ton element over the starter bars requires more time than at a 15 ton elements since it's likely that the heavier element is longer and contains more starter bars. By increasing the length of the edge bars, the difference is reduced to a minimum.

For example, the horizontal norm time of a precast wall element of 30 ton is 24 minutes. A precast wall element of 15 ton has a horizontal norm time of 20 minutes, but since two elements are required, the total norm time is 40 minutes. Again, this is almost twice as large as the heavier element of 30 ton.

In the previous two examples, one 30 ton element has been compared with two 15 ton elements. Changing the parameters, for example 18 elements with a total mass of 489 ton versus 25 elements with the same mass doesn't influence the outcome of the

²¹ One might say that smaller elements have a shorter duration of crane related actions, but the difference between attaching, detaching and orientating a 15 or 30 ton element is negligible at the vertical transport cycle.

calculation: the higher transport speed can't make up for the additional elements and actions.

8.3.3 Conclusion

The time that is required to complete one level is denoted as the cycle time. The cycle time consists of many actions and per action a certain norm time is obtained. This norm time is composed out of the crane related actions (attaching, detaching or positioning the element) and the horizontal/vertical transport time. At a separated transport system (hoisting shed) it's either the horizontal or vertical norm time and at a non-separated system (tower crane) it's a combination.

At a well-designed separated transport system, the horizontal cycle times are always leading, ensuring no delays occur at the construction floor. Since the horizontal system is leading, the vertical system is able to provide a small stock of elements at the construction floor and the cycle time isn't affected by the building height.

When the element mass is also taken into consideration, it may be concluded that the maximum element mass should be transported at every vertical transport action. This is because the relation between the mass and vertical transport speed isn't linear: 50% less weight results in 33% more transport speed. Besides the non-linear relation, two elements of 15 ton require twice as many vertical crane related actions. Therefore two elements of 15 ton obtain a vertical cycle time that is almost twice as large as the cycle time of one 30 ton element.

At the horizontal cycle time, the mass and building height exert no influence on the cycle time. Therefore two elements will obtain a cycle time twice as large as one element. Since the single 30 ton element is larger than a single 15 ton element, the crane related actions of the heavier elements will be slightly longer (it's more difficult to place the element over the starter bars), but this increment is marginal.

It may therefore be concluded that it's more attractive to use one 30 ton element instead of two 15 ton elements for the horizontal and vertical transport cycle: at every transport movement, the maximum allowable mass should be transported.

8.4 Conclusion

In this chapter the influence of the horizontal and vertical connections have been examined. Since relatively large elements are utilised in the structural walls, also the influence of the element mass on the cycle time has been considered. From the results the following conclusions can be made with respect to the horizontal connection:

- Increasing the shear stiffness of the horizontal connection has more effect when the current shear stiffness is relatively low.
- A lower shear stiffness of the horizontal connection results in larger normal stresses in the outer fibre.
- Using a monolithic schematisation of the connections to design a staggered precast wall with open vertical joints will result in non-realistic values. The top deflection will be underestimated and the shear stresses are overestimated.
- Using an elaborated and iterative method to calculate the actual shear stiffness is not required since a constant shear stiffness over the height and width results in relative accurate and acceptable values.

For the vertical connection it may be concluded that:

- The vertical connection has nearly no influence on the stiffness of the building. Furthermore, the distribution of normal force and moments is hardly affected either.
- The shear distribution is considerably influenced by the open vertical joint. Between 14 and 26% more shear force may be expected according to the two 2D models.
- As a result of the higher shear force, the actual 3D model has shown that 18% more reinforcement is required in the centre area of the dowel elements.

From these aspects the question arises: is it structurally attractive to utilise the vertical connections in the bottom of the building? To activate the vertical connections, 25% more connections have to be made per floor. Since these vertical connections are more labour intensive than for example horizontal connections, it's concluded that the 18% more reinforcement in the centre of the element and the coinciding additional labour outweigh the disadvantages of using the vertical connection structurally (this preference is confirmed by the building practise: [Vambersky 2007] and [Zonneveld ingenieurs 2012]). The masonry configuration with open vertical joint remains the best solution.

The relation between the mass and cycle time can be characterized by:

- The relation between the mass and vertical transport speed isn't linear: 50% less weight results in 33% more transport speed.
- Two elements of 15 ton require twice as many vertical crane related actions when compared to one 30 ton element.
- Due to the non-linear relation and the increased amount of actions, the vertical cycle time of two 15 ton elements is almost twice as long as one 30 ton element.
- At the horizontal cycle time, the transport speed is equal for all the elements. Therefore also the horizontal cycle time of two 15 ton elements will be twice as long as one 30 ton element.

The previous relations are valid when the crane related actions of one 30 ton element are identical to one 15 ton element. Due to the larger size and mass of the 30 ton element the crane related actions will slightly increase (it may be more difficult to place the element over a larger amount of starter bars), but this increase is negligible. Even if a longer time for the crane related actions would be included (for example 7 or 8 minutes instead of 6), the two 15 ton elements will always obtain a longer cycle time. It may be concluded that the maximum mass should be transported at every vertical movement.

9 Results of the FEM analysis

In this chapter the results of the FEM analysis will be discussed and analysed. In chapter 7 it's described how the structure is modelled in AxisVM and the loads acting on the structure are calculated in chapter 5. The FEM results shown in this chapter are preliminary results and as this chapter will show that there are several opportunities for optimisation.

The goal of this chapter is to analyse the behaviour of the precast structure based on the distribution of forces, the value of the forces, the deflections, second order effects, shear lag, structural factor and vibrations. With the acquired insight, the reinforcement will be designed for a lintel and a wall element. During the examination of these aspects, differences will be distinguished and analysed between the precast and monolithic model, providing insight in how the structures behave under identical circumstances.

This chapter will start with the distribution of forces of a precast and monolithic model in section 9.1. Since this section only includes the distribution of forces, section 9.2 will continue with a short examination of the value of the forces in the precast model. Consequentially, the deformations are discussed in section 9.3. The second order effects and shear lag are examined in section 9.4 and 9.5. The structural factor is included in section 9.6, combined with the vibrations. In section 9.7 the reinforcement is designed for a lintel and wall element. Since a Young's modulus was assumed in section 7.4, this value will be validated in section 9.8. This chapter will end with an evaluation of concept 3 in section 9.9 and a conclusion in section 9.10.

9.1 Distribution of forces

Precast structures are composed out of separate elements and are assembled on the building site. This method results in multiple connections, differentiating precast from cast in situ structures. But how do these connections influence the distribution of forces and what is the effect of the masonry configuration? Before the results of the FEM analysis can be discussed, these important questions have to be examined and analysed.

Due to the size of the examination and analysis, only the results are included in this section. The entire examination and analysis can be found in appendix E.1.

9.1.1 Model scheme

The analysis of the distribution of forces is based on eight different models:

1. simplified 2D precast wall without openings,
2. simplified 2D monolithic wall without openings,
3. 2D precast wall with openings,
4. 2D monolithic wall with openings,
5. simplified 3D precast model without openings,
6. simplified 3D monolithic model without openings,
7. 3D precast model with openings,
8. 3D monolithic model with openings.

By slowly increasing the level of detail, the effects of several aspects, for example the wall openings and the connection between perpendicular walls can be studied without other disruptions.

For the 2D calculations, wall 4 from section 4.3.2 is used. The normal stiffness is equal to the surrounding concrete and the shear stiffness is based on a slip of 1mm and an average normal stress of 25N/mm^2 (see section 7.8 for more details on the stiffness

calculations). The wind load is placed in the positive x-direction (from left to right) and the forces are equivalent to the values calculated in section 5.3. The dead load of the structure is obtained from section 5.2 and placed at every floor. In the 2D calculations a mesh size of 250mm is used for the bottom section ($1/3^{\text{rd}}$ of the building height) and 750mm for the top section. For the 3D model, the mesh size is increased to respectively 750mm and 2000mm due to the limited memory capacity of the program (see section 7.6).

9.1.2 Results

During the extensive analysis, the distribution of forces is dissected and several interesting observations and conclusions can be made:

- When the simplified 2D precast wall without openings is observed, a disruption can be distinguished at the intersection between the vertical open joint and the horizontal connection. This disruption isn't present at the monolithic models and is most likely created by the location of the interface element and how AxisVM retrieves the results from the postprocessor (how the results are extrapolated from the calculation unit to the graphical unit within the program). This assumption is based on the value of the disruptions, the fact that the disruption is always contained within one mesh element and the location of the disruption relative to the interface element (if the interface element is transferred to the second connecting domain, the peak value also shifts). Therefore these disruptions may be neglected and shouldn't be incorporated in the reinforcement design. By neglecting these disruptions, the simplified precast 2D wall has a similar distribution of normal forces compared with the simplified monolithic 2D wall.
- Despite the similar distribution of normal force, the local distribution of shear force (n_{xy}) is considerably different between a precast and monolithic model. This difference is created by the open vertical joint of the precast structure, which is unable to transfer any shear or normal forces. Due to this property, the forces of the element are transferred to the over and underlying dowel elements. By activating these elements, the shear force increases between the open vertical joints (only 50% of the original structural area is available) and shear force reinforcement is required in the lower section of the wall. This also holds for the horizontal normal force. Despite these local differences at the vertical open joints, the global distribution of forces remains more or less comparable.
- The introduction of shear force into the dowel elements isn't linear and a large peak force is located at the connection point between the horizontal and vertical open joint. In the last 5% of the connection length, the element transfers 11% of its shear force. Furthermore, this peak value is always contained within one mesh element and the shear force value increases when the size of the mesh element is reduced. Between the two horizontal connections, the shear force spreads out in the dowel element. This distribution of shear force originates in the underlying behaviour of the elements and is concentrated by the linear calculation and smeared stiffness. It's known of linear calculations that a large portion of the force is often transferred at the corners (last possible location without redistribution) and by neglecting important mechanisms of the connection (non-smeared stiffness and starter bars) the forces remain concentrated. Therefore this peak value may be smoothed in the actual design. A non-linear calculation in combination with the actual connection behaviour should determine the exact reduction of this peak value.
- When the 2D walls with openings are examined, it can be noted that the normal and shear force increase. This can be explained by the reduced structural area. For example, in the simplified 2D precast wall with openings, the entire floor height of 3.05m was available to transfer the shear force around the open vertical joint. At the model with door openings, all the forces have to be transferred via a

lintel with a height of 0.75m, resulting in a considerable increase of shear force. This phenomenon also occurs in the monolithic wall, but the values are lower since this wall doesn't contain an open vertical joint.

- In the 3D model, the perpendicular walls increase the structural area (similar to the flanges at an I-profile). As a result of this increased area, the normal force is reduced when compared with the 2D models. The effect of the perpendicular walls on the shear force distributions is considerably smaller since most of the shear force is taken up by longitudinal wall (the web of an I-profile).
- The floors of the Zalmhaven tower are supported by the three walls in the y-direction, resulting in the shortest floor span. The two walls in the x-direction are only loaded by dead load. Therefore one might expect that at the foundation the three walls will receive the largest dead load, but in fact the two walls in the x-direction receive 14% more dead load. This distribution can be explained by the thickness and resulting stiffness of the walls: the three walls have a thickness of 400mm while the two walls have a thickness of 500mm. The larger thickness results in a higher stiffness and stiffer elements attract more forces. This distribution is favourable since the two walls have a lower moment of inertia, resulting in a larger tension forces due to wind load.

When all the results are compared, it may be concluded that the 3D models with openings are a combination of the results of the 2D walls with openings and the simplified 3D models without openings. The precast and monolithic models contain many similarities and differences are difficult to differentiate. The only difference visible in the models and which is also present in the actual structure is the local shear force distribution. Due to the open joint, the dowel elements are activated and higher shear forces will be encountered.

Besides the conclusions, there also remains one aspect which acquires more attention: peak values. During the analysis of all the models, many disruptions have been encountered. For all the disruptions a likely cause has been identified, but it should be examined if they are the main reason for the peak value or if other aspects also contribute. Due to the limited time of this thesis, a more thorough analysis has not been performed, but for future examinations it's recommended to do so.

9.2 Forces in the structure

In the previous section the distribution of forces was discussed. It was examined how the forces flow through a monolithic and precast structure in 2D and 3D, with or without openings. The value of the forces was of minor importance and only used to compare the results between the models. In the upcoming chapters, only section 9.7 requires accurate values to design the reinforcement. A structural design is not a structural design without forces, but since they are not required for any calculations, the values will only be discussed shortly in this section.

9.2.1 Load combination SLS1

Load combination SLS1 is required for stiffness calculations and all the loads are multiplied by a load factor of 1.0. Figure 61 shows the results of the vertical force per meter at wall 5. Figure 62 shows a more detailed view at the bottom of the model.

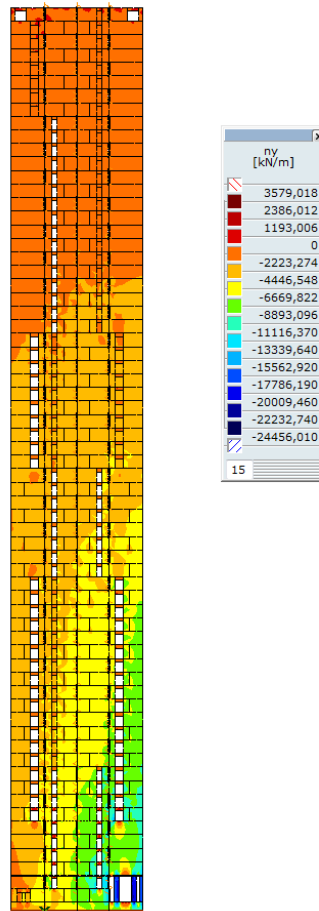


Figure 61 Load combination SLS1, ny distribution of wall 5

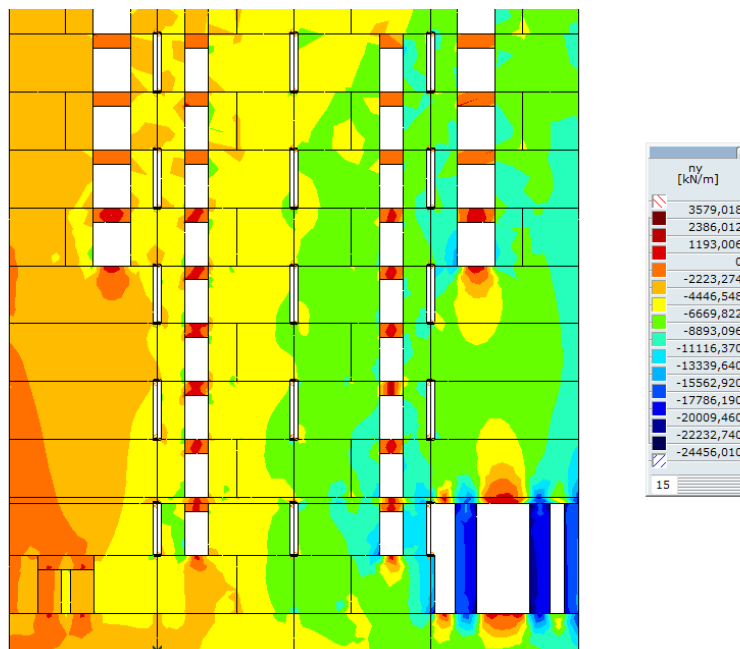


Figure 62 Detailed view of load combination SLS1, ny distribution of wall 5

Figure 62 shows that there is no tensile force in the wall elements. In the centre of several lintels and the wall element above the lobby, a vertical tension force is encountered. Due to the large openings at the lobby, a large compression force can be distinguished in the columns. The lack of tension is beneficial for the deformation

calculations because tension would reduce the stiffness of the horizontal connections considerably. To verify the model, the total horizontal and vertical foundation reactions are compared with the applied loads. According to the sections made at the foundation the following two forces occur (see Figure 63):

$$N=791.1\text{MN}$$

$$H=13.8\text{MN}$$

According to the load calculations, the following loads should occur at the foundation:

$$N=800.6\text{MN}$$

$$H=13.9\text{MN}$$

The calculated values are respectively 1.2 and 0.9% higher than the measure values: somewhere the load has disappeared. This difference is likely caused by the connection between the perpendicular walls, shown in Figure 64. To create an area for the vertical spring, which models the starter bars between the elements, a small notch is removed from every uneven floor. As a result of this notch, the dead floor load and the wind load is temporarily intersected, resulting in a smaller load than expected. The 1.2% larger dead load will not result in any problems since the normal resistance isn't exceeded at any location (see section 9.2.2). In fact, the higher normal force is beneficial since a small tension force occurs at ULS2 (see section 9.2.3). The slightly larger wind load will result in a larger wind moment at the foundation and here the difference will be bigger than 0.9% since the relation isn't linear. The overestimation of the second order effects will counteract the reduced wind load in the SLS (see section 9.4.2). In the ULS, there is no additional safety in the second order effect and the small additional force has to be taken up by the elements.

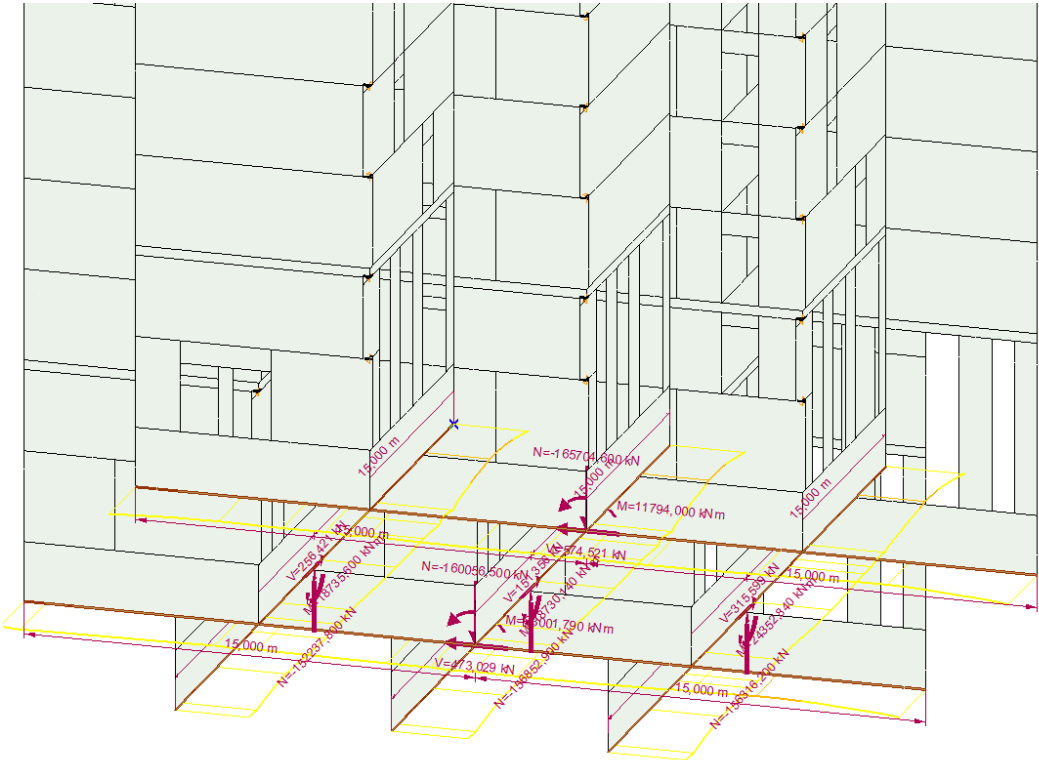


Figure 63 Vertical load at the foundation in SLS1

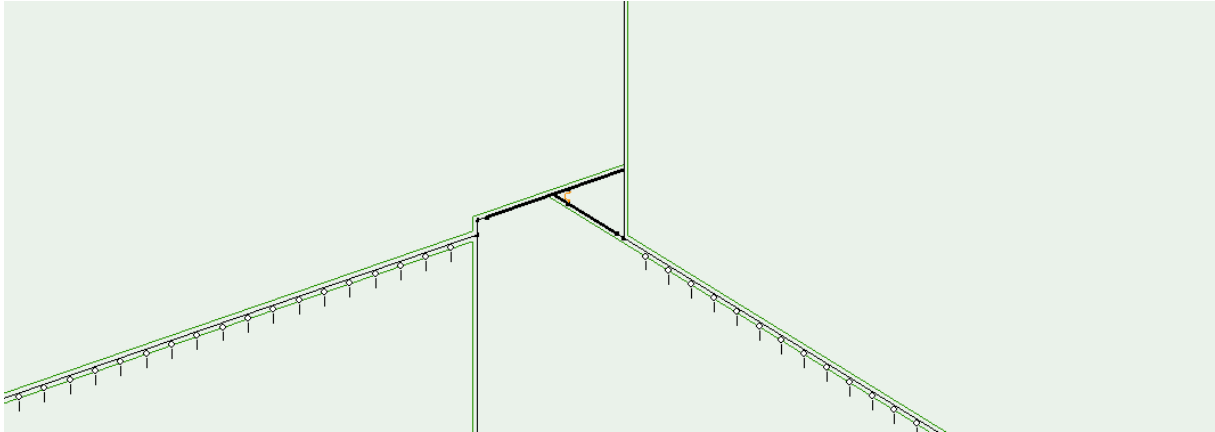


Figure 64 Connection between perpendicular walls

When the normal force value $N=800.6\text{MN}$ is compared with the normal force $N=964.1\text{MN}$ of section 9.6.1, a large difference can be distinguished. This difference is created by how the structure is modelled: the load bearing facade isn't included and the load of the floor section which is supported by the load bearing facade isn't included either (26% of the floor area). This decision was made to reduce the complexity of the model (see appendix B.1)

9.2.2 Load combination ULS1

At the load combination ULS1, the following load factors are applied:

$$\text{ULS1} = 1.3 * \text{dead load} + 1.65 * \text{wind load} + 1.65 * \text{instantaneous live load}$$

Compared with SLS1, the normal force has increased considerably, as can be seen in Figure 65. Nevertheless, all the wall elements are still loaded with compression. For example: in the left corner element at the first floor a compression stress of 3.2N/mm^2 is encountered. A more detailed view of the load distribution is shown in Figure 66.

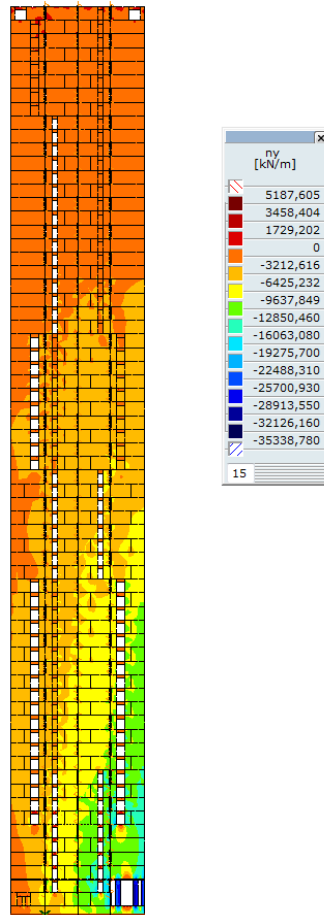


Figure 65 Load combination ULS1, ny distribution of wall 5

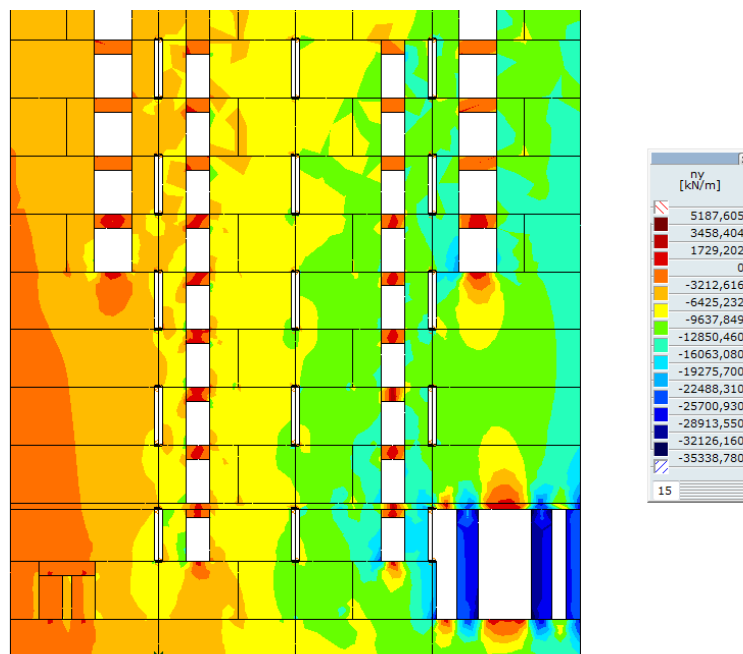


Figure 66 Detailed view of load combination ULS1, ny distribution of wall 5

The wall element at the right hand side on the third floor has a compression stress of 21.1N/mm^2 . The columns in the lobby obtain a compression stress of 33.8N/mm^2 .

9.2.3 Load combination ULS2

Load combination ULS2 has the largest possibility of creating tension stresses in the structure since the dead load is multiplied by 0.9, the instantaneous live floor load by 0.0 while the wind load is still multiplied by 1.65:

$$\text{ULS2} = 0.9 \cdot \text{dead load} + 1.65 \cdot \text{wind load} + 0.0 \cdot \text{instantaneous live load}$$

This combination is encountered when due to errors 10% of the calculated mass isn't applied, no occupants have settled in the building and an extreme (once in every 50 years) storm occurs. While the combination of these events is highly unlikely, the structural requirements should still be satisfied. Therefore the reinforcement design of section 9.7 is based on this load combination.

In Figure 67 it can be observed that a small section at the left bottom corner endures a tensile stress. In Figure 68 a more detailed view is depicted of this tensile area.

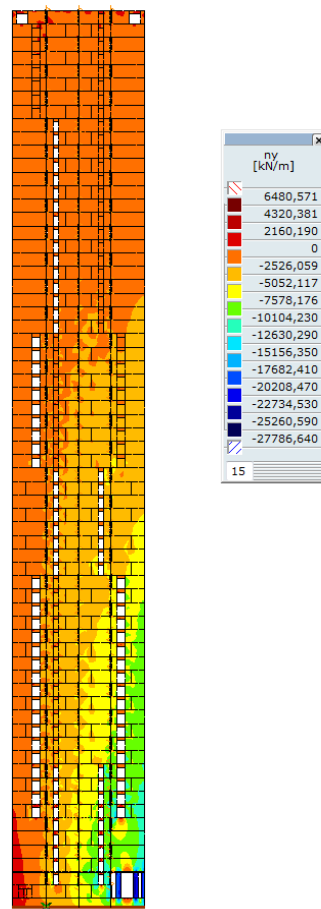


Figure 67 Load combination ULS2, ny distribution of wall 5

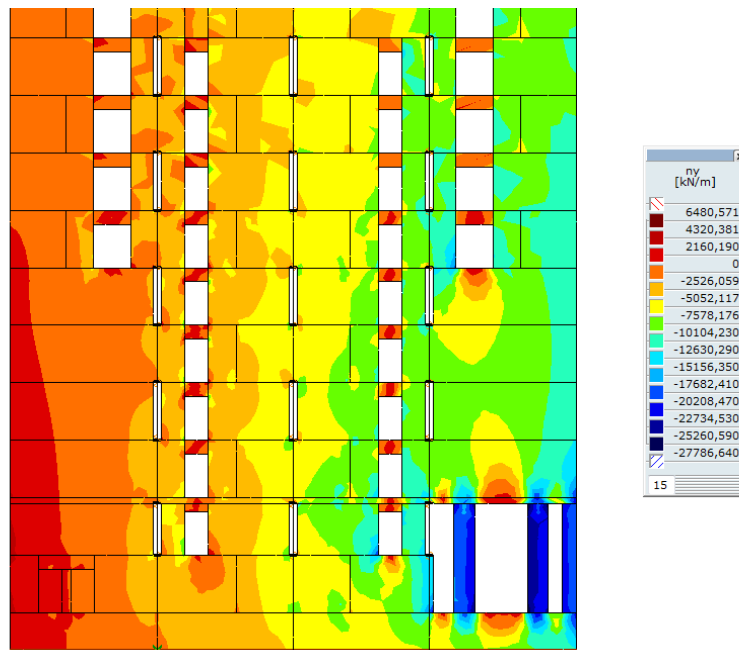


Figure 68 Detailed view of load combination ULS2, ny distribution of wall 5

At the first floor, the tensile area has a width of approximately 3m and continues until the sixth floor. At the outer fibre of the first floor a tensile stress of 3.9N/mm^2 is encountered, while this reduces to a tensile stress of 1.8N/mm^2 when the force is integrated of the entire tensile width. When the tensile strength of C90/105 ($f_{ctd}=2.3\text{N/mm}^2$) is considered, only a small section of the concrete will crack. As a result of these cracks, the stiffness is permanently reduced at this area. According to a second calculation with a reduced stiffness for the entire tensile area ($E=14667\text{N/mm}^2$) this has no significant influence on the distribution of forces and the deflection. According to Figure 69 the deflection in the x-direction will increase with 2% as a result of the cracked concrete at the left bottom corner. This will be an upper limit since the reduced stiffness is applied to the entire tensile area. Furthermore, the tensile stress will slightly diminish (from 3.9 to 3.8N/mm^2), while the compression stress slightly increases. It can be concluded that the forces are redistributed as a result of the lower stiffness, but due to the small area this is nearly negligible.

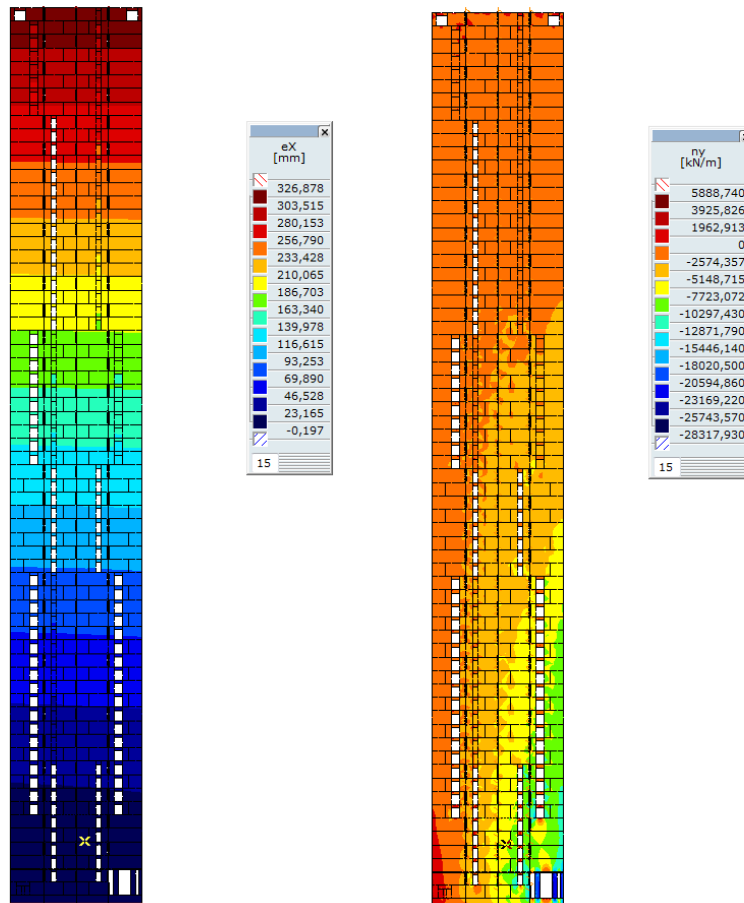


Figure 69 Deflection (left) and normal force (right) values as a result of tensile stresses at the bottom

9.2.4 Load combination ULS3

In the ULS combination 3, the largest distributed normal force is created:

$$\text{ULS3} = 1.5 * \text{dead load} + 0.0 * \text{wind load} + 1.65 * \text{instantaneous live load}$$

Though this combination creates a large distributed normal force, the largest absolute value is obtained at the right hand side in ULS1. This is because of the wind load and the load factor of 1.65 in this combination. The fact that wind load isn't included in ULS3 is clearly visible in Figure 70: the colour lines are nearly horizontally.

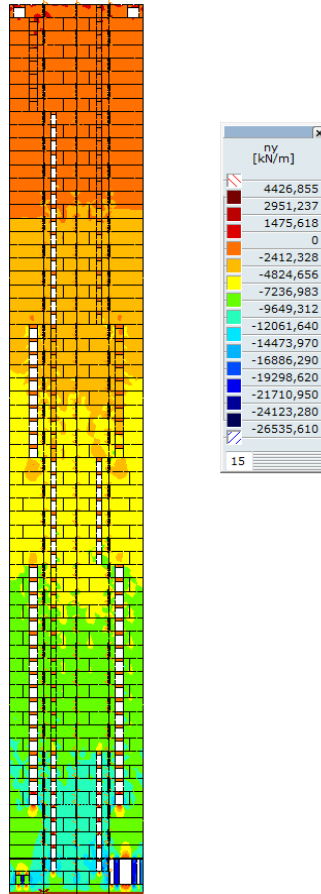


Figure 70 Load combination ULS3, ny distribution of wall 5

In Figure 71 a more detailed view of the bottom of wall 5 is depicted. It's clearly visible how the normal force flows around the openings (distribution between blue and green). The red areas show bending above the openings. At the left hand side, a normal force of 16.6N/mm^2 is obtained at the second floor. In the centre this increases to 23.4N/mm^2 . At the right hand side, a normal force of 18.3N/mm^2 occurs at the third floor. The two dark blue columns at the lobby are stressed by 24N/mm^2 of normal force.

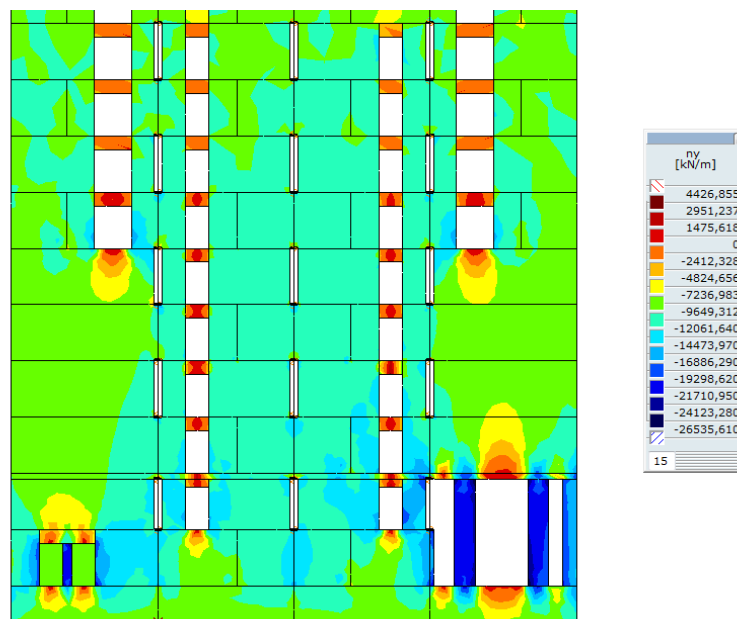


Figure 71 Detailed view of load combination ULS3, ny distribution of wall 5

While ULS1 contains the highest absolute value, it can be concluded that the distributed stresses of ULS3 are higher.

9.2.5 Conclusion

Although this section only provides a glimpse of all the forces and stresses in the structure, a small insight is provided in the differences between the four load combinations. For an actual structural design, this will not be enough, but since these values aren't shown in any other calculation, this section was created.

From the results it may be concluded that there are some inaccuracies between the calculated loads and the reactions at the foundation. This difference is created by a modelling technique: to incorporate the spring between the perpendicular wall elements a small notch is removed. As a result, the load isn't applied at this small notch.

Only in ULS2 a tensile force is encountered at the outer fibre. The combination of events leading to this load combination are highly unlikely, but the requirements should be satisfied. Due to this tensile force, a small concrete area will crack, resulting in a permanent loss of stiffness. A second calculation has shown that this reduced stiffness has nearly no influence on the force distribution and deflections. Therefore no additional measures are required.

The other three load combinations ensure that all the elements are loaded with compression (except the tension force above and beneath the openings in all the combinations). This compression stress may go up to 23.4N/mm^2 at load combination ULS3. Due to the lobby, the columns at the right hand side are loaded with a maximum stress of 33.8N/mm^2 , which is considerably smaller than the resistance ($f_{cd}=60\text{N/mm}^2$).

9.3 Deformations

The deformations of the structure are often decisive in high-rise design. Due to the reduced stiffness of the precast connections, the deformations become even more important. In this section the deformations of the precast model will be analysed and compared with the monolithic model. Also the effects of the foundation and wall reduction discussed during the cycle time will be analysed. Based on the results, quantitative conclusions will be formulated.

9.3.1 Model scheme

For this analysis, the final two models are used: a precast and monolithic structure with wall openings and a foundation. A mesh size according to the height is applied, resulting in mesh elements of 750mm at the bottom section and 1500mm at the top section. In section 7.6.2 it was already discussed that the mesh size has nearly no influence on the deflection since the deflection is the primary unknown variable. Concrete class C90/105 is used with $E_x=E_y=29333\text{ N/mm}^2$. Due to the large forces in the lintels above the door openings, the concrete section is likely cracked, resulting in a reduced Young's modulus of $E_x=E_y=14667\text{ N/mm}^2$ (see section 7.4). The normal stiffness is equal to the surrounding concrete: $k_y=7.33*10^8\text{kN/m}$. The shear stiffness is constant over the building height and width and is based on a compression stress of 25N/mm^2 and a slip value of $s=0.4\text{mm}$: $k_x=1.44*10^7\text{kN/m}$. In section 7.8.2 and 7.8.3, the normal and shear stiffness are discussed in more detail. The normal stiffness of the foundation is based on the applied diaphragm walls: $k_z=6.97*10^5\text{kN/m}$. The horizontal stiffness of the foundation is set at: $k_y=k_x=1*10^7\text{kN/m}$ (no horizontal deformation). The monolithic model is created without interface elements (see section 7.5) and therefore no stiffness has to be entered. Both models are loaded by a non-uniform wind load (the wind load

increases with the building height), dead load and live load as described in 5.2 and 5.3. SLS1 is applied as load combination, since only the deflections are calculated (see section 5.5).

9.3.2 Results of the models

In Table 15, the deflections of the following three different models are depicted:

1. Precast model in the x and y-direction,
2. Monolithic model in the x and y-direction,
3. Monolithic model of Zonneveld ingenieurs in the x and y-direction.

Table 15 Deflections of the models

Model	e_x [mm]	e_y [mm]
Precast model	321.6	292.2
Monolithic model	309.0	289.1
Monolithic model Zonneveld	305	244

In Figure 72 the deflection of the final precast model with foundation is shown in the x-direction. The top deflection is within the limit of (National Annex of NEN-EN 1990):

$$u_{\max} = h/500 = 202.25 \cdot 10^3 / 500 = 404.5 \text{ mm}$$

The original monolithic design of Zonneveld ingenieurs had a top deflection of 305mm in the x-direction (see Figure 74 or the literature study), which is only 5% smaller than the precast design. The monolithic design made in this thesis has a top deflection of 309.0mm (see Figure 72), providing a reduction of 4% with the precast model. The deviation between the two monolithic models can be explained by the different concrete strength class, loads, FEM-program and modelling methods which are used.

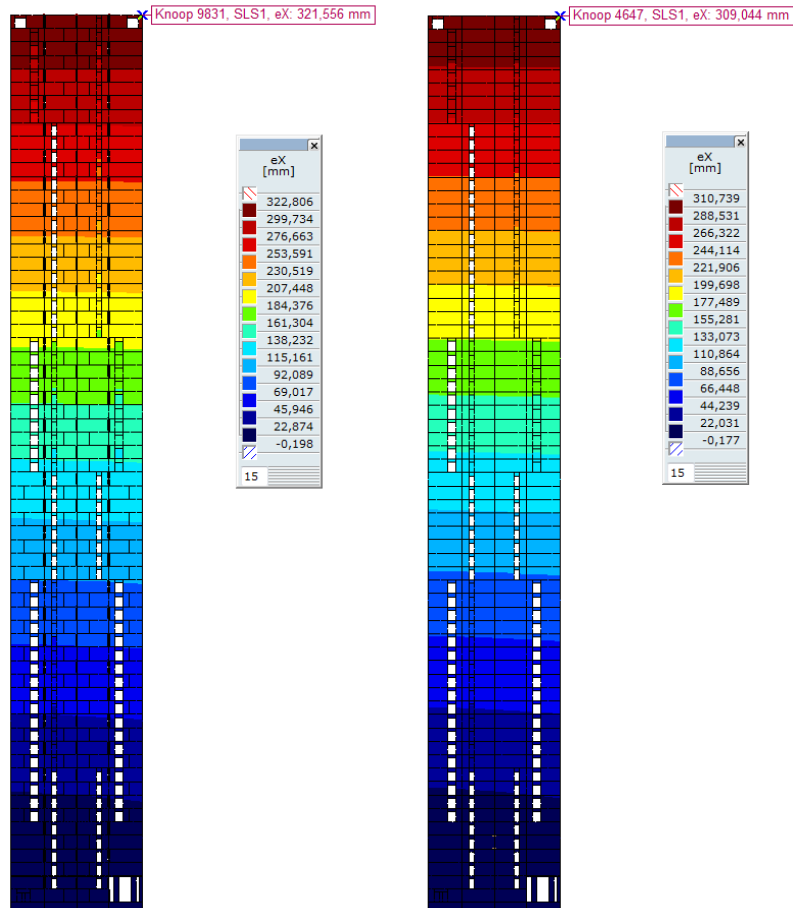


Figure 72 Deflection of the final precast (left) and monolithic (right) model with foundation in the x-direction

In the y-direction, the deflection of the precast model is slightly smaller: 292.2mm (see Figure 73). The reduced deflection (9%) with respect to the x-direction can be explained by the increased stiffness: three walls of 400mm versus two walls of 500mm. The three walls in the y-direction result in a total thickness of 1200mm, which is 20% more than the 1000mm in the x-direction.

When the precast design in the y-direction is compared with the monolithic design made in this thesis, the difference is only 0.4%: they are nearly identical. The difference between the precast design of this thesis and the monolithic design of Zonneveld ingenieurs is considerably larger: 16%. The reason for this larger difference originates in how the model of Zonneveld ingenieurs is crated and will be examined in more detail in the next paragraphs.

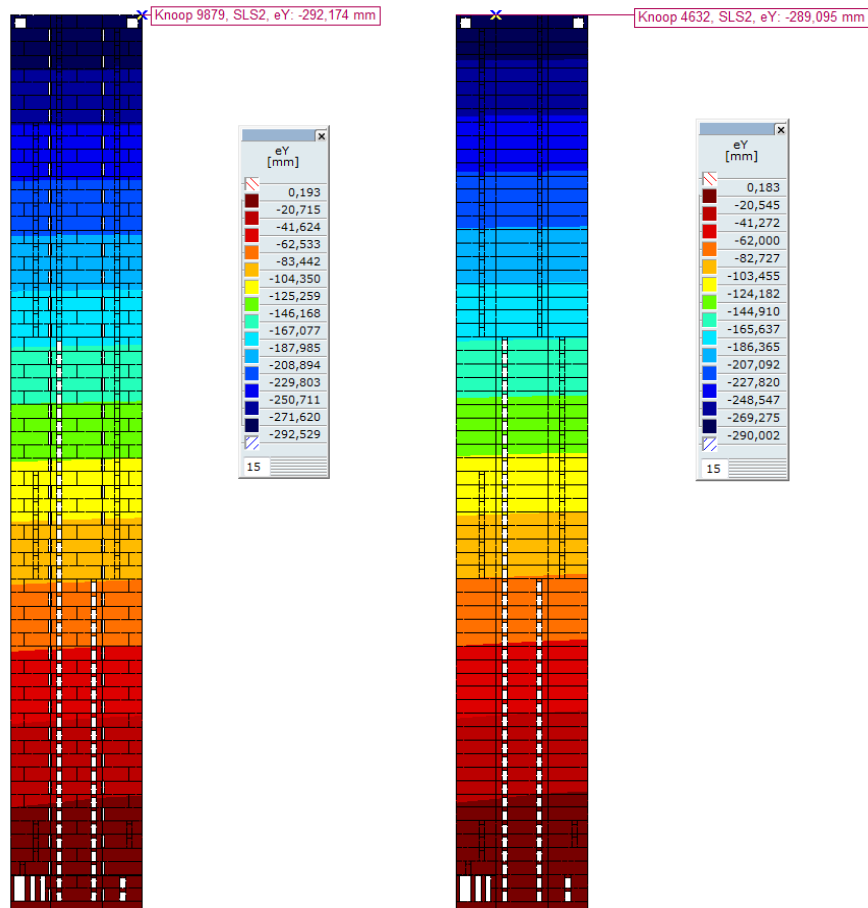


Figure 73 Deflection of the final precast (left) and monolithic (right) model with foundation in the y-direction

In the monolithic model made in this thesis, the difference in deflection between the x and y-direction is 19.9mm. This is a difference of 7%, which is slightly smaller than the 9% difference of the precast model. This small deviation between the two values is probably created by the connection between the vertical walls: at the precast wall they are only connected at a small area at the top and bottom of the element while the walls in the monolithic model are connected over the entire length.

The monolithic model made by Zonneveld ingenieurs has a deflection of 305mm in the x-direction and 244mm in the y-direction, resulting in a difference of 20%. This percentage is identical to the increased stiffness of the walls (1000mm to 1200mm). Why the differences in the precast and monolithic model made in AxisVM are only 9 and 7% can be explained by how the model of Zonneveld ingenieurs is made. In Figure 74 two large openings can be seen at the right hand side (the x and y-direction haven been reversed), while all the drawings and models made in AxisVM only contain one opening²². Therefore the difference between the x and y-direction will decrease to values comparable with the AxisVM results if only one opening is examined in the Zonneveld ingenieurs model.

With the reduced value in the x-direction, the deformations of the model made by Zonneveld ingenieurs are considerable smaller than the deformations of the monolithic model made in this thesis. The cause for this difference lies mainly within the distribution of openings (the models made in this thesis contain more openings).

²² The drawings on which this thesis is based are more recent than the drawings on which the model of Zonneveld ingenieurs is based.

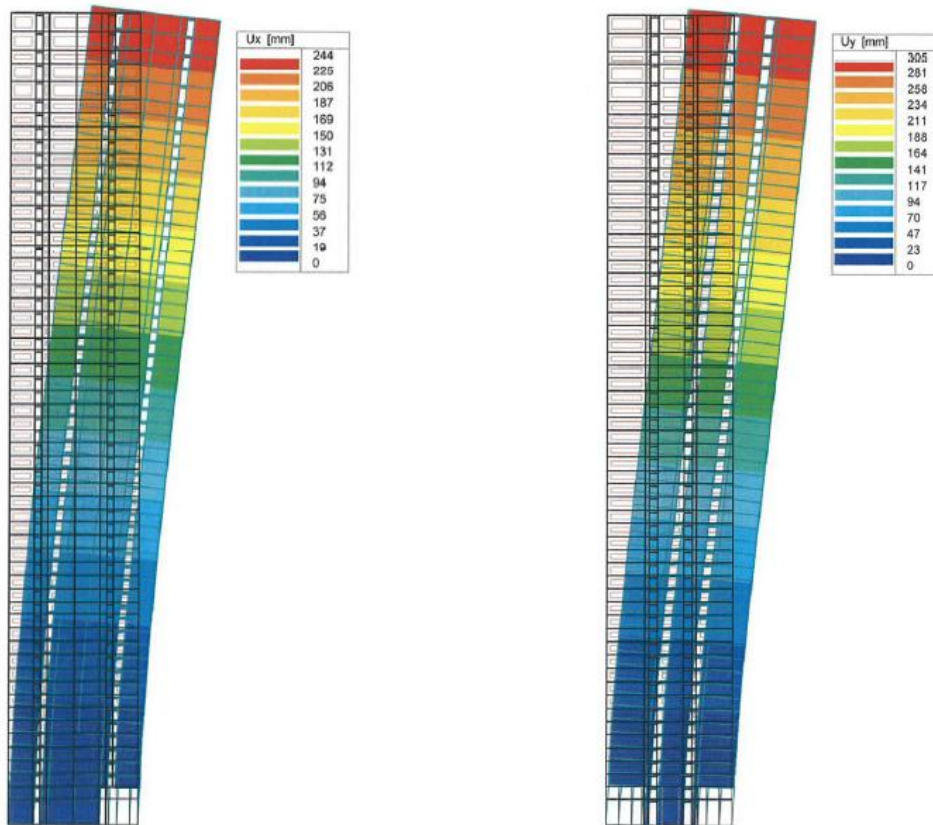


Figure 74 Deformations of the model of Zonneveld ingenieurs [Zonneveld ingenieurs 2004]

Besides the separate x and y-direction in the precast model, also a combination of the two directions has been examined. What happens if the building is loaded by 50% wind load from the x-direction and 50% from the y-direction? In this situation the orientation of the stability structure changes relative to the load, resulting in a less stiff structure. To obtain the top deflection, the following formula is used:

$$u_{\text{max,combination}} = \sqrt{u_{\text{max,y}}^2 + u_{\text{max,x}}^2} = \sqrt{156.973^2 + 167.156^2} = 229.3\text{mm}$$

This combination value is considerably lower than maximum deflection in the x or y-direction and is therefore not leading.

Aside from the wind load, the dead load of the structure and the live floor load also play an important role in the top deflection. Due to only dead and live floor load, the structure deflects 14.7mm in the x-direction and 21.2mm in the y-direction (see Figure 75). These deflections can be explained by the large openings in the walls at the lobby and the asymmetrical wall openings over the height of the building. To prevent deflections by dead load, the elements and columns can be given a small additional length at the side which deforms more. It's also advised to make the elements slightly larger since they shrink due to the dead load (elastic deformation and creep) and because of dehydration (shrinkage). As depicted in Figure 75, the building will be 57.6mm shorter than designed at the top because of elastic deformation. The creep and shrinkage effects aren't calculated and therefore this value will increase.

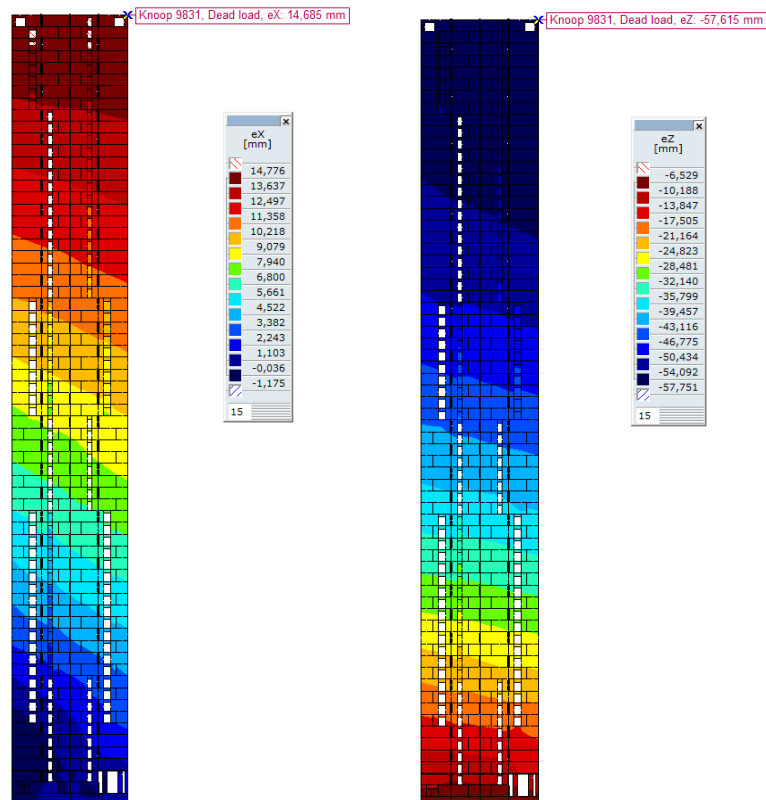


Figure 75 Horizontal deformation (left) and vertical deformation (right) due to dead load

For the deflections a different shear stiffness is used in the horizontal connections: $k_x=1.44 \cdot 10^7 \text{ kN/m/m}$ instead of $k_x=5.76 \cdot 10^6 \text{ kN/m/m}$ (see section 7.8.3). The stiffness has increased since a different slip value is applied: $s=0.4$ instead of $s=1.0 \text{ mm}$. As a result, the deflections of the precast model decrease with 3mm in the x and y-direction. This low reduction of the deflections can be explained by the already high stiffness values, resulting in a low sensitivity for changes. Furthermore, the model is mainly dominated by bending deformation and increasing the shear stiffness has nearly no influence.

9.3.3 Influence of the foundation

The foundation plays an important role in the total deflection of the building. During preliminary design, it is often assumed that one-third of the total deflections is caused by the foundation. A simple way to incorporate the foundation into the design without any knowledge of the foundation is to limit the maximum deflections from $u_{\max}=h/500$ to $u_{\max}=h/750$. In a later stage, when a preliminary design is made for the foundation, the deflections because of the rotation can be calculated. By using an very stiff foundation ($k_x=k_y=k_z=1\text{E}+7$), the influence of the foundation can be examined. Figure 76 shows the deflection with a very stiff foundation. From the original 321.6mm, the deflection has been reduced to 257.5mm, which is a reduction of 20%. This is considerable lower than the first estimation of 33%. The large diaphragm walls with a length of 60m, which are required for the load bearing capacity, provide a very large stiffness and ensure a small rotation in the foundation.

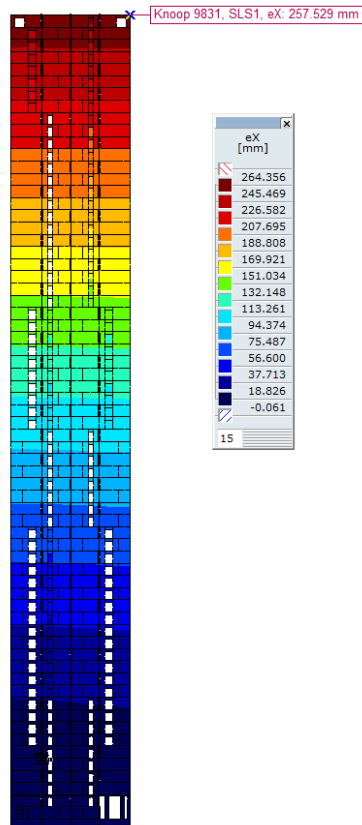


Figure 76 Deflection of the final precast model without foundation in the x-direction

In the y-direction, the difference is 18% between the model with and without foundation. The values of the monolithic model are in the same order of magnitude (18% in the x-direction and 17% in the y-direction).

The influence of the foundation will diminish even more in the actual design because the foundation slab and diaphragm walls around the circumference aren't included in this model (see section 7.11).

9.3.4 The influence of the wall reductions

During the design and analysis of the Zalmhaven tower, only a wall reduction of 500 to 400mm at wall 4 and 5 at level 27 was considered. During the examination of the cycle time, two additional wall reductions will be considered: from 400 to 300mm at wall 4 and 5 at level 45 and from 400 to 300mm at wall 1, 2 and 3 at level 27. As a result, the mass is reduced and a shorter vertical transport time is obtained. These two wall reductions aren't taken into account in the structural analysis, but in this section it will be determined what the effects are on the deformation. In Figure 77 the deflection in the x-direction is shown: 327.1mm, which is 1.8% larger than the value of Table 15. In the y-direction the deflection is 1.2% larger. It may be concluded that while the wall reductions are considerable, the increase of deformations is nearly negligible. This is because the top deflections are mainly based on the stiffness at the bottom, which isn't affected by the wall reductions.

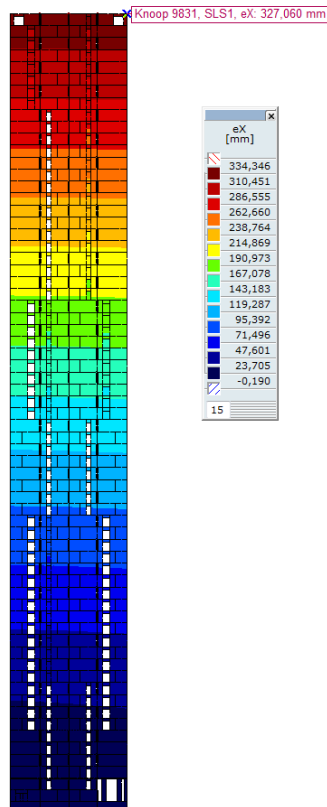


Figure 77 Deformation in the x-direction with wall reductions

9.3.5 Conclusion

From the previous sections it may be concluded that the deflections in the x and y-direction of the precast model are within the limit of $u_{max}=h/500=404.5\text{mm}$. The deflections are respectively 321.6mm and 292.2mm. Besides the precast model, also a monolithic model has been examined: 309.0mm in the x-direction and 289.1mm in the y-direction. These values are respectively 4 and 0.4% lower than the precast values. The reductions are very small and it may be concluded that the deformations of a precast structure with a masonry configuration and open vertical joints is nearly identical to a precast structure. Besides these two models, also the original design of Zonneveld ingenieurs was considered. Since this model contains several differences (mainly the openings), the result are less comparable.

Besides the separate directions, also a combination has been analysed: 50% wind load from the x-direction and 50% from the y-direction. The resulting deformation was only 229.3mm and is therefore not leading.

The dead load and live floor load also affects the deflection of Zalmhaven tower since there are large openings in the structural walls at the lobby and because the wall openings aren't distributed symmetrically over the height. As a result, the precast model will deflect 14.7mm in the x-direction and 21.2mm in the y-direction. To prevent permanent deflections from the dead load, slightly longer elements and columns can be applied. The dead load and live floor load also ensure a vertical reduction in height due to the compression force. The top floor will be 57.6mm lower than designed. Also this phenomenon can be counteracted by slightly longer elements.

During the preliminary design it's often assumed that a third of the top deflection is created by the rotation of the foundation. By comparing a model with the actual foundation stiffness to a model with a very stiff foundation, the effect of the foundation

could be analysed. The result show that at the stiff foundation of the Zalmhaven tower only increase the top deflection with 18% or 20% (x and y-direction). This is considerable lower than the assumed 33% in the preliminary stage.

By reducing the wall thickness at level 27 and 45, the costs and construction time are reduced. Since the top deflection is mainly based on the stiffness at the bottom, the wall reductions have a negligible effect.

The shear stiffness applied at the deformation calculations has nearly no influence on the results (the reduction is only 1%). The additional required work to change all the stiffness parameters of the horizontal connections isn't compensated by a large reduction. This is because the original high stiffness isn't sensitive to changes and the model is mainly dominated by bending deformation. Therefore it can be concluded that applying slip value of $s=0.4$ instead of $s=1.0\text{mm}$ is not required.

9.4 Second order effects

As a result of the first order wind deflection, the building mass is shifted away from the centre of gravity. Due to the distance between the mass and centre of gravity, a moment is created, which results in a second order deflection. Due to this second order deflection an additional third order moment is created. The higher order deflections decrease rapidly and therefore only the first and second order deflections are calculated. Usually the second order effects are small (smaller than 10%), but in extreme cases a high second order effect may lead to structural failure. In the preliminary design stage the effects can be calculated with simple formulas, providing insight in the behaviour of the structure. After the calculation model is created, the assumed second order effects have to be verified. This section will start with the second order calculation already made in the literature study.

9.4.1 Hand calculation of the second order effects

During the literature study the second order effects of the original design were examined. Since the structural layout hasn't changed, the calculation is still valid. Due to the increased mass of the structure the magnification factor will increase. The following formula is used to obtain the second order effects:

$$\frac{1}{F_{\text{crit}}} = \frac{H}{2C} + \frac{H^2}{8EI} + \frac{1}{2GA}$$

in which:

- F_{crit} is the critical load which is used to calculate the second order effects,
- H is the building height,
- C is the rotation stiffness of the foundation,
- EI is the bending stiffness of the building,
- GA is the shear stiffness of the building.

With the values calculated during the literature study, the following critical force is obtained:

$$\frac{1}{F_{\text{crit}}} = \frac{202.5}{2 * 8.52 * 10^9} + \frac{202.5^2}{8 * 2.17 * 10^7 * 3.05 * 10^3} + \frac{1}{2 * 9,04 * 10^6 * 6,41 * 10^1} = 8.8 * 10^{-8} \text{ [kN}^{-1}\text{]}$$

This results in $F_{\text{crit}}=11337417.4\text{kN}$. Now the factor n can be calculated. Due to the larger mass, the new value will be smaller than the original value calculated during the literature study (13.37):

$$n_k = \frac{F_{crit}}{F_{total,k}} = \frac{11337417.4}{964144.25 + 53087.91} = 11.15$$

The magnification factor for SLS calculated in the literature was 1.08. The new magnification factor becomes:

$$n/(n-1) = 11.15/10.15 = 1.099$$

The factor n for ULS can be calculated with (was 10.1 during the literature study):

$$n_d = \frac{F_{crit}}{F_{total,d}} = \frac{11337417.4}{1.3 \cdot 964144.25 + 1.65 \cdot 53087.91} = 8.45$$

The magnification factor for the ULS becomes $n/(n-1) = 8.45/7.45 = 1.13$. In the literature study a value of 1.11 was obtained.

The SLS magnification factor is within the limit of 10%, but the ULS factor is just outside the boundary. Since this preliminary calculation is based on estimations, a second order effect of 10% was assumed. To incorporate the second order effects in a linear calculation, the wind load is increased by 10%. The verification has to show whether this assumption is reasonable. It should be noted that increasing the wind load by the second order magnification factor may provide an accurate deflection value, but this also increases the horizontal load. Therefore the horizontal reaction force is overestimated by the second order factor. If a non-linear calculation is performed, this additional deflection is created by the eccentrically dead load, which doesn't create a horizontal reaction force.

9.4.2 Verification of the calculated second order effects

Since the calculations of the previous section only provide basic insight in the behaviour of the structure, a geometrical nonlinear-elastic static calculation was conducted. This calculation includes the second order deflection, geometrical imperfections of the structure and the computed response is nonlinearly related to the applied loads.

First the second order effects are determined for the SLS. Only the x-direction is examined, since this direction contains the largest deformations (lower stiffness of the structure). To obtain the multiplication factor for the second order, the deformation of the geometrical nonlinear calculation is divided by the linear deformation:

$$\text{Second order effect in SLS} = \frac{n}{n-1} = \frac{u_2}{u_1} = \frac{343.3}{321.6} = 1.07$$

This factor is 0.03 lower than the value calculated in the previous section. During the preliminary calculations, a second order effect of 1.1 was assumed instead of 1.07 because of uncertainties. After the nonlinear calculation it may be concluded that the deformations are overestimated due to this decision.

The second order effects were also examined in the ULS. For this comparison ULS1 (see section 5.5) is used and only the x-direction is analysed. The following magnification factor in ULS is obtained:

$$\text{Second order effect in ULS} = \frac{n}{n-1} = \frac{u_2}{u_1} = \frac{583.9}{532.2} = 1.0971 = 1.10$$

The ULS magnification factor is just within the limit of 10% and the assumed value of 1.13 during the preliminary stage is too large. While the deformations are slightly overestimated because of the second order effects, the forces in the elements aren't.

The fact that the SLS and ULS factor calculated by AxisVM are lower than the values of the hand calculation can be explained by the more exact calculation. For example, the foundation stiffness and the stiffness of the structure are based on estimations in the hand calculation.

An important remark should be made: the second order calculation is performed with the original model which contains the second order effect already in the wind load. Therefore the first order deflection is 10% too large (there is a linear relation between the wind load and deflection), resulting in a larger second order moment. Therefore the second order effect is slightly overestimated. A second overestimation is made by the geometrical imperfections included in this analysis. According to section 5.2 (3) of NEN-EN 1992-1-1, this isn't required for the SLS, only for the ULS. Therefore the actual SLS factor will be reduced even more. Another second order calculation is required to examine the magnitude of the two overestimations. Since a smaller second order effect won't have any negative influence on the results, this will be reserved for a future optimisation phase which is not included in the thesis.

9.4.3 Conclusion

After the FEM verification calculations, it can be concluded that the second order effects are smaller than 10%: in SLS the magnification factor is 1.07 and in ULS 1.10. Since a magnification factor of 1.10 was assumed in the preliminary phase (applied at the wind load), the deformations are slightly overestimated. As a result, more safety is available in the SLS, which may be beneficial during the optimisation phase. In the ULS, the load on the elements increases due to the additional second order moment. The calculated value is almost identical to the estimated value applied in the wind load and therefore no additional safety is available above the already applied safety factors.

It should be noted that the second order effects calculated by AxisVM are slightly too large: the calculation is performed with the original model including a 10% larger wind load. During the optimisation phase another second order calculation should be performed without the increased wind load.

9.5 Shear lag

The Euler-Bernoulli beam theory is often used for beam analyses and is based on two important assumptions: the material is linear elastic and plane sections remain plane. According to these assumptions, stresses as a result of bending should be linearly distributed, as shown in Figure 78 (a). However, this assumption only holds when there is no shear force in the beam or when the beam has an infinite shear stiffness. In reality, a shear force is always present in combination with a finite shear stiffness. Therefore the beam will always be subjected to shear deformation. Because of this shear deformation, the longitudinal deformation in the centre of the beam will lag behind the longitudinal deformation at the outer fibre of the beam and the stresses increase quadratically instead of linear. In Figure 78 (b) an example is given of a stress distribution subjected to shear lag. Due to these stress concentration areas near the outer fibre of the beam, problems might occur with the resistance of the used materials.

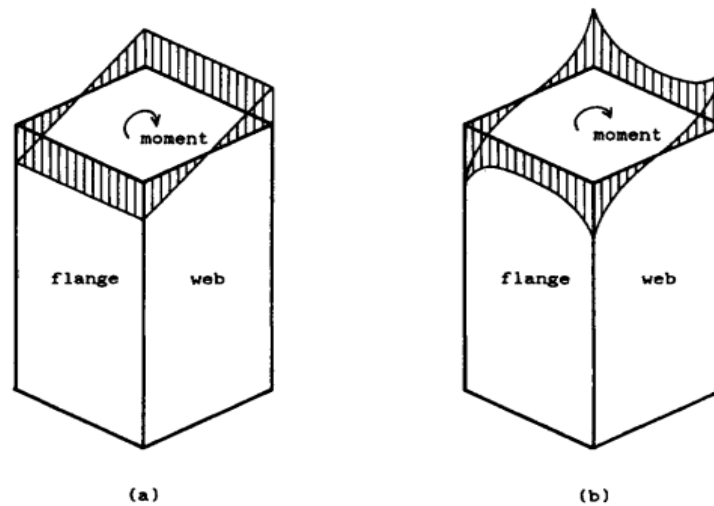


Figure 78 Axial stress distribution in a beam structure: (a) no shear lag: (b) shear lag [Kwan, 1996]

Therefore several models will be analysed to examine the effects of shear lag:

- a precast 2D wall without any openings,
- a precast 2D wall with openings,
- a precast 3D model without openings,
- a precast 3D model with openings.

During the literature study it was already concluded that the strength class of the concrete has a small effect on the amount of shear lag. Besides the strength class, the foundation also plays an important role in the shear stress distribution. This will be elaborated in more detail in the following sections.

9.5.1 Shear lag in a precast 2D wall without openings

The first wall which will be examined is the precast 2D wall without openings. The element configuration is based on wall 4 of section 4.3.2. The normal stiffness is identical to the surrounding concrete (see section 7.8.2) and a high shear stiffness (see section 7.8.3) is applied at the horizontal connections. The vertical connections are left open. Furthermore, a mesh size according to the height is used (250mm at the bottom and 750mm at the top, see section 7.6.2). At first the wall is clamped at the foundation. When the wall is loaded by wind, Figure 79 is obtained.

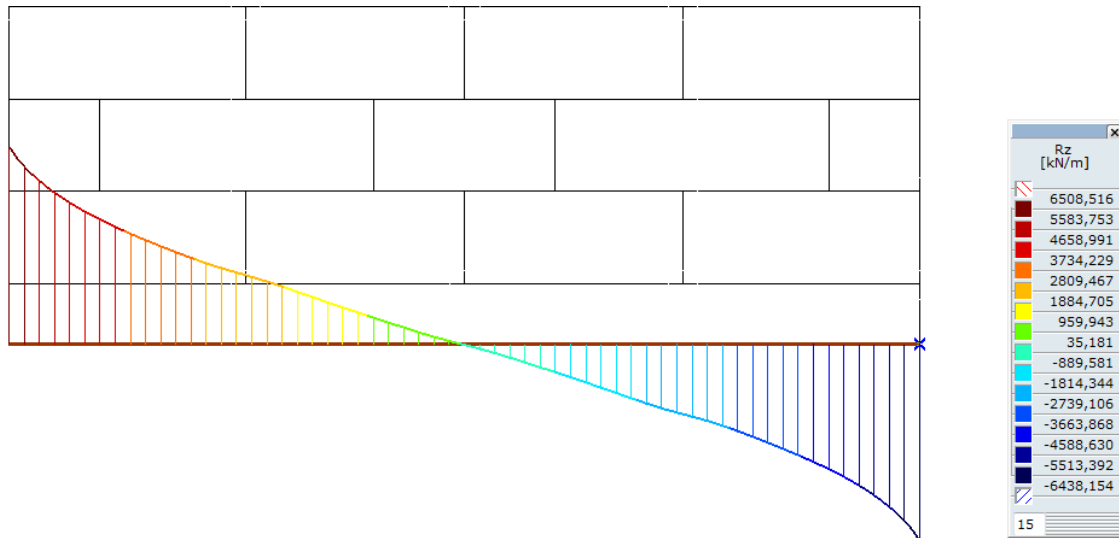


Figure 79 Force distribution as a result of wind load in a 2D precast wall without openings (stiff foundation)

The increase of reaction force towards the outer fibres is clearly visible. When a linear distribution is considered²³, it can be calculated that the reaction force increases with 23% at the outer fibre due to shear lag. The shear lag effect is also visible at the normal force distribution due to dead load. In Figure 80 the normal force increases with 29% towards the edge of the structure.

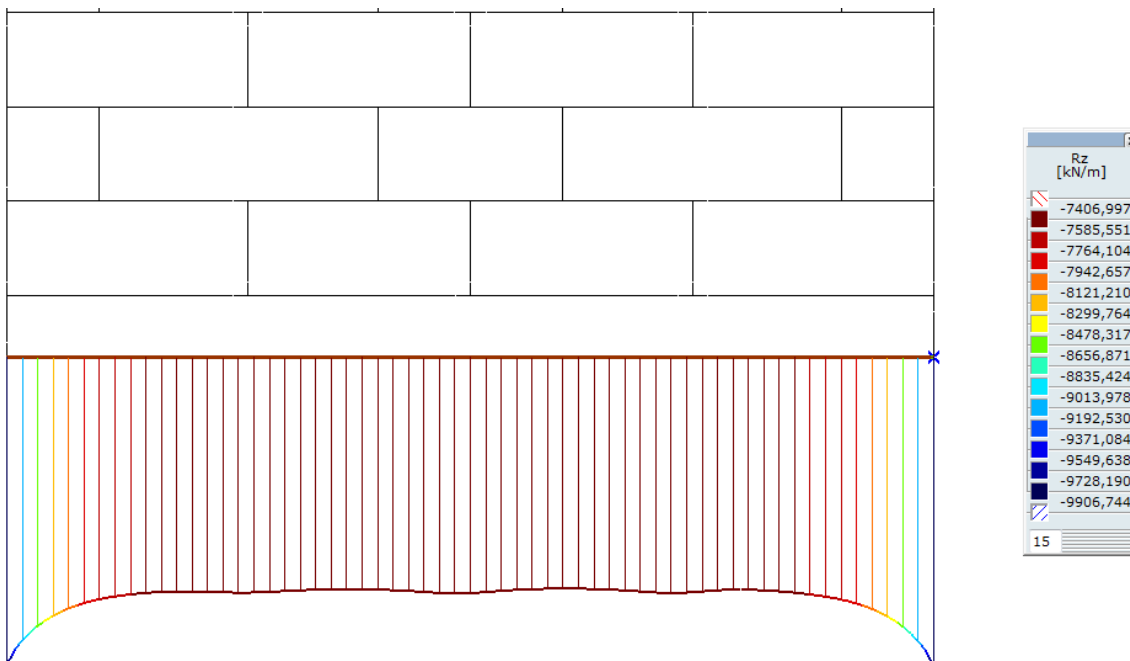


Figure 80 Force distribution as a result of dead load in a 2D precast wall without openings (stiff foundation)

The previous two figures used a stiff foundation as support. When the actual foundation stiffness of $k_{\text{foundation}}=697190\text{kN/m}$ is entered (see section 7.11), the shear lag effect changes considerable. Figure 81 depicts a nearly linear distribution and the normal force as a result of the wind load only increases with 4% due to shear lag.

²³ Based on the section forces at the foundation, the linear distribution can be obtained.

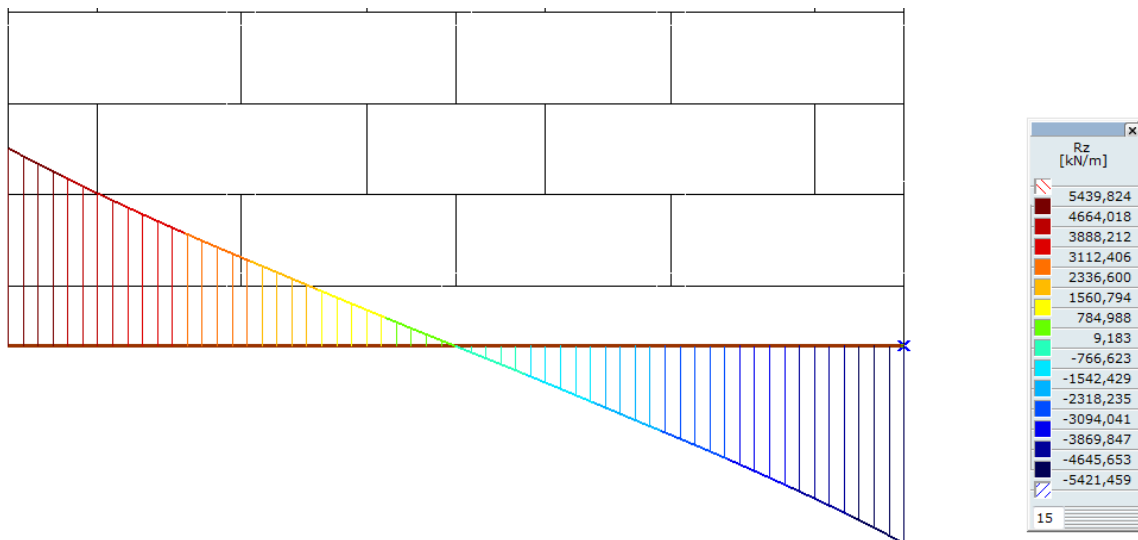


Figure 81 Force distribution as a result of wind load in a 2D precast wall without openings

This difference can be explained by the stiffness of the foundation. When a stiff foundation is applied, the peak forces near the edge are absorbed without deformations: the corner is able to take up large forces. When the stiff foundation is replaced by the actual foundation, small deformations may occur, resulting in a redistribution of the forces. This redistribution is also visible in Figure 82. At the edge, the normal force only increases with 5% due to shear lag.

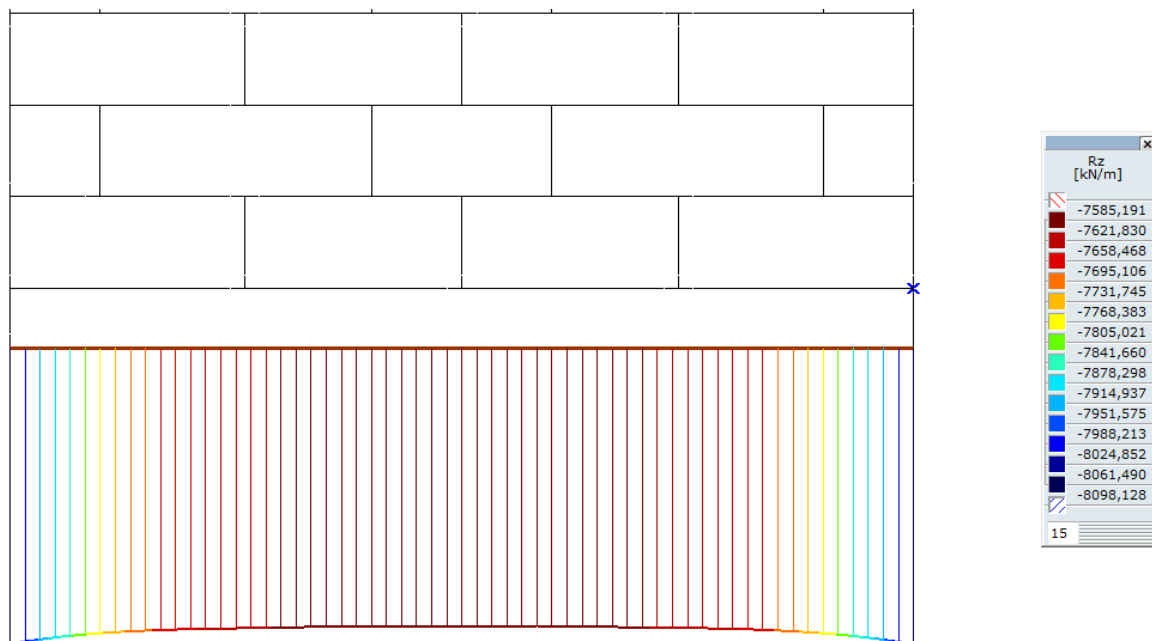


Figure 82 Force distribution as a result of dead load in a 2D precast wall without openings

9.5.2 Shear lag in a precast 2D wall with openings

When the openings are added to the precast 2D wall, the distribution of forces changes noticeable compared to the wall without openings. Figure 83 shows a large disruption on the right hand side of the foundation. Due to the openings, the linear distribution of forces is slightly affected, increasing the shear lag effect.

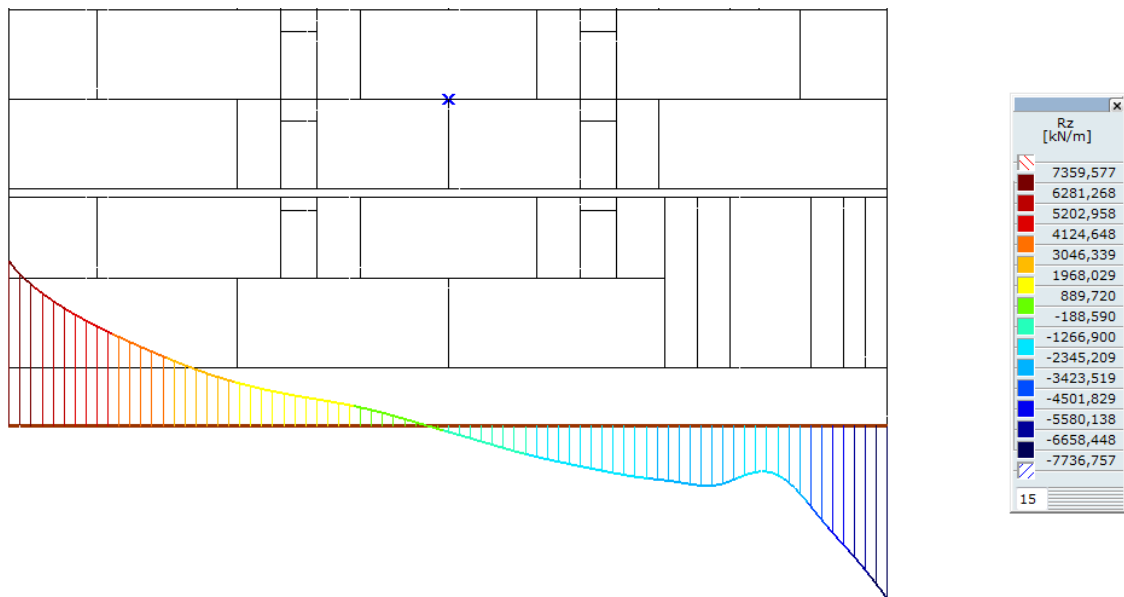


Figure 83 Force distribution as a result of wind load in a 2D precast wall with openings (stiff foundation)

The large disruption at the lobby has almost disappeared in Figure 84. Due to shear lag, the normal force as a result of wind load increases with 6%. This is slightly more than the 4% of the closed model in Figure 81 and this difference is created by the non-linear distribution.

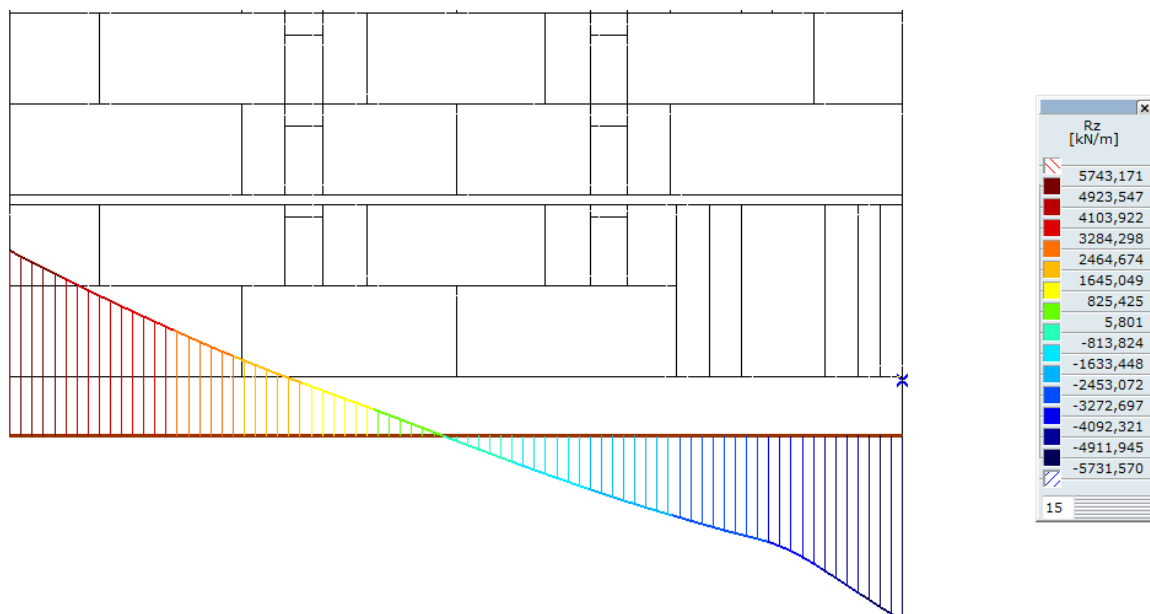


Figure 84 Force distribution as a result of wind load in a 2D precast wall with openings

In Figure 85 the normal force as a result of dead load is shown. Again a peak force area can be distinguished on the right hand side of the stiff foundation model. By replacing the stiff foundation by the actual foundation this peak area is reduced. At the corners, the normal force increases with 7% due to shear lag. This value is slightly larger than the 5% of Figure 82.

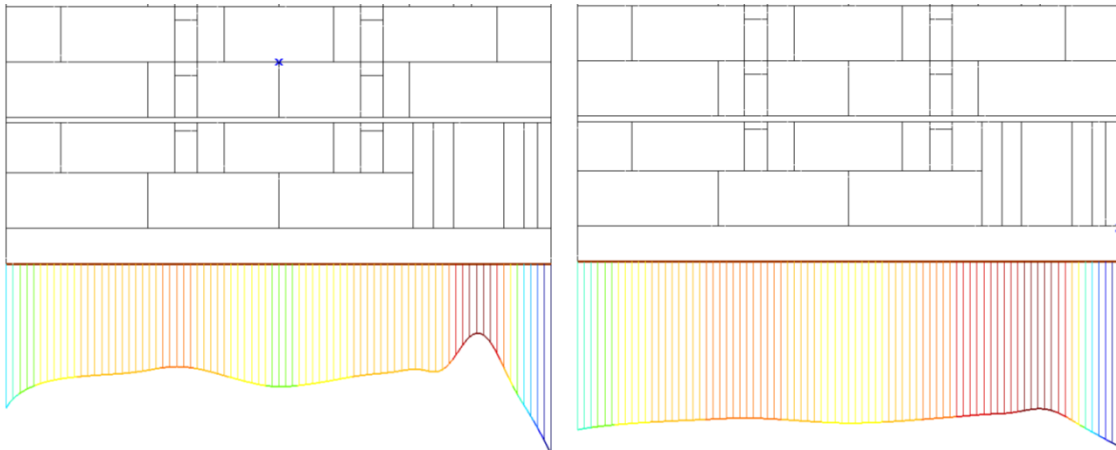


Figure 85 Force distribution as a result of dead load in a 2D precast wall with openings and stiff foundation (left) and actual foundation (right)

9.5.3 Shear lag in a precast 3D model with and without openings

The distribution of forces obtained at the precast 2D wall with and without openings also holds for the 3D model. Figure 86 shows the normal force distribution due to wind and dead load in a 3D model without openings and a stiff foundation. The shear lag effect is clearly visible.

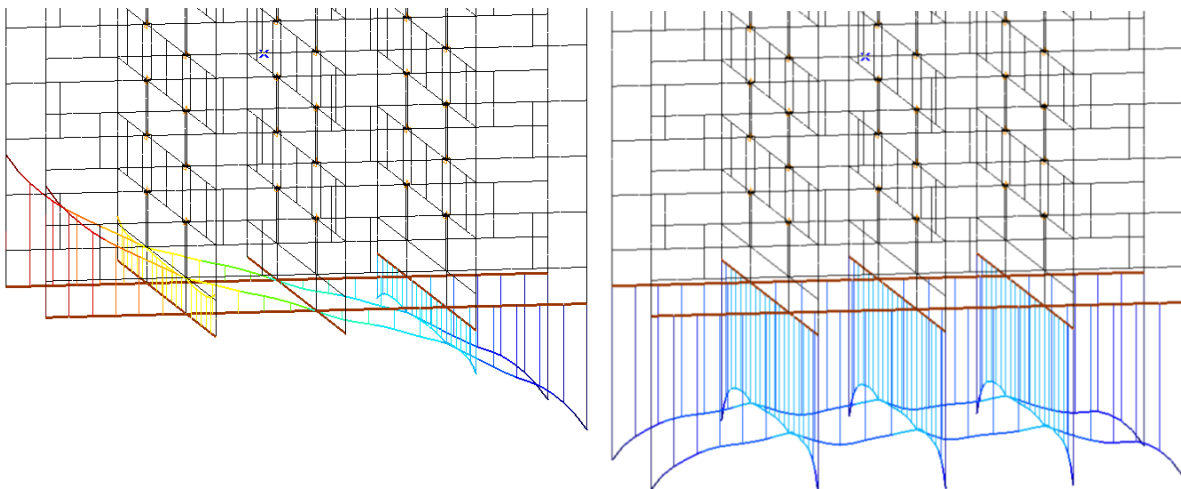


Figure 86 Force distribution as a result of wind load (left) and dead load (right) in a 3D precast model without openings (stiff foundation)

Modelling the actual stiffness ensures that the normal force due to wind load only increases with 7% at the outer fibre of the structure as a result of shear lag. The dead load increases with 8% due to shear lag. In Figure 87 the results are depicted.

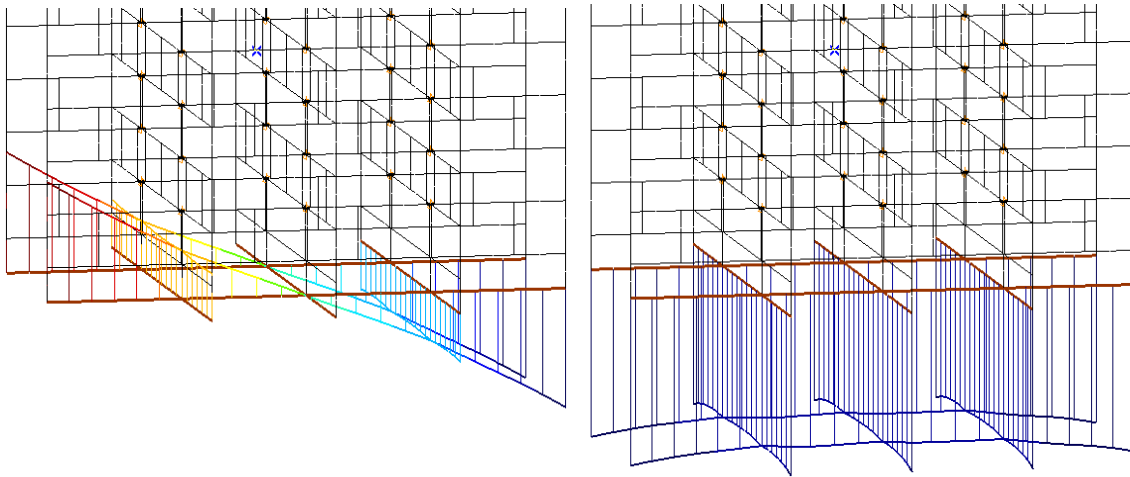


Figure 87 Force distribution as a result of wind load (left) and dead load (right) in a 3D precast model without openings

When the 3D model with openings is considered, several disruptions can be distinguished in Figure 88. Just as with the 2D wall with openings, the disruptions almost disappear completely when the actual stiffness is entered in the model, see Figure 89.

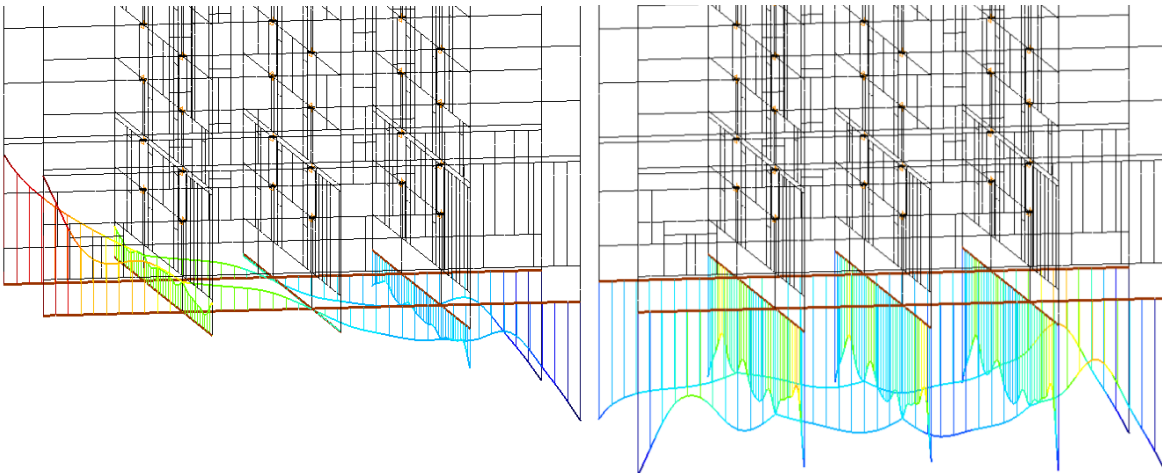


Figure 88 Force distribution as a result of wind load (left) and dead load (right) in a 3D precast model with openings (stiff foundation)

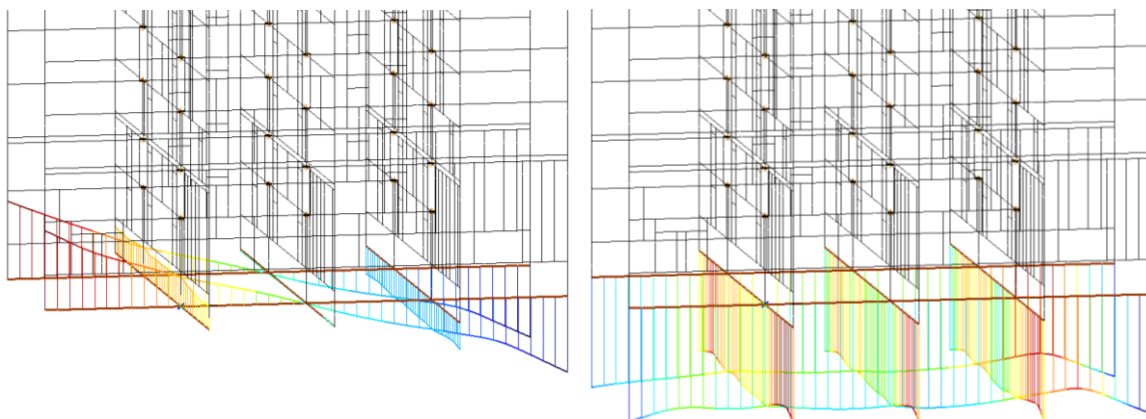


Figure 89 Force distribution as a result of wind load (left) and dead load (right) in a 3D precast model with openings

Modelling the actual stiffness ensures that the normal force due to wind load only increases with 8% at the outer fibre of the structure as a result of shear lag. The dead load increases with 10% due to shear lag.

All the models show an increase of forces of maximum 10% due to shear lag when the actual foundation stiffness is used. During the literature study it was noted that forces may increase up to 50%. The high shear stiffness of this structure (the masonry configuration in combination with the low amount of openings in the walls) ensures that the shear lag is limited at 10%.

9.5.4 Conclusion

When all the previous models are compared, it can be concluded that shear lag is mainly a problem at structures that contain a very stiff foundation and a low shear resistance. The models of the Zalmhaven tower show that compared to a linear distribution, the actual normal forces might increase up to 10%. This is very interesting, since the Zalmhaven tower is supported by 60m long diaphragm walls, which create a rather stiff foundation. Apparently, the stiffness isn't too high to create large shear lag effects.

A maximum shear lag effect of 10% is an acceptable value. It's interesting to know how large this increase in force is, since a very large shear lag effect may endanger the capacity of the materials. The small disruptions that are still visible in Figure 89 will not be present at the end of the foundation. This is due to the distribution effect of the diaphragm walls underneath the foundation slab and structural walls. The diaphragm walls can be seen as structural walls in the ground without openings until a depth of 60m below NAP.

9.6 Structural factor and acceleration of the building

With the desire to construct higher buildings, the dynamic effects become more important. Taller buildings are more sensitive to wind load and vibrations induced by wind load may be experienced as uncomfortable by the occupants. Therefore requirements are included in the standards which limit the intensity of vibrations in the SLS. Besides the comfort requirements, the fluctuating wind load also has an effect on the maximum value of the loads: due to the dynamic behaviour of the building, the loads may be larger than the loads created by a quasi-static behaviour. To incorporate this in the standards, the quasi-static load is increased with a dynamic factor in the ULS: c_d . If the requirements aren't met or errors are made, large financial losses may be expected (structurally but also with respect to the comfort).

During the literature study, the standards were analysed very thoroughly. Since no design was made, the existing monolithic design was examined. The calculations resulted in a structural factor of $c_s c_d = 1.11$ and an acceleration of $a_{tot} = 0.081 \text{ m/s}^2$. The structural factor is larger than 1, resulting in a magnification. Now that the design has been made, the results have to be verified.

9.6.1 Verification of the structural factor $c_s c_d$ and acceleration a_{tot}

In the literature study an extensive analysis of the structural factor and the acceleration can be found. In this chapter the most important findings of this analysis are recapitulated and the new structural factor and acceleration value are calculated. This section will start with the findings:

- The mass of the building is one of the aspects which determine the frequency of the vibrations: a high mass results in a low frequency. In the NEN 6702 it's allowed to use the dead load and instantaneous live load as building mass. In the

NEN 1991-1-4, only the dead load may be used (see Annex F.5 (3), μ_e). This is an interesting aspect since if there is no live load, there are also no occupants inside the building. Therefore no one will experience the vibrations. Besides this peculiarity, the dynamic factor does influence the load, also when there are no occupants inside.

- The magnification factor Φ_1 of NEN 6702 uses a damping value of $D=0.02$ for concrete buildings. When the accelerations are examined (Φ_2), this factor is reduced to $D=0.01$ (if $f_e < 1\text{Hz}$). In NEN-EN 1991-1-4, the damping is described by the logarithmic decrement δ , which is 0.1 for concrete buildings. The damping value of NEN 6702 can be rewritten to a logarithmic decrement value by the following formula: $\delta = 2 \cdot \pi \cdot D = 2 \cdot \pi \cdot 0.01 = 0.063$. But the Eurocode uses $\delta = 0.1$, which is 59% higher the value from the NEN 6702. It may be concluded that the Eurocode utilises a higher damping value, resulting in a lower acceleration.
- To calculate the structural factor, the first natural building frequency is required. Annex F2 of NEN-EN 1991-1-4 provides an easy equation to calculate the frequency (multi-story buildings with a height larger than 50m): $n_1 = 46/h$ [Hz]. But this easy equation is inaccurate, resulting in an incorrect structural factor. Therefore it's advised to use the equation of NEN 6702, section A4: $f_e = \sqrt{a/\delta}$. This equation incorporates more structural effects and provides a more accurate approximation of the natural frequency.
- The load on the main load bearing structure is determined by the pressure distribution on the outer shell. This pressure distribution consists out of a wind trust multiplied by a form factor. In the NEN 6702 a form factor of $0.8 - (-0.4) = 1.2$ was applied regardless of the building seize. In the EN 1991-1-4, the form factors are depending on the slenderness of the building. For example: at a slenderness of $h/d > 5$, a form factor of 1.3 has to be applied. Therefore the form factor increases with 8% at the Zalmhaven tower ($h/d = 202.25/30 = 6.74$).

With these aspects in mind and the structural values of the precast design, the new structural factor and acceleration can be determined. First the natural frequency will be calculated:

$$f_e = \sqrt{a/\delta} \text{ [Hz]}$$

in which:

- a is the numerical value of the oscillation acceleration, depending on the static system and distribution of the mass: $a = 0.384\text{m/s}^2$
- δ is the numerical value of the largest deformation of the structure as a result of the instantaneous load combination.

The deformation δ can be calculated with the following equation:

$$\delta = \frac{M \cdot l}{C} + \frac{M \cdot l^2}{4EI}$$

in which:

- M is the moment as a result of the dead load and instantaneous live floor load placed vertical²⁴, according to the load combination of section 6.3.5.2 of NEN 6702:

$$q = \frac{G_{rep} + \psi Q_{rep}}{l}$$

$$M = \frac{1}{2}ql^2$$

²⁴ By placing the vertical load horizontally, a large deflection is obtained. The wind load isn't considered in this calculation.

in which:

G_{rep} is the dead load

ψ is the correction factor for the instantaneous live load

Q_{rep} is the instantaneous live floor load.

l is the height of the structure

C is the rotation stiffness of the foundation

EI is the bending stiffness of the structure.

In appendix E.2, the calculation sheet can be found. According to this calculation, a natural frequency of $f_e = 0.151\text{Hz}$ is obtained. According to section A.5 of NEN 6702, this value may be multiplied by a factor $(1+20/h)$:

$$f_{e,corrected} = f_e \cdot (1 + 20/h) = 0.151 \cdot (1 + 20/202.25) = 0.165\text{Hz}$$

This value is substantial lower than the value calculated using NEN-EN 1991-1-4, section F.2:

$$n_1 = \frac{46}{h} = \frac{46}{202.25} = 0.227\text{Hz}$$

As a result of the lower eigenfrequency, the acceleration and structural factor will increase.

With the eigenfrequency, structural mass, building height and width, the structural factor and acceleration can be calculated. The calculation sheet which is used is shown in appendix E.2 and the following results are obtained:

$$c_s c_d = 1.111, a_{\text{parabolic,bending}} = 0.050\text{m/s}^2 \text{ and } a_{\text{torsion}} = 0.062\text{m/s}^2$$

A parabolic mode shape is chosen for the bending acceleration since this provides the most accurate approximation of the behaviour of the Zalmhaven tower. The linear mode shape should be applied when shear deformation is leading instead of bending. To acquire the total acceleration, the bending and shear values have to be combined as following:

$$a_{\text{total}} = \sqrt{a_{\text{parabolic,bending}}^2 + a_{\text{torsion}}^2} = \sqrt{0.05^2 + 0.062^2} = 0.080\text{m/s}^2$$

At a frequency of 0.165Hz, the acceleration of 0.080m/s² is allowable according to Figure 90. At a frequency of 0.165Hz, the acceleration may go up to 0.18m/s², but in practise the value is limited at 0.15m/s² for residential high-rise buildings.

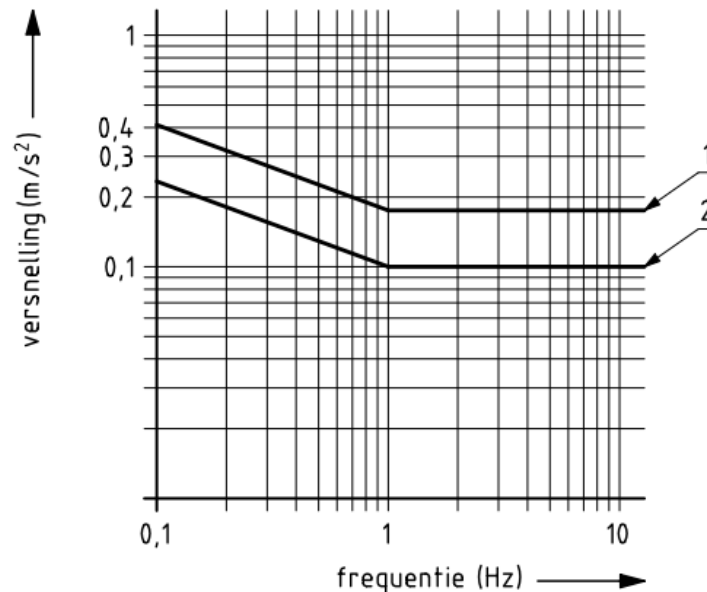


Figure 90 Comfort criteria for Dutch office buildings (1) and residential buildings (2) [NEN 6702]

It's an interesting aspect that a high-rise tower of 202.25m satisfies the requirements so easily since generally the accelerations are a leading aspect. The main reason for this low acceleration of the Zalmhaven tower can be ascribed to the structural material and the high dead load. The connections between the precast elements will also have a beneficial influence on the damping since they dissipate energy. It's estimated²⁵ that a precast structure may have a logarithmic decrement value up to $\delta=0.15$ instead of $\delta=0.10$. Since no research is available on this aspect to validate this assumption, the value of $\delta=0.10$ is maintained.

9.6.2 Conclusion

During the extensive analysis of the NEN-EN 1991-1-4 in the literature study, several interesting aspects have been discovered. For example:

- In the Eurocode it's not allowed to incorporate the live floor load in the acceleration calculation. This is remarkable since if there is no live floor load, there are commonly also no occupants present. Adding the live load will reduce the acceleration with approximately 4% (depending on the parameters).
- With the introduction of the Eurocode, the damping value D has been replaced by the logarithmic decrement value δ . But a damping value of $D=0.01$ results in a 59% lower logarithmic decrement value than assumed in the Eurocode. In other words: the Eurocode provides much more damping than the NEN 6702.
- In the NEN 6702 an accurate set of equations is available to calculate the first natural frequency. In the NEN-EN 1991-1-4, this has been replaced by a very simple and inaccurate equation. Because of these properties, it's advised to apply the equations of the NEN 6702.
- A constant form factor of 1.2 was applied at the NEN 6702. By incorporating the slenderness, the NEN-EN 1991-1-4 provides more realistic values. For high-rise buildings, this often results in a higher form factor (1.3 instead of 1.2).

²⁵ This estimation is made by dr.ir. R.D.J.M. Steenbergen from TNO during a consult on the dynamic properties of the Zalmhaven tower.

9.7 Reinforcement design

Until now, only global aspects have been discussed. In this section, two local aspects are examined: the reinforcement design of a lintel and a wall element. By choosing the correct location, an upper limit is obtained for the reinforcement design of all the lintels and wall elements.

9.7.1 Location of the lintel and wall element

Figure 91 shows the location of lintel and wall element. These two specific elements are chosen since they contain the highest representable moment and shear force. Therefore, the obtained reinforcement design will be an upper limit for all the other lintels and wall elements. To reduce the production costs of the elements, the reinforcement ratio may be decreased at a higher floor level until the practical reinforcement ratio is achieved²⁶. Reducing the reinforcement ratio or concrete strength class is often more attractive than reducing the element thickness because of repetition.

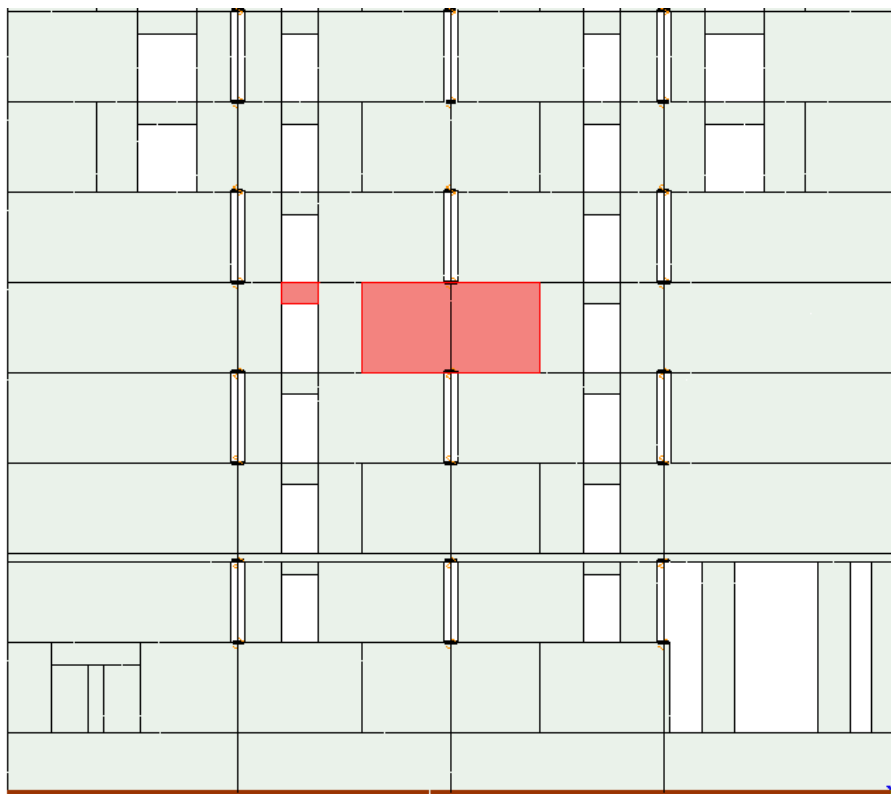


Figure 91 Location of the lintel and wall element

9.7.2 Model scheme

For this analysis, the final precast model is used with foundation. All the properties which have been assigned to the model can be found in 9.3.1 section. The only difference between the two model schemes is the load combination: the deflections are calculated in SLS while the reinforcement is calculated in the ULS. In this section load combination ULS1 will be applied: $1.3 \cdot \text{dead load} + 1.65 \cdot \text{wind load} + 1.65 \cdot \psi \cdot \text{live load}$ (see section 5.5).

²⁶ The practical reinforcement ratio is higher than the minimal reinforcement ratio, which prevents brittle cracking.

9.7.3 Reinforcement design of the lintel

The design will start with the lintel. Based on the FEM calculations, the lintel is loaded with the forces shown in Figure 92. The three diagrams are consistent with the deformation of the lintel. The lintel is 1250mm long, 750mm high and 500mm thick.

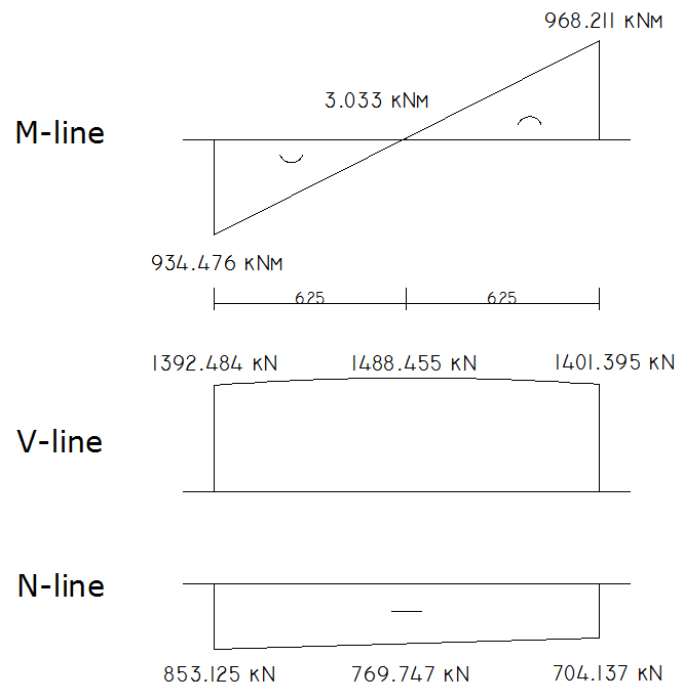


Figure 92 Forces in the lintel

The normal force in this lintel results in a compression stress of 2.23N/mm^2 . Since the compression stress is relatively low compared with the shear force and bending moment, it's assumed that there is no normal force during the shear force and bending moment calculations. As a result, the reinforcement calculation for this lintel will be conservative since the normal force has a positive influence.

The bending moment in Figure 92 is determined at the end of the lintel. In reality, the bending moment might still increase at the wall (there is a minimal connection length). Therefore the moment is increased with 25% (comparable to a corbel). This results in a bending moment of 1210.3kNm. The shear force decreases towards the ends and is not increased by 25%.

Bending moment reinforcement design of the lintel

Figure 92 shows a linear bending moment distribution. Therefore the reinforcement has to be applied at the bottom and at the top of the lintel. Based on $M_{Ed}=1210.3\text{kNm}$, the reinforcement ratio can be determined with the GTB 2010 tables. Table "11.10 bending without normal force at a rectangular cross section" is used.

Properties for the calculation:

- concrete strength class: C90/105,
- environmental class: XC2,
- minimum cover²⁷: $c_{min} = c_{min,dur} + \Delta c_{dev} = 25 + 5 = 30\text{mm}$.

With these values the effective height can be determined²⁸:

$$d = h - \left(\frac{3}{2} \phi + \phi_{stirrup} + c \right) = 750 - \left(\frac{3}{2} \cdot 25 + 16 + 30 \right) = 666.5\text{mm}$$

With table 11.10 of GTB 2010, the reinforcement ratio can be determined:

$$\frac{M_{Ed}}{b d^2} = \frac{1210.3}{0.5 \cdot 0.6665^2} = 5449 \rightarrow \rho = 1.33\%$$

This results in a minimum reinforcement area of:

$$A_s = \rho \cdot b \cdot d = 0.0133 \cdot 500 \cdot 666.5 = 4432\text{mm}^2$$

With 10x $\Phi 25$ a reinforcement area of 4909mm² is obtained ($\rho=1.46\%$). In Figure 93 the reinforcement layout is depicted. Due to the minimal diameter of the curved stirrups ($4 \cdot \Phi_{stirrup}$), the corner reinforcement is moved to the centre of the lintel. The anchor length of the stirrups is minimal $10 \cdot \Phi_{stirrup} = 140\text{mm}$.

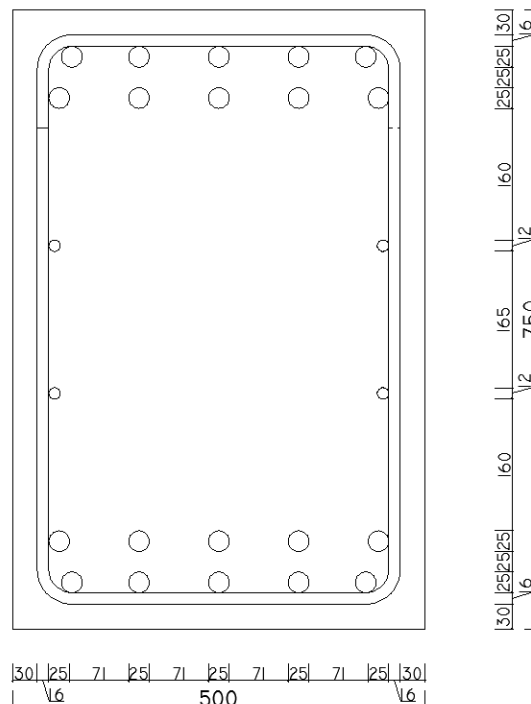


Figure 93 reinforcement layout of the lintel

A total reinforcement ratio in the lintel of 2.92% is not very high for a building of 202.5m. At the bottom lintels, reinforcement ratios up to 4% are applied in lower buildings. It may therefore be concluded that there are possibilities for further optimisation. For example: a lower concrete strength or thinner elements.

²⁷ Based on the structural class S4 and the national annex.

²⁸ 3/2 is used instead of 1/2 since two rows of reinforcement are required.

Shear force reinforcement design of the lintel

According to 6.2.2 of NEN-EN 1992-1-1, the shear force capacity can be determined with the following equation:

$$V_{Rd,c} = [C_{Rd,c}k(100\rho_l f_{ck})^{1/3} + k_1\sigma_{cp}]b_w d$$

in which:

$V_{Rd,c}$ is the shear resistance,

$C_{Rd,c} = 0.12$,

f_{ck} is the characteristic compression strength,

$k = 1 + \sqrt{\frac{200}{d}} \leq 2.0$ with d in mm,

$\rho_l = \frac{A_{sl}}{b_w d} \leq 0.02$,

A_{sl} is the area of the tension reinforcement,

b_w is the smallest width,

$k_1 = 0.15$,

$\sigma_{cp} = \frac{N_{Ed}}{A_c} \leq 0.2f_{cd}$,

N_{Ed} is the normal force in the cross section as a result of the load or pre-stress force,

A_c is the area of the concrete cross section.

When the capacity is lower than the present shear force, all the force has to be taken up by the shear reinforcement. The following properties are calculated:

$f_{ck} = 90\text{Mpa}$,

$k = 1 + \sqrt{\frac{200}{d}} = 1 + \sqrt{\frac{200}{668.5}} = 1.55$,

$\rho_l = \frac{4909}{500 \cdot 668.5} = 0.0147$,

$\sigma_{cp} = \frac{704 \cdot 10^3}{500 \cdot 750} = 1.88\text{N/mm}^2$.

This results in the following shear capacity:

$$V_{Rd,c} = [0.12 \cdot 1.55(100 \cdot 0.0147 \cdot 90)^{1/3} + 0.15 \cdot 1.88] \cdot 500 \cdot 666.5 \cdot 10^{-3} = 411.0 \ll 1488\text{kN}$$

The capacity is much lower than the present shear force and shear reinforcement is required. Stirrups with a diameter of 16mm will be used. To determine the minimum distance between the stirrups, the following equation is utilised:

$$\frac{A_{sw}}{s} = \frac{V_{Ed}}{z \cdot \cot \alpha \cdot f_{yd}}$$

in which:

A_{sw} is the area of the shear force reinforcement,

s is the centre to centre distance of the shear force reinforcement,

f_{yd} is the calculation value of the yield strength of the reinforcement,

z is the internal lever arm. When there is no normal force: $z=0.9d$,

α is the angle between the compression diagonals: $1 \leq \cot \alpha \leq 2.5$,

V_{Ed} is the present shear force.

The following properties are calculated:

$A_{sw} = 2 \cdot \pi \cdot 8^2 = 402.1\text{mm}^2$ (the 2 is added since one stirrup has two legs that cross the crack),

$f_{yd} = 435\text{N/mm}^2$,

$z = 0.9 \cdot 666.5 = 599.9\text{mm}$,

$$\alpha : 1 \leq \cot \alpha \leq 2.5, \\ V_{Ed} = 1488 \cdot 10^3 \text{ N.}$$

With $\cot \alpha = 1$ (45°), the following centre to centre distance is obtained:

$$\frac{402.1}{s} = \frac{1488 \cdot 10^3}{599.9 \cdot 1 \cdot 435} \rightarrow s = 70.5 \text{ mm}$$

When $\cot \alpha = 2.5$ (21.8°) is applied, a centre to centre distance is obtained of:

$$\frac{402.1}{s} = \frac{1488 \cdot 10^3}{599.9 \cdot 2.5 \cdot 435} \rightarrow s = 176.3 \text{ mm}$$

In theory, the stirrup centre to centre distance may vary between 70.5 and 176.3 mm. In practice the last value is commonly used in beams and lintels and this results in a shear reinforcement of $\Phi 16$ -170. This distance complies with the maximum centre to centre distances of the stirrups stated in NEN-EN 1992-1-1, section 9.2.2 (6):

$$s_{l,\max} = 0.75d(1 + \cot \alpha) = 0.75 \cdot 666.5 \cdot (1 + 0) = 500 \leq 300 = 300 \text{ mm}$$

It should be noted that α now represents the angle between the stirrups and longitudinal direction of the beam: $\alpha = 90^\circ$. Besides the maximum centre to centre distance, the stirrups also have a maximum distance in the transverse direction (section 9.2.2 (8)):

$$s_{t,\max} = 0.75d = 0.75 \cdot 666.5 = 499.9 \text{ mm} \leq 600 \text{ mm}$$

Also this requirement is satisfied since the transverse distance is:

$$s_t = 500 - 2 \cdot (30 + 8) = 424 \text{ mm}$$

According to section 9.2.2 (5), the minimum shear reinforcement ratio is:

$$\rho_{\min} = \frac{0.08 \cdot \sqrt{f_{ck}}}{f_{yk}} = \frac{0.08 \cdot \sqrt{90}}{500} = 0.0015 = 0.15\%$$

$$\rho = \frac{A_{sw}}{b \cdot s} = \frac{402.1}{500 \cdot 170} = 0.0047 = 0.47\% > 0.15\%$$

The final aspect which should be verified is if the resistance of the compression diagonal isn't exceeded. This is an important aspect since a very small angle results in a large compression force. The concrete diagonal fails when the compression force is larger than $V_{Rd,\max}$ from equation 6.9 of NEN-EN 1992-1-1:

$$V_{Rd,\max} = \frac{\alpha_{cw} b_w z v_1 f_{cd}}{\cot \theta + \tan \theta}$$

in which:

- b_w is the width of the lintel,
- z is the internal lever arm. When there is no normal force: $z = 0.9d$,
- θ is the angle between the compression diagonals,
- v_1 is the strength reduction factor for concrete cracked by shear force:
 $v_1 = 0.9 - f_{ck}/200 > 0.5$,
- α_{cw} is a factor to take the axial stress into account: $\alpha_{cw} = 1$ for non prestressed structures.

With the National Annex, the following properties are calculated:

$$\begin{aligned} b_w &= 500\text{mm}, \\ z &= 599.9, \\ \theta &= 21.8^\circ, \\ v_1 &= 0.9 - 90/200 = 0.45 = 0.5, \\ \alpha_{cw} &= 1. \end{aligned}$$

This results in a resistance of the compression diagonal of:

$$V_{Rd,max} = \frac{1 \cdot 500 \cdot 599.9 \cdot 0.5 \cdot 60}{2.5 + 0.4} \cdot 10^{-3} = 3102.9\text{kN}$$

The force in the diagonal is:

$$V_{Ed,diagonal} = \frac{V_{Ed}}{\sin\theta} = \frac{1488}{\sin 21.8} = 4006.8 > 3102.9\text{kN}$$

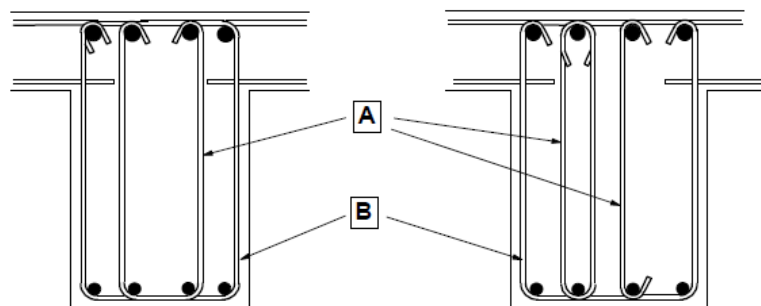
The compression diagonal fails and a larger angle has to be used. When an angle of 27° is applied, the stirrups require a centre to centre distance of $s=130\text{mm}$: $\Phi 16-130$. The resistance of the compression diagonal becomes:

$$V_{Rd,max} = \frac{1 \cdot 500 \cdot 599.9 \cdot 0.5 \cdot 60}{1.96 + 0.51} \cdot 10^{-3} = 3640.0\text{kN}$$

The new force in the diagonal is:

$$V_{Ed,diagonal} = \frac{V_{Ed}}{\sin\theta} = \frac{1488}{\sin 27} = 3277.6 < 3640.0\text{kN}$$

The requirement is satisfied and stirrups of $\Phi 16-130$ are applied. These stirrups are relatively large, but for a 202.5m high building it's not unrealistic. The diameter of the stirrups can be reduced by applying internal stirrups, shown in Figure 94.



Verklaring

- A alternatieven voor binnenbeugels
- B omsluitende beugel

Figure 94 Example of internal stirrups [NEN, 2011]

A point of attention is the top opening in the centre stirrups at the left example of Figure 94. This opening should be located in the compression zone. Since the moment reverses in the lintel (see Figure 92), the stirrups shouldn't contain any openings (according to the wind direction the compression and tension zone alternate).

When the total reinforcement volume in the lintel is divided by the volume of the lintel and multiplied by the volumetric mass, the amount of reinforcement per cubic meter of concrete is obtained: 292kg/m^3 . Values up to 450kg/m^3 aren't exceptional at the bottom lintels of high-rise buildings and there is room for optimisation.

9.7.4 Reinforcement design of the wall

The reinforcement design of the wall element shown in Figure 91 is slightly different from the previous discussed lintel. Figure 95 shows the forces in the wall element based on multiple vertical section lines in AxisVM and the diagrams are consistent with the deformations of the wall element, see Figure 96.

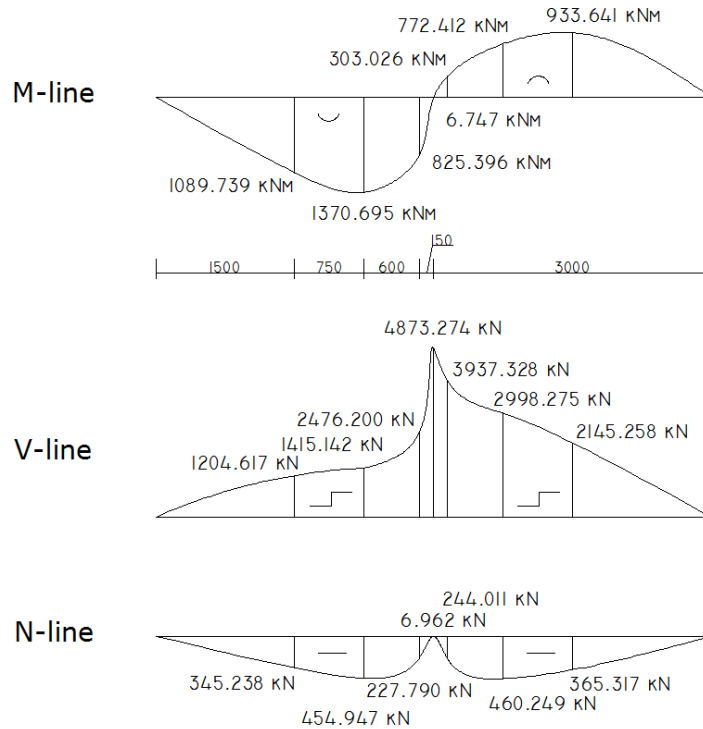


Figure 95 Forces in the wall element

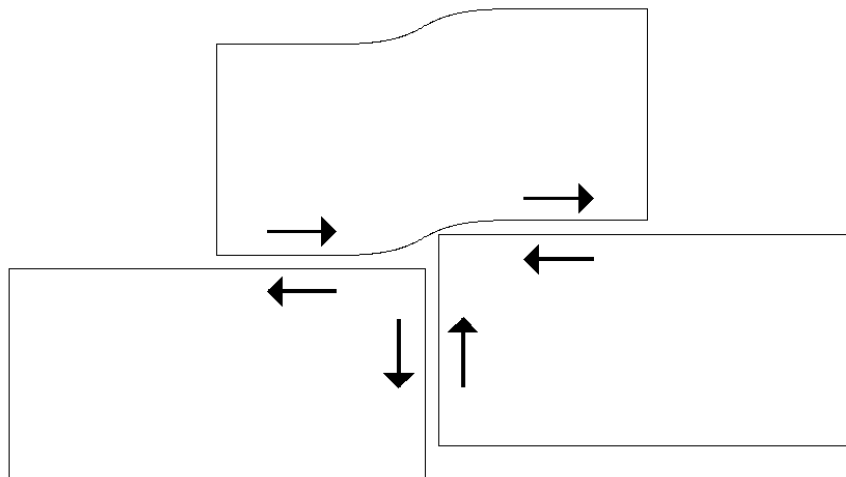


Figure 96 Deformation and forces in the wall element

The shear force diagram n_{xy} of Figure 95 shows a large peak value at the location of the vertical open joint. When the properties of the open joint are taken into consideration, this peak value can be explained easily: due to the lack of stiffness, the over and underlying dowel elements have to take up the vertical shear force. These forces are mainly transferred at the edge of two elements, resulting in a large peak value in the dowel element. When a section is made over the entire height exactly at the open vertical joint, only half of the elements are available to transfer the vertical shear force.

Bending moment reinforcement design of the wall

The bending moment distribution of Figure 95 is non-linear and the reinforcement has to be placed at the bottom and at the top. The reinforcement calculation will be based on the bottom value of $M_{Ed}=1370.7\text{kNm}$. Since this is relatively low for an wall element, it was also examined if the transport would create a higher moment. Due to the dead load of 37.4kN/m a moment of 201.8kNm is created. This is considerably lower than the present moment and the transport isn't governing. To obtain the reinforcement ratio, Table "11.10 bending without normal force at a rectangular cross section" of GTB 2010 is used.

Properties for the calculation:

- concrete strength class: C90/105,
- environmental class: XC2,
- minimum cover²⁹: $c_{min}=c_{min,dur}+\Delta c_{dev}=25+5=30\text{mm}$.

With these values the effective height can be determined:

$$d = h - \left(\frac{1}{2} \phi + \phi_{stirrup} + c \right) = 3050 - \left(\frac{1}{2} \cdot 20 + 16 + 30 \right) = 2994\text{mm}$$

With table 11.10 of GTB 2010, the reinforcement ratio can be determined:

$$\frac{M_{Ed}}{b d^2} = \frac{1370.7}{0.5 \cdot 2.994^2} = 306 \ll 2100$$

The lowest value of the table is 2100, which is far larger than the required value of 306. At 2100, a reinforcement ratio of $\rho=0.49\%$ is obtained. This low value seems plausible, but with the large concrete area a minimum reinforcement area is required of:

$$A_s = \rho \cdot b \cdot d = 0.0049 \cdot 500 \cdot 2994 = 7335\text{mm}^2$$

With $10 \times \Phi 32$ a reinforcement area of 8043mm^2 is obtained ($\rho=0.54\%$). This is an enormous amount of reinforcement for a wall element which is mainly loaded by shear force. To accommodate this low bending moment, table 11.4 of C25/30 is used. Since this table contains a lower concrete strength, the reinforcement ratio is increased with 25%: $\rho=1.25 \cdot 0.09=0.113\%$. This ratio is considerable lower than the minimum reinforcement ratio of:

$$\rho_{min} = 0.26 \cdot \frac{f_{ctm}}{f_{yk}} = 0.26 \cdot \frac{5}{500} \cdot 10^2 = 0.26\%$$

or the previous calculated value of $\rho=0.54\%$, but due to low bending moment the element won't fail at bending. The reinforcement ratio of $\rho=0.113\%$ results in a steel area of:

$$A_s = \rho \cdot b \cdot d = 0.00113 \cdot 500 \cdot 2994 = 1692\text{mm}^2$$

With $6 \times \Phi 20$ a reinforcement area of 1885mm^2 is obtained ($\rho_{moment}=0.126\%$). In Figure 97 the reinforcement layout is depicted. Due to the minimal diameter of the curved stirrups ($4 \times \Phi_{stirrup}$), the corner reinforcement is moved to the centre of the lintel. The anchor length of the stirrups is minimal $10 \times \Phi_{stirrup}=140\text{mm}$.

²⁹ Based on the structural class S4 and the national annex.

Since the shear force in Figure 95 shows a large peak at the centre, the wall element is divided into two areas: the hatched areas of Figure 99 provide the base net and at the centre area reinforcement is added to accommodate the higher load.

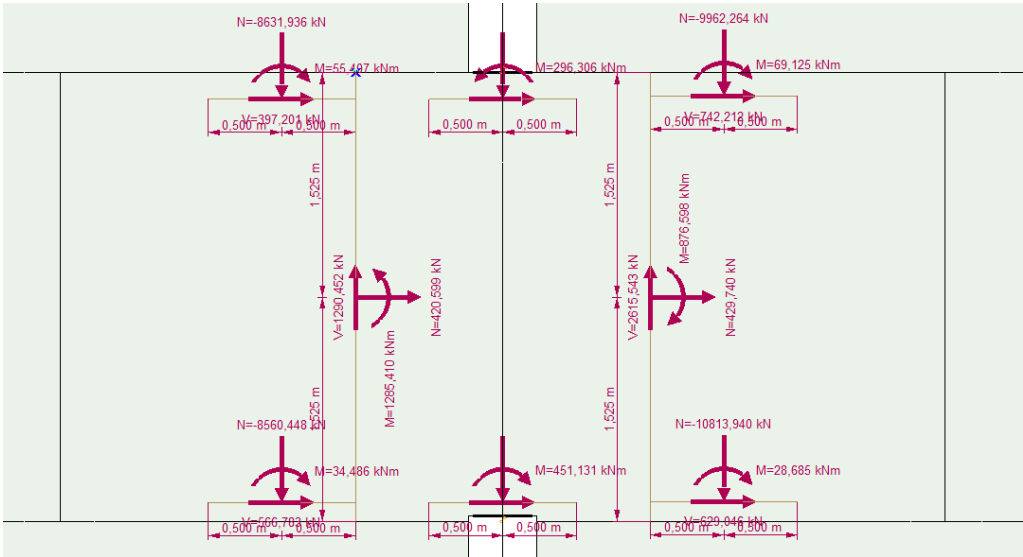


Figure 98 Sections for the vertical net of the wall element

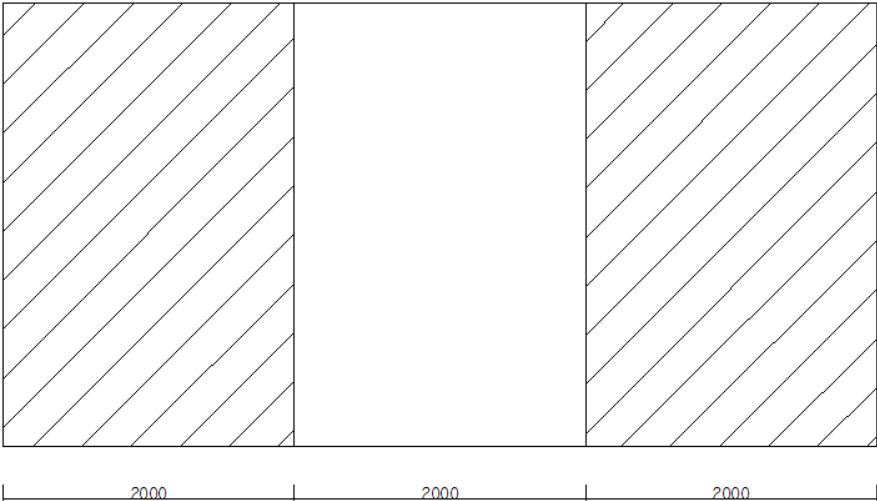


Figure 99 Division of reinforcement net

For the base net, the hatched area on the right hand side provides the highest $n_{y,d}^*$:

$$n_{y,d}^* = n_{y,d} + |n_{xy,d}| = 10813.9 + 2615.5 = 13429.4 \text{ kN/m}$$

This force is accompanied by a moment at the top and the bottom:

$$M_{top,d} = 69.1 \text{ kNm/m}$$

$$M_{bottom,d} = 28.7 \text{ kNm/m}$$

With these values and a column program of Zonneveld ingenieurs, the required reinforcement area can be calculated. It may be uncommon to use a column program for a wall, but a 1m strip of the wall is calculated, making the program very suitable to determine the reinforcement area. In appendix E.2.3, an overview is provided of the calculation. The calculation results in a minimum reinforcement area of $3087 \text{ mm}^2/\text{m}$. This is the total amount of required reinforcement and this value has to be divided by two to

obtain the area per side: $A_s=1543.5\text{mm}^2/\text{m}$ per side. With a net of $16\Phi-125$ a reinforcement area of $1608.5\text{mm}^2/\text{m}$ is created.

In the central area the following values are obtained:

$$\begin{aligned}n_{y,d}^* &= n_{y,d} + |n_{xy,d}| = 10087.1 + 4873.3 = 14960.4\text{kN/m} \\M_{\text{top},d} &= 296.3\text{kNm/m} \\M_{\text{bottom},d} &= 451.1\text{kNm/m}\end{aligned}$$

This results in a minimum reinforcement area of $3439\text{mm}^2/\text{m}$. Since this area already contains the base net of $16\Phi-125$, only a slight amount of reinforcement has to be added: $A_s=(3439-3087)/2=176\text{mm}^2/\text{m}$. With a net of $10\Phi-250$, this value is easily obtained: $A_s=314\text{mm}^2/\text{m}$. Applying $8\Phi-125$ is also possible ($A_s=314\text{mm}^2/\text{m}$), but the difference in diameter is more than two steps (8-10-12-16) and is therefore not allowed. It's also possible to reduce the centre to centre distance of the base net in the centre area from $16\Phi-125$ to $16\Phi-100$ ($A_s=2011\text{mm}^2/\text{m} > 3439/2=1720\text{mm}^2/\text{m}$), but the production speed will be higher when a base net is applied and locally small bars are added.

The two hatched areas of Figure 99 have a total vertical reinforcement ratio of:

$$\rho_{y,\text{hatched}} = \frac{A_s}{b \cdot d} = \frac{3217}{500 \cdot 1000} = 0.0064 = 0.64\%$$

At the centre area this increases to:

$$\rho_{y,\text{centre}} = \frac{A_s}{b \cdot d} = \frac{3845}{500 \cdot 1000} = 0.0077 = 0.77\%$$

A base net of $16\Phi-125$ is relatively large and it isn't a standard net size. A standard net size is for example $12\Phi-150$. Therefore this net has to be made specific for this project at the factory. Since these high forces are still obtained at the 14th floor, the repetition will overcome this problem. Compared with a monolithic structure it may be concluded that a precast structure requires more vertical reinforcement: at the central area, the precast element requires a net of $16\Phi-125$ in combination with $10\Phi-250$. The monolithic model requires a net of $16\Phi-140$, which is a difference of 25%. The difference decreases to 18% when not the applied reinforcement but the required reinforcement is considered.

To obtain the horizontal net, again several sections have been made (see Figure 100). Compared with Figure 98, the division of forces in Figure 100 is more constant.

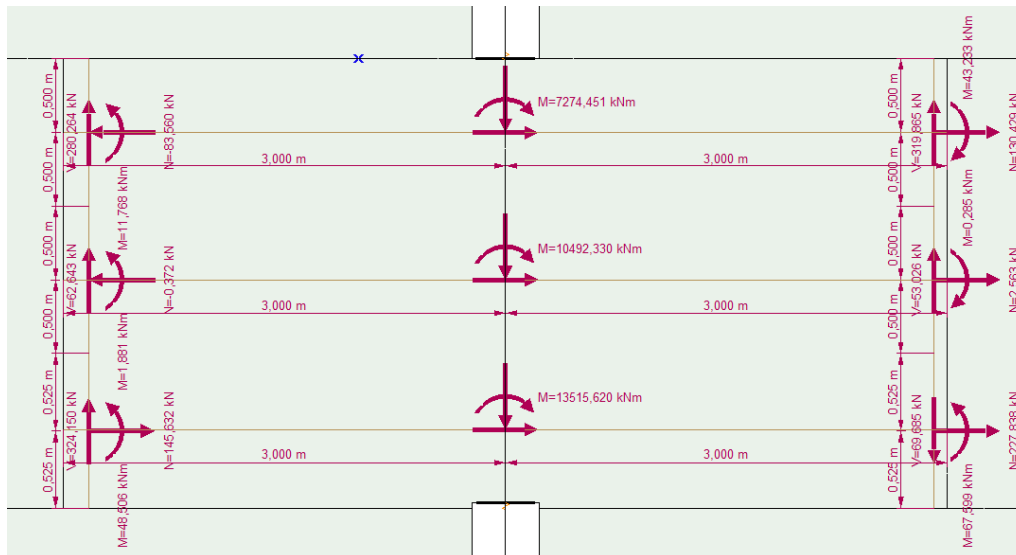


Figure 100 Sections for the horizontal net of the wall element³⁰

The lowest section provides the highest values:

$$n_{x,d}^* = n_{x,d} + |n_{xy,d}| = 227.8 + 3658.8 = 3886.6 \text{ kN/m}$$

$$M_{\text{top},d} = 48.6 \text{ kNm/m}$$

$$M_{\text{bottom},d} = 67.6 \text{ kNm/m}$$

This results in a minimum reinforcement area of $1000 \text{ mm}^2/\text{m}$ in total. Per side this is: $A_s = 500 \text{ mm}^2/\text{m}$. With a net of $12\Phi-150$, this requirement is satisfied ($A_s = 755 \text{ mm}^2/\text{m}$). The following total reinforcement ratio is obtained in the horizontal direction:

$$\rho_x = \frac{A_s}{b \cdot d} = \frac{1510}{500 \cdot 1000} = 0.0030 = 0.30\%$$

With the reinforcement net in x and y-direction and the moment reinforcement, the total reinforcement ratio can be determined:

$$\rho_{\text{total}} = 2 \cdot \rho_{\text{moment}} + \frac{4 \cdot \rho_{y,\text{hatched}} + 2 \cdot \rho_{y,\text{centre}}}{6} + \rho_x$$

$$\rho_{\text{total}} = 2 \cdot 0.126 + \frac{4 \cdot 0.64 + 2 \cdot 0.77}{6} + 0.3 = 0.0124 = 1.24\%$$

A total reinforcement ratio of 1.24% isn't a very high value for a wall element at the bottom of a 202.5m high tower. It may be concluded that there is some room left for optimisation. Just as with the lintel, the amount of reinforcement per cubic meter can be determined. It should be noted that this is based on the previous calculated values and that the anchor reinforcement of the lintel isn't included. The calculation provides 117kg steel per cubic meter of concrete. Often a minimal amount 120 kg/m^3 or more is applied, which confirms the assumption of the low reinforcement ratio (for example, at Het Strijkijzer they applied 250 kg/m^3 at the bottom section).

³⁰ Unfortunately, the shear force of the horizontal sections aren't shown in this figure due to the element in front of it (the perpendicular wall). From top to bottom, the following values are obtained: 3657.1kN, 3657.0kN and 3658.8kN.

9.7.5 Conclusion

After designing the reinforcement of a lintel and wall element, it may be concluded that the reinforcement ratios are slightly too low for a 202.5m high-rise tower. The material isn't used to its full capacity. This is mainly caused by the concrete strength class C90/105, which was applied to counteract the stiffness reduction of the precast connections. In section 9.3.2, it's concluded that the deflection of the precast model is only 4% larger, making the stiffness not leading. Therefore the concrete strength class may be lowered. A second possibility is to reduce the wall thickness. In the x-direction two walls of 500mm are applied, which is enormous. These two solutions can also be combined. When the wall thickness is reduced over the height (for example 500mm between level 1 and 26, 400mm between 27 and 44 and 300mm between 45 and 65), the stiffness isn't affected considerably, but the amount of concrete is reduced significantly. This also has a positive effect on the cycle times of the elements (see section 11.1.1.4). Unfortunately, the accelerations will increase when the mass at the top is reduced.

When the reinforcement ratios of a precast and cast in situ element are examined, it can be concluded that the precast element requires 18% more shear reinforcement in the centre of the element (the location where the shear forces are introduced by the dowel action). At the sides, the reinforcement ratio remains identical.

9.8 Verification of the Young's modulus

In section 7.4 of this thesis, a Young's modulus of $E=29333\text{N/mm}^2$ was applied for uncracked concrete and $E=14667\text{N/mm}^2$ for cracked concrete. The Young's modulus of cracked concrete is lower than that of uncracked concrete since the cracking reduces the stiffness. But are the applied values realistic? This is an interesting question since a high Young's modulus results in a large stiffness and therefore attracts more forces. As a result, it may be possible that the large reinforcement area cannot be placed within the small lintel. Furthermore, if the stiffness is too high, the model will not behave comparable to the actual building. Therefore the Young's modulus will be verified in this section.

9.8.1 Calculation method

There are two methods to calculate the actual Young's modulus: the M-N-Kappa diagram or the fictitious Young's modulus according to table NB1 of NEN-EN 1992-1-1. The first method is more complicated and time consuming than the second method. In determining the M-N-Kappa diagram, the external normal force N_{Ed} is kept constant and it's examined which moment can be endured by the cross section in different loading stages. When the cross section is loaded until failure, the following stages can be distinguished:

1. no tension in the concrete: $\sigma_c=0$,
2. no tension in the reinforcement at the tension side: $\sigma_s=0$,
3. the yield stress in the compression reinforcement is reached:
 $\sigma_{s,compress}=f_{yd}=435\text{N/mm}^2$,
4. the strain limit of the concrete is reached: $\epsilon_{c3}=2.3\text{‰}$,
5. the yield stress in the tension reinforcement is reached: $\sigma_{s,tension}=f_{yd}=435\text{N/mm}^2$,
6. the concrete cross section fails: $\epsilon_{cu3}=2.6\text{‰}$.

By examining all the stages, the bending stiffness ($E_{eff(\infty)}I$) can be determined. Since the compression area is known, the Young's modulus can be calculated. Applying this method is time consuming, but it provides accurate results. The fictitious Young's modulus calculation of table NB1 only requires the tension and/or compression reinforcement ratio and provides quick results. Compared with the M-N-Kappa diagram, the fictitious Young's

modulus values are more conservative. It should be noted that the fictitious Young's modulus may only be applied when the cross-section is rectangular.

In this calculation the second method will be applied since the results are conservative, but representative. In the final design an M-N-Kappa diagram should be considered, since it provides more accurate results.

9.8.2 Verification Young's modulus of the lintel

In section 9.7.3 the reinforcement of the lintel was calculated. This resulted in a reinforcement ratio of $\rho_{\text{tension}}=1.46\%$ for the tension reinforcement and of $\rho_{\text{compression}}=1.46\%$ for the compression reinforcement. The total reinforcement ratio is therefore $\rho_{\text{total}}=2.92\%$. When the cross section is reinforced symmetrically and loaded by bending and a normal force, the following formula may be applied ($\alpha_n \leq 0.5$)³¹:

$$[3.10+470\rho+(51.0-170\rho)\alpha_n]10^3 \geq 6400$$

in which:

$$\rho = \frac{(A_{st}+A_{sc})}{A_c},$$

$$\alpha_n = \frac{N_{Ed}}{f_{cd}A_c + (A_{st}+A_{sc})f_{yd}}$$

A_{st} is the reinforcement area at the tension side,

A_{sc} is the reinforcement area at the compression side.

The value of α_n depends on the normal force. In this section α_n will be calculated for $N=0$, $N=704.1\text{kN}$ (see Figure 92) and $N=-1018.8\text{kN}$ (this is the largest tension force present in a lintel). When there is a tensile force in the lintel, α_n will obtain a negative value resulting in a lower Young's modulus.

For $N=0$, $\alpha_n=0$. For $N=704.1 \cdot 10^3\text{N}$, the following value is derived:

$$\alpha_n = \frac{N_{Ed}}{f_{cd}A_c + (A_{st} + A_{sc})f_{yd}} = \frac{704.1 \cdot 10^3}{60 \cdot 500 \cdot 666.5 + (4909 + 4909) \cdot 435} = 0.02895$$

For $N=-1018.8 \cdot 10^3\text{N}$, $\alpha_n=-0.04198$.

When there is no normal force ($N=0$) included in the calculation, the following fictitious Young's modulus is obtained:

$$E_f = [3.10+470 \cdot 0.0292 + (51.0-170 \cdot 0.0292) \cdot 0] \cdot 10^3 = 16824\text{N/mm}^2$$

When the normal force is incorporated ($N=704.1 \cdot 10^3\text{N}$), the calculation results in the following value:

$$E_{f,\text{comp}} = [3.10+470 \cdot 0.0292 + (51.0-170 \cdot 0.0292) \cdot 0.02895] \cdot 10^3 = 18157\text{N/mm}^2$$

With a tension force of $N=-1018.8 \cdot 10^3\text{N}$ is applied, a fictitious Young's modulus is acquired of (this value is only illustrative, see annotation 31):

$$E_{f,\text{tension}} = [3.10+470 \cdot 0.0292 - (51.0-170 \cdot 0.0292) \cdot 0.04198] \cdot 10^3 = 14891\text{N/mm}^2$$

³¹ This is actually the column formula which includes the contribution of the normal force (α_n). Because of the symmetrical reinforcement and the normal force, this formula is applied. When beam formula is utilised, a fictitious Young's modulus of 15337N/mm^2 would be obtained, which is larger than the applied Young's modulus of $E=14667\text{N/mm}^2$. It should be noted that the column formula only holds for compression and that the fictitious Young's modulus for tensions is only illustrative.

The three values are higher than the applied Young's modulus of $E=14667\text{N/mm}^2$. The fictitious Young's modulus for compression will be an upper limit³² and the fictitious Young's modulus for tension will be a lower limit. Since most lintels are loaded with compression, the stiffness will commonly have a value between 16824 and 18157 N/mm^2 . The increase of stiffness between 16824 and 14667 N/mm^2 is 15%.

Since the lintels have an influence on the deflection, a higher stiffness of the lintels will reduce the deflection (the lintels make the difference between two or three different walls or one continuous wall, see section 10.4.4 of the literature study). Therefore the obtained deflection values of section 9.3.2 are slightly overestimated.

Due to the higher stiffness of the lintels, the forces in the lintels will increase. Since the reinforcement area in the calculation is always larger than required, this increase of stiffness should not provide any problems. To make sure the reinforcement area isn't insufficient, the largest stiffness of $E_{f,\text{compression}}=18157$ is applied at all the lintels. This value isn't representable for all the lintels, but with this method the largest forces are obtained, resulting in an upper limit. According to the new model, all the forces in the lintel increase with approximately 5%. As a result of the higher shear force (which is leading in the lintel design), the compression diagonal should be verified:

$$V_{\text{Ed,diagonal}} = \frac{V_{\text{Ed}}}{\sin\theta} = \frac{1560}{\sin 27} = 3436.2 < 3640.0\text{kN}$$

The lintel satisfies the requirements and no difficulties should be encountered by a higher force in the lintel.

9.8.3 Verification Young's modulus of the wall

When the Young's modulus of the wall is verified, a problem occurs: there is almost no bending in the element and the reinforcement is mainly based on shear and normal force (compression). Therefore the reinforcement ratio is considerably lower than at the lintel. The following fictitious Young's modulus is obtained ($\alpha_n \leq 0.5$)³³:

$$\alpha_n = \frac{N_{\text{Ed}}}{f_{\text{cd}}A_c + (A_{\text{st}} + A_{\text{sc}})f_{\text{yd}}} = \frac{56809.920 \cdot 10^3}{60 \cdot 500 \cdot 6000 + (4 \cdot 3217 + 2 \cdot 3842) \cdot 435} = 0.30068$$

$$E_{f,\text{comp}} = [3.10 + 470 \cdot 0.00685 + (51.0 - 170 \cdot 0.00685) \cdot 0.30068] \cdot 10^3 = 21304\text{N/mm}^2$$

This is considerably lower than the assumed value of $E=29334\text{N/mm}^2$. Therefore a more elaborated method is required based on creep to calculate the exact value (see equation 5.27 of NEN-EN 1992-1-1):

$$E_{\text{cd,eff}} = \frac{E_{\text{cd}}}{1 + \varphi_{\text{ref}}}$$

Since 2/3rd of the original Young's modulus is a good approximation for compressed concrete wall elements, the assumed value of $E=29334\text{N/mm}^2$ is maintained.

9.8.4 Conclusion

At the start of the thesis a Young's modulus value was assumed for concrete under tension ($E=14667\text{N/mm}^2$) and under compression ($E=29334\text{N/mm}^2$). After the reinforcement was designed for a lintel and wall element, the values could be validated. For the validation two methods are available: the M-N-Kappa diagram or the fictitious

³² Most lintels have a lower compression force.

³³ The column formula is used because of the symmetric reinforcement and normal force.

Young's modulus formulas. The M-N-Kappa diagram provides more accurate values, but the calculation is extensive and time consuming. Therefore engineers in practise commonly apply the fictitious Young's modulus formulas, which provide a quick and conservative result. In a final design the M-N-Kappa diagrams may be considered, but in this thesis the fictitious formulas are applied.

The validation of the lintel shows that assumed value is too low: the fictitious Young's modulus will vary between 14891 and 18157N/mm². As a result of the higher stiffness of the lintels, the deformations will decrease and the forces in the lintels will increase. Therefore an upper limit verification has been applied: all the lintels were given a Young's modulus of 18157N/mm². With the increased forces, the new required reinforcement was calculated. The calculated reinforcement remained below the applied value and a higher stiffness will not result in a failure of the lintel.

The verification of the wall element resulted in a very low fictitious Young's modulus of 21304N/mm². This is considerably lower than the applied value of 29334N/mm². The small reinforcement ratio of the wall can be considered as the cause of this large difference. Since 2/3rd of the original Young's modulus is an acceptable value for a concrete wall element under compression, this value is maintained.

It can be concluded that the initial estimations were quite accurate and that the validation didn't result in any adjustments.

9.9 Evaluation concept 3

In section 4.2.4 two concepts were considered for the load bearing structure: concept 1 were the original layout is maintained and concept 3 were the original layout is supplemented by a facade tube. Due to the limited amount of time in this thesis and the extensive analysis of concept 1, concept 3 was never designed and modelled. Therefore concept 3 will be evaluated based on the obtained knowledge of concept 1.

During the preliminary analysis it was concluded that concept 3 has the lowest dead load while the moment of inertia of the load bearing structure was considerable larger than that of concept 1. This is because the bundled tube system of concept 3 utilises its material far more efficient. Concept 3 will be evaluated on the same aspects as concept 1 in this chapter:

- The distribution of forces will not change considerably when the internal walls in combination with a facade tube are considered. This is because the underlying behaviour of the elements remains identical. Due to the larger openings in the internal walls (larger lintels), the flow of forces will be slightly more disrupted. The distribution of forces in the facade tube will be comparable to the structural walls, but the large amount of window openings will also create disruptions.
- The absolute values of the forces in the internal structural walls will change since a considerable section of the load is taken up by the facade tube. Due to this more efficient structure the tension and compression forces will be smaller.
- Aside from the smaller forces, the deformations will also be reduced. Since the stiffness isn't leading in the current design of concept 1, this may result in large openings in the structural walls. This will increase the flexibility, creating the possibility to combine two apartments as one (identical to Het Strijkijzer in The Hague).
- The second order effect is based on the load, bending and shear stiffness of the structure and the stiffness of the foundation. The shear stiffness isn't leading and the foundation remains nearly identical. Because of the higher bending stiffness and lower mass, the second order effect will diminish.

- Shear lag occurs at structures with a finite shear stiffness. Because of the internal walls, the shear lag effect of the facade tube is reduced considerable. Due to the larger amount of openings, the shear lag effect in the internal walls will slightly increase (because of the openings, the shear stiffness is reduced).
- The structural factor and building acceleration are two complex aspects. The exact behaviour is difficult to predict, but increasing the stiffness results in a lower building frequency and a lower frequency results in a smaller structural factor and acceleration. The building acceleration slightly increases because also the mass is reduced. Since the mass reduction is limited, the structural factor and building acceleration will reduce.
- The reinforcement design will change due to the larger door openings (longer lintels) and smaller forces. By optimizing the wall thickness and concrete strength class, an economic reinforcement design is created.

Besides the structural properties also the construction methodology is influenced. As a result of the facade tube, more structural connections are required. Since the structural walls and facade elements will be thinner and the maximum element length is limited to 12m, multiple elements have to be transported per vertical transport movement to optimise this process. The hoisting shed itself may use the same system (supports on the end faces of facade elements) or the Erasmus MC system could be utilised (see section 4.5.4). Considering the construction methodology, there are no large disadvantageous or advantageous attached to concept 3.

From the previous evaluation it may be concluded that concept 3 is the best solution for the Zalmhaven tower. It should be noted that the architectural design will change considerably when the facade tube is applied. Furthermore, creating balconies at all the apartments will be challenging because this ensures that the facade element is interrupted at the door openings (no lintel at the bottom of the elements). In association with the architect, structural engineer, contractor and client, it has to be determined which concept provides the best results corresponding to the wishes.

9.10 Conclusion

In this chapter many structural aspects have been calculated, examined and compared. The goal of this chapter was to analyse the behaviour of the precast structure based on the distribution of forces, the value of the forces, the deflections, second order effects, shear lag, structural factor and vibrations. The distribution of forces is also represented by the reinforcement and by comparing the results of the precast and cast in situ structures, interesting conclusions can be made:

- Despite the similar distribution of normal force, the local distribution of shear force is considerably different between a precast and monolithic model. This difference is created by the open vertical joint of the precast structure, which is unable to transfer any shear and normal forces. Due to this property, the forces of the element are transferred to the over and underlying dowel elements. By activating these elements, the shear force increases between the open vertical joints (only 50% of the original structural area is available). It may be concluded that the underlying behaviour of the elements is considerably different when it comes to shear forces and additional shear force reinforcement is required.
- The previous mentioned shear force is transferred to the dowel element by a peak force in the connection point of the horizontal and vertical connection. This peak value is present because the shear force is concentrated by the linear calculation and smeared stiffness. It's known of linear calculations that a large portion of the force is often transferred at the corners (last possible location without redistribution) and by neglecting important mechanisms of the connection (non-smeared stiffness and starter bars) the forces remain concentrated. Therefore this

peak value may be smoothed in the actual design. A non-linear calculation in combination with the actual connection behaviour should determine the exact reduction of this peak value.

- When the deflections are considered, a stiffness reduction between 0.4 and 4% is obtained for precast concrete, depending on which direction of the Zalmhaven tower is considered. This stiffness reduction is significantly low and can be explained by three important aspects: the high Young's modulus of the concrete, the stiff behaviour of the masonry element configuration and the high slenderness of the tower. By using the masonry element configuration, the dowel elements are activated which have a stiffness equal or higher than traditional vertical connections. The high slenderness ensures that the elements are mainly loaded by bending. As long as all the connections are loaded by compression, the normal stiffness is equal to the surrounding concrete, approximating the stiffness and strength of a monolithic structure.
- Precast concrete also influence the damping of the structure. Due to the high amount of connections more energy is dissipated, providing a higher damping value. It's estimated that the damping value may be up to 50% higher. Since very little is known on the exact behaviour of the damping value and currently no research has proven this assumption, the values provided by the standards should be maintained.

Besides the comparison between precast and cast in situ concrete, multiple aspects of the precast design have been examined which are worth mentioning:

- The influence between the foundation and top deflection for the Zalmhaven tower has been analysed. Commonly it's expected that the foundation creates 1/3rd of the total deflection, but the analysis provided values between 18 and 20%. This reduction is created by the very stiff diaphragm walls with a length of 62.3m.
- When the structure has a finite shear stiffness, shear lag occurs. Due to the stiffness of the foundation, the negative effects of shear lag are reduced considerably: the shear lag effect is limited to a maximum of 10%.
- Despite the height of 202.25m, the acceleration of the building due to cyclic wind loading remains comfortable within the boundaries. These low values are created by the enormous dead load of the structure and the high damping values of concrete (the damping values for concrete buildings in the NEN-EN 1991-1-4 are 59% higher than the values of the NEN 6702. The difference is slightly diminished by other factors).
- When the reinforcement ratios at the bottom of the Zalmhaven tower are examined, it may be concluded that the values are too low. Since the deflections aren't leading, the concrete strength class or concrete thickness may be reduced to optimise the design.
- The evaluation of concept 3 reveals multiple benefits and several disadvantages. In consultation with architect, structural engineer, contractor and client, it has to be determined which concept provides the best results corresponding to the wishes.

The previous conclusions have shown several aspects on which a precast structure distinguishes itself from a monolithic design. It may also be concluded that there is still room for optimisation and that this current design isn't finished.

10 Dimensional control

Dimensional control is becoming more important with the increasing amount of prefabrication. With precast concrete lower tolerances can be achieved, but the freedom to adapt has been reduced compared to cast in situ structures. To maintain an economically viable process, it has to be prevented that elements won't fit. When the dimensional deviations are within the tolerances and the connections are designed to absorb the dimensional deviations, the structure can be easily assembled without delays and unwanted modifications.

But what is dimensional control, who is responsible and how do the standards define tolerances and deviations? Furthermore, how are the deviations controlled, on a local or global scale?

The goal of this section is to approach the deviations and tolerances from the basis. By examining this specific for a precast high-rise building, it can be determined whether the traditional solutions will result in problems. This is interesting since the large number of separate precast elements may require a different technique.

In section 10.1 the dimensional control will be discussed in more detail. How the standards define tolerances and deviations is described in section 10.2. In section 10.3 it's examined whether the deviations have to be controlled locally or globally. This chapter on dimensional control ends with a conclusion in section 10.4.

In the creation of this chapter the following three articles have been used [Hoof, 1997A], [Hoof, 1997B] and [Boonekamp, 1979].

In this chapter only a small insight is given on the phenomenon dimensional control. More information on this subject and the possibilities of computer aided dimensional control can be found in the following two dissertation reports: [Hoof, 1986] and [Wu, 2002].

10.1 Dimensional control

Dimensional control in the building industry can be defined as the operational techniques and activities that are necessary for the assurance of the dimensional quality of a building [Hoof, 1986]. Together with the material quality and its quality control, the dimensional control will have a direct impact on whether or not the building will perform or operate as designed. But before the dimensional control can be discussed in more detail, a different aspect has to be evaluated first: dimensional deviations. A dimensional deviation can be explained as the difference between a target size and the measured size and the phenomena can be approached in two ways: from the cause and from the effect.

10.1.1 The cause of dimensional deviations

The most important cause of dimensional deviations are human actions. The inability to make something perfectly is simply an irrefutable fact and a deviation of 0mm is impossible. This means that at the allocation of the measurement points, the adjustment and manufacturing of the element, no size is perfect. Besides the human actions, tools or other equipment (for example the falsework and formwork) may also result in deviations. Because after all, these components have also been made by humans.

A second cause of deviations are the changing physical conditions to which the elements, entire structure but also the equipment is exposed or subjected to. Examples of different physical conditions are temperature, relative humidity and load.

Final, also a variation occurring in the applied material over time can cause dimensional deviations. These deviations are inevitable and not the occurrence but only the size can be influenced by adjusting the working method, equipment, materials, loads or care.

When the dimensional deviations of multiple equal elements are plotted, a normal or Gaussian distribution is obtained. From this distribution it's possible to obtain the expected value μ (and this should be equal to the target size) and the standard deviation σ (see Figure 101). Δ represents the inaccuracy, a symmetric area around the expected value that contains 98% of the deviations.

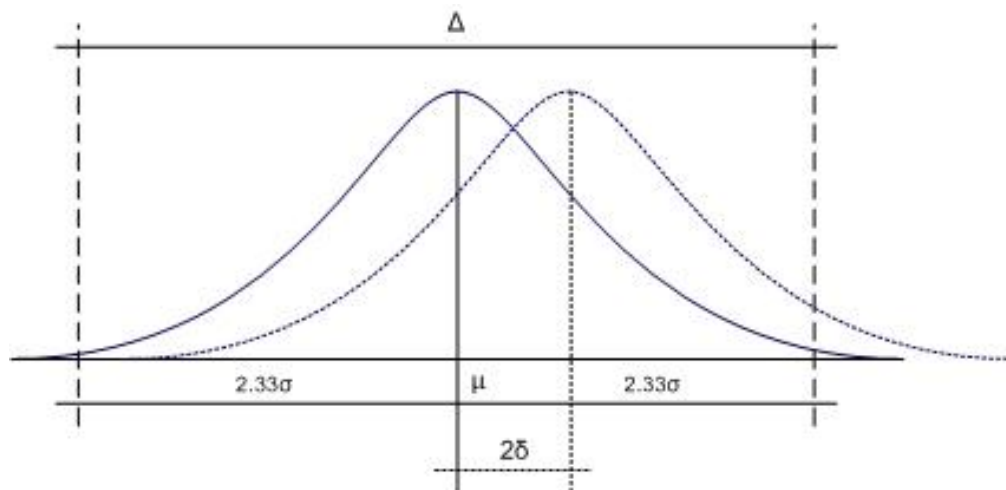


Figure 101 Gaussian distribution of the dimensional deviation

Besides the accidental deviations that create the Gaussian distribution, there are also systematic deviations. Systematic deviations can for example be created in the formwork or by an error in the measurement equipment and they are equal for every element. Though most production processes are often verified and the machines and equipment are adjusted according to the observed systematic deviation, it's nearly impossible to produce a set of elements without any systematic dimensional deviation. In Figure 101 a positive systematic deviation is depicted by a second Gaussian curvature. The inaccuracy now becomes $\Delta = 2(|\delta| + 2.33\sigma)$ and still contains 98% of all the deviations. The probability that the deviation is outside the 98% zone is therefore only 2%. This is a small probability, but there are no safety factors used during the dimensional design of a connection to assure a proper fit. This is in contrast with the structural design where substantial safety factors are used. The consequence of an error is likely the cause of this difference (the element doesn't fit versus a (partial) collapse).

10.1.2 The effect dimensional deviations

Occurring dimensional deviations that exceed a certain limit will affect two important groups: the clients/users and the manufacturers. For the clients and users too large deviations will result in a loss of function of the building with respect to the aesthetics, structure or building physics. For example unsightly connections, unsafe structures, draught, noise nuisance or ponds of water on the roof or floor. For the manufacturers (contractors and suppliers) large deviations will result in financial losses. For example the costs that are associated with the rejection of material, followed by replacement or repair and the stagnation of the work. Besides the two already mentioned groups, there's a third group which is confronted with too large deviations: the persons directly involved in a project as supervisors, administrators, architects, engineers, project managers, craftsmen or planners. In many projects disagreements or huge arguments arise due to too large deviations, with disturbed relationships as a result.

10.1.3 Responsibility

Now that the causes and the effects of deviations that are too large have been discussed, the question arises: who is responsible? Contractors and producers are the obvious

candidates since they produce and construct the building with all the resulting deviations. But do they have exclusive responsibility for the obtained deviations? The sheer additional effort and resulting costs these parties have to make to restore undesirable situations make it unlikely that they voluntarily and intentionally produce deviations. It's more obvious to blame multiple parties for a failing dimensional control. Creating an accurate and dimensional acceptable project is therefore a collective effort of all the involved partners.

The ultimate goal of the partners should be: minimizing the negative results of dimensional deviations with respect to the functioning of the building and the costs. Thereby the following three propositions have to be taken into account:

1. dimensional deviations are inevitable,
2. high accuracies will result in disproportional high costs,
3. for each connection or situation in a building it holds that deviations will impair the proper functioning. However, this will only become a problem if a certain limit is exceeded.

The design process

The first partners that play an important role in the dimensional control are the designers of the building (architects, structural and installation engineers). Of them it may be desired that they specify how large the sizes or deviations may be. It would be impossible for the contractor or supplier to create anything without a proper size specification including maximum allowable dimensional deviations. A question that arises is which sizes and deviations should be specified? It's impossible to distinguish all the sizes in a building and fortunately this is not required. Only for a limited amount of sizes a project specific determination is required. In the other cases it's sufficient to specify the maximum allowable deviations as provided by the standards. This implicitly ensures an acceptable performance of the building, or at least this is assumed.

A first selection criterion for a project specific approach is the status of a size: is it a 'partial result' or an 'end result'? In fact, only the 'end results' are of importance: dimensions and situations where there is a direct relationship between deviations and proper functioning. An example of an 'end result' is a connection between concrete sandwich elements (joint thickness and thickness variation over the length) where deviations endanger aesthetic, structural and building physics functions. The warpage or thickness of a concrete facade element can be seen as a "partial" result, which is only significant in combination with the allocation of the measurement points and adjustment of the element.

A further limitation of the project specific dimensional tolerances can be obtained by using the sensitivity criterion. As a scale for the sensitivity, the difference between the initial estimated required accuracy and the initial estimated occurring accuracy can be used. If the difference is relatively small (it's difficult to add an exact value to the aspect small, but values below 2 or 3mm can be regarded as small), the connection or situation may be considered as critical. For all the non-critical connections or situations the maximum allowable deviations as provided by the standards may be used.

The next step is to verify if the critical project specific maximum allowable deviation is indeed technically achievable. This should be combined with a verification of the financial consequences due to the critical and small allowable deviations. In other words: does the increased performance justify the increased accuracy?

Finally, it should be examined if there are alternatives for the designed connections or situations that are functionally equivalent, but result in less negative effects. Towards the end of the design stage a design becomes available with all the size specifications (dimensions with the corresponding maximum allowable deviations). Because of the relation between accuracy and costs, it's only more than fair to present the dimensions

with corresponding deviations before the tender. In Figure 102 the design process is shown in combination with the execution process.

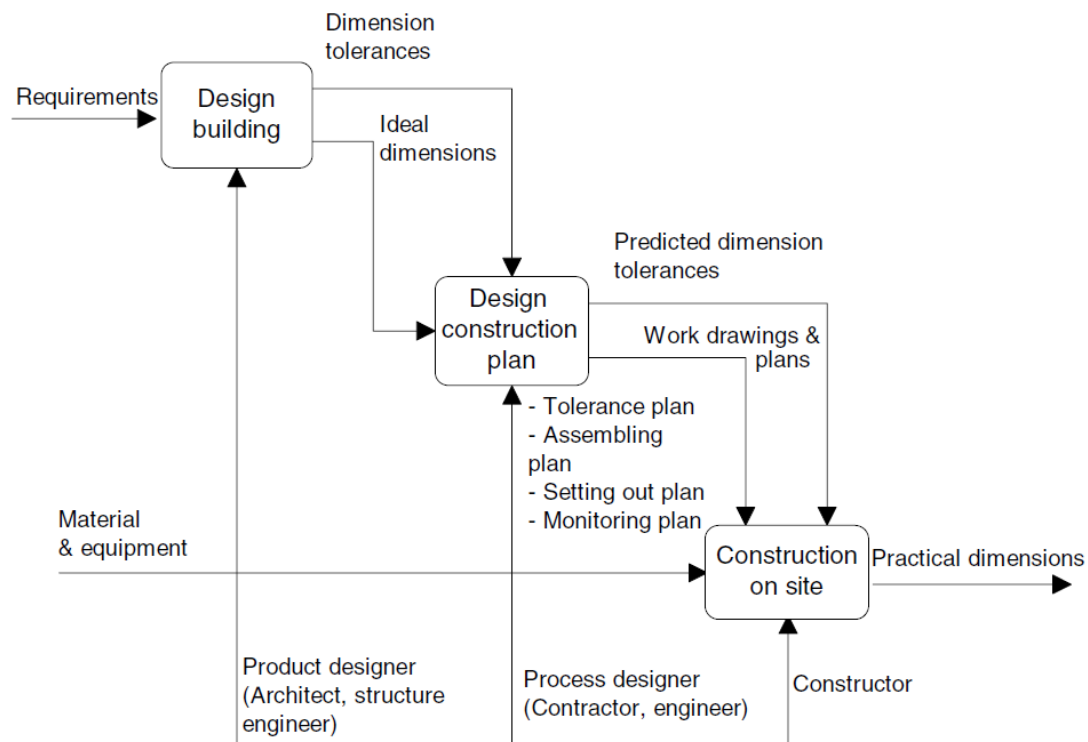


Figure 102 The role of dimensional control in building design and construction [Wu, 2002]

The execution process

An important task for the designers of the execution process (process designer) is to develop a plan which results in a finished building that satisfies the requirements. The first step to develop this plan is to describe how the critical connections or situations can be realised. This means preparing an execution plan, which describes where and how the measurement points are allocated. Parallel to the preparation of the execution plan an assembly plan is developed. In the assembly plan it's specified which points of an element or building section are used during the placing and adjusting. The execution and assembly plan together can be seen as a collection of allocation and adjustment points, which unambiguously fixates the location of an element or building section. When the product sizes are added, a full overview of the connections and situations can be formed.

Although we now have a complete collection of allocation sizes, adjustment sizes and product sizes with their relationships, the essence is still lacking: an overview of the consequences of the choices made in relation to the dimensional accuracy. For each connection or situation, a forecast of the expected accuracy is made. This forecast is based on many previous and similar experiences or based on a more objective mathematical approach through accuracy calculations. Eventually, it's possibly to determine with a certain reliability between which limits a deviation probably will remain. The expected value is compared with the maximum allowable values and changes are made concerning the construction method, equipment and care if the requirements aren't met or the costs are too high.

Towards the end of the design of the execution process an execution plan is obtained, in which the building is constructed on paper (model based). The occurring deviations have to be smaller than the maximum allowable dimensional deviations and the resulting costs should be as low as possible. What the process designer managed to do on paper has to be matched by the contractor on site.

The contractors on the building site are given work plans, execution plans and assembly plans, which show how and with what accuracy the allocation points, the assembly and the manufacturing of the elements have to be realised (with a precast structure the elements are produced at a factory). Also agreements are made with the subcontractors and suppliers with respect to the maximum allowable deviations of their products.

The implementation of dimensional control is only complete if the execution process is constantly monitored. In other words: quality control has to be implemented. The purpose of measuring and verifying the structure is that the actual deviations can be compared with the designed and forecasted values. If there are significant differences, it may be possible to adapt the process without large additional costs. The described control measurements can also be considered as an internal justification towards the process designers and as an external justification from the contractors and process designers towards the client and designers.

10.1.4 Conclusion

There are arguments why a professional implementation of dimensional control is the only option for the future, in terms of quality and costs. For example, more and more precast elements are used at the construction site, which require little to no modifications and have to fit the first time, every time. In addition, the higher amount of prefabrication is accompanied by increasingly more complex building shapes; building layouts are rarely straightforward and facades aren't flat and vertical anymore but show slopes and curves. Add the preferred reduced construction time, which results in more parallel processes, and it will be clear that acting on a basis of experience (which experience?) will only by coincidence lead to acceptable results. It's likely that clients will also become more aware of dimensional control and include it in the contracts. Why would they take the unnecessary risk of dimensional deviations and all the adverse consequences?

10.2 Dimensional accuracy in the standards

With the slogan "nothing ventured, nothing gained" many standards are imposed in the contract documents. The NEN-collection 14 "Maten en meten" is a good example of the latter, which contains standards about modular coordination, dimensional tolerances and dimensional control. In contrast to the intentions, it appears that the standards in practise do not guarantee the quality assurance that was presumed by the unsuspecting specifications employee (bestekschrijver in Dutch). The prescribed standards are rarely sufficient for a proper functioning building. Often the standards provide a (legitimate) opportunity for (sub)contractors to exonerate themselves if problems due to dimensional deviations occur.

In this section standards on dimensional accuracy will be discussed, including possible reduction factors. The main question is: which aspects are defined by the standards?

10.2.1 NEN 2881: dimensional tolerances for structures

The first important standard of the NEN-collection 14 is NEN 2881 "maattoleranties voor de bouw". The main goal of NEN 2881 is to unambiguously specify concepts such as dimensional deviations, tolerances and maximum allowable dimensional deviations. According to the standard a dimensional deviation can be explained as the difference between a target size and the measured size, negative or positive. For example 7992 or 8005mm, where 8000 is the target size. Note that the deviation of the size is defined including measurement inaccuracies. The tolerance of an object can be described as the tolerated deviation between the largest allowable size and the smallest allowable size. For example, a tolerance of 10mm and a target size of 8000mm results in a symmetric (a tolerance is often symmetric, but this is not mandatory) area of allowable sizes between

7995 and 8005mm. The first measured size (7992mm) is outside the tolerance area and actions have to be taken. In practice the term tolerance is often used inappropriately, for example it's often stated that the element has a tolerance of 5mm while the measured length is 5mm too long (dimensional deviation).

NEN 2886 until 2889 create confusion by specifying tolerances with a different method. These standards use a maximum allowable dimensional deviation A, equal to 50% of the tolerance. For example: the target size is 8000mm and the tolerance (T) is 10mm. This results in an area of allowable sizes between 7995 and 8005mm. In the previous example, the maximum allowable dimensional deviation (A) would be 5mm, resulting in the same allowable area of 7995 till 8005mm. NEN 2881 also specifies how tolerances should be added together. It's not allowed to normally add tolerances (T) or allowable deviations (A), but they have to be quadratically added: $T_{\text{total}}^2 = T_i^2 + T_s^2 + T_u^2$ or $A_{\text{total}}^2 = A_i^2 + A_s^2 + A_u^2$. For example two elements that are stacked on top of each other with a target size and height tolerance of 3300 (+3;-3)mm and 3300 (+4;-4)mm will result in a total target size and tolerance of 6600 (+5;-5)mm.

10.2.2 NEN 2886: maximum allowable dimensional deviations for concrete structures

In NEN 2886 "Maximaal toelaatbare maatafwijkingen voor gebouwen" the maximum allowable dimensional deviations are provided for structural and spatial dimensions. These values serve as boundary limit and the deviations due to the allocation of measurement points, adjustment and manufacturing of the elements should be smaller than the provided A_e -values. The A_e -values of NEN 2886 are obtained by applying a mathematical model on a basic project execution process, taking NEN 2887, 2888 and 2889 into account. The results of this model are given via the term dimensional tolerance (T_e), defined as: the tolerance of that point with respect to the location of that point in the building. As a result of this method, every point in the structure can be given a dimensional tolerance (the designated point has a certain area in which it should be located). But in practice there is no use for the dimensional tolerance because it's impossible to determine the location a point without a reference system. To overcome this problem, the location of one point is determined relative to another point. Now that the relative location is known, it's also possible to determine the maximum allowable deviation:

$$A_e = \frac{1}{2} \sqrt{T_{e,1}^2 + T_{e,2}^2 + 8l} \text{ [mm]}$$

The A_e -value for the position of the two points relative to each other is dependent on the dimensional tolerance of both points [mm] and the mutual distance l [m]. The values for the dimensional tolerances of walls and floors can be found in Table 24

Table 16 Maximum allowable deviations for concrete structures (A_e) [NEN, 1990]

gebouwdelen	rich-ting	plaats		plaatstolerantie T_e mm	illustratie voor de definiëring van richtingen en punten waarvoor de plaatstoleranties gelden
		R	M		
wanden	x	o	o	32	
	y	o		33	
	y		o	$\sqrt{424 + (4 + 2,8 l)^2}$	
	z	o	o	22	
vloeren	x	o	o	61	
	z	o		26	
	y	o		34	
	y		o	$\sqrt{424 + (2 + 5,6 l)^2}$	
	z		o	$\sqrt{164 + (2 + 4 l)^2}$	
balkons	x	o	o	29	
en	y	o	o	30	
galerijen	z	o	o	23	

In 1995 a code of practice has been introduced: NPR 3685 "Maattoleranties in de bouw". In this code of practise instructions and many examples are provided. Unfortunately, the examples are for non-professionals difficult to understand. This is partly explained by the complexity of the material and how the examples are elaborated. As a result, the examples are rarely used.

10.2.3 NEN 2887: maximum allowable deviations for the allocation of the measurement points

The allocation of the measurement points is described in NEN 2887 "Maximaal toelaatbare maatafwijkingen voor het uitzetten op de bouwplaats". The allocation of the measurement points is part of the execution process and requires measuring and marking of points. To obtain the A_u -values, two formulas are provided in the standard:

1. Maximum allowable deviations for distances: $A_{u,1} = \sqrt{16 + 2l}$ [mm]
2. Maximum allowable deviations for perpendicular angles:

$$A_{u,2} = \sqrt{16 + 2l_{12} + \left(\frac{l_{12}}{l_{23}}\right)^2 \cdot (16 + 2l_{23})}$$
 [mm]

The second formula provides the maximum allowable angle deviation $A_{u,2}$ (or A_1 in Figure 103) of point 1 in relation to point 2 and 3 in Figure 103. The distance between the points is entered in meters.

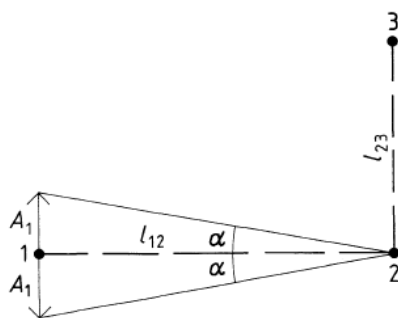


Figure 103 Maximum allowable deviations for right angles [NEN, 1990]

No tables with maximum allowable dimensional deviations are given, since the values are project specific (the value depends on the length between the points). Due to the introduction of more advanced tools in the last two decades, the A-values can be reduced. When a modern total station is used, the deviations may be reduced with 50% [Hoof, 1997B].

10.2.4 NEN 2888: maximum allowable deviations for the adjustment of the structure

In NEN 2888 "Maximaal toelaatbare maatafwijkingen voor het stellen van draagconstructies van gebouwen" the maximum allowable dimensional deviations for the adjustment process are given (see Table 17). During the adjustment process the elements are placed on their final location, requiring an iterative method of adjusting and measuring. From a limited amount of points on the element the coordinates are measured relative to a central point (for example three corner points of a wall element relative to a central point on the floor).

Table 17 Maximum allowable dimensional deviations for the adjustment process (A_s) [NEN, 1990]

vorm van het bouwelement	maximaal toelaatbare stelafwijking A _s mm			illustratie voor de definiëring van de punten en richtingen waarvoor de maximaal toelaatbare stelafwijkingen gelden
	x	y	z	
verticaal schijfvormig $b \ll h \leq l$ (wand)	10	7	5	
horizontaal schijfvormig $h \ll b \leq l$ (vloerplaat)	10	5	7	

NEN 2888 dates from December 1990 and in the past 22 years a lot has changed. Total stations are an important cause of this change and they combine a digital theodolite with a digital distance meter. The first total station was introduced in 1968 (Reg Elta 14 from Zeiss [deHilster, 2012]), but in the last decade the total station has become the tool to use on the construction site. The A-values of NEN 2888 are unnecessarily large and the maximum allowable value of 10mm in the x-direction can be achieved without any instruments. The standard already contains a chapter with reduction factors and it's recommended to apply them (chapter 3.3 from NEN 2888). The suggested reduction factors are $\frac{1}{2}\sqrt{2}$ or $\frac{1}{2}$.

10.2.5 NEN 2889: maximum allowable deviations of the concrete element

From all the dimensional standards, NEN 2889 "Betonelementen, Maximaal toelaatbare maatafwijkingen" is probably the most well known-standard. For many years only this standard or its predecessor (NPR 2889) was used in tenders [Hoof, 1997B]. In Table 18 the used A_i-values of the NEN 2889 are depicted.

Table 18 Maximum allowable dimensional deviations for concrete elements (A_i) [NEN, 1990]

produkt	grootte ¹⁾					vorm ¹⁾					voorzieningen ²⁾	
	lengte ³⁾	breedte	dikte	hoogte	diagonaal ⁴⁾	kromte	buiging ⁵⁾	scheluwte	haaksheid		eenling	groep
									kop-eind	opleg-vlak		
mm	mm	mm	mm	mm	mm	mm/m	mm/m	mm	mm	mm	mm	
kolommen	–	7	7	11	–	1,4	–	5	10	6	11	5
balken:												
≤ 10 m NVS ⁶⁾	11	–	7	11	–	1,4	1,4	8	10	6	11	5
≤ 10 m VS ⁷⁾	17	–	7	11	–	2,0	2,8	10	14	6	14	5
> 10 m VS ⁷⁾	21	–	8	11	–	2,0	2,0	14	16	8	14	5
spantvormige elementen	11	7	7	11	–	1,4	2,0	10	10	6	11	5
vloerplaten NVS ⁶⁾	28	12	12	–	28	2,0	1,6	8	20	–	50	–
vloerplaten VS ⁷⁾	28	12	12	–	28	1,0	2,0	8	20	–	50	–
vloerplaten TT ⁸⁾	21	7	7	7	21	2,0	2,8	10	20	6	28	5
wanden	11	–	7	8	11	1,4	–	8	10	–	11	5
gevelelementen – binnenspuwbladen	7	–	5	7	9	2,0	–	8	10	–	11	5
trapelementen	14	11	11	–	–	2,0	–	8	10	–	11	5
balkonelementen	7	7	5	–	9	1,4	2,0	8	10	–	11	5

1) Zie illustraties in de bijlage C bij NEN 3682.

2) Bijvoorbeeld een opening c.q. sparing is eenling.

Maatafwijkingen bij een voorzieningengroep zijn maatafwijkingen in de onderlinge posities van eenlingen binnen een groep.

3) Voor de lengte van balken als onderdelen van systeemvloeren gelden dezelfde maximaal toelaatbare maatafwijkingen als bij vloerplaten zijn vermeld.

4) Bedoeld worden alle diagonalen.

5) Buiging ten opzichte van berekende doorbuiging of opbuiging.

6) NVS: niet-voorgespannen.

7) VS: voorgespannen.

8) Vloerplaten TT: dubbel T vloerplaten.

Manufacturers may individually or collectively specify smaller tolerances than the previous mentioned standard. An example of the latter can be found in the BELTON publication "Connections in precast" (see Table 19) and Facades in precast".

10.2.7 NEN 3682: dimensional control for structures

It's expected that every contractor, supplier and supervisor periodically verifies if the dimensions of the building or product satisfy the required accuracy. However, in practise too little control measurements are conducted. Moreover, the results are often poor and inconsistent. This applies to the measurement method, the use of equipment, the registration and interpretation of measurement results. The goal of NEN 3682 is to make dimensional control organised and accessible. This goal is achieved by giving many illustrative examples and methods. In Figure 105 an example is given where the measurement points on walls and floors should be located.

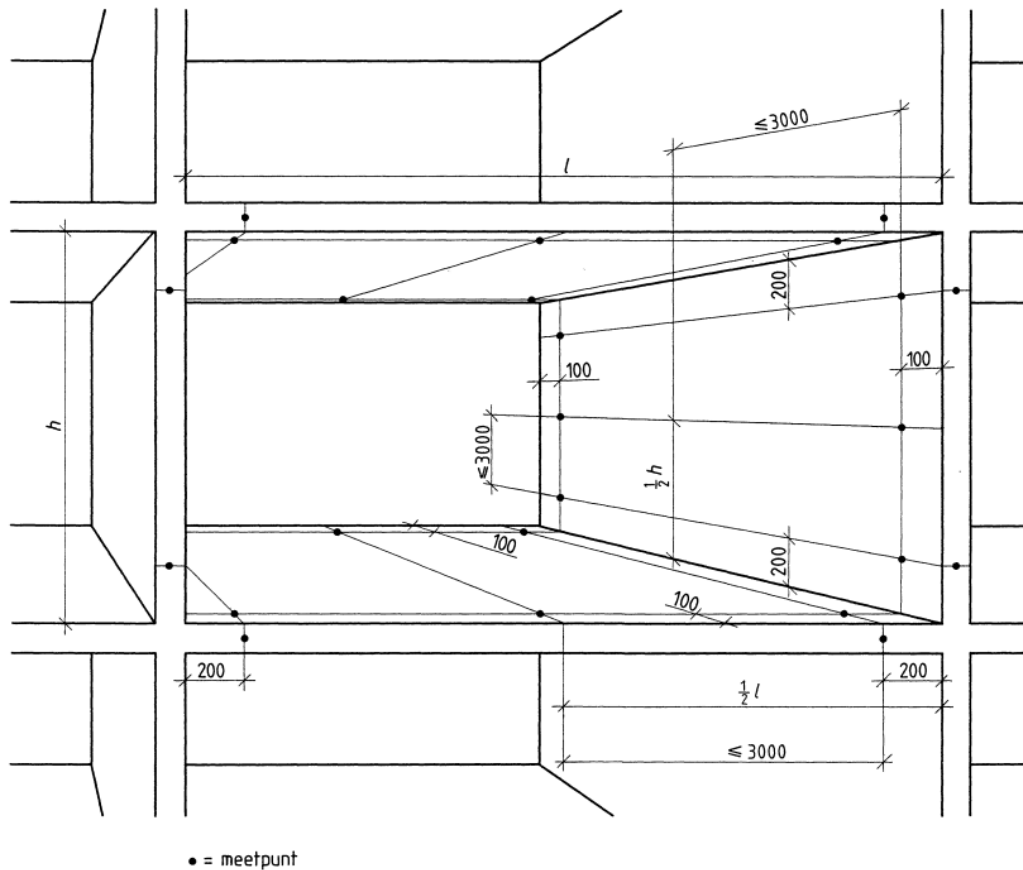


Figure 105 Location of the measurement points at walls and floors [NEN, 1990]

10.2.8 Conclusion

With the NEN 2881, 2886, 2887, 2888, 2889, 2890, 3682 and NPR 3685 it's possible to determine the maximum allowable dimensional deviations and the deviations due to the allocation of measurement points, adjusting and manufacturing of the element. Because the standards are dated, reduction factors between 30 and 50% can be applied without an increase of costs. In the next section it will be examined how these standards affect a precast high-rise structure.

10.3 Dimensional tolerances and deviations in a precast high-rise building

In the previous sections dimensional control, tolerances and deviations have been discussed. It can be concluded that deviations are inevitable and that only the magnitude can be controlled. When a precast high-rise building is compared with a low rise precast building, the high-rise building distinguishes itself by the repetitive nature of the construction method. Because of this repetition, deviations and tolerances become leading in a high-rise design. How does this influence the functional requirements³⁴ and how are the deviations absorbed?

First the deviations will be examined. There are several methods to absorb deviations, for example at every level (locally) or on every n-levels (globally). During the compensation of the deviations it should also be known how the structure reacts. Quay walls are an interesting example of these aspects: in a precast quay wall, all the massive concrete blocks are placed relative to the previous block. The global deviations aren't leading at this stage because the precast blocks are difficult to adjust underneath the water level and the wall will deform during the construction. This deformation occurs because the quay wall is constructed under an angle and levels when the ballast behind the wall is placed. Pre-loading the quay wall also creates additional deformations. Therefore placing the elements at their desired location before the ballast is placed and the wall is pre-loaded is pointless. Since it's difficult to determine the exact location of the precast elements after all the deformations have occurred, a cast in situ top beam is placed on top of the precast elements adsorbing all the deviations. As a result, the ships are able to moor to a perfectly straight quay wall at the desired location.

To determine how the deviations at a precast high-rise tower should be adsorbed, it's first examined at which level the deviations are larger than the tolerances. Therefore the deviations due to the allocation of the measurement points, the adjustment and manufacturing of the element will be estimated in this section and compared with the boundary values according to the standard. Based on these results, the functional requirements and the behaviour of the structure, a method will be designed how to absorb the deviations.

10.3.1 Model scheme

To calculate at which level the deviations are larger than the tolerances, the hatched area with walls 1 until 3 of Figure 106 has been chosen. This area has the largest dimensions and this will result in larger deviations. Because the walls are stacked in a masonry configuration, difficulties arise with elements that are placed above each other (different allocation points on the walls for even and uneven floors). Therefore walls from corner to corner without a masonry configuration are used in this calculation. The error that is created is very small since most deviations and tolerances do not depend on the wall length (for the deviations that do depend on the length, the dependency of the calculation on the wall length is very low).

³⁴ Functional requirements are the properties that the product should provide. For a structural wall this are for example: strength, stiffness, stability, aesthetics or building physics properties

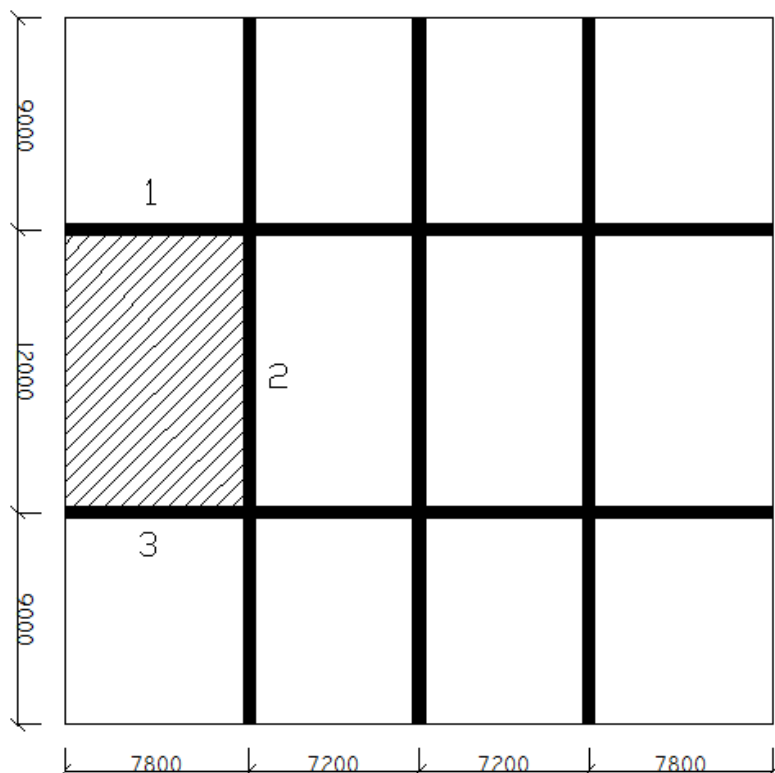


Figure 106 Overview of the floor

Most structures are constructed with no or very little internal walls and therefore they only require a few vertical allocation points (it's advised to use at least two points with the largest possible mutual distance). Due to the structural walls in the Zalmhaven tower, every floor area requires its own vertical allocation point. It's possible to use only four allocation points at the corners and place all the walls according to these points, but this requires a specific construction sequence and after all the walls are placed, the central walls cannot be measured anymore. The small additional costs of placing a tube in every floor centre outweighs the limitations of only four vertical allocation points in the corners and therefore every floor area is equipped with its own vertical allocation point.

The deviations of the walls depend on the building height. The deviations of the floors are less interesting since they are placed between the walls and are therefore influenced by the walls. Furthermore, a new wall element depends on the previous element while the floor element doesn't. Therefore only the walls will be examined in this research on tolerances.

10.3.2 Maximum allowable deviations of the concrete element

The first deviations that will be calculated are due to the production of the elements: NEN 2889. In Table 20 the used A_i -values of the NEN 2889 are depicted.

Table 20 Maximum allowable dimensional deviations for concrete elements (A_i) [NEN, 1990]

produkt	grootte ¹⁾					vorm ¹⁾					voorzieningen ²⁾	
	lengte ³⁾	breedte	dikte	hoogte	diagonaal ⁴⁾	kromte	buiging ⁵⁾	scheluwte	haaksheid		eenling	groep
									kop-eind mm	opleg-vlak mm		
	mm	mm	mm	mm	mm	mm/m	mm/m	mm	mm	mm	mm	mm
kolommen	–	7	7	11	–	1,4	–	5	10	6	11	5
balken:												
≤ 10 m NVS ⁶⁾	11	–	7	11	–	1,4	1,4	8	10	6	11	5
≤ 10 m VS ⁷⁾	17	–	7	11	–	2,0	2,8	10	14	6	14	5
> 10 m VS ⁷⁾	21	–	8	11	–	2,0	2,0	14	16	8	14	5
spantvormige elementen	11	7	7	11	–	1,4	2,0	10	10	6	11	5
vloerplaten NVS ⁶⁾	28	12	12	–	28	2,0	1,6	8	20	–	50	–
vloerplaten VS ⁷⁾	28	12	12	–	28	1,0	2,0	8	20	–	50	–
vloerplaten TT ⁸⁾	21	7	7	7	21	2,0	2,8	10	20	6	28	5
wanden	11	–	7	8	11	1,4	–	8	10	–	11	5
gevelelementen – binnenspouwbladen	7	–	5	7	9	2,0	–	8	10	–	11	5
trapelementen	14	11	11	–	–	2,0	–	8	10	–	11	5
balkonelementen	7	7	5	–	9	1,4	2,0	8	10	–	11	5

1) Zie illustraties in de bijlage C bij NEN 3682.

2) Bijvoorbeeld een opening c.q. sparing is eenling.

Maatafwijkingen bij een voorzieningengroep zijn maatafwijkingen in de onderlinge posities van eenlingen binnen een groep.

3) Voor de lengte van balken als onderdelen van systeemvloeren gelden dezelfde maximaal toelaatbare maatafwijkingen als bij vloerplaten zijn vermeld.

4) Bedoeld worden alle diagonalen.

5) Buiging ten opzichte van berekende doorbuiging of opbuiging.

6) NVS: niet-voorgespannen.

7) VS: voorgespannen.

8) Vloerplaten TT: dubbel T vloerplaten.

The A-values in the standard are based on a large-scale study of BFBN on dimensional deviations in precast elements. This research was done already 35 years ago and since then the techniques and quality control have changed considerably. A reduction of 30% of the values for walls, columns and facade elements is easily achievable [Hoof, 1997B]. Elements with a deviation smaller than 1mm can be produced, but normal workmanship will not be sufficient anymore. These high accuracies will also result in a disproportional increase of costs.

In Table 21 the values are depicted that will be used in this research on tolerances, based on Table 20 and a reduction of 30%. The coordinate system is depicted in Figure 107.

Table 21 Reduced A_i-values based on NEN 2889

	Length (x)	Height (z)	Thickness (y)	Squareness (x)	Warpage (y)
	[mm]	[mm]	[mm]	[mm/m]	[mm]
Deviation at the bottom	8	0*	5	0	0
Deviation at the top	8	6*	5	7	6

* Normally the element would be adjusted at the bottom connection resulting in the desired height at the top of the element. In this stage the elements are placed of top of each other without any connection thickness, resulting in a deviation at the top.

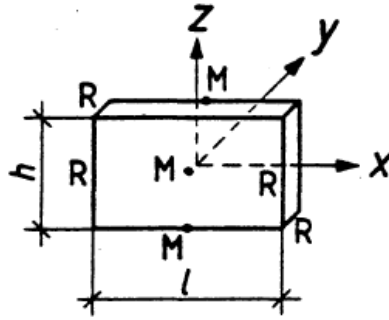


Figure 107 Coordinate system of the wall [NEN, 1990]

When a new section of elements is placed on top of the first wall, these new elements may have the same deviations. To combine these values, they have to be added quadratically. The deviations at the bottom of the second wall (first floor) are:

- $A_{i,1,x} = \sqrt{8^2 + 21^2 + 8^2} = 25\text{mm}$
- $A_{i,1,y} = \sqrt{5^2 + 6^2 + 5^2} = 9\text{mm}$
- $A_{i,1,z} = \sqrt{6^2 + 0^2} = 6\text{mm}$

It can be noted that the x-direction has the largest deviations. This is because of the large perpendicular deviation of $7 \cdot 3.05 = 21\text{mm}$. The deviation in the z-direction contains only one value because the deviation is examined at the bottom of the element (see Table 21). This method can be repeated for all the other walls above the first two walls.

10.3.3 Maximum allowable deviations for the adjustment of the structure

In NEN 2888 the maximum allowable dimensional deviations for the adjustment process are given (see Table 22). In this section the deviations due to the iterative method of adjusting and measuring will be calculated.

Table 22 Maximum allowable dimensional deviations for the adjustment process (A_s) [NEN, 1990]

vorm van het bouwelement	maximaal toelaatbare stelafwijking A_s mm			illustratie voor de definiëring van de punten en richtingen wavoor de maximaal toelaatbare stelafwijkingen gelden
	x	y	z	
verticaal schijfvormig $b \ll h \leq l$ (wand)	10	7	5	
horizontaal schijfvormig $h \ll b \leq l$ (vloerplaat)	10	5	7	

NEN 2888 dates from December 1990 and in the past 22 years a lot has changed. The stated A-values in the standard are unnecessarily large and the maximum allowable value of 10mm in the x-direction can be achieved without any instruments. NEN 2888 already contains a chapter with reduction factors and it's recommended to apply them (chapter 3.3 from NEN 2888). The suggested reduction factors are $\frac{1}{2}\sqrt{2}$ or $\frac{1}{2}$.

Due to the high accuracy of the current total stations, a reduction factor of 50% will be used in this research on tolerances. Table 23 shows the reduced values that will be applied in the calculation. The coordinate system is depicted in Figure 107.

Table 23 Reduced A_s-values according to NEN 2888

Element shape	Maximum allowable deviation for the adjustment process		
	x [mm]	y[mm]	z [mm]
Wall	5	4	3
Floor	5	3	4

When the wall on the first floor is adjusted, the same deviations occur as on the ground floor. Therefore the deviations have to be summed quadratically. The following deviations are obtained at the bottom of the wall on the first floor:

- $A_{s,1,x} = \sqrt{5^2 + 5^2} = 7\text{mm}$
- $A_{s,1,y} = \sqrt{4^2 + 4^2} = 5\text{mm}$
- $A_{s,1,z} = \sqrt{3^2 + 0^2} = 3\text{mm}$

Again the largest deviations are obtained in the x-direction.

10.3.4 Maximum allowable deviations for the allocation of the measurement points

The allocation of the measurement points is described in NEN 2887. To obtain the A_u-values, two formulas are provided in the standard:

3. Maximum allowable deviations for distances: $A_{u,1} = \sqrt{16 + 2l}$ [mm]
4. Maximum allowable deviations for perpendicular angles:

$$A_{u,2} = \sqrt{16 + 2l_{12} + \left(\frac{l_{12}}{l_{23}}\right)^2 \cdot (16 + 2l_{23})} \text{ [mm]}$$

The second formula provides the maximum allowable deviation A_{u,2} (or A₁ in Figure 108) of point 1 in relation to point 2 and 3 in Figure 108. The distance between the points is entered in meters.

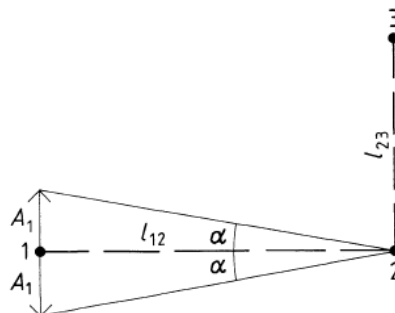


Figure 108 Maximum allowable deviations for right angles [NEN, 1990]

Just as the previous two standards, the A-values can be reduced due to the introduction of more advanced tools in the last two decades. When a modern total station is used, the deviations may be reduced with 50% [Hoof, 1997B].

As shown in section 10.3.1, the hatched area is chosen for this research on tolerances. From these three walls, wall 2 will be used. In Figure 109 the location of the three allocation points are depicted. Normally these points are placed a certain distance from the ground, edge or ceiling (100 to 200mm) because it's unpractical and difficult to measure the corners. For simplicity this research uses the actual corners.

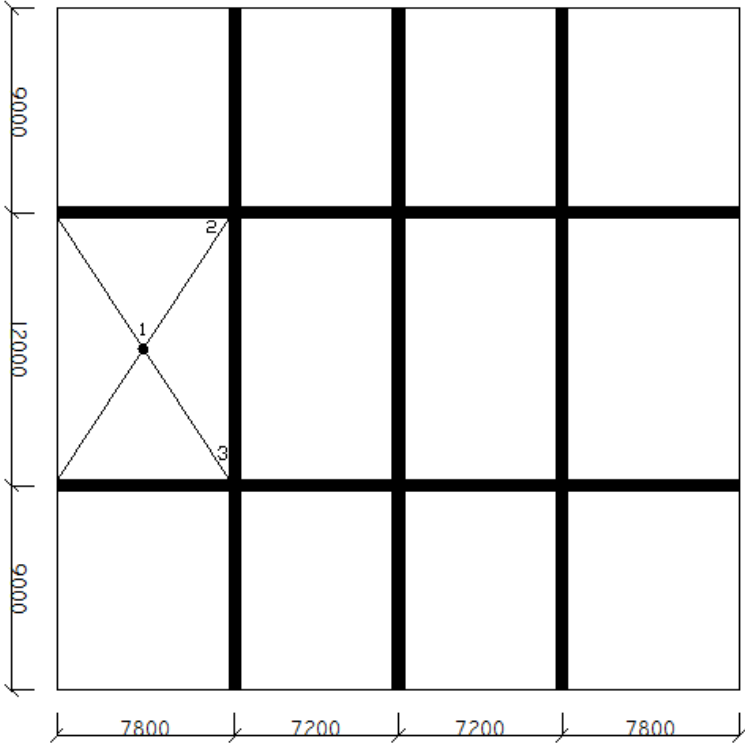


Figure 109 Location of the allocation points

Above allocation point 2 another point is located, point 4. This is depicted in Figure 110 and with these three points the location of the wall element can be determined relative to point 1. To measure the curvature of the element, additional points in the centre are required.

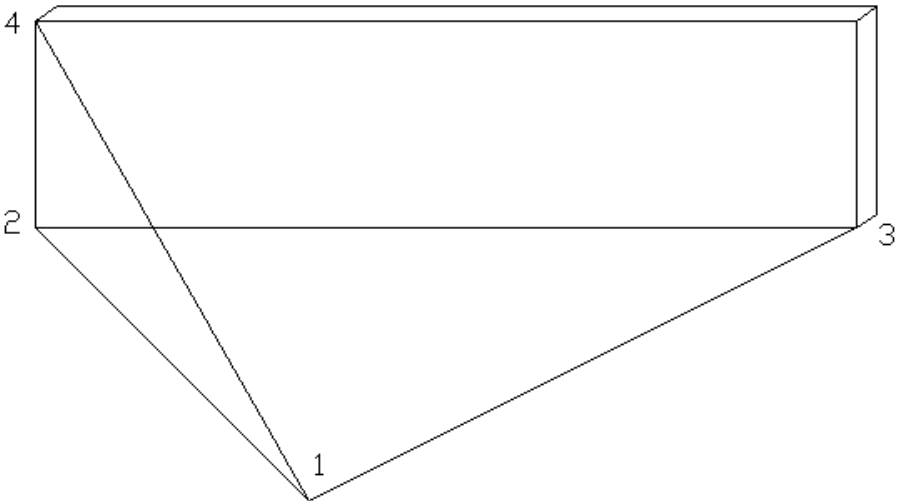


Figure 110 Location of the allocation points on the element

The maximum allowable deviations of point 2, 3 and 4 relative to point 1 are:

- $A_{u,1-2} = \sqrt{16 + 2 \cdot 7.2} = 6\text{mm}$
- $A_{u,1-3} = \sqrt{16 + 2 \cdot 7.2} = 6\text{mm}$
- $A_{u,1-4} = \sqrt{16 + 2 \cdot 7.8} = 6\text{mm}$

These deviations are in the direction of the line and therefore have to be rewritten to x, y and z-values:

- $A_{u,1-2}=6\text{mm}$
 - $A_{u,1-2,x} = \frac{5.5}{7.2} \cdot 6 = 5\text{mm}$
 - $A_{u,1-2,y} = \frac{5.5}{7.2} \cdot 3.9 = 3\text{mm}$
 - $A_{u,1-2,z} = 0\text{mm}$
- $A_{u,1-3}=6\text{mm}$
 - $A_{u,1-3,x} = \frac{5.5}{7.2} \cdot 6 = 5\text{mm}$
 - $A_{u,1-3,y} = \frac{5.5}{7.2} \cdot 3.9 = 3\text{mm}$
 - $A_{u,1-3,z} = 0\text{mm}$
- $A_{u,1-4}=6\text{mm}$
 - $A_{u,1-4,x} = \frac{5.6}{7.8} \cdot 6 = 4\text{mm}$
 - $A_{u,1-4,y} = \frac{5.6}{7.8} \cdot 3.9 = 3\text{mm}$
 - $A_{u,1-4,z} = \frac{5.6}{7.8} \cdot 3.05 = 2\text{mm}$

Though the distance between $A_{u,1-2}$ and $A_{u,1-4}$ has increased, the allowable deviation has decreased. This is caused by how the deviations are calculated: the distance in this formula is only of minor influence.

Placing and measuring points on the ground floor is relatively easy with a total station, but how are the main measurement points obtained at the overlying floors? A solution is to raise these points via a small hollow tube in the floor. A well known system that is capable of doing this is the MOUS system (Markeren, Oploden/ophalen van peil, Uitzetten van afstanden en richtingen en het maken van Sparingen). In Figure 111 it's depicted how the main measurement points are raised at a cast in situ floor. There are also many solutions for precast floors.

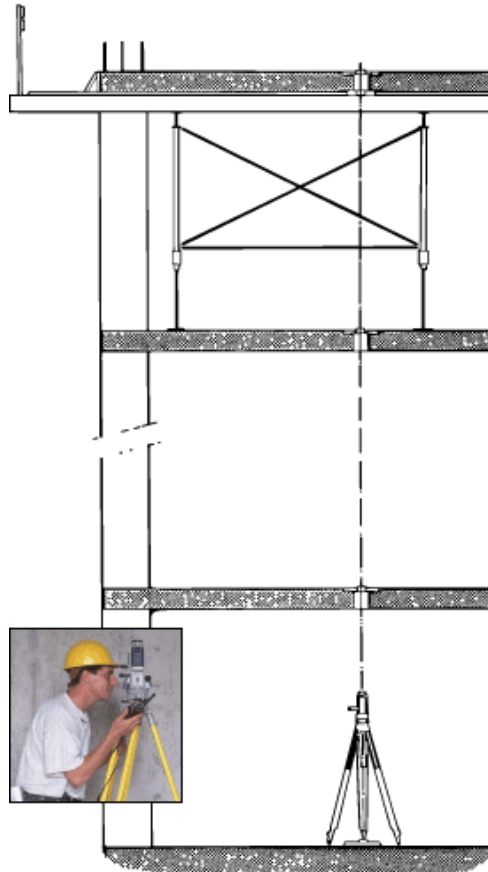


Figure 111 Raising measurement points with the MOUS system [MOUS, 2005]

Just as with the in-plane measurement points, the raising of a measurement point is subjected to deviations in the x, y and z-direction. Between point 1 and point 5 (same location as point 1 but then on the first floor) the following deviations occur:

- $A_{u,1-5,y} = \sqrt{16 + 2 \cdot 3,05} = 5\text{mm}$
- $A_{u,1-5,x} = \sqrt{16 + 2 \cdot 3,05 + \left(\frac{3,05}{22,2}\right)^2 \cdot (16 + 2 \cdot 22,2)} = 5\text{mm}$
- $A_{u,1-5,z} = \sqrt{16 + 2 \cdot 3,05 + \left(\frac{3,05}{10,5}\right)^2 \cdot (16 + 2 \cdot 10,5)} = 5\text{mm}$

The l_{23} (22.2 and 10.5m) distance used in $A_{u,1-5,x}$ and $A_{u,1-5,z}$ is shown in Figure 112. A longer distance results in a more accurate angle (smaller deviation).

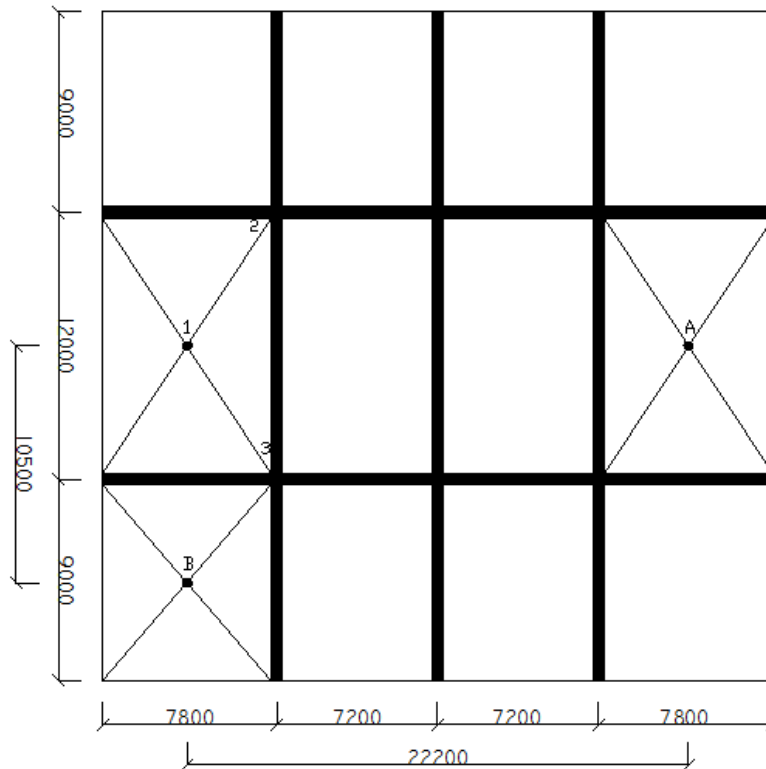


Figure 112 Location of the vertical allocation points

These deviations also have an influence on point 6, 7 and 8 (the same points as 2, 3 and 4, but then on the first floor). This results in the following deviations for point 6 (left bottom corner point on the first floor):

$A_{u,5-6,rel1}$:

- $A_{u,5-6,rel1,x} = \sqrt{5^2 + 5^2} = 7\text{mm}$
- $A_{u,5-6,rel1,y} = \sqrt{3^2 + 5^2} = 6\text{mm}$
- $A_{u,5-6,rel1,z} = \sqrt{0^2 + 5^2} = 5\text{mm}$

This process can be repeated for point 7 and 8 and all the other overlying floors. When a modern total station is used, the above values may be reduced with 50%.

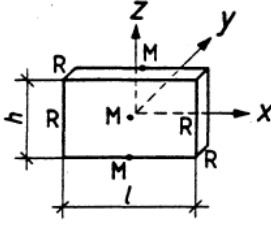
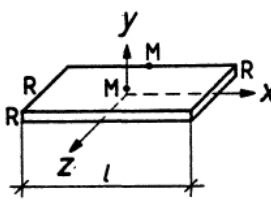
10.3.5 Maximum allowable deviations for concrete structures

In the previous three sections maximum values have been calculated which can occur due to the allocation of measurement points, adjustment and manufacturing of the element. When these values are quadratic combined (the deviations may not be normally added to each other), the total deviation is obtained. This deviation should be lower than the maximum allowable deviation, provided by NEN 2886. The maximum allowable deviations can be calculated with the following formula:

$$A_e = \frac{1}{2} \sqrt{T_{e,1}^2 + T_{e,2}^2 + 8l} \text{ [mm]}$$

The A_u -value for the position of the two points relative to each other is dependent on the dimensional tolerance of both points [mm] and the mutual distance [m]. The values for the dimensional tolerances of floors and walls can be found in Table 24.

Table 24 Maximum allowable deviations for concrete structures [NEN, 1990]

gebouwdelen	richting	plaats		plaatstolerantie T_e mm	illustratie voor de definiëring van richtingen en punten waarvoor de plaatstoleranties gelden
		R	M		
wanden	x	o	o	32	
	y	o		33	
	y		o	$\sqrt{424 + (4 + 2,8 l)^2}$	
	z	o	o	22	
vloeren	x	o	o	61	
	z	o		26	
	y	o		34	
	y		o	$\sqrt{424 + (2 + 5,6 l)^2}$	
	z		o	$\sqrt{164 + (2 + 4 l)^2}$	
balkons en galerijen	x	o	o	29	
	y	o	o	30	
	z	o	o	23	

At the ground floor the maximum allowable deviation between point 1 and 2 (see Figure 112) in the x, y and z-direction are:

- $A_{e,1-2,x} = \frac{1}{2} \sqrt{T_{e,1,z}^2 + T_{e,2,x}^2 + 8l_{1-2}} = \frac{1}{2} \sqrt{(164 + (2 + 4 \cdot 7.8)^2 + 32^2 + 8 \cdot 7.2} = 23\text{mm}$
- $A_{e,1-2,y} = \frac{1}{2} \sqrt{T_{e,1,x}^2 + T_{e,2,y}^2 + 8l_{1-2}} = \frac{1}{2} \sqrt{61^2 + 33^2 + 8 \cdot 7.2} = 35\text{mm}$
- $A_{e,1-2,z} = \frac{1}{2} \sqrt{T_{e,1,y}^2 + T_{e,2,z}^2 + 8l_{1-2}} = \frac{1}{2} \sqrt{(424 + (2 + 5.6 \cdot 7.8)^2 + 22^2 + 8 \cdot 7.2} = 26\text{mm}$

To calculate the maximum allowable deviations between point 1 and 5, the same formulas can be used, but the mutual distance changes. This provides in the following results:

- $A_{e,1-5,x} = \frac{1}{2} \sqrt{T_{e,5,z}^2 + T_{e,5,x}^2 + 8l_{1-5}} = \frac{1}{2} \sqrt{(164 + (2 + 4 \cdot 7.8)^2 + 32^2 + 8 \cdot 7.8} = 23\text{mm}$
- $A_{e,1-5,y} = \frac{1}{2} \sqrt{T_{e,5,x}^2 + T_{e,5,y}^2 + 8l_{1-5}} = \frac{1}{2} \sqrt{61^2 + 33^2 + 8 \cdot 7.8} = 35\text{mm}$
- $A_{e,1-5,z} = \frac{1}{2} \sqrt{T_{e,5,y}^2 + T_{e,5,z}^2 + 8l_{1-5}} = \frac{1}{2} \sqrt{(424 + (2 + 5.6 \cdot 7.8)^2 + 22^2 + 8 \cdot 7.8} = 26\text{mm}$

For the deviations the global coordinate system is used, equal to the coordinate system of the wall 2. For the dimensional tolerances in the previous calculations the coordinate system is shown in Table 24. An overview of the coordinate systems is shown in Figure 113.

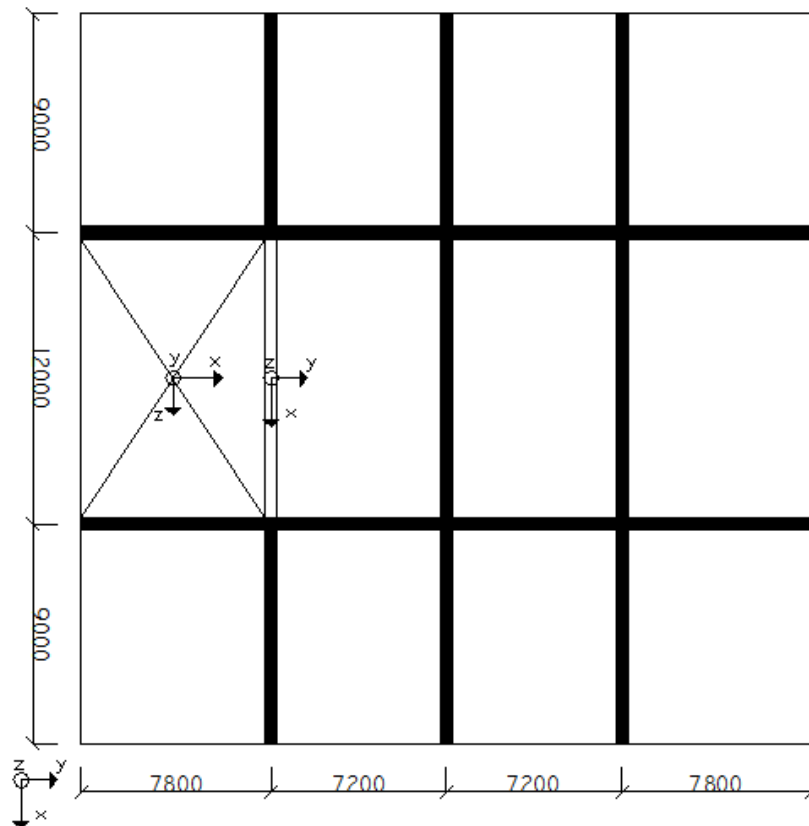


Figure 113 Overview of the coordinate systems

An interesting aspect is that the maximum allowable deviation for concrete structures has the smallest values in the x-direction, while the largest deviations are encountered in this direction due to the allocation of the measurement points, the adjustment and manufacturing of the element. It's likely that the x-direction will limit the amount of floors before the deviations have to be corrected.

10.3.6 Calculation of the deviations at the Zalmhaven tower

Now that the maximum allowable deviations due to the allocation of the measurement points, the adjustment and manufacturing of the elements are known, it can be calculated at which level the boundary conditions are exceeded. An important question that arises with the results is: how are these deviations controlled? Are they controlled on a local scale at every connection or only on a global scale at the calculated levels? And what about the traditional connections, can they control the deviations?

In Table 25 the total dimensional deviations due to the allocation of the measurement points, the adjustment and manufacturing of the elements are shown. In Table 26 the maximum allowable dimensional deviations are depicted. It can be seen that due to the large deviation in the x-direction the maximum allowable deviation is already exceeded at the first wall: the walls have to be corrected at every floor. A full oversight of the calculation sheet can be found in appendix E.

Table 25 Total dimensional deviation due to allocation of measurement points, the adjustment and manufacturing of the element

	gf	1	2	3	4	5	6	7	8	9	10
Height (z) [mm]	0	7	9	11	13	14	15	17	18	19	20
Length (x) [mm]	9	25	27	29	30	32	33	34	36	37	39
Thickness (y) [mm]	6	11	12	14	15	16	18	19	20	21	22

Table 26 Allowable dimensional deviation

	gf	1	2	3	4	5	6	7	8	9	10
Height (z) [mm]	26	26	26	26	27	27	27	27	27	27	27
Length (x) [mm]	23	23	24	24	24	24	24	24	24	24	24
Thickness (y) [mm]	35	35	35	35	35	35	35	35	35	35	36

When the x-direction deviations of the concrete wall element (A_i) are reduced with 50 instead of 30%, only every sixth wall has to be corrected. In Table 27 the results are shown when all the x-direction deviations (A_i , A_u and A_s) are reduced with 60%.

Table 27 Reduced total dimensional deviation due to allocation of measurement points, the adjustment and manufacturing of the element

	gf	1	2	3	4	5	6	7	8	9	10
Height (z) [mm]	0	7	9	11	13	14	15	17	18	19	20
Length (x) [mm]	6	15	16	17	19	20	21	22	23	24	25
Thickness (y) [mm]	6	11	12	14	15	16	18	19	20	21	22

A 60% reduction of all the x-direction deviations is feasible with normal to accurate workmanship and now only every tenth³⁵ wall has to be corrected. Though according to this calculation only every tenth wall has to be set at a deviation of approximately 0mm relative to point 1 on the ground floor, the deviation of every wall in between should still be checked (quality control). Due to accidental errors and the fact that the inaccuracy area only contains 98% of the deviations, larger deviations might occur. This will result in an exceeded maximum allowable value at the tenth wall and a possibility that the element won't fit or that several wall sections might have to be replaced. Since open vertical joints are used that have no structural property, the joint thickness might be larger compared to a structural connection. Due to this larger joint thickness, larger deviations can be absorbed without any structural consequences.

It may be concluded that the deviations can be controlled on a global scale: place every element relative to the previous element and absorb the deviations at the tenth floor. Due to errors or inaccuracies, the deviations might be larger than calculated in Table 27, but this should provide no problems because in the z and y-direction there is still plenty of tolerance left to absorb the deviations. In the x-direction the tolerances might in that case be exceeded but since the open vertical connection doesn't contain any structural properties, the joint thickness can be enlarged.

³⁵ On the ninth floor the tenth wall is located. The tenth wall is the first wall that exceeds the limits.

When the tenth wall is corrected, a difference of 24mm in the x- direction, 21mm in the y-direction and 19 mm in the z-direction will occur between wall 4 and 5. These differences will create an eccentricity, resulting in an additional moment. In the y- direction (thickness off the wall) the deviation will have the largest influence; there is a difference of 15mm between correcting at every wall and correcting only every tenth wall (see Table 27: $e=21-6=15\text{mm}$). Due to the enormous thickness of the wall (500mm) the additional 15mm will not result in a larger reinforcement ratio of the wall.

To absorb the additional accidental deviations at every tenth wall, it's recommended to provide adjustment possibilities. For example, the normal joint thickness in a precast structure is 20mm. In case a 20mm open vertical joint would be applied, it might be possible that due to a positive deviation in the x-direction, the open joint would be reduced to -4mm. Combine this with an accidental error and the element won't fit. To overcome this problem, the joint thickness is increased. In Table 28 the results are depicted.

Table 28 Joint thickness due to deviations

Location	Normal thickness	Additional thickness	Total thickness
	[mm]	[mm]	[mm]
Height (z: horizontal joint)	20	15	35
Length (x: vertical joint)	20	20	40

In case a positive deviation of 24mm occurs in the x-direction, there is still 16mm left for accidental deviations and the placing of the element. When there is a negative deviation on all the underlying walls, the joint thickness increases to 64mm. In the z-direction (there is no joint in the y-direction) an additional thickness of 15mm is required to accommodate deviations. The calculated deviations are a maximum value and it's likely that the actual deviations will be smaller (the probability that ten walls have a maximum positive deviation due to the allocation of the measurement points, adjusting and manufacturing of the element is relatively small).

In the previous calculation the deviations for wall 2 (see Figure 106) have been examined. Since the distance only plays a minor role in the calculation, the results of wall 1 and 3 will be nearly identical. The deviations of the floor are not considered since they do not increase with the structural height.

10.3.7 Functional requirements and reaction of the structure

From the previous section it may be concluded that when every element is placed relative to the previous element, the deviations only have to be adsorbed every tenth level. But how are the deviations and tolerances influenced by the functional requirements and the reaction of the structure?

Traditionally the deviations are controlled locally in precast high-rise buildings (for example Het Strijkijzer in The Hague or the Erasmus MC tower in Rotterdam): the walls are placed on their predestined location and the floor elements are levelled (at the supports or by a thin screed layer). This method is utilised because skew elements will create additional loads, building physic properties are jeopardized and connections might not fit anymore or become aesthetically unpleasant. By placing the elements relative to each other, the building physic and connection properties aren't endangered. Furthermore, the calculation has shown that the small eccentricity at the tenth floor doesn't require additional reinforcement. To prevent any unexpected deviations due to errors, the placement of the elements relative to each other should be monitored (quality control). The question remains: do the benefits of only absorbing the deviations at every tenth level outweigh the disadvantageous? Unfortunately the answer to this question is

no. The risk of unexpected abnormalities and the possible resulting repair works is present and due to the repetition it's likely that errors might occur. When this is combined with the very small time reduction (adjusting the element relative to the previous element or relative to a central point with the help of a total station doesn't differ considerably), the traditional method is preferred. Since the precast wall of the Zalmhaven tower use a wet horizontal connection, the deviations in the x-, y- and z-direction can be adsorbed per level. If for instance a horizontal connection with welded steel plates would be utilised (or a cold connection which is often applied at steel columns), it would be impossible to absorb the deviations per level and the calculated method of every then levels should be applied.

Aside from the functional requirements, the behaviour of the structure also plays an important role. Just the quay walls, which are commonly constructed under an angle, the Zalmhaven tower is constructed completely level. This is because of the lobby, which reduces the structural area at one side, creating an initial deflection due to the dead load. As a result, columns with a small overlength are used. If this overlength isn't taken into account in the floors above, the overlength is absorbed in the connections, neutralizing the effect. Besides the walls, the floors are also subjected to deformations. By pre-stressing the element, deformations due to dead load may be prevented. Any deviations that occur during the placement can be absorbed by a thin screed layer.

10.3.8 Conclusion

The standards for the allocation of the measurement points, the adjustment and manufacturing of the element are dated and reduction factors should be applied. When all the deviations are calculated for the Zalmhaven tower and quadratically added, the total deviations are obtained. When these values are compared with the maximum allowable deviations for a concrete structure, it can be concluded that the deviations have to be corrected at least every tenth level (global scale). Nevertheless, the deviations of the walls in between should still be checked since an accidental deviation may lead to an exceeded maximum allowable deviation at every tenth wall (quality control). By monitoring all the walls it can be checked if all the deviations are as large as calculated. Despite the reduced labour, this method isn't applied in practise since it creates large risk with respect to unknown errors. Since the Zalmhaven tower utilises concrete walls with a wet horizontal connection and floor elements with a thin screed layer, the traditional method of absorbing the deviations per level can be applied. If a different connection would be utilised (welded or cold connection), the deviations should be accumulated and only absorbed on a global scale (for example every ten levels).

10.4 Conclusion

Dimensional control in the building industry can be defined as the operational techniques and activities that are necessary for the assurance of the dimensional quality of a building [Hoof, 1986]. By defining tolerances based on their result and sensitivity, a small amount of project specific tolerances can be determined by the designers of the building. Combined with the general tolerances for all the other connections and situations, the process designer is able to construct the building on paper with an execution and assembly plan. The task of the contractor is to match the process that was constructed on paper.

Creating an accurate and dimensional acceptable project is a collective effort of all the involved partners and the ultimate goal should be: minimizing the negative results of dimensional deviations with respect to the functioning of the building and the costs. An important statement that should be taken into account is: deviations are inevitable and only the size can be controlled.

The standards provide rules and maximum values for occurring deviations and maximum allowable deviations. Because the standards were introduced in 1990, the values are slightly outdated and reduction factors should be applied. Reduction factors of 30 to 50% are realistic.

When the occurring and maximum allowable deviations are calculated for a precast high-rise building, it can be concluded that every tenth level the maximum allowable values (tolerances) are exceeded. By placing the intermediate nine levels relative to the previous level the required actions are reduced. Despite the quality control and reduced amount of actions, this technique isn't applied in practise since the risk or errors and delays increases drastically.

With wet connections and a thin screed layer the deviations in the x-, y- and z-direction can be adsorbed per level and don't have to be accumulated. The behaviour of the structure should be taken into account when the elements are adjusted. If for example the overlength of columns isn't considered, the effect of this action may be neutralized in the horizontal connections.

11 Project realisation

After the structural and construction methodology design, the project has to be realised. The cycle time plays an important role in the project realisation and has a considerable influence on the total construction time and costs.

The goal of this chapter is to calculate the required cycle time of the precast building method. Just like the structural behaviour, the cycle time of the precast building method will be compared with the cast in situ building method. By examining and comparing the results, insight is gained on how the two methods behave under identical circumstances. These values are mainly influenced by the structural properties (the mass and number of elements) and based on completed projects.

Besides the cycle time, the project realisation also contains the total building time and costs. These aspects aren't compared on a quantitative level since they are influenced by many non-structural aspects and are subjective to several assumptions. Therefore statement like "the total precast building time is 50% shorter than the cast in situ building time" or "the precast building method is 10% less expensive than the cast in situ building method" are difficult to support. Since the goal of this thesis is to examine if it's structurally and logistically possible to construct a 200m high-rise precast tower in the Netherlands, the total building time of the precast building method is calculated. The total costs of the precast tower are not since these exact values highly depend on the market (currently the price for a concrete wall element varies between €80 and €400/m², which is a factor of 5) and on the organisation calculating the costs (level of expertise and how eager is the company to attain the project?). Therefore the boundary conditions of the costs will be provided and the determination of the exact value is up to the reader.

In section 11.1 quantitative values will be determined for the cycle time of the precast and cast in situ building method. Based on the results of the precast cycle time an estimation is made for the total building time of the Zalmhaven tower in section 11.2. In section 11.3 the boundary conditions for the precast cost calculation are provided. This chapter ends with a conclusion in section 11.4.

11.1 Cycle time

In section 8.3, the cycle time in relation to the building height and mass of the elements was already discussed. The examined relation only holds for the precast building method. The cast in situ building isn't influenced directly by the building height (the quantity of elements that have to be transported is relatively low), but the amount of weather delays are related to the building height, influencing the cycle time. In this section the cycle time will be determined for both methods. Based on these values, a comparison is made between both methods.

11.1.1 Cycle time of the precast structure

In this section the horizontal and vertical cycle time for the Zalmhaven tower will be determined. During the structural analysis, only a wall reduction of 500mm to 400 of wall 4 and 5 at level 27 was taken into account. In section 9.3.4 it's shown that reducing the wall thickness of wall 1, 2 and 3 from 400 to 300 mm at level 27 and wall 4 and 5 from 400 to 300mm at level 45 results in almost no additional deflections. Therefore these wall reductions will be taken into account during the calculation of the cycle time. All the figures in this section start at level 6 since the first 5 levels are created by a heavy load crawler crane (see section 4.5).

11.1.1.1 Vertical cycle time

The cycle time includes the sum of activities that are required to complete a building layer. During the vertical cycle time, all the elements and materials are transported to the construction floor. The following elements and materials are transported:

- structural wall elements,
- floor elements,
- facade elements,
- bathroom units,
- scissor stairs (wokkeltrap in Dutch),
- pallets with aerated concrete blocks,
- equipment and building materials.

In appendix F a complete overview is provided of the amount of elements and materials that are transported per floor. Per vertical movement a constant amount of time is maintained for the crane related actions: 6 minutes. Within these 6 minutes, the element is attached, orientated for transport/storage and detached. With these aspects, Figure 114 is created.

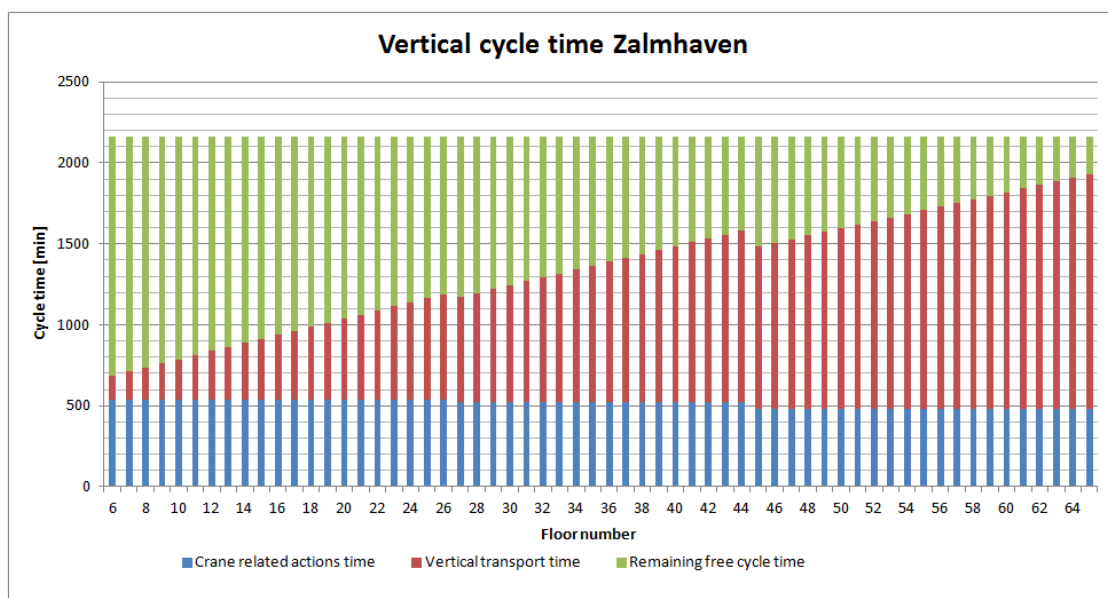


Figure 114 Vertical cycle time of the Zalmhaven tower

The blue line represents the total amount of crane related actions per floor. At floor 5 to 26 this equals $89.5 \times 6 = 537$ minutes. From the 27th floor, every even floor has four elements less (see the structural design of section 4.3) and therefore the time for the crane related actions is reduced to: $87.5 \times 6 = 525$ minutes³⁶. At the 45th floor, the pallets with aerated concrete blocks and the container with building materials are transported outside the cycle time, providing a new reduction. The new total time due to crane related actions is: $80.5 \times 6 = 483$ minutes.

The red line represents the vertical transport time. At the 5th floor all the elements and materials are transported within 126 minutes. At the 65th floor this takes 1447 minutes or 24.1 hours (when the crane related actions are included, the total vertical time becomes 1930 minutes). At the 27th floor the transport time is reduced because per even floor four elements less have to be transported. Furthermore, the wall thickness of wall 1, 2 and 3 is reduced from 400mm to 300mm and the thickness of wall 4 and 5 is

³⁶ Only the even floors obtain an element reduction. Therefore the average amount of elements per floor is 87.5 instead of 89.5. The average amount is used because the even and uneven floors don't have the same amount of elements.

reduced from 500mm to 400mm. At the 45th floor the reduction of vertical transport time is slightly larger since the pallets with aerated concrete blocks and the container with building materials are transported outside the cycle time. Furthermore, the wall thickness of wall 4 and 5 is reduced from 400mm to 300mm. If these reductions at the 27th and 45th floor were not applied, a cycle time of 1632 minutes would be obtained (14% higher).

A total cycle time of 2160 minutes (3 days of 12 hours) is maintained, providing an utilisation ratio of 31% at the bottom and 89% at the top. It can be concluded that at the bottom the vertical transport system is inefficient (it's only utilised 31% of the total time) and could be used to help the horizontal transport system. At the top, the limit of 90% is almost reached. By helping the horizontal transport system at the bottom, the inefficiency during the start-up of the project is minimized.

When the total load per floor is divided by the amount of transport movements per floor, the average load per movement can be calculated. In order to obtain an efficient transport system, this load should be as high as possible (see section 8.3). Between level 5 and 26, the average mass per movement is only 15.3 ton. Between level 27 and 45 this reduces to 14.4 ton because of the smaller wall thickness. Since the pallets with concrete blocks and the equipment are not part of the cycle time between floor 45 and 65, the average mass increases to 15.2 ton, despite a second wall reduction. These average loads are very low compared to the maximum capacity of 36 ton of the hoisting shed. The main cause for this low number is that the floor (40 elements per floor level with a maximum mass of 17.9 ton) and facade (16 elements per floor level with a maximum mass of 14 ton) elements are transported separately. When these elements are transported by two, the average mass would increase considerably: from 15.3 ton to 22.3 ton between level 5 and 26, from 14.4 to 21.2 ton between 27 and 44 and from 15.2 to 23.5 ton between 45 and 65 on average per movement. As a result of the increased mass per vertical movement, the vertical cycle at the 65th floor is reduced from 1436 to 1105 minutes (a reduction of 23%). This mass per movement can be increased even more when several structural wall elements are transported together.

Unfortunately, transporting two elements at once also provides difficulties: how are the two elements lifted simultaneously from a truck without any damage? It's possibly to transport the elements in a special steel structure, making sure that the elements don't move during transport. A similar system was also applied at the Erasmus MC tower and six thin floor elements were transported at once. It should be noted that this aspect considers two elements of 17.9 ton, which aren't very lightweight.

Because of these difficulties (and section 11.1.1.4), this optimisation isn't applied at the Zalmhaven tower yet. Without the reductions already a cycle time of 3 days is reached and the possible reduction to 2.5 days only provides a workweek of 5 days instead of 6. If the contractor wishes to reduce the vertical cycle times, an innovative system should be designed which makes transporting two floor and wall elements at once possible. A second method to reduce the vertical transport time is to apply a more powerful driving unit with gears (higher transport speed). Since the horizontal cycle time should always be leading, a reduction of vertical cycle times may not lead to an increased construction rate. Therefore, the optimisations will be discussed in more detail in section 11.1.1.4.

11.1.1.2 Horizontal cycle time

Just as the vertical cycle time, the horizontal cycle time is composed out of the transport time and the crane related actions. But in contrast to the vertical cycle time, the horizontal cycle time isn't affected by the building height and element mass. Therefore only the crane related actions provide a difference between the norm times of different elements. In Table 29 the average horizontal cycle time is determined.

Table 29 Horizontal cycle time

Object	Norm time	Level 5-26		Level 27-65	
		Amount	Total	Amount	Total
	[min]	[-]	[min]	[-]	[min]
Wall element	24	19.5	468	17.5	420
Facade element	24	16	384	16	384
Floor element	20	40	800	40	800
Bathroom unit	20	6	120	6	120
Staircase	20	2	40	2	40
Pallets with blocks	10	6	60	6	60
Equipment/material	20	1	20	1	20
Total		89.5	1892	87.5	1844

The horizontal cycle time is a summation of all the norm times. The values used in Table 29 are based on a reference project, the Erasmus MC tower [Meij, 2012] and validated with Zonneveld ingenieurs. At level 27, the cycle time is reduced by 48 minutes since on average two elements less are transported per floor (every even floor has four elements less). At Figure 114 there was also a reduction visible at the 45th floor (the pallets and container with equipment are transported outside the cycle time). This reduction isn't visible in Table 29 since it's only transported outside the vertical cycle time.

11.1.1.3 Total cycle time

When the vertical and horizontal cycle time are combined, the total cycle time is obtained. The largest value of Figure 114 or Table 29 determines the cycle time, as shown in Figure 115.

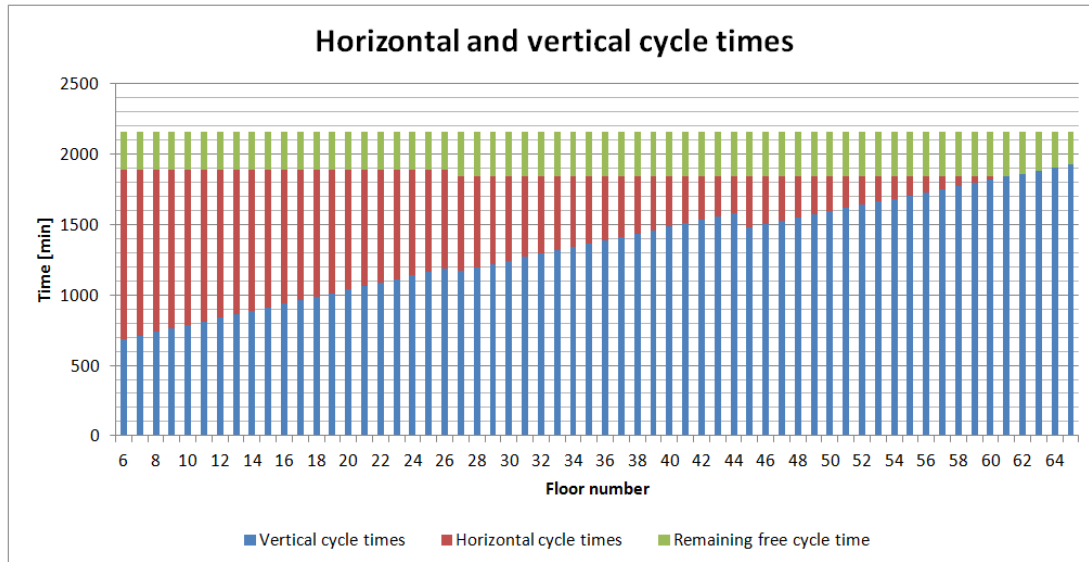


Figure 115 Total cycle time of the Zalmhaven tower

The blue lines represent the vertical cycle times and they are identical to Figure 114. The red lines represent the horizontal cycle times, as shown in Table 29. The green lines represent the remaining free cycle times. Between level 5 and 26 this is 12.4%. Between level 27 and 61 this increases to 14.6%. At level 62, the vertical transport time becomes larger than the horizontal transport time and the utilisation ratio increases to 89.3% (10.7% free cycle time) at the 65th floor. Due to the larger vertical cycle time, the construction workers have to wait 86 minutes distributed over 3 days of 12 hours per day. To prevent any delays, breaks can be scheduled during the time the horizontal cycle

has to wait, the vertical cycle could start a little bit earlier the last four floors creating a buffer or optimisations can be applied.

11.1.1.4 Possible optimisations

Already several possibilities have been discussed to optimise the cycle times. According to Figure 115, the vertical and horizontal cycle times are nearly identical at the top of the Zalmhaven tower. Therefore, a reduction of the total cycle time is only obtained if both the vertical and horizontal cycle time are reduced.

Horizontal optimisation

First several solutions will be discussed for the horizontal system. The element mass, transport speed and building height have no influence on the horizontal cycle time and therefore the amount of possible optimisation solutions is diminished. The following three solutions remain:

- reduce the amount of elements,
- reduce the required time for the crane related actions,
- utilise the vertical transport system.

Due to the structural properties, the wall elements are already very large (average mass of 24.6 ton). At level 27 it's possible to reduce the amount of wall elements even more, but then elements with a length of 15m are created. These long elements are difficult to construct in the factory and an exemption is required for the transport. Furthermore, handling and storing these elements on the construction floor is very cumbersome. Therefore this optimisation isn't considered.

The length of the facade elements varies between 6 and 7.8m. Two facade elements of 6m may be combined as one element of 12m, but then problems arise with the structural integrity of the concrete inner leaf (small concrete area with a large length). Therefore no facade elements are combined.

Per floor level, 40 floor elements are applied with a width of 3m. The mass of the elements varies between 16.6 and 17.9 ton (according to the length) and it's possible to transport two elements at once. The width may also be increased to 4.5m (an exemption is required since the element exceeds the allowed dimension of the truck), resulting in only 28 elements per floor with a mass varying between 25 and 26.8 ton. Since there are 12 elements less with a total time of $12 \cdot 20 = 240$ minutes, the horizontal cycle time is reduced with 13%. Due to the higher load, it's now impossible to transport two elements at once. The vertical optimisation is therefore no longer applicable and more vertical transports are created (20 double loads versus 28 single loads).

The bathroom units and pallets cannot be reduced furthermore since every apartment requires its own bathroom and the mass of the concrete aerated blocks should be limited because of the floor capacity (the pallets should be placed near the support of the floor to prevent any failure).

The second method to optimise the cycle time is to reduce the required time for the crane related actions. Since the transport time and crane related actions aren't discussed separately, the total norm time has to be reduced. The current applied norm times, see Table 29, are already very strict: attaching the wall element (1), orientating the wall element for transport (2), transporting (3), orientation and adjustment at the final location (4), detaching (5) and returning (6) all within 24 minutes for a wall or facade element doesn't leave much room for any errors or optimisation. Therefore the norm time will not be reduced furthermore.

At the bottom of the Zalmhaven tower, the vertical transport system is very inefficient (it's only utilised for 31% at level 6). Therefore several elements can be placed by this gantry crane. For example, when the horizontal crane places facade elements at the back of the layout, the vertical transport system could place the stairs, bathroom units or floor

elements in the front of the layout (smaller norm time). When the two stairs, four bathroom units and fourteen floor elements are placed with the horizontal transport system, Figure 116 is obtained. Between level 6 and 15, only 69% of the cycle time is used.

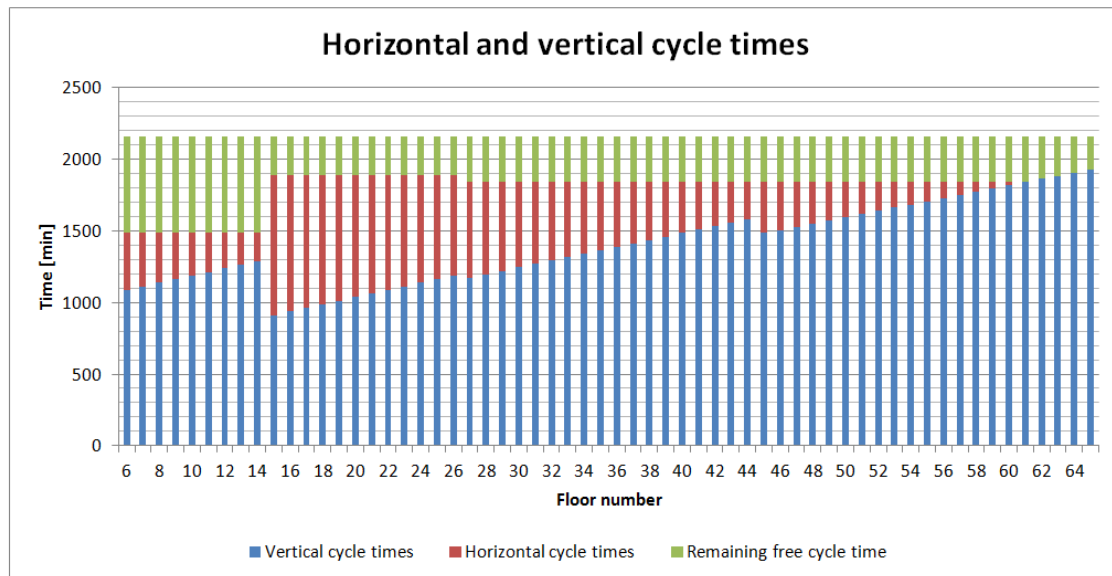


Figure 116 Utilisation vertical transport system

This method can also be applied at higher levels, but the horizontal system is able to assist less because the vertical transport time will become more important. Therefore this solution is mainly used to counteract the inefficiency³⁷ at the start-up of the construction.

It can be concluded that the easiest method to reduce the entire horizontal transport cycle is to reduce the amount of floors. This will result in a 13% reduction of the horizontal cycle time. Other methods may be applied (reducing the amount of facade elements or the norm time), but these solutions will be accompanied by difficulties. The inefficiency at the start-up of the construction may be counteracted by utilising the vertical transport system.

Vertical optimisation

The vertical cycle time is dependent on the height and mass. Since the horizontal cycle time can only be optimised by 13% without creating elements that are nearly impossible to construct, transport and handle, a vertical reduction larger than 18% would be needless (the vertical cycle time is 5% larger than the horizontal cycle time at the 65th floor). The following solutions can be used to optimise the vertical transport cycle:

- reduce the amount of elements,
- reduce the required time for the crane related actions,
- reduce the transport time.

By reducing the amount of elements, the average mass per transport movement increases, resulting in a higher efficiency. At the horizontal optimisation it was already discussed that reducing the amount of floor elements is the easiest method to reduce the horizontal cycle time. Reducing the amount of other elements provides several problems. When the width of the floor elements is increased from 3 to 4.5m, the amount of floor elements is reduced from 40 to 28. As a result, the vertical cycle time is reduced by 11%.

³⁷ The construction workers have to become familiar with the process.

Besides reducing the amount of elements, it's also possible to transport two elements at once. Because the floor width has increased from 3 to 4.5m for the horizontal cycle, it has become impossible to transport two floor elements at once (maximum weight of 53.6 ton). But several wall and facade elements can still be transported simultaneously. As a result of the floor reduction and transporting two elements at once, the vertical transport time is reduced from 1930 to 1494 minutes, a 23% reduction.

Per vertical movement, 6 minutes are calculated for the crane related actions. This value is already very low and reducing it to 5 or 4 minutes might create more problems than benefits (the possibility of delays increases). Therefore this value will not be reduced.

The third method is to reduce the transport time by increasing the transport speed. At the current design of the Erasmus MC tower, a drive unit of approximately 110kW without gears is applied. By replacing this unit with a more powerful one, for example 150kW, the transport speed is increased with 38%. As a result of this more powerful unit, the vertical cycle time is reduced with 20%. Though increasing the power of the driving unit is a simple solution, it doesn't increase the efficiency (the average mass per movement remains identical).

It can be concluded that reducing the amount of elements or increasing the amount of elements per movement is the only solution to increase the efficiency. Applying a more powerful driving unit is a simple solution, but it increases the costs. But the larger floor elements (exemption required for the transport) and transporting two elements at once (a special steel structure has to be engineered) also increase the costs. When floor elements of 4.5m are applied in combination with transporting two facade elements at once, Figure 117 is obtained.

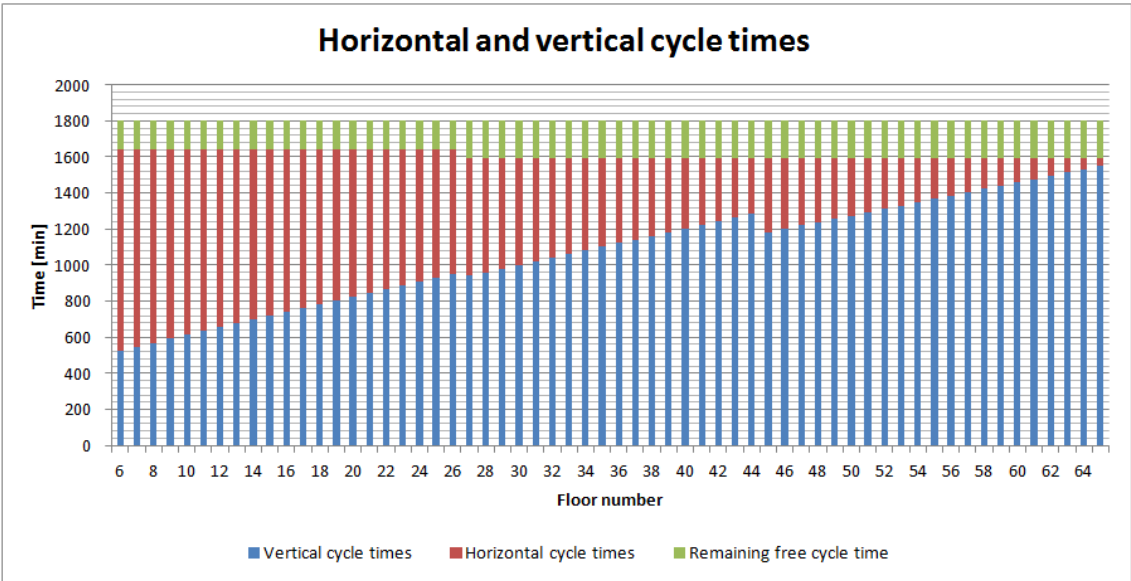


Figure 117 Optimised vertical and horizontal cycle time

At the 65th floor, the horizontal cycle is slightly larger than the vertical cycle time, providing an optimal system. Between level 5 and 26, the utilisation ratio is 91%, which is higher than the allowable limit of 90%. Therefore the horizontal crane should be utilised to decrease this ratio (see Figure 116). Between level 27 and 65, the utilisation ratio is 88%. When the cycle time of the 65th floor of Figure 115 and Figure 117 are compared, it can be denoted that the cycle time is reduced with 18% due to the optimisations. As a result, the total cycle time of 3 days with 12 hours can be reduced to 2.5 days of 12 hours. But does the additional free day per week outweigh the additional costs? It's unlikely that this day will be used for construction (12 floors per 5 weeks) and this day could be used for other activities and absorbing delays. Since the original cycle

time already had more available free cycle time (14.6% instead of the minimum 10%), these actions can also be performed at the original cycle time without optimisation or the Sunday could be used. To make a definite conclusion, the risks should be considered.

11.1.1.5 Risks, quality and costs resulting from the cycle time

When the cycle time is considered, the aspects costs and quality should also be examined. It's possible to reduce the cycle time, but does the shorter cycle time justify the resulting costs and quality? Another aspect which shouldn't be forgotten are the risks. The cycle time shouldn't be optimized by reducing the time for crane related options or buffers since this leaves less room for the construction workers to perform their work. Optimizing the cycle time without making it more efficient will only result in a higher probability of delays. Therefore the optimisation of the previous section only contains a floor element reduction and transporting two elements at once: this won't increase the work load for the construction workers (or decrease the resulting quality) but it makes the process more efficient. Now only one question remains: do the benefits of the additional free day outweigh the higher cost of the special steel structure to transport two elements at once and the higher costs for the floor transport (exemption required)? The answer would be yes if the original non-optimized cycle contained no buffer to absorb any delays. But with an exemption it's possible to work on Sunday³⁸. With this additional day (Saturday or Sunday), the delays are adsorbed in the same week as they are created and an accumulation of delays is prevented.

It should be noted that the non-optimised cycle time of two floors per five or six days is very short. Since the values are based on a reference project (the Erasmus MC tower) and other projects have been executed with similar cycle times (at Het Strijkijzer also two floors were constructed per six days), the risks, quality and costs shouldn't be disproportional to the corresponding cycle time.

11.1.1.6 Conclusion

In the previous section the composition of the horizontal and vertical cycle times have been examined. An entire level can be constructed within three days, resulting in two finished levels per week. At the start-up, the efficiency of the construction crew is rather low and the vertical transport system may be utilised to counteract this. At level 62, the vertical transport cycle becomes leading, resulting in a small stagnation of the work at the last four levels. There are many possibilities to optimise the cycle times (up to 18%), but this results in higher costs. To prevent an accumulation of delays, every week should contain a buffer to absorb the delays. When a three day cycle is used, the only day left in the week to absorb the delays is Sunday. An examination of the costs has to determine if the additional costs of occasionally working on Sunday is more efficient than using very large floor elements which require an exemption.

11.1.2 Cycle time of the monolithic structure

The monolithic structure is created with a tunnel system. One tower crane will be applied, transporting the tunnel system and remaining material (scissor stairs, bathroom units and aerated blocks) and equipment. Since this is a non-separated system, there is only one cycle time (the horizontal and vertical cycle time are combined). The facade is placed by a crane independent system and is therefore not included in the cycle time (An example is the JuBi project in The Hague). This facade working platform (hefsteiger in Dutch) also ensures that the facade is closed quickly after the structure (6 levels below

³⁸ If the noise level of the construction process is higher than 60dB, an exemption is required. Since the hoisting shed absorbs a large part of the noise and they will only work on Sundays sporadically, acquiring an exemption should be possible.

the construction level). It's also possible to use a second crane for the facade, but this drastically increases the weather dependency.

11.1.2.1 Total cycle time

Before the cycle time can be calculated, the construction sequence of the tunnel system has to be determined. In Figure 118 the construction sequence of the tunnel system is shown.

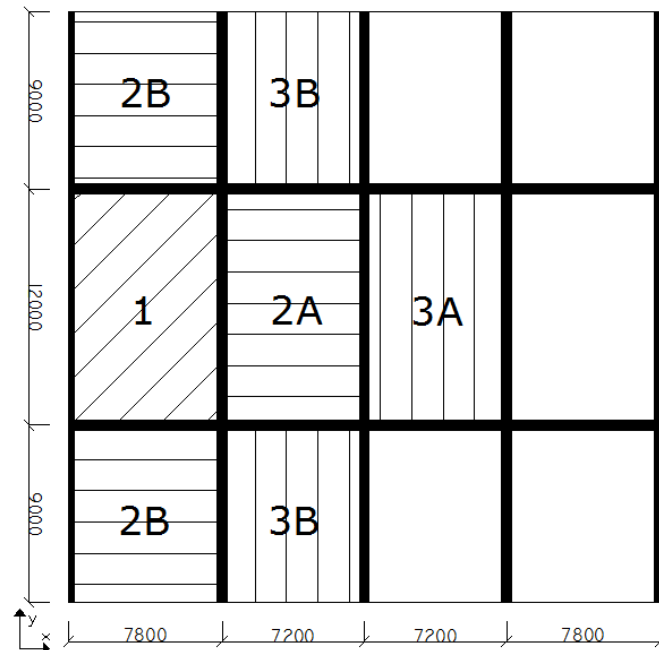


Figure 118 Construction sequence of the tunnel system

First area 1 is created on day 1. On day 2, the tunnel system of area 1 is removed and placed at area 2A. Simultaneously, two tunnel sections with an end wall are placed at area 2B. With a foldable steel wall formwork in area 1, it's now also possible to cast the two 500mm thick walls (this formwork section has to be transported via the door openings to the next area). On the third day, the tunnel section of 2A is transported to 3A and the two sections of 2B to 3B. At the fifth day section 4A is transported to the new floor level. Because the current floor level still has to be finished by the two 5B areas, a cycle time of 5 days is maintained. Per level the following actions relating to the tunnel section take place:

- removing tunnel system,
- transporting tunnel system,
- placing and adjusting tunnel system,
- placing reinforcement, ducts and pipes,
- pouring concrete,
- finishing concrete.

These actions have to take place within approximately 8 hours because the concrete has to dry for the next cycle. It's possible to remove the tunnel system the next day because the concrete is covered from the elements and heated. To achieve all these actions within 8 hours, the amount of construction workers on the building site will be considerably higher than at the precast construction method.

The previously mentioned actions only include the load bearing structure. The staircase, aerated concrete blocks and other materials required for the finishing stage still have to be transported by the tower crane. Because of the wet construction method, these

materials have to be placed at a lower level. Since the concrete is poured with a concrete pump and the facade by a crane independent system, the tower crane is available to transport these materials after the tunnel system is transported.

It's also possible to create one entire bay per day. Because the tunnel system has to be removed, the internal walls have to be casted at a later stage with foldable formwork (to create a proper connection between the wall and the floor, the floor section above the wall isn't casted by the tunnel system). On average, it requires one week to complete one building layer with a tunnel system formwork. To operate this building method only one tower crane is required.

11.1.2.2 Possible optimisations

The process itself can't be optimized anymore because the heated concrete requires approximately 16 hours to become stiff enough to remove the formwork. Within the remaining 8 hours all the other actions have to be executed. The only solution to optimize the construction speed is to use multiple cycles: by using two cranes and two tunnel systems it's possible to create two bays per day with the last mentioned method. Per level, another day is required to cast the internal walls. As a result, two levels can be completed per week. Since this reduces the amount of repetition and increases the amount of cranes, tunnel systems and construction workers, this optimisation isn't applied very often.

11.1.2.3 Risks, quality and costs resulting from the cycle time

Traditionally one layer per week is constructed when a tunnel system is used³⁹. When two tunnel systems, construction crews and tower cranes are used, the complexity of the small construction floor will increase considerably. This has a negative influence on the risks, quality and costs. On the other hand, reducing the construction time will result in less interest loss and more revenues at an earlier stage. In collaboration with the contractor a decision has to be made (how much personnel and equipment does he have available). Since this building method isn't protected from the environment additional buffers preventing an accumulation of delays becomes important. Because the environment isn't protected from the building method either it may be more difficult to work during the weekends and late hours.

11.1.2.4 Conclusion

With a tunnel system, it takes one week to construct a new level. By using two cranes, construction crews and two tunnel systems it's possible to create two bays per day, resulting in two levels per week. This optimisation isn't applied very often because of the large amount of construction workers on the small area (450m² of gross floor area has to be finished within 8 hours). Therefore this optimisation isn't considered. Within this week, only the load bearing structure is finished. The facade and all the materials for the finishing still have to be transported to all the underlying levels. To prevent a high crane utilisation ratio, a crane independent system can be applied for the facade and the concrete pouring.

11.1.3 Comparison cycle times

Now that the cycle time has been determined for the precast and monolithic structure, they can be compared on a quantitative level.

³⁹ An example is 100 hoog in Rotterdam. One level with 563m² and five bays was finished in one week.

The first difference between the methods which can be distinguished is the facade: in the precast building method the facade is included in the cycle time, while this is excluded in the cast in situ building method. Furthermore, all the materials and elements are placed at the desired location while the wet construction method of the tunnel system requires that all the materials are placed at a structurally completed level.

The precast building method has a cycle time of 2160 minutes (3 days of 12 hours). When this is compared with the cast in situ method of 2400 minutes (5 days of 8 hours), a difference of only 10% is obtained. But where the cycle time of the precast method can be incorporated in double shifts, the cast in situ method can't because the concrete has to harden. Therefore the precast cycle time may only be 10% lower, the construction time per level is reduced by 50%.

The previous comparison is based on the total cycle time, including non-structural aspects. When only the structural cycle time is compared, the value of the precast building method is reduced from 2160 to 1800 minutes (now only the walls, floors and load bearing facade elements are considered). The cycle time of the cast in situ method remains 1800 minutes since this process can't accelerate (the concrete has to harden). As a result, the structural cycle time of the precast building method is 25% lower than the in situ building method. The reduction of the total construction time per level remains 50%.

Besides the shorter structural cycle time, the risk of weather delays also plays an important role. Due to the conditioned construction area at the precast building method no weather delays are incorporated (this was also done at the Erasmus MC tower). At the tunnel system it's very plausible that due to the weather conditions the concrete cannot be casted or the tunnel system cannot be transported. Therefore this building method has a higher risk of not accomplishing the designed cycle times.

11.1.4 Conclusion

With the precast building method a cycle time of one floor every three days can be achieved. This cycle time can be reduced by optimizing the vertical and horizontal cycle time. The optimisation ensures that two levels can be completed in five days, resulting in an additional buffer to prevent an accumulation of delays (all the delays should be absorbed in the same week to prevent any delays in the next cycle). This optimisation is accompanied by additional costs, but to create a buffer at the six day cycle also additional costs are required (working on Sunday). Therefore the exact value of the exemptions will determine which cycle time is favoured.

The cast in situ building method with a tunnel system requires five days of eight hours to complete a level. Due to the nature of this building method, only the load bearing structure is finished within these five days. By utilising a crane independent system for the facade, the structure may be weather proof several layers below the construction level. The construction speed can't accelerate because the concrete has to harden to remove the tunnel system the next day. To reduce the cycle time a second tunnel system in combination with tower crane and crew is required. Unfortunately this results in an overcrowded construction area which is prone to delays. Therefore is optimisation isn't recommended and not considered in this thesis.

When the cycle times of both systems are compared it may be concluded that the cycle time of the precast method is only 10% shorter than the cast in situ building method. When the total construction time per floor is considered, this difference increases to 50%. The reduction of the total construction time is considerable larger because the cycle time of the tunnel system can't be incorporated in two shifts while this possible with the hoisting shed. When only the load bearing structure is considered, the difference between the cycle times increases from 10 to 25%. This larger difference is created by the fact

- During the first 24 weeks most of the actions take place consecutive: the first 5 levels can only be constructed when the foundation is finished and the hoisting shed can only be assembled when the 5th level has been completed. Of course several smaller actions can be performed simultaneously (assembling the crawler crane during the construction of the foundation or the assembling of small truss sections to one large truss while the 5th level is created), but the main actions have a sequential nature. Since these actions aren't protected from the environment, weather delays are incorporated.
- The finishing stage can only start when the hoisting shed is assembled. This is because the hoisting shed provides a weather proof occlusion at the top floor. By applying massive floors with integrated ducts and reinforcement for the diaphragm action, sandwich elements and prefabricated bathroom units, it's estimated that 6 levels under the hoisting shed the finishing stage is completed (see section 4.4). Because of this incredibly high finishing speed the finishing stage isn't leading.
- The total process of assembling, disassembling and climbing back of the hoisting shed requires 8 weeks, which is 27% of the time required to construct level 6 to 65. This value is considerably high because a special system (hoisting shed) is required to reach the short cycle times.

The previous building time is an example of what is possible with the precast building method and the previous values should not be mistaken for facts. Unlike other aspects, the building time between the precast and cast in situ building method isn't compared because there are too many aspects influencing the relation. Providing an exact comparison would therefore be difficult to support and substantiate. Since the goal of this thesis is to examine if it's structurally and logistically possible to construct a 200m precast tower in the Netherlands, the relation between the two building times isn't examined any further.

11.3 Costs

The costs are an important aspect of the feasibility of a project. The costs (one of the three main control factors) often determine the building method. Unfortunately the costs are subjected to large fluctuations and only represent the current market status. Therefore it's difficult to obtain valid conclusions when the basis may change the day after tomorrow. Since the focus of this thesis lies on the structural and logistically feasibility, it has been decided not to calculate the costs of the Zalmhaven tower with a precast building method. Determining the costs is therefore left to the knowledge of the reader and the market circumstances at that point of time. To facilitate this calculation several boundary conditions will be provided for the precast structure:

- 70 diaphragm walls with a dimension of $l \times w \times d = 63.2 \times 3.3 \times 1.5 \text{m}^3$ are required.
- A concrete slab with a volume of 900m^3 is required for the foundation. Since all the diaphragm walls are located underneath the structural walls, the reinforcement ratio is limited.
- In total 1209 concrete elements with a concrete strength class of C90/105 are used. Because of this high strength class only 117kg reinforcement per cubic meter of concrete is required at the bottom. These walls are subdivided as following:
 - 243 elements with a thickness of 500mm and a total area of 4941m^2 ,
 - 410 elements with a thickness of 400mm and a total area of 10705.5m^2 ,
 - 556 elements with a thickness of 300mm and a total area of 14548.5m^2 ,
 - 66 elements with a thickness of 200mm and a total area of 1494m^2 (partition walls between the stairs).

- In total 2624 floor elements with a thickness of 320mm are required. These elements are subdivided as following:
 - 1312 elements with a length of 7.3m,
 - 1312 elements with a length 6.8m.
- 1008 facade elements with a total area of 23538m². These elements are subdivided as following:
 - 252 load bearing facade elements (l×h=9×3.05m²) with an inner leaf thickness of 300mm,
 - 252 load bearing facade elements (l×h=6×3.05m²) with an inner leaf thickness of 300mm,
 - 252 non-load bearing facade elements (l×h=7.8×3.05m²) with an inner leaf thickness of 200mm,
 - 252 non-load bearing facade elements (l×h=7.2×3.05m²) with an inner leaf thickness of 200mm.

With these boundary conditions an estimation can be made for the load bearing structure.

11.4 Conclusion

When the building height increases, the influence of the cycle time becomes more important. At the Zalmhaven tower the cycle time is leading (approximately 50% of the total precast construction time). When the precast and cast in situ building time are compared, an interesting conclusion can be made: while the difference in actual cycle time may be small (10 to 25%), the difference between the total construction time per level is considerably larger. The precast building method is able to construct 2 levels per week where the monolithic method only finishes 1 level, a reduction of 50%. It can be stated that due to prefabrication, the precast construction method has obtained a smaller lead time, ensuring that more actions can be performed in the same time span. Aside from shorter total construction time, the precast building method also distinguished itself from the cast in situ method by the level at which the finishing stage starts. At the precast building method the sandwich facade elements and other material (bathroom units or aerated concrete blocks) are placed at the construction level while these aspects are placed several levels lower at the cast in situ method.

Besides the cycle time, the project realisation also contains the total building time and costs. These aspects aren't compared on a quantitative level with the in situ building method since they are influenced by many non-structural aspects and are subjective to many assumptions. Despite the lack of a quantitative comparison, an example is provided of the possibilities of the precast building method. By partly integrating the finishing stage in the cycle times, the finishing stage isn't leading anymore. This reduction is interesting since traditionally the finishing stage determines the completion date. A second interesting aspect is the total process of assembling, disassembling and climbing back of the hoisting shed. These actions require 8 weeks, which is 27% of the time required to construct level 6 to 65. This value is considerably high because a special system (hoisting shed) is required to reach the short cycle times.

For the total costs of the project only boundary conditions are provided. Due to large fluctuations which the costs are subject to, the cost calculation would only represent the current market status. Therefore the determination of the exact value is left up to the reader.

12 Conclusion

In the previous chapters many precast properties have been compared to the traditional building method. The goal of this thesis is to examine if it's structurally and logistically feasible to construct a 202.25m precast tower in Rotterdam, the Netherlands. An underlying goal of this thesis is to provide an overview of the properties which characterise a precast high-rise building with respect to an identical cast in situ building. By providing this overview more awareness is created on which aspects should be considered during the initiation and design phase.

By examining the Zalmhaven tower and creating a structural and logistical design it can be concluded that heights up to 200m are achievable in precast concrete. During the structural design of a precast structure the following aspects should be taken into consideration:

- The stiffness reduction is marginal. As a result of the large precast concrete elements in a masonry configuration, a high concrete strength class and a large building slenderness, the stiffness reduction of the precast structure is smaller than 4% compared to the cast in situ variant.
- No strength reduction is encountered as a result of the connections. Due to the high dead load of the structure the horizontal connections behave as stiff as the surrounding concrete.
- The shear stiffness of the horizontal connections has a marginal influence on the stiffness of the building. This effect is created by the high slenderness of the building, making the normal stiffness governing.
- The vertical connections have a marginal influence of the stiffness of the building. The large dowel elements above and below the vertical connection take up the shear force originally transferred by the vertical connection, making this connection ineffective with respect to the building stiffness.
- The distribution of shear force is considerably influenced when the masonry element configuration is utilised. As a result of the open vertical joint, the shear force has to be transported to the over- and underlying dowel elements. Locally the structural area is reduced by 50%, requiring more shear reinforcement.
- The deviations of the stacked precast elements do not accumulate. The horizontal wet connections in combination with a thin screed layer on the floors are able to absorb the deviations in x-, y- and z-direction.
- An optimal element configuration results in a time reduction during the execution phase. Designing all the elements with respect to the maximum load capacity ensures that the transport efficiency is optimal. When the element thickness is reduced over the height while maintaining the same dimensions, no significant reductions are obtained. When the lower mass creates opportunities to combine elements, a considerable time reduction can be expected.

Aside from the previous structural characteristic aspects of precast concrete, several other aspects concerning a high-rise design should be regarded:

- Using the Eurocode doesn't result higher loads for the Zalmhaven tower. With the transition from the TGB standards to the Eurocode, the method to calculate the wind load has changed considerably. Nevertheless, the wind load on the Zalmhaven tower remains more or less identical.
- The building vibrations induced by wind load aren't governing at the Zalmhaven tower. With the introduction of the Eurocode the vibration calculation has been revised extensively. According to the extensive calculation method, the Zalmhaven tower meets the requirements with ease.

Four aspects should be considered during the design of the transport system of a precast structure:

- Precast concrete is able to maintain a high amount of actions within a short time span. The precast elements require fewer actions since they only have to be assembled on the building site. Furthermore, the amount of wet concrete is reduced considerably, decreasing the lead time between actions. A cycle time of two layers per week is feasible
- The highest efficiency per transport movement is obtained when the maximum load is transported at every cycle. The non-linear relation between mass and transport speed and the crane related actions per transport movement ensure that the efficiency is optimal at high loads.
- The cycle times become independent of the building height when a separated transport system is applied. This relation is beneficial for high-rise buildings, but only holds when the horizontal cycle is governing.
- A hoisting shed with vertical guided transport system reduces the weather dependency significantly. The construction floor is protected from the environment and the vertical transport is able to operate at high wind speeds.

During the initiation phase when the building method is determined the previous aspects should be taken into account. These aspects can be reformulated as following:

- By prefabricating the elements, the building only has to be assembled on site. As a result of this assembly process, the construction time at the site is reduced considerably. Furthermore, fewer different disciplines and personnel are required in combination with a cleaner building site.
- With prefabrication, the construction process is shifted from building site to factory. The conditions in the factory are better and this part of the building process becomes less dependent of the weather. The controlled environment also provides better working circumstances and a higher quality of the elements. This also holds for the hoisting shed.
- Because all the elements are prefabricated and only a small wet connection is required, the lead time between actions of a precast structure is very small. Therefore a large amount of actions can be performed in a short time span. Cast in situ concrete is limited by the hardening time of the wet concrete.
- With prefabrication, actions can be combined. Sandwich facade elements or floor elements with incorporated ducts and reinforcement are a good example of this aspect, reducing the required amount of actions per object. As a result of this integration, the construction and finishing time at the construction site are reduced.
- By reducing the construction time at site, the interest costs are reduced and revenues are obtained at an earlier stage. Therefore a precast structure may be economically more attractive. By outsourcing the work to subcontractors at a factory the financial risks are reduced as well.

Besides the benefits of introducing connections in the structure, they also create limitations. The research of this thesis has shown that the characteristic disadvantageous with respect the reduced stiffness and accumulation of deviations of a precast structure aren't governing. From this feasibility study it can be concluded that there are opportunities for precast buildings passing the psychological limit of 200m.

13 Recommendations

During this thesis not every aspect could be analysed and several assumptions have been made. Furthermore, several aspects have been encountered which require further optimisation. It's recommended to examine the following subjects in more detail:

- Precast concrete in the masonry configuration has been used as structural layout because of its structural properties and the reduced amount of work. Unfortunately the masonry configuration increases the amount of different elements and creating an optimal element configuration with the openings and wall intersections is relatively complex. Research by Keulen [Keulen, 2012] has shown that a normal layout with a continues vertical connection over the height (indented non-reinforce mortar connection) is nearly as stiff as the masonry configuration. It should be examined if the higher repetition factor and simplified layout are more beneficial than the slightly higher stiffness, reduced labour and different connection details⁴⁰.
- The structural analysis has been performed by a linear elastic calculation with a smeared stiffness for the horizontal connection. The peak values at the vertical connections are likely caused by this schematisation and it should be analysed if the peak values are smoothened when a non-linear calculation method is used with the actual connection properties. Furthermore, the effect of the exact calculation on the other results should be examined.
- AxisVM was chosen as FEM program, but it's unknown how the programs and the corresponding optimisation techniques influence the results. It's recommended to examine the actual behaviour with experiments and validate the AxisVM results.
- During the literature study an extensive analysis was made of progressive collapse. The available time of this thesis was too limited to continue this analysis and isn't considered in the design. It should be examined how the new consequence class influences a precast structure: is it still possible to create simple and fast connections and how do the measures to mitigate risks influence the design?
- In this thesis a hoisting shed is applied. To increase the economical feasibility of this production system it's recommended to utilise techniques already applied in self climbing system. It's also advised to make the system modular to make it reusable. These aspects haven't been validated with companies providing these systems and it's recommended to analyse the possibilities and solutions more thoroughly.
- A very high concrete strength class (C90/105) was applied at the Zalmhaven tower to absorb the stiffness reduction of the precast connections. Since the reinforcement design resulted in low reinforcement ratios at the bottom of the structure and the stiffness isn't governing, the concrete strength class should be optimized. It's recommended to examine how this optimisation influences the results.
- The structural damping of buildings is determined by the possibility to dissipate energy. By introducing connections, it's predicted that more energy could be dissipated, providing a more pleasant living environment. It should be examined how precast concrete influences the damping behaviour of high-rise buildings.

⁴⁰ Tension ties in the floor are required to prevent the unreinforced connection to open up when loaded by tension.

14 Evaluation and level of accuracy

The last chapter of this thesis contains the evaluation of the results. Within the evaluation the level of accuracy is an important aspect since it determines how applicable and useful the obtained results are.

First of all, it should be stated that the design for the structure and construction methodology are based on the boundary conditions and preferences (point of view) of the designer. Different boundary conditions or preferences may lead to considerably different results.

With these aspects in mind and the results of the previous chapters, it may be concluded that the structural design is in the preliminary design phase. Some aspect may be slightly further (the amount of FEM analyses, reinforcement calculation and tolerances), but the results aren't optimised yet. Furthermore, several aspects of the preliminary phase are still missing (economical viability and a global risk analysis). Because the design is still in the preliminary design phase, it might be interesting to compare the results of this design with a different precast design. A trade-off matrix⁴¹ could be used to compare the different concepts.

The design of the construction methodology is approximately at the same level of accuracy. Several aspects are still unknown, for example the dimensions of the steel trusses and load bearing capacity of the hydraulic jacks of the hoisting shed. On the other hand, important aspects required for the design have been determined: the transport and climbing speed of the hoisting shed or the transport of elements via the road.

Aside from the global design result more aspects should be evaluated. For example the correctness of the calculated results. The structural examination is based on a FEM analysis and this complex method is susceptible to errors. Therefore multiple actions have been taken to validate the results:

- the loads applied at the structure haven been compared with the results obtained at the foundation,
- the obtained results have been validated with hand calculations and results of the original design made by Zonneveld ingenieurs,
- the behaviour of the entire structure has been compared with small scale models in two different FEM programs (AxisVM and Scia Engineer).

The results of the construction methodology are validated by reference projects and consults with experts. Because of these actions it's assumed that the bandwidth of the inaccuracy is relatively low for the structural and construction methodology results (in appendix I a short feasibility check is provided of the hoisting shed).

It may be concluded that still many aspects have to be considered before the Zalmhaven tower can be constructed. Therefore the obtained preliminary results are susceptible to changes. Nevertheless, the results which are obtained are relatively accurate and will only change due to new boundary conditions or an optimisation of the results.

⁴¹ A variant of the Multi Criteria Evaluation (MCE).

Bibliography

Literature study

- Hagen, S.J. (2012). *The Zalmhaven tower, an investigation on the feasibility of precast concrete in a high-rise tower, Literature study*. Delft: TU Delft.

Books

- Bennenk, H.W. *Handboek Prefab-Beton*. bfnb.

Internet:

- Bing maps. <http://www.bing.com/maps/>. Used on 17-11-2011.
- D9t. <http://www.skyscrapercity.com/showthread.php?t=36290&page=63>. Used on 18-10-2012.
- deHilster. <http://www.dehilster.info/index.php?doc=http://www.dehilster.info/instrumenten/totalstation1/index.html?n=20120331>. Used on 13-05-2012.
- Doka. <http://www.doka.com/web/references/index.in.php?refid=9073>. Used on 05-10-2012.
- Faay. http://www.faay.nl/newsletters/nl/januari_2010.html. used on 18-09-2012.
- Google maps. <http://maps.google.nl/>. Used on 15-11-2011.
- Gyproc. <http://www.gyproc.nl/producten/wanden/scheidingswanden/soundbloc-wandsystemen>. Used on 19-06-2012.
- Het strijkijzer. <http://www.hetstrijkijzer.nl/strijkijzer?waxtrapp=nzfmEsHunObnOhIYW>. Used on 02-12-2011.
- Hurks group. http://www.hurksprefabbeton.nl/show/nl/projecten/item/70,Woontoren_de_Stads_heer.html. Used on 09-09-2012.
- Knight. http://www.ece.ualberta.ca/~knight/ece632/fea/rectangles/r_hi.html. Used on 13-06-2012.
- Kwint. <http://www.kwintgroep.nl/docs/products/Staalkabel%20en%20toebehoren.pdf>. Used on 09-09-2012.
- Mous. <http://www.moussystem.nl/nl/systemen/mssv-5.html>. Used on 08-05-2012.
- Peri. http://www.peri.com/ww/en/products.cfm/fuseaction/showproduct/product_ID/1057/app_id/6.cfm. Used on 13-10-2012.
- Rotterdam. http://www.rotterdam.nl/grondwatermeetnet_online. Used on 03-05-2012.
- Topaas. <http://www.skyscrapercity.com/showthread.php?t=36290&page=123>. Used on 18-10-2012.
- Top100.nl. http://www.top010.nl/html/woontoren_zalmhaven.htm. Used on 16-11-2011.
- Wikipedia. <http://en.wikipedia.org/wiki/Skyscraper>. Used on 05-04-2012.
- Zalmhaven. <http://www.zalmhaven.com/?item=downloads&count=true&selected=4>. Used on 16-11-2011.
-

Master thesis reports:

- Falger, M.M.J. (2004). *Prefab stabiliteitsconstructies met open verticale voegen, Onderzoeksrapport*. Delft: TU Delft.
- Meij, M. van der (2012). *Een bouwmethode van geprefabriceerde betonnen hoogbouw (>200m)*. Delft: TU Delft.

- Pieterse, E.A. (2006). *Deuvelwerking van randbalken als onderdeel van vloeren in prefabbouw*. Delft: TU Delft.
- Tolsma, K.V. (2010). *Precast concrete cores in high-rise buildings*. Delft: TU Delft.

Readers:

- Abspoel, R., Bijlaard, F.S.K., Samsor, R. (2008). *Constructieleer 2B CT2051B Deel Staalconstructies*. Delft: TU Delft.

Reports:

- Cement online
 - Boonekamp, H.A.L., Meischke, J.C. (1979). *Efficiënter bouwen door betere maatcontrole*. Cement, vol. 1979-9, p. 387-399.
 - Herwijnen, R. Van & Reuvers, M. (2011). *Organisatie van de uitvoering*. Cement, vol. 2011-7, p. 20-26.
 - Hoof, P.A.J. (1997A). *Maatbeheersing in de bouw*. Cement, vol. 1997-1, p. 15-19.
 - Hoof, P.A.J. (1997B). *Maatbeheersing in de bouw (III)*. Cement, vol. 1997-9, p. 16-21.
 - Keulen, D. (2012). *Vervorming prefab wandconstructies*. Cement, vol. 2012-6, p. 80-84.
- Others
 - Hoof, P.A.J. (1986). *Maatbeheersing in de bouw, een ontwikkeling van uitzetmethoden*. Eindhoven: TU Eindhoven.
 - ING (2010). *Samen duurzaam bouwen aan innovatie*. Presented at Bouwend Nederland at 2 October 2010.
 - Hayden, T. (2009). *Crowding Our Planet*. National Geographic, p. 10-29.
 - Kwan, A.K.H. (1996). *Shear Lag in Shear/Core Walls*. Journal of structural engineering (www.ascelibrary.org), vol. September 1996.
 - Nederlandse Normalisatie-instituut (2011). *NEN-EN 1991-1-4*. Nederlandse Normalisatie-instituut: Delft.
 - Nederlandse Normalisatie-instituut (2011). *NEN-EN 1992-1-1*. Nederlandse Normalisatie-instituut: Delft.
 - Nederlandse Normalisatie-instituut (2007). *NEN 6702*. Nederlandse Normalisatie-instituut: Delft.
 - Nederlandse Normalisatie-instituut (1990). *NEN 2886*. Nederlandse Normalisatie-instituut: Delft.
 - Nederlandse Normalisatie-instituut (1990). *NEN 2887*. Nederlandse Normalisatie-instituut: Delft.
 - Nederlandse Normalisatie-instituut (1990). *NEN 2888*. Nederlandse Normalisatie-instituut: Delft.
 - Nederlandse Normalisatie-instituut (1990). *NEN 2889*. Nederlandse Normalisatie-instituut: Delft.
 - Nederlandse Normalisatie-instituut (1990). *NEN 3682*. Nederlandse Normalisatie-instituut: Delft.
 - Straman, J.P. (1988). *Geprefabriceerde stabiliteitsconstructies, de invloed van de verticale voegen*. TU Delft, Delft.
 - Vambersky, J.N.J.A. *Superhoog in Prefab*. Beton in Beeld 006-2007.
 - Wu, R. (2002). *Computer Aided Dimensional Control in Building Construction*. Eindhoven: TU Eindhoven.

Others:

- Corsmit PowerPoint presentation. Received from Jan Font Freide personally.
- DCK 2012. Calculation sheet received personally.
- TNO. Calculation sheet received personally.
- Zonneveld ingenieurs. Documents received personally.

Appendix A: Element configuration

In this appendix the final element configuration of the Zalmhaven tower is depicted. More information on the size, mass and how this configuration is obtained can be found in chapter 4.

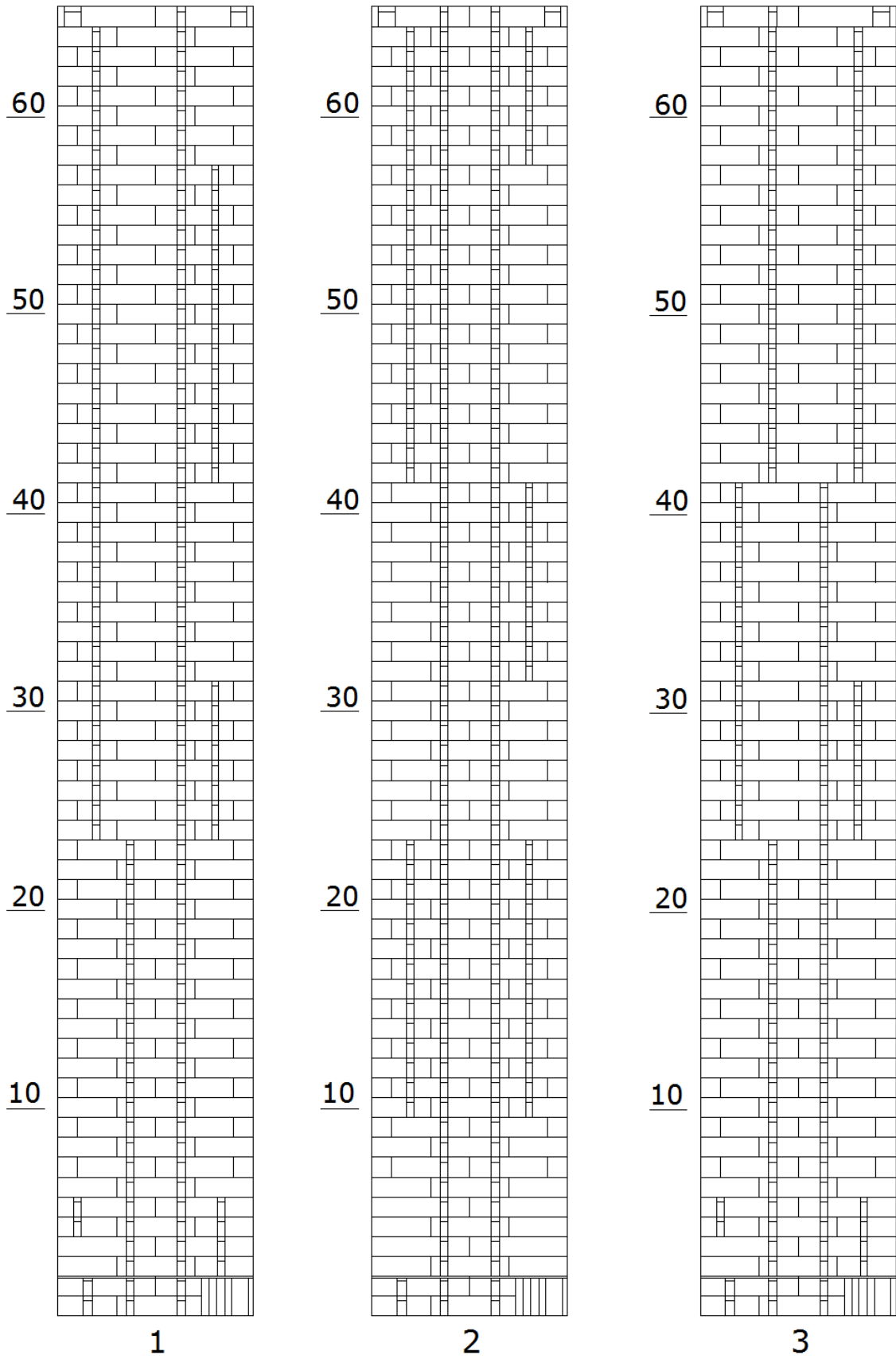


Figure 120 Element configuration of wall 1, 2 and 3

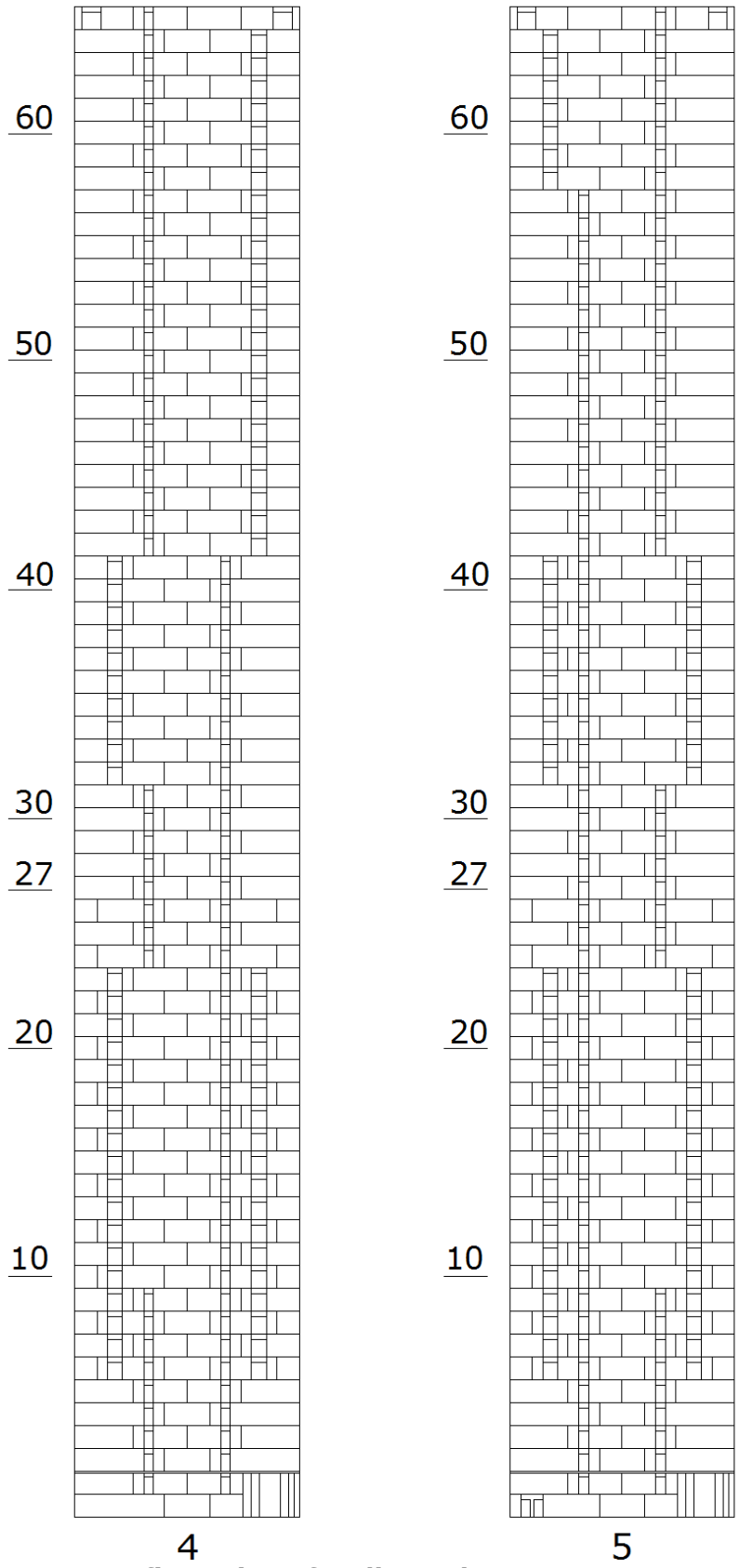


Figure 121 Element configuration of wall 4 and 5

Appendix B: Loads on the structure

In chapter 0 all the loads acting on the Zalmhaven tower are discussed. In this appendix the exact determination will be given of the horizontal and vertical loads. The same division as in chapter 0 will be maintained: section B.1 will discuss the vertical loads and section B.2 the horizontal loads.

B.1 Vertical loads

The vertical loads consist of dead load and live floor load. The dead load is composed out of the following aspects:

- dead load of the floors, including the screed layer and distributed floor load,
- dead load of the structural walls, excluding the wall openings,
- dead load of the facade.

For the floors a massive slab of 320mm thick will be used, to satisfy the requirements of contact sounds (minimal 800kg/m²). A thin screed layer (50mm) will be applied to provide a smooth finish. The internal apartment walls are based on a Gyproc SoundBloc metal stud wall with a dead load of 0.86kN/m [Gyproc, 2012]. According to section 6.3.1.2 of NEN-EN 1991-1-1, this may be replaced by a distributed load of 0.5kN/m². When these three loads are combined, a total floor load of 9.75kN/m² is obtained.

The structural walls have a thickness of 400 to 500mm. With approximately 10% openings, this results in a vertical load of 9 or 11.25kN/m² wall area. During the load calculation any possible optimisations (reduction of the wall thickness over the height) aren't included.

The Zalmhaven tower contains two load bearing facades with a dead load of 5kN/m². The two remaining non-load bearing facades have a dead load of 3kN/m². These values are based on the original design of Zonneveld ingenieurs.

The live floor load depends on the function of the floor. According to table NB.1-6.2 of NEN-EN 1991-1-1, dwellings are subjected to a live load of 1.75kN/m². When this load is combined with another live load (for example wind), it may be reduced by 60% ($\Psi=0.4$ in table NB.2-A1.1 of NEN-EN 1990).

Due to the function of the ground floor (lobby area), a live load of 5.0kN/m² is assumed. A reduction factor of $\Psi=0.6$ may be applied when combined with other live loads. A reduction factor of 0.6 is applied instead of $\Psi=0.4$ because this area will be used as an escape route during emergencies.

The first two floors will be used for storage and installations, which results in a live load of 5kN/m². Due to the nature of this load, no reduction factor may be applied ($\Psi=1.0$). The panorama floor on 65th floor is subjected to a live load of 5kN/m². In contrast to the ground floor this area isn't used as an escape route and a reduction factor of 0.4 may be applied in combination with other live loads ($\Psi=0.4$).

The previous aspects have been shortly summarized:

<u>Dwelling floor</u>		
Floor slab (d=320mm)	<u>G</u>	<u>Q</u>
Screed layer (50mm)	8.00kN/m ²	
Distributed wall load	1.25kN/m ²	
Live load ($\Psi_0=0.4$)	0.50kN/m ²	
Total		<u>1.75kN/m²</u>
	9.75kN/m ²	1.75kN/m ²
<u>Lobby floor (ground floor)</u>		
Floor slab (d=1000mm)	<u>G</u>	<u>Q</u>
Live load ($\Psi_0=0.6$)	25.0kN/m ²	
Total		<u>5.00kN/m²</u>
	25.0kN/m ²	5.00kN/m ²
<u>Installation/storage floor</u>		
Floor slab (d=320mm)	<u>G</u>	<u>Q</u>
Screed layer (50mm)	8.00kN/m ²	
Distributed wall load	1.25kN/m ²	
Live load ($\Psi_0=1.0$)	0.50kN/m ²	
Total		<u>5.00kN/m²</u>
	9.75kN/m ²	5.00kN/m ²
<u>Panorama floor</u>		
Floor slab (d=320mm)	<u>G</u>	<u>Q</u>
Screed layer (50mm)	8.00kN/m ²	
Distributed wall load	1.25kN/m ²	
Live load ($\Psi_0=0.4$)	0.50kN/m ²	
Total		<u>5.00kN/m²</u>
	9.75kN/m ²	5.00kN/m ²
<u>Structural walls</u>		
500mm wall (10% reduction)	<u>G</u>	
400mm wall (10% reduction)	9.00kN/m ²	
	11.25kN/m ²	
<u>Facade</u>		
Load bearing facade	<u>G</u>	
Non-load bearing facade	5.00kN/m ²	
	3.00kN/m ²	

With these values, an excel calculation was created, see Figure 122. The total load of the AxisVM calculations can't be used because only a part of the structure is modelled: the floors and the facade aren't included. The load resulting from the floors and facade which are supported by the structural walls is included, but a large part of the facade is self-bearing. This self-bearing facade, which supports approximately 26% of the floor area, isn't included. This decision to exclude the floors and the facade was made to reduce the amount of modelling work and because the facade doesn't provide any stability. The floors have a load introducing function (wind load from the facade to the structural walls), but due to their large structural area (the EA is relatively large) the actual distribution of forces is disrupted. The floors will increase the effective width of the walls, absorbing loads which should be taken up by the structural walls. Because of this decision, the excel sheet has to be used for the load calculation.

According to Figure 122, a total dead load of 964.1Mn and a total instantaneous live floor load of 53.1Mn is present at the foundation. The Zalmhaven tower has a total area of 55618m² of which 71.6% is lettable.

B.2 Horizontal loads

The horizontal loads are created by the wind. The wind load can be determined by the following equation from section 5.3 of NEN-EN 1991-1-4:

$$F_w = c_s c_d * c_f * q_p(z_e) * A_{ref} * n$$

in which:

- $c_s c_d$ is the structural factor for taking into account the effect of wind actions from the non-simultaneous occurrence of peak wind pressures on the surface (c_s) together with the effect of the vibrations of the structure due to turbulence (c_d).
- c_f is the force coefficient for the structure or a structural element.
- $q_p(z_e)$ is the peak velocity pressure at the reference height.
- A_{ref} is the reference area of the surface.
- n is the second order effect of the structure. This is incorporated in the wind load to prevent a non-linear calculation during the first stages of the design. The estimated second order is validated at the end with a non-linear calculation (see section 9.4).

An aspect which is missing in this calculation is the wind friction. In the Eurocode, the wind friction may be neglected at tall buildings since this only provides a minor component. For low and elongated buildings the friction should be incorporated.

The structural factor $c_s c_d$ can be calculated with the maple sheet created in the literature study or the excel sheet created by TNO for Zonneveld ingenieurs. Due to simplicity and organized overview of the TNO sheet, this calculation method will be used. In the literature study, the calculation of the structural factor is discussed in detail. In this section, the calculation will be discussed shortly.

In Figure 123 the calculation sheet of TNO is depicted. The following parameters are entered: the height, width, natural frequency, damping, mass, wind velocity, the roughness length and the vibration mode. The frequency could be calculated with formula F.2 of NEN-EN 1991-1-4, but this provides inaccurate results. Therefore it's strongly recommended to apply the method used in the Annex A.4 of NEN 6702:

$$f_e = \sqrt{\frac{a}{\delta}} \text{ [Hz]}$$

in which:

- a is the numerical value of the oscillation acceleration, depending on the static system and distribution of the mass: $a=0.384\text{m/s}^2$
- δ is the numerical value of the largest deformation of the structure as a result of the instantaneous load combination.

The calculation of the natural frequency of the Zalmhaven tower is provided in section 9.6 and E.2.1. According to this calculation, the first natural frequency is 0.165Hz. The damping used in this calculation is 0.02 (concrete buildings), but the Eurocode uses a logarithmic decrement value of $\delta=0.1$. This logarithmic decrement value can be expressed as a damping value:

$$D = \delta / 2n = 0.1 / 2n = 0.016 < 0.02$$

The logarithmic decrement value is 20% lower than the damping value of the NEN 6702. But when the acceleration is calculated, the NEN 6702 uses a damping value of $D=0.01$ (when $f_e < 1\text{Hz}$, see Annex A.5 of NEN 6702). The logarithmic decrement remains $\delta=0.1$ and now the logarithmic decrement is 59% larger than the damping value of the NEN 6702. On this subject dr.ir. R.D.J.M. Steenbergen from TNO was consulted and he agreed that there are differences between the NEN 6702 and NEN-EN 1991-1-4. Because there is still little known on the damping of structures, it's impossible to say which value is correct. The current damping values are too general and more research is required. Currently R. Van den Berg is starting his promotion research on this aspect in combination with TNO, Zonneveld ingenieurs and several other companies.

For the mass, only the dead load may be used in NEN-EN 1991-1-4 (see Annex F.5 (3) μ_e). This is an interesting aspect since if there is no live load, there are also no occupants inside the building. Therefore no one will experience the vibrations. This peculiarity applies to the accelerations, but is more understandable for the building factor: the dynamic factor influences the load, also when there are no occupants inside.

The next aspects are the basic wind velocity and roughness factor. When the accelerations are calculated, a basic wind velocity of 19.4m/s may be assumed for wind area II. This value is provided in the "NTA Hoogbouw (03-A Wind) report and represents the SLS wind velocity (repetition period of 1 year). When the structural factor is calculated, the original 27m/s has to be maintained for area II (ULS value, repetition period of 50 years). Therefore the acceleration value provided in Figure 123 isn't representable. For the roughness length at high-rise buildings $z_0=0.2\text{m}$ should be applied (non-build area). Even though the structure is located in the centre of a city, the roughness length should remain 0.2m (this is because of the height of the building relative to the surroundings).

The last aspect is the vibration mode. Unlike the acceleration, where bending and torsion is combined, the structural factor is calculated with the bending vibration mode. The parabolic bending mode is utilised since the deflection behaviour is dominated by bending. If the deflection is dominated by shear, the linear bending mode should be applied.

Due to confidentiality, this figure cannot be displayed.

Figure 123 Calculation c_s, c_d [TNO 2012] (acceleration isn't representable)

According to Figure 123, a structural factor of 1.111 is obtained.

The next factor in the wind load calculation is the force coefficient. In Figure 124 the force coefficient values from table NB.6-7.6, NEN-EN 1991-1-4 are shown. The Zalmhaven tower has a slenderness value of $h/d=202.25/30=6.7$. Therefore the $c_{pe,10}$ values of zone 5D and 5E should be used: $c_f=0.8-(-0.7)=1.5$. Due to the ac of correlation between the two sides, the value has to be multiplied by 0.85 (NB 7.2.2 (4)). This results in a force coefficient of $c_f=1.5*0.85=1.3$

Zone	A		B		C		D		E	
	$c_{pe,10}$	$c_{pe,1}$	$c_{pe,10}$	$c_{pe,1}$	$c_{pe,10}$	$c_{pe,1}$	$c_{pe,10}$	$c_{pe,1}$	$c_{pe,10}$	$c_{pe,1}$
5	-1,2	-1,4	-0,8	-1,1	-0,5		+0,8	+1,0	-0,7	
≤ 1	-1,2	-1,4	-0,8	-1,1	-0,5		+0,8	+1,0	-0,5	

Figure 124 Force coefficient values [NEN-EN, 2011]

The peak velocity pressure can be found in table NB.5 of NEN-EN 1991-1-4 or calculated with the maple sheet created in the literature study.

A_{ref} depends on the considered area. In this thesis the wind force will be calculated per meter height and therefore the force will only be calculated with the width: 30m. When wind load is calculated per meter of height, a parabolic line is created. This is very difficult to enter in AxisVM and therefore Figure 125 of NEN-EN 1991-1-4, section 7.2.2 will be used. For z_{strip} a height of three storeys will be maintained (9.15m). The height of the strip isn't specified in the Eurocode and therefore any value could be used. A strip height of three storeys is a good compromise between accurate results and an acceptable amount of modelling work.

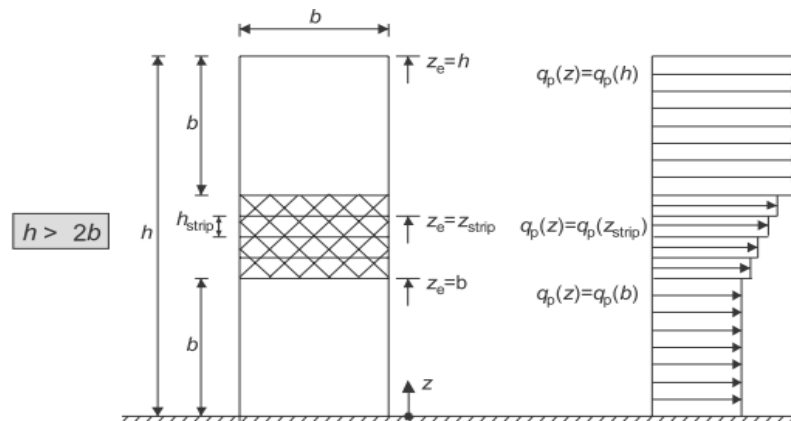


Figure 125 Wind load distribution [NEN-EN, 2011]

The last aspect of the wind load calculation is the second order effect. Due to the first order deflection of the wind, the structure isn't loaded centrally anymore (initial skewness neglected) and a second order moment is created. As a result of this additional moment, the deflection increases. An easy method to include these actions is to multiply the wind load by a second order factor. It should be noted that this does not provide exact result: by multiplying the wind load by a second order factor, the resulting deformation may be equal but at the foundation the horizontal resulting force has also increased with the same factor. Therefore the horizontal forces are overestimated by the same value as the second order factor. This should be taken into account when the horizontal resistance of the foundation is considered.

After the vertical loads were determined, the second order magnification factor was determined. In section 9.4 this calculation is shown. According to this calculation the SLS magnification factor is equal to 1.1 and the ULS factor is equal to 1.13. Due to inaccuracies in this calculation (the foundation and structural stiffness are estimated), a magnification factor of 1.1 is assumed.

Now that all the values of the different aspects are determined, the total wind load per meter height can be determined. The results are shown in Table 30.

Table 30 Distributed wind load over the height

Height [m]	$C_s C_{d_i}$ [-]	C_f [-]	q_p [kN/m ²]	w [m]	n [-]	q_{wind} [kN/m]
0-30.5	1.11	1.3	1.202	30	1.1	57.29
30.5-39.65	1.11	1.3	1.265	30	1.1	60.29
39.65-48.80	1.11	1.3	1.343	30	1.1	64.01
48.80-57.95	1.11	1.3	1.409	30	1.1	67.15
57.95-67.10	1.11	1.3	1.471	30	1.1	70.11
67.10-76.25	1.11	1.3	1.520	30	1.1	72.44
76.25-85.40	1.11	1.3	1.564	30	1.1	74.54
85.40-94.55	1.11	1.3	1.604	30	1.1	76.44
94.55-103.70	1.11	1.3	1.640	30	1.1	78.16
103.70-112.85	1.11	1.3	1.674	30	1.1	79.78

112.85-122.00	1.11	1.3	1.705	30	1.1	81.26
122.00-131.15	1.11	1.3	1.737	30	1.1	82.78
131.15-140.30	1.11	1.3	1.765	30	1.1	84.12
140.30-149.45	1.11	1.3	1.791	30	1.1	85.36
149.45-158.60	1.11	1.3	1.815	30	1.1	86.50
158.60-170.80	1.11	1.3	1.839	30	1.1	87.64
170.80-202.25	1.11	1.3	1.923	30	1.1	91.65

Because the wind load isn't placed at the facade, but as a horizontal line load on the structural walls per floor, the values of Table 30 have to be converted. The following formula is used:

$$q_{\text{wind,line load}} = \frac{q_{\text{wind}} \cdot h_{\text{floor}}}{n \cdot d_{\text{building}}}$$

in which:

$q_{\text{wind,line load}}$ is the wind line load on the structural wall
 q_{wind} is the wind load per meter height
 n is the amount of walls in the considered direction
 d_{building} is the building depth (30m).

With this formula, Table 31 is obtained.

Table 31 Distributed wind load per structural wall

Area	Height	Force per meter height	Line load x-direction per wall	Line load y-direction per wall
	[m]	[kN/m]	[kN/m]	[kN/m]
1	0-30.5	57.29	2.91	1.94
2	30.5-39.65	60.29	3.06	2.04
3	39.65-48.80	64.01	3.25	2.17
4	48.80-57.95	67.15	3.41	2.28
5	57.95-67.10	70.11	3.56	2.38
6	67.10-76.25	72.44	3.68	2.45
7	76.25-85.40	74.54	3.79	2.53
8	85.40-94.55	76.44	3.89	2.59
9	94.55-103.70	78.16	3.97	2.65
10	103.70-112.85	79.78	4.06	2.70
11	112.85-122.00	81.26	4.13	2.75
12	122.00-131.15	82.78	4.21	2.81
13	131.15-140.30	84.12	4.28	2.85
14	140.30-149.45	85.36	4.34	2.89
15	149.45-158.60	86.50	4.40	2.93
16	158.60-170.80	87.64	4.46	2.97
17	170.80-202.25	91.65	4.66	3.11

With this calculation one aspect still hasn't been considered: geometrical imperfections. Due to deviations in the geometry of the building, the structure is loaded eccentrically. This aspect is comparable to the second order effect.

Section 5.2 of NEN-EN 1992-1-1 provides methods to incorporate geometrical imperfections into the calculation. It should be noted that the geometrical imperfections only have to be considered in the ULS (see 5.2 (3) of NEN-EN 1992-1-1). Therefore the values of Table 31 still suffice for the SLS. The geometrical imperfections are calculated with the following equation:

$$\theta_i = \theta_0 \cdot \alpha_h \cdot \alpha_m$$

in which:

θ_0 is the initial value: $\theta_0=1/300$

α_h is a reduction factor for the height: $\alpha_h = 2/\sqrt{l}$; $2/3 \leq \alpha_h \leq 1$

α_m is a reduction factor for the amount of elements/floors: $\alpha_m = \sqrt{0.5(1 + 1/m)}$

l is the height (in meters)

m is the amount of elements/floors.

With a height of 202.25m the following values are obtained: $\alpha_h=2/3$ and $\alpha_m=\sqrt{0.5}$. This results in a rotation of:

$$\theta_i = \theta_0 \cdot \alpha_h \cdot \alpha_m = 1/300 \cdot 2/3 \cdot \sqrt{0.5} = 1.58 \cdot 10^{-3} \text{ [rad]}$$

Because of this small rotation, an additional horizontal load is created (H_i), shown in Figure 126. This horizontal load is obtained by multiplying the dead and instantaneous live floor load by the rotation (this is allowed because the rotation is small):

$$H_i = \theta_i \cdot N = 1.58 \cdot 10^{-3} \cdot (964144.25 + 53087.91) = 1611 \text{ kN}$$

This can be rewritten to a horizontal live load of:

$$q_i = H_i/l = 1611/202.25 = 7.96 \text{ kN/m}$$

With the same equation used at the wind load, this can be rewritten to a horizontal line load per structural wall:

$$q_{i,x\text{-direction}} = 0.40 \text{ kN/m}$$

$$q_{i,y\text{-direction}} = 0.27 \text{ kN/m}$$

These values should be added to Table 31 for the ULS calculations.

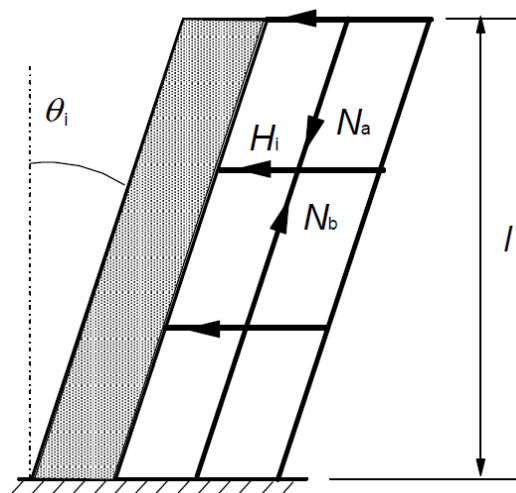


Figure 126 geometrical imperfections [NEN-EN, 2011]

The non-linear calculation performed by AxisVM to verify the second order effects also took geometrical imperfections into account. Therefore the previous calculated values of 0.4 and 0.27kN/m don't have to be added to the wind load: the values presented in Table 31 are the final values which have to be entered in AxisVM for the FEM calculations in SLS and ULS.

Appendix C: Modelling in AxisVM

In this appendix the detailed background information of chapter 6 is provided. Section B.1 will start with the influence of the domains. Section B.2 continues with the optimal mesh size and section B.3 concludes the with the connections

C.1 The influence of the domains

When a structure is modelled in a finite element method program, domains are used for separating structural elements. For example, a single floor slab, wall element or column may be represented by one domain. When a monolithic structure is modelled, the entire structure should be made with one domain since there are no joints or connections⁴². Because of practical reasons (constructing the model), it may be more convenient to use multiple domains in a monolithic model. But do the multiple domains influence the structural properties?

C.1.1 Model scheme of the investigation

To answer this question, three structures are modelled (see Figure 127). The first structure contains a domain for every wall element and between these elements interface elements are applied. The second structure is also modelled with a domain for every wall element, but there are no interface elements. Without the interface elements, AxisVM automatically connects the domains to each other. The third structure is composed of one domain element, representing a wall that was cast in a continuous process.

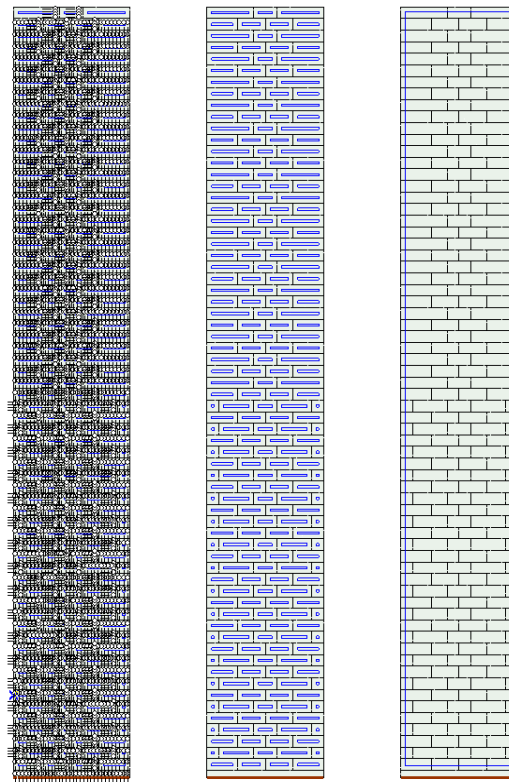


Figure 127 Three structure from the domain investigation

For the three structures wall 4 (see section 4.3.2) is used without any openings. Maintaining the openings would make it more difficult to construct a wall with one

⁴² There may be connections visible in the concrete due to the casting sequence, but these connections have a strength that approximates the surrounding concrete and are therefore not considered as a real connection.

domain. Furthermore, the openings should not have any effect on the results since they do not interfere with the behaviour between different domains.

A mesh size of 750mm is used which results in four mesh elements over the height of one domain (only the first two structures). Because there are no openings in the three structures, this mesh size is relative accurate. A smaller mesh size would provide more accurate values, but the goal of this investigation is not to obtain an accurate shear force value to design and reinforce a wall element, but to find out if multiple domains influence the structural results. Using the same mesh size in the three structures assures that all the values have the same accuracy.

The three structures are clamped at the foundation ($R_x=R_z=1*10^7$ kN/m/m and $R_y=0$ kN/m/m) and a 2D calculation with membrane elements is used in the X-Z plane (hence $R_y=0$ kN/m/m). Concrete class C90/105 is used with $E_x=E_y=29333$ N/mm² (the concrete is uncracked due to the high dead load of the structure). The stiffness of the horizontal and vertical connections of structure 1 (the interface elements) are iteratively⁴³ determined at $k_x=k_y=1*10^{10}$ kN/m/m. The three structures are loaded by dead load and a non-uniform wind load (the wind load increases with the building height) as described in section 5.2 and 5.3.

C.1.2 Results

In Figure 128, Figure 129 and Figure 130 the result of the investigation on the influence of the domains are depicted. Based on the figures it can be concluded that the three structures are identical on a global scale. For example, Figure 128 shows that the first structure has a top displacement of 253.989mm. The second structure has a top displacement of 253.941mm, only 0.001% smaller than the first structure. The top displacement of the third structure is identical to the second structure: 253.941mm.

⁴³ The iterative method was applied since it was unknown at which stiffness the models would behave nearly identical. After several models with a different stiffness, this value was obtained.

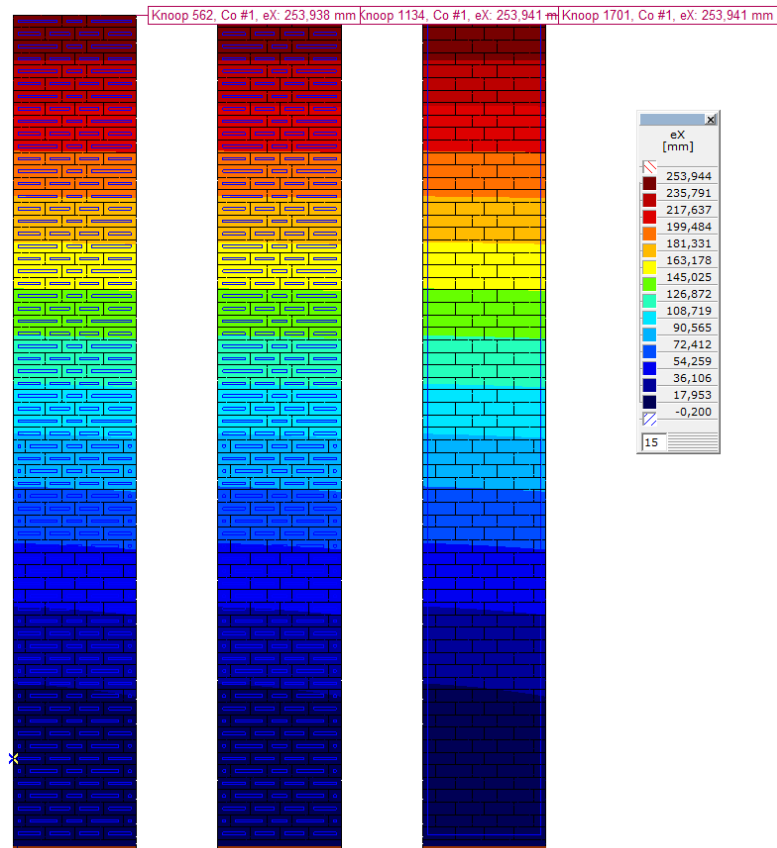


Figure 128 Displacement e_x

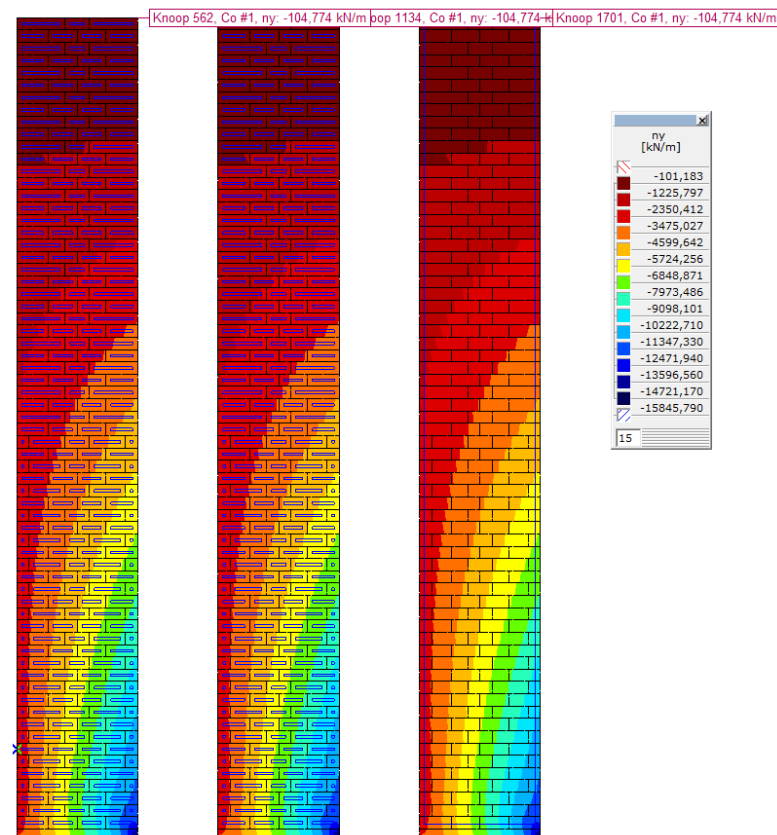


Figure 129 Normal force n_y

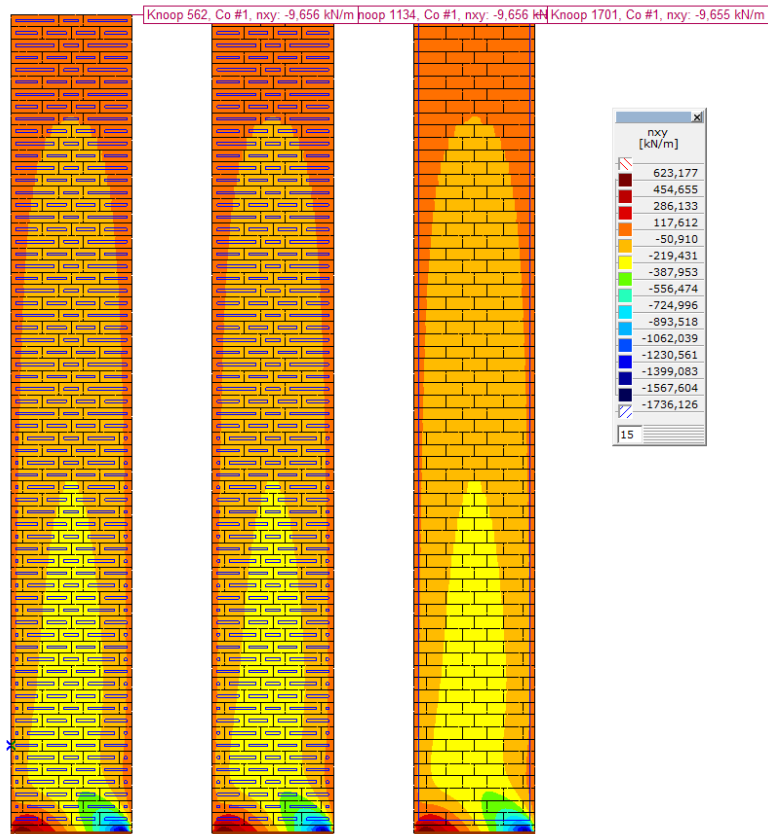


Figure 130 Shear force n_{xy}

To compare the results of Figure 129 and Figure 130 is slightly more difficult based on the graphical values and therefore three sections have been made per structure, see Figure 131.

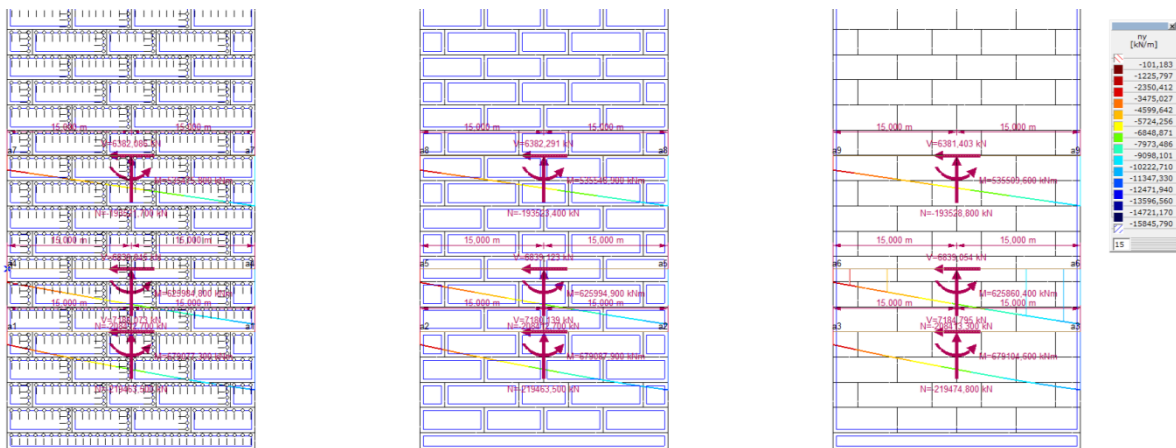


Figure 131 Sections

In Table 32 the results are shown. It can be noticed that the maximum difference between the three structures is never larger than 0.066% (difference between the shear force of structure 1 and 3 at section 1). For the integrity of the conclusions made in this section, a second calculation has been made with a mesh size of 1500mm. The results are shown in Table 33 and it can be observed that the mesh size has nearly no influence on the results: the differences are in the same order of magnitude and the largest difference can be found at the shear force between structure 1 and 3 at section 3 (0.094%).

Table 32 Section forces at a mesh size of 750mm

Structure		Section 1	Difference with structure 1 [%]	Difference between str. 2 and 3 [%]	Section 2	Difference with structure 1 [%]	Difference between str. 2 and 3 [%]	Section 3	Difference with structure 1 [%]	Difference between str. 2 and 3 [%]
1	M [kNm]	679077,3	-	-	625984,8	-	-	535475,8	-	-
	V [kN]	7180,073	-	-	6839,045	-	-	6382,086	-	-
	N [kN]	219463,5	-	-	208412,7	-	-	193521,7	-	-
2	M [kNm]	679087,9	0,002	-	625994,9	0,002	-	535548,9	0,014	-
	V [kN]	7180,139	0,001	-	6839,123	0,001	-	6382,291	0,003	-
	N [kN]	219463,5	0,000	-	208417,7	0,002	-	193523,4	0,001	-
3	M [kNm]	679104,6	0,004	0,002	625860,4	-0,020	-0,021	535509,6	0,006	-0,007
	V [kN]	7184,795	0,066	0,065	6839,054	0,000	-0,001	6381,403	-0,011	-0,014
	N [kN]	219474,8	0,005	0,005	208413,3	0,000	-0,002	193528,8	0,004	0,003

Table 33 Section forces at a mesh size of 1500mm

Structure		Section 1	Difference with structure 1 [%]	Difference between str. 2 and 3 [%]	Section 2	Difference with structure 1 [%]	Difference between str. 2 and 3 [%]	Section 3	Difference with structure 1 [%]	Difference between str. 2 and 3 [%]
1	M [kNm]	679029,9	-	-	625835,4	-	-	535444,6	-	-
	V [kN]	7177,032	-	-	6838,371	-	-	6375,241	-	-
	N [kN]	219477,8	-	-	208414,1	-	-	193535,3	-	-
2	M [kNm]	679043,8	0,002	-	625848,7	0,002	-	535521,4	0,014	-
	V [kN]	7177,11	0,001	-	6838,984	0,009	-	6375,526	0,004	-
	N [kN]	219470	-0,004	-	208414,1	0,000	-	193536	0,000	-
3	M [kNm]	679099,1	0,010	0,008	625813,1	-0,004	-0,006	535518,1	0,014	-0,001
	V [kN]	7181,781	0,066	0,065	6836,565	-0,026	-0,035	6381,231	0,094	0,089
	N [kN]	219405,4	-0,033	-0,029	208411,1	-0,001	-0,001	193543,3	0,004	0,004

C.1.3 Conclusion

When the results are compared it can be concluded that there is a difference between a monolithic structure composed out of one domain and a monolithic structure with multiple domains (with or without interface elements). Since the differences are relatively small, it's acceptable to use multiple domains or multiple domains with interface elements for a monolithic structure. To obtain monolithic results with interface elements, a stiffness equal or larger than $k_x=k_y=1*10^{10}$ kN/m/m is required. By using a high stiffness, the interface elements become very stiff. This high stiffness makes the interface elements obsolete and values are obtained which are comparable to model 2 (no interface element, resulting in an infinite stiffness between the two elements). When the actual normal stiffness and a very high shear stiffness are entered in the first model ($k_y=7.33*10^8$ kN/m/m and $k_x=1*10^{10}$ kN/m/m), the differences become larger between model 1 and model 2 and 3. This is unexpected because the normal stiffness is based on the stiffness of the surrounding concrete (see section 7.8) and this should provide monolithic values. It can be concluded that the lower stiffness in combination with the interface elements provide too much deformation in the connections. Because these differences are smaller than 0.5% (660% larger than the largest value of Table 32), this less stiff behaviour is neglected.

C.2 Mesh size

The mesh size is one of the important factors that determine the accuracy of the calculations. A large mesh size will result in a short calculation time but it may not provide accurate calculation results. Therefore the effect of different mesh sizes and the resulting calculation time have to be researched. If the calculation results converge with a decreasing mesh size, an optimal mesh size can be chosen.

This research on the mesh size is composed out of four different parts: first an uniform mesh size will be used for the entire structure. The size of the mesh is the only variable and will be reduced in several steps. In the second part, the mesh size will be reduced locally and in the third part of this research, the mesh size will have a different size according to the height. Part 1 until 3 will be based on a 2D wall. Based on these results, an optimal mesh size will be determined for a 3D structure in part 4.

C.2.1 Part 1: uniform mesh size

The mesh size research will start with a uniform mesh size. Creating a uniform mesh is relatively easy, but compared with locally increased mesh size and a mesh size according to the height, it may be inefficient. First of all several assumptions will be made.

Assumptions

For this research wall 4 is used, as described in section 4.3.2. The mesh size is uniform over the building height and will be automatically generated by AxisVM. AxisVM 10 only uses triangles for the mesh and Figure 132 shows how a square wall element is meshed with triangles.

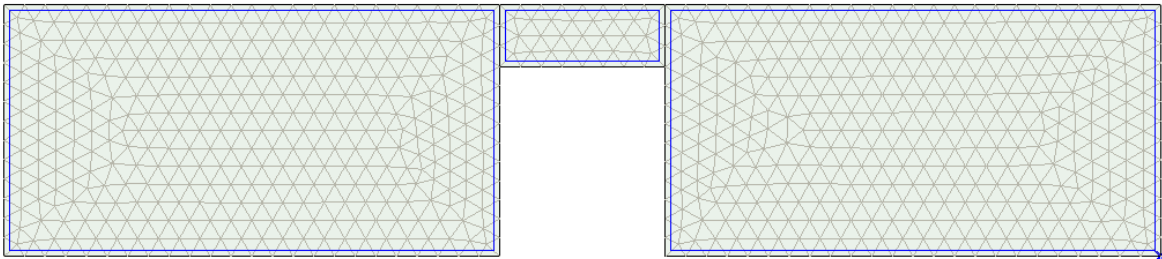


Figure 132 Triangular mesh in a square element

In AxisVM 11 and other FEM programs (for example ATENA) it's possible to construct the mesh out of quadrangles or a combination of triangles and quadrangles. Theoretically this should have no effect on the result, but it's known that the mesh shape may influence crack direction in ATENA for example. Since all the results are obtained by first order linear analysis, crack formation is not taken into account and therefore the mesh form should have no influence on the results⁴⁴.

The differences between the meshes will be determined by the maximum top deflection and by three sections. The considered sections are shown in Figure 133 and they are located at the sixth floor. The sixth floor is chosen because of the intersections at the lower floors. It should be noted that there may be sections with higher forces and that the current three sections are only chosen for comparison purposes. In section I, the shear force and moments will be considered, in section II the normal force and in section III the moments. These three locations on the sixth floor are chosen because they often contain the largest forces at that level.

⁴⁴ This assumption is confirmed by Dr.ir. M.A.N. Hendriks from the Structural Mechanics Department of Civil Engineering and Geosciences.

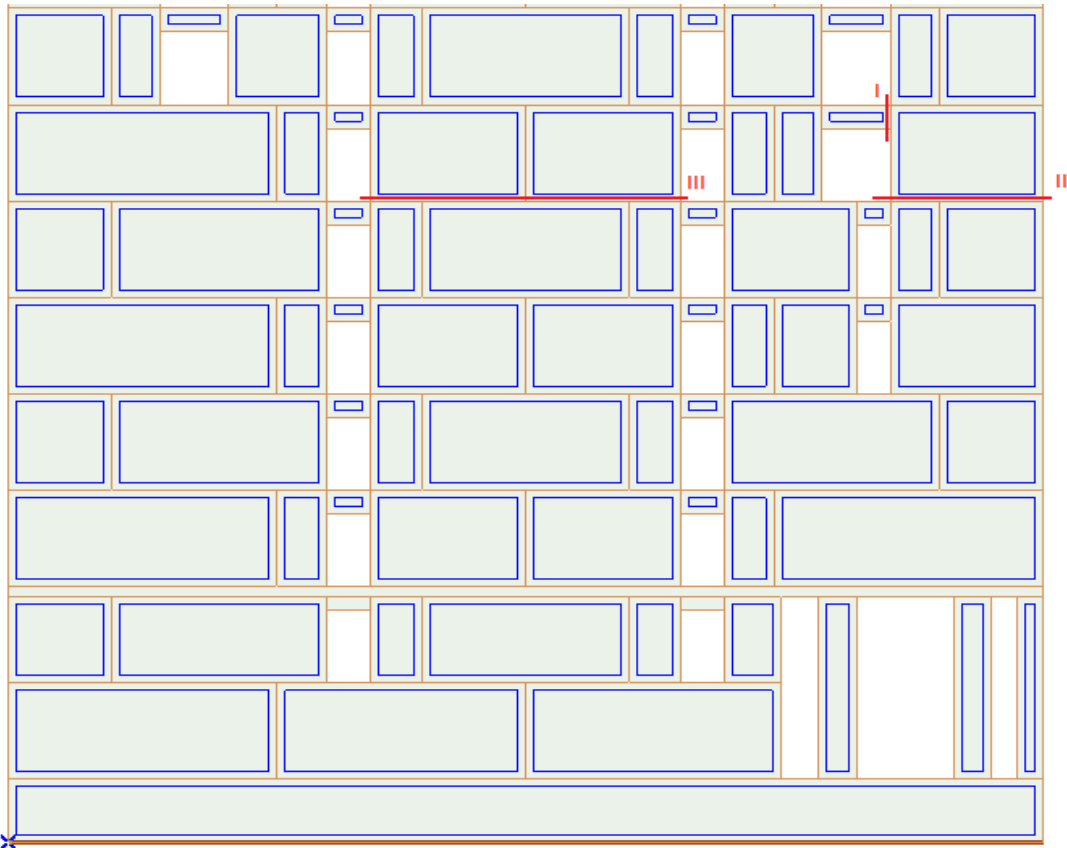


Figure 133 Location of the sections

To obtain accurate results, the mesh size should decrease with a factor of 2 in the smallest elements (the lintels) per step. Therefore the following mesh sizes will be examined: 1500, 1000, 750, 500, 375, 250 and 150mm. In Figure 134 it can be seen that a mesh size of 1500 and 1000mm contain one layer of mesh elements in the lintels. Between a mesh size of 750mm and 375mm there are two layers (Figure 135 and Figure 136). When a mesh size of 250mm is observed, it can be seen that there are 4 layers (Figure 136) and a mesh size of 150mm results in 6 layers (Figure 137). Reducing the mesh size by 2 for every step would have resulted in very large steps and obtaining 8 layers in the last step would cause a disproportionate long calculation time (8 layers can only be achieved by a mesh size smaller than 100mm). Therefore the mesh sizes of 1500, 1000, 750, 500, 375, 250 and 150mm are maintained.

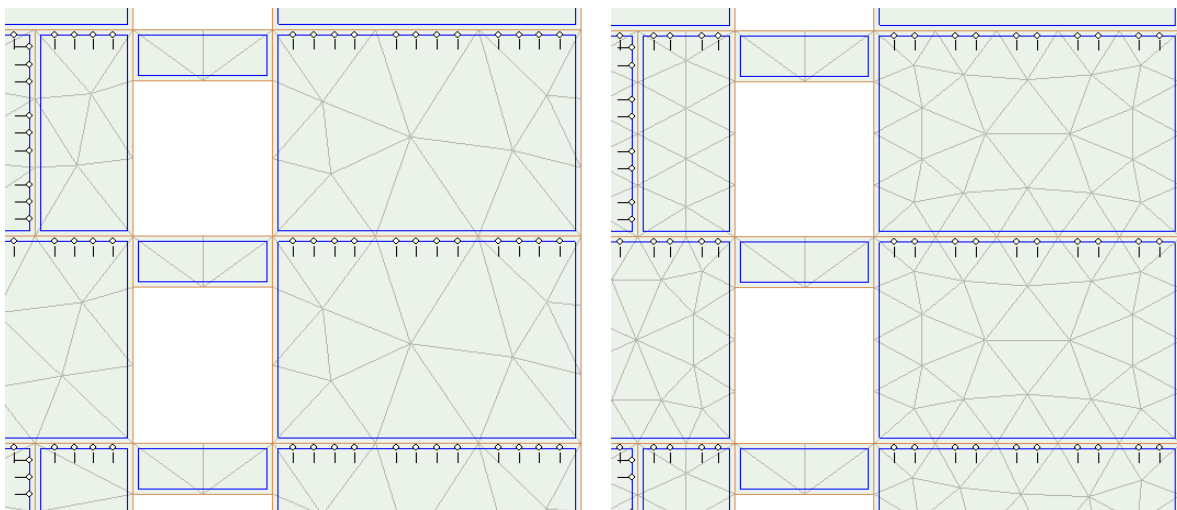


Figure 134 Mesh size of 1500mm (left) and 1000mm (right)

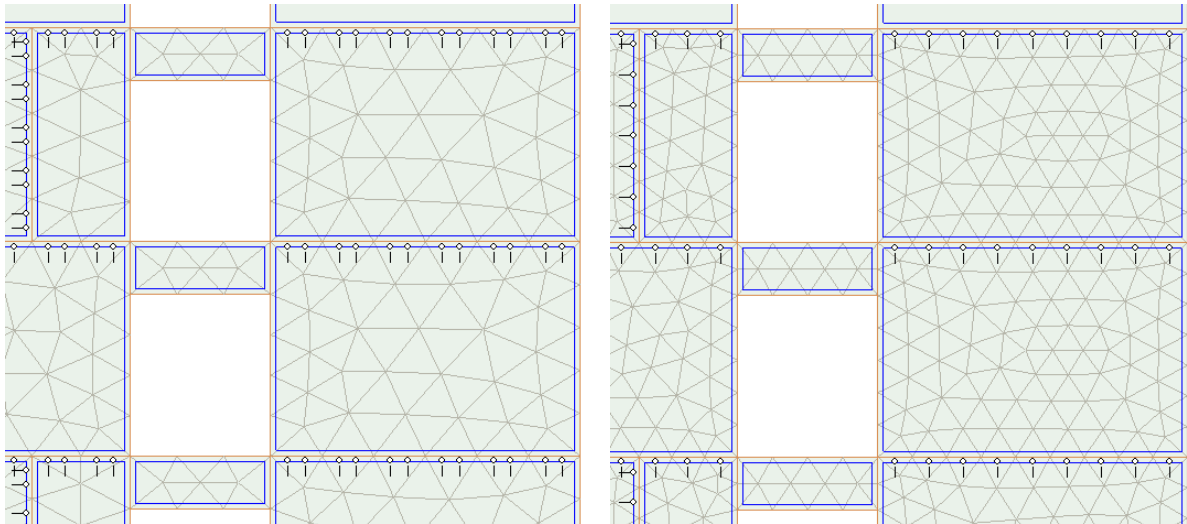


Figure 135 Mesh size of 750m (left) and 500mm (right)

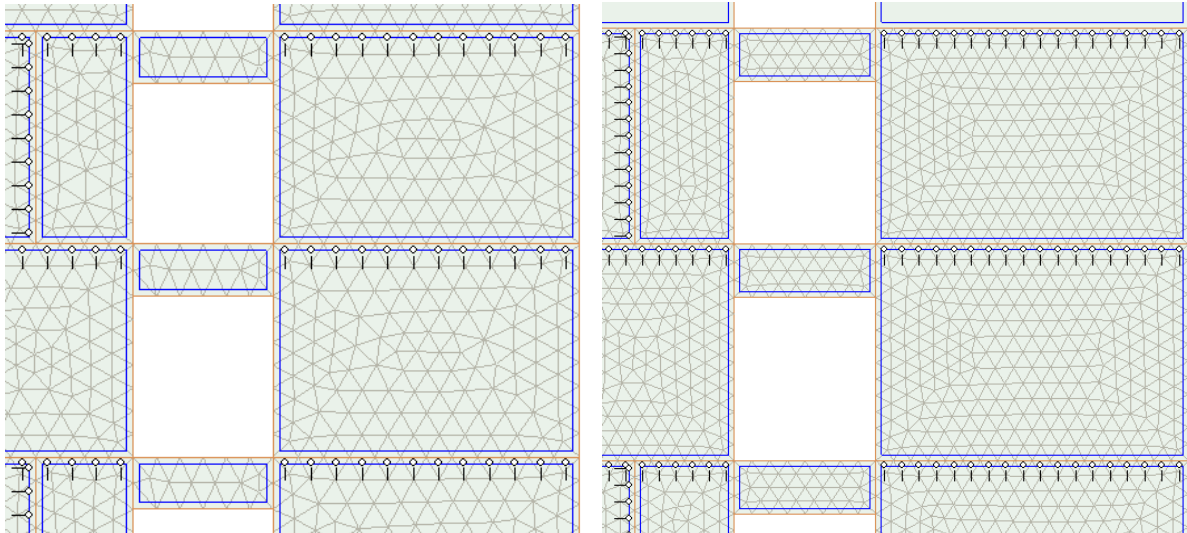


Figure 136 Mesh size of 375mm (left) and 250mm (right)

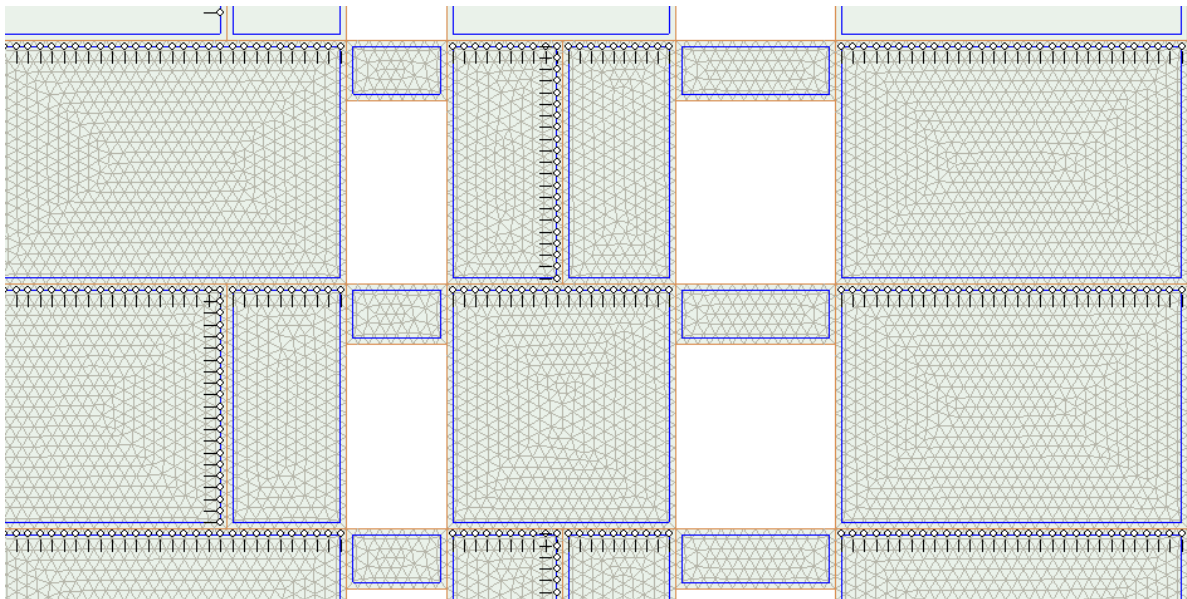


Figure 137 Mesh size of 150mm

Results

In Table 34 the results are shown of the analysis with different mesh sizes. Besides the calculated values, the table also contains the relative difference with the previous calculated value.

Table 34 Results of the research on different mesh sizes

Mesh size	Top deflection U_{\max}		Shear force at section 1		Moment at section 1		Normal force at section 2		Moment at section 3		Calculation time
	[mm]	Difference [%]	[kN]	Difference [%]	[kNm]	Difference [%]	[kN]	Difference [%]	[kNm]	Difference [%]	
1500	379.5	-	174.9	-	148.1	-	59872.1	-	30057.1	-	5
1000	377.9	-0.4	235.5	34.6	184.9	24.8	59491.5	-0.6	28810.8	-4.1	16
750	378.6	0.2	296.7	26.0	189.4	2.4	59377.4	-0.2	29621.4	2.8	27
500	378.6	0.0	296.7	0.0	193.9	2.4	59271.3	-0.2	29035.5	-2.0	107
375	378.3	-0.1	323.3	9.3	217.3	12.1	59210.1	-0.1	28847.2	-0.6	652
300	378.4	0.0	315.6	-2.7	215.9	-0.6	59186.2	0.0	28752.9	-0.3	805*
250	x										
150	x										

* This calculation was done by a faster computer.

A mesh size of 250mm and 150mm could not be calculated due to a memory problem in AxisVM. AxisVM is written as a 32-bit application and only supports 2GB of physical memory and 2GB of virtual memory. When a mesh size of 250mm is calculated, 1.1 million equations have to be solved which requires more than 4GB of memory. AxisVM 12, which will be released next year, is written as 64-bit application and will support more than 4GB of memory. It's recommended to do the mesh size on a part of the structure, making sure that all the mesh sizes can be analysed. Based on the section results, conclusions can be made for the entire structure.

The second column of Table 34 shows that there is only a lateral deflection difference of 0.3% between the largest and smallest mesh size: the deflection is only slightly dependent on the mesh size. This small relationship can be explained by the calculation method of AxisVM (and most other FEM programs): the deflection of the nodes is the primary unknown variable and the mesh size has little influence on the deflection of the nodes. Creating a smaller mesh will result in more nodes and more points where the deflection is known, but the overall deflection will not become more accurate. The mesh size does have an influence on the strains, stresses and forces because they are derived from the deflections in the nodes. A smaller mesh will result in more nodes and as a result there are more points where the stain, stress and force are known. A smaller distance between the known points will result in a better derivation.

The size of the element that is meshed also plays an important role. When section 1 is compared with section 2 and 3, large fluctuations can be seen at section 1. It's likely that there is a relation between the amount of meshed elements in the domain and the accuracy: in the lintel the amount of meshed elements changes drastically compared to the domain of section 2 and 3. The observed differences between section 1 and section 2 & 3 are also confirmed by several graphics of the normal force in the local y direction (n_y) in Figure 138, Figure 139 and Figure 140. In these three graphics the same scale is used and large differences can be seen in the lintels while the adjacent walls stay merely the same.

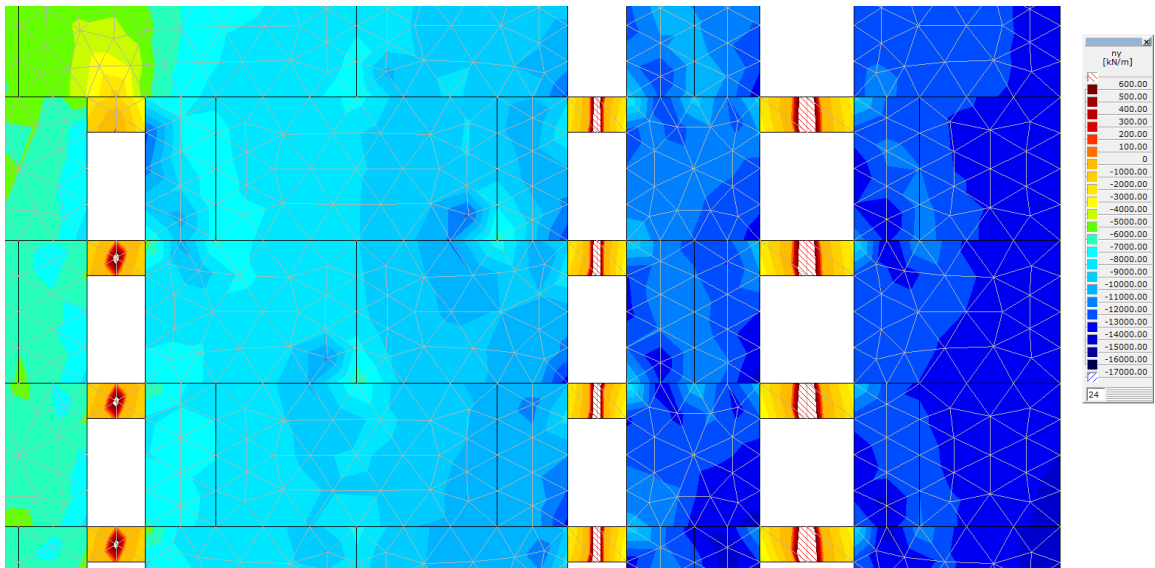


Figure 138 Normal force in the local y direction (mesh is 1000mm)

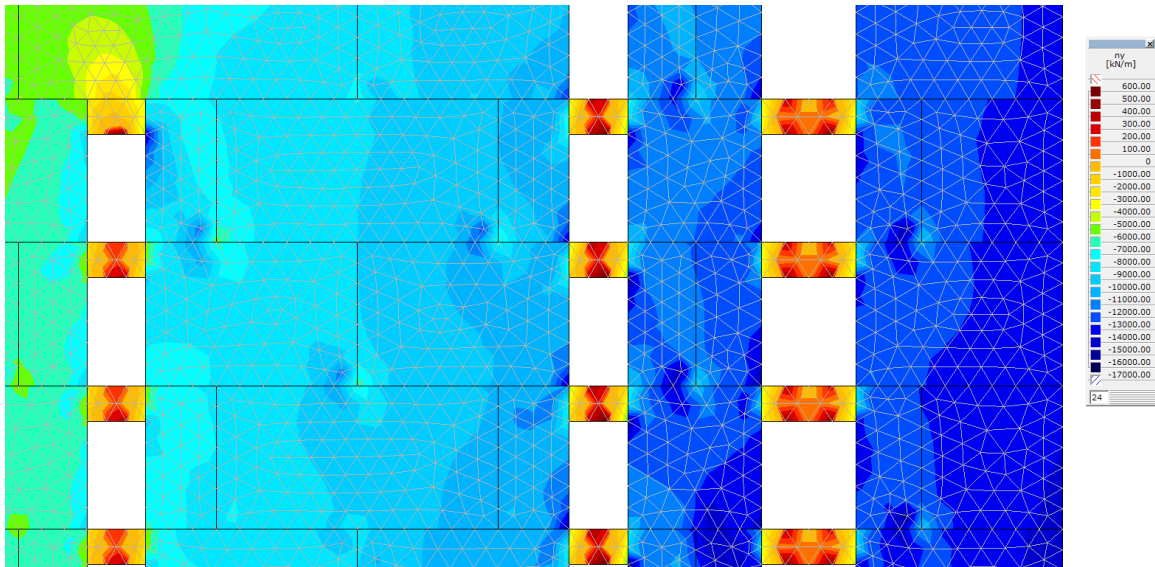


Figure 139 Normal force in the local y direction (mesh is 500mm)

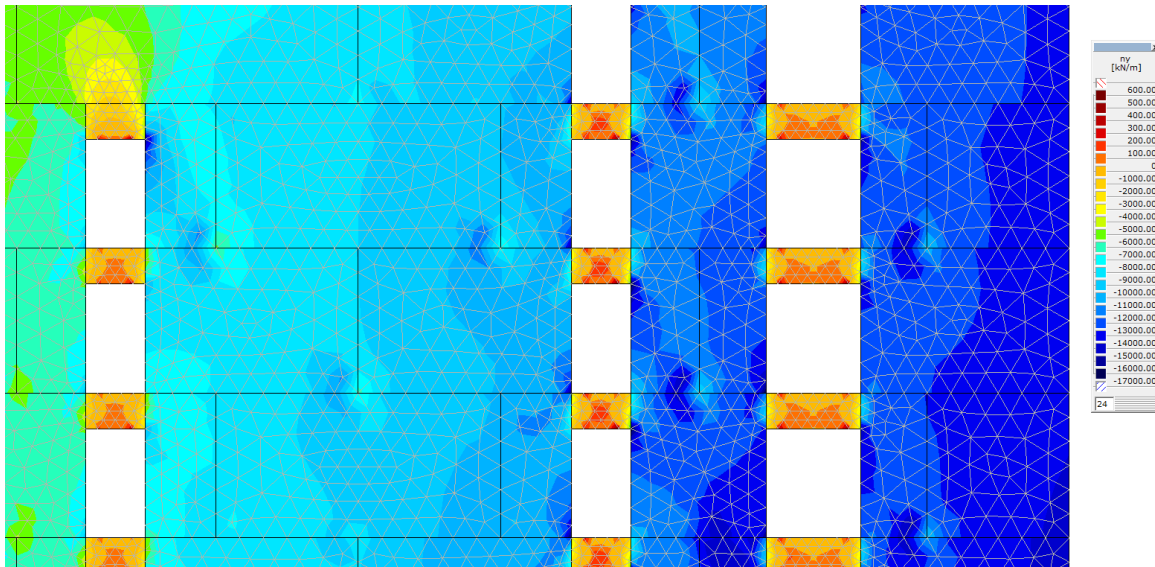


Figure 140 Normal force in the local y direction (mesh is 250mm)

A second observation that can be made in Table 34 is the reduction of the relative difference with a decreasing mesh size: the values are converging. The mesh size of 300mm provides the most accurate values, but unfortunately smaller mesh sizes can't be examined. Therefore the mesh size and results will also be evaluated by using a locally increased mesh (part 2) and a mesh size according to the height (part 3).

C.2.2 Part 2: local mesh size

Part 1 of the mesh size research shows that the deflection is almost equal for all mesh sizes. The forces in section II and III also change very little, but section I shows large variations with different sizes. To overcome this problem without decreasing the entire mesh size, the mesh is only locally reduced at the lintels. This is depicted in Figure 141.

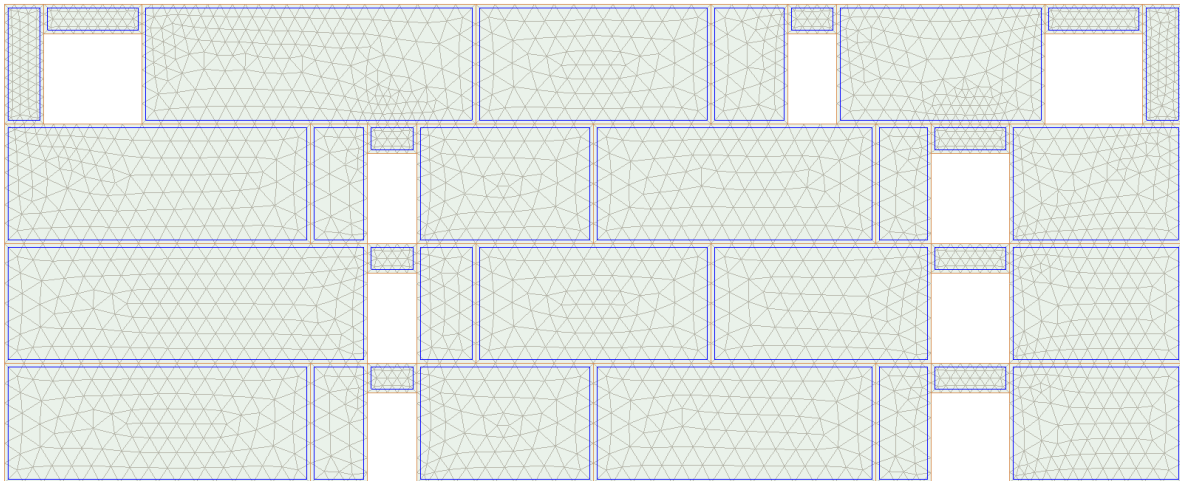


Figure 141 Local mesh reduction

By locally reducing the mesh size, the calculation time remains acceptable and the variation at section I should become less. For part 2 of the mesh research the same assumptions as in part 1 are made. The only difference is the mesh size in the lintels (section I). To provide a smooth transition between the mesh size in the lintels and the adjacent walls, a transition mesh is automatically generated by AxisVM. This transition mesh can also be seen in Figure 141.

Results

Table 35 shows the result of the research on local different mesh sizes. The first value in column 1 represents the mesh size of the adjacent walls, the second value represents the mesh size of the lintels. Besides the results, the table also contains the relative difference with the previous calculated value.

Table 35 Results of the research on local different mesh sizes

Mesh size	Top deflection U_{max}		Shear force at section 1		Moment at section 1		Normal force at section 2		Moment at section 3		Calculation time
	[mm]	Difference [%]	[kN]	Difference [%]	[kNm]	Difference [%]	[kN]	Difference [%]	[kNm]	Difference [%]	
500/500	378.6	-	296.7	-	193.9	-	59271.3	-	29035.5	-2.0	107
500/375	379.1	0.1	322.4	8.7	215.5	11.1	59220.0	-0.1	29305.0	0.9	184
500/250	379.2	0.0	319.2	-1.0	216.0	0.2	59119.0	-0.2	28635.4	-2.3	373
500/150	379.7	0.1	330.4	3.5	208.0	-3.7	59090.1	0.0	28614.1	-0.1	650
375/375	378.3	-0.4	324.3	1.8	217.3	4.5	59210.1	0.2	28847.2	0.8	652
375/250	378.7	0.1	319.8	-1.4	217.8	0.2	59195.6	0.0	28494.1	-1.2	811
375/150	x										
250/250	x										
250/150	x										
150/150	x										

The differences between 500/500 and 375/250 at section II, III and the top deflection are relatively small and this is comparable to the results of Table 34. The differences at section I are smaller than in Table 34, but this is caused by the smaller mesh sizes that have been examined (500/500 versus 1500). When the values of 500/250 and 375/250 in section I are compared, it can be concluded that the differences are less than 0.8%. In section II and III the differences are also relatively small: less than 0.5%. To obtain these slightly more accurate values, the calculation time increases with 117%.

Just as with Table 34 it can be observed that the values converge. Unfortunately, smaller mesh sizes couldn't be examined due to a memory problem. A second method to create a local reduced mesh size is to apply a smaller mesh at all the elements that contain openings. Compared to the previous method where only the lintels are given a smaller mesh, the amount of equations that have to be solved will increase. Therefore this method has not been examined.

C.2.3 Part 3: mesh size according to height

Commonly the largest forces occur in the lower section of the structure. To obtain accurate results at the three sections without a long calculation time, the wall is divided into two regions. The lower region has a height of 81.3m¹ (approximately 1/3rd of the structure height) and will be meshed with small elements. The top region has a height of 120.95m¹ and will be meshed with larger elements. This method should provide accurate values for the lower section and reduce the required memory. Due to the large mesh size in the top area of the structure, this method should not be used to design lintels or elements at that location. Locally reducing the mesh size around the considered element in the top section may circumvent this problem.

Results

Table 36 shows the result of the research on different mesh sizes over the height. The first value in column 1 represents the mesh size at the lower region and the second value represents the mesh size of the top region. Besides the results, the table also contains the relative difference with the previous calculated value.

Table 36 Results of the research on local different mesh sizes

Mesh size	Top deflection U _{max}		Shear force at section 1		Moment at section 1		Normal force at section 2		Moment at section 3		Calculation time
	[mm]	Difference [%]	[kN]	Difference [%]	[kNm]	Difference [%]	[kN]	Difference [%]	[kNm]	Difference [%]	
375/750	378.4	-	324.2	-	217.1	-	59212.9	-	28846.8	-	130
375/500	378.4	0.0	324.3	0.0	217.3	0.1	59210.4	0.0	28847.1	0.0	367
375/375	378.3	0.0	324.3	0.0	217.3	0.0	59210.1	0.0	28847.2	0.0	652
250/750	378.3	0.0	320.8	-1.1	218.9	0.7	59170.4	-0.1	28682.4	-0.6	680
250/500	378.3	0.0	321.0	0.1	219.0	0.0	59167.8	0.0	28682.8	0.0	913
250/250	x										
150/750	x										
150/500	x										
150/250	x										
150/150	x										

When all the results are compared, it can be concluded that there is almost no difference between a mesh size of 375/750 and 250/500. The only value that increases drastically is the calculation time: there is a difference of 600% between the smallest and largest mesh size. It can be concluded that the top section has nearly no influence on the bottom section and this has a positive effect on the results and calculation time. When the mesh results of 250/750 are compared with 250/500, the calculation time increases with 34% while the differences are less or equal than 0.1%.

C.2.4 Part 4: mesh size in a 3D structure

From the results of the previous sections it can be concluded that the mesh size according to the height provides the most accurate results with the shortest calculation time. This is important for the 3D model since the amount of equations that have to be solved will drastically increase compared to the 2D models.

The smallest mesh size that can be applied is 750mm at the bottom ($1/4^{\text{th}}$ of the building height) and 1500mm at the top ($3/4^{\text{th}}$ of the building height). But this mesh size is too large to provide accurate local results. Therefore the mesh size will be reduced to 250mm around the considered element. This method is applicable since the local distribution of forces is highly dependent on the mesh size while the global distribution of forces is only slightly dependant.

C.2.5 Conclusion

A small mesh size is the key to obtain accurate results, but a small mesh also increases the calculation time considerably. Therefore the results of different mesh sizes have been analysed in order to find a mesh size that results in accurate values combined with an acceptable calculation time.

In Table 37 the most accurate values of the first three parts are combined. With a mesh size according to the height the smallest mesh is obtained (250mm) at the cross-sections and the results can be considered as the most accurate values that can be calculated.

Table 37 Results of the research on local different mesh sizes

Mesh size	Top deflection U_{\max}		Shear force at section 1		Moment at section 1		Normal force at section 2		Moment at section 3		Calculation time
	[mm]	Difference [%]	[kN]	Difference [%]	[kNm]	Difference [%]	[kN]	Difference [%]	[kNm]	Difference [%]	
300	378.4	-	315.6	-	215.9	-	59186.2	-	28752.9	-	805
375/250	378.7	0.1	319.8	1.3	217.8	0.9	59195.6	0.0	28494.1	-0.9	811
250/500	378.3	-0.1	321.0	0.4	219.0	0.6	59167.8	0.0	28682.8	0.7	913

If it would be possible to calculate an even smaller mesh size in part 3 (for example 150/750), the values would probably still change relative to the 250/500 values. Due to the converging values of Table 36, it's estimated that these relative differences will be smaller than 1%. This difference may be positive or negative since there will always be a bandwidth around which the values will deviate. Unfortunately, it's impossible to calculate smaller mesh sizes due to a memory problem of AxisVM.

In part 3 it was already concluded that the results of 250/750 and 250/500 are nearly identical. Due to the reduced calculation time, a mesh size of 250mm at the bottom section ($1/3^{\text{rd}}$ of the height) and 750mm at the top section ($2/3^{\text{rd}}$ of the height) is recommended for all the calculations at the bottom of a 2D structure. If the forces in the top section have to be determined, the method of part 2 is recommended.

An entire structural wall was used for this analysis and the smallest mesh size which was examined was 250mm. A smaller mesh size couldn't be analysed because this resulted in a memory problem. Therefore it's unknown if the results converge even more at lower mesh values. Therefore it's recommended to perform the mesh analysis only on a section of the entire model. With these result, the optimal mesh size can be determined without any memory problems.

For the 3D structure, a mesh size of 250mm at the bottom and 750mm at the top is too small. Since the mesh size only has a small influence on the global distribution of forces, it's allowed to use a larger mesh size, for example 750mm at the bottom and 1500mm at

the top. By locally reducing the mesh size around the considered elements, it's still possible to achieve accurate results.

C.3 Determining the connection stiffness

The stiffness of the connections determines the behaviour of the entire structure. Therefore obtaining realistic values for the normal and shear stiffness is essential. In this section it's explained how the values are calculated.

C.3.1 Description of connection geometry

Before the connections stiffness can be determined, there must be consensus on the connection geometry. Therefore Figure 142 has been created.

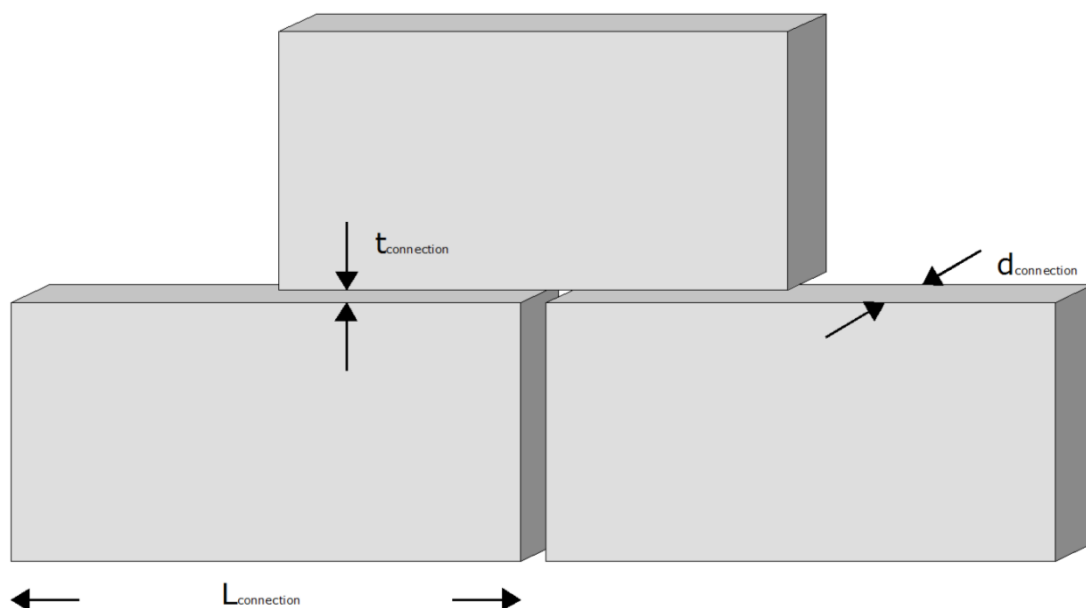


Figure 142 Connection geometry

There are three important parameters: the length, thickness and depth of the connection. These parameters will be used in the following sections

C.3.2 Normal stiffness of the horizontal connection k_y

The horizontal connection endures large forces in a high-rise building. To prevent local weaknesses, fluid or thixotropic mortar with a stiffness equal or higher than the surrounding concrete is often applied. Under compression, this should in theory result in a stiffness equal to the surrounding concrete. With this assumption, enclosed air bubbles (up to 3% with pump grouting) are neglected. Under tension, the stiffness is reduced considerably since all the forces are transferred by the reinforcement. As a result of the large dead load of the Zalmhaven tower, no tensile stress occurs in the horizontal connections and only compression is considered.

To calculate the normal stiffness of the horizontal connection, the following equations are used:

$$F = k \cdot \Delta L \quad (1) \quad \varepsilon = \Delta L / L \quad (2) \quad \sigma = \varepsilon \cdot E \quad (3) \quad F = \sigma \cdot A \quad (4)$$

They can be combined as following:

$$2 \text{ in } 3: \sigma = \frac{\Delta L \cdot E}{L} \Rightarrow \Delta L = \frac{\sigma \cdot L}{E} \quad (5)$$

$$5 \text{ in } 1: F = \frac{k \cdot \sigma \cdot L}{E} \quad (6)$$

$$4 \text{ in } 6: \sigma \cdot A = \frac{k \cdot \sigma \cdot L}{E} \quad (7)$$

Since σ isn't equal to 0, σ can be removed from equation 7. When equation 7 is rewritten, the following equation is obtained:

$$k = \frac{A \cdot E}{L} \quad [\text{N/mm}]$$

in which:

- k is the stiffness of the connection
- A is the considered area
- E is the Young's modulus of the mortar
- L is the thickness of the connection ($t_{\text{connection}}$ in Figure 142).

When the stiffness is determined for a certain area and a connection thickness of 1mm is taken into account the equation can be rewritten to:

$$k = \frac{A \cdot E}{L} = \frac{A \cdot E}{A \cdot 1} = E \quad [\text{N/mm}^3]$$

This stiffness of the connection is now identical to the Young's modulus of the mortar. When mortar with a Young's modulus equal or higher than the surrounding concrete is applied, the stiffness of the connection will be equal or higher than the surrounding concrete.

In AxisVM the stiffness is entered per meter, resulting in following equation:

$$k = \frac{A \cdot E}{L \cdot 1} \quad [\text{N/mm/m} = \text{kN/m/m}]$$

For the Young's modulus of the mortar the same value is used as the surrounding concrete: $E_{\text{uncracked}} = 29333 \text{ N/mm}^2$. The thickness of the connection is 20mm. As a result of a different wall thickness a different normal stiffness is obtained for the walls, shown in Table 38.

Table 38 Normal stiffness horizontal connection k_y

Wall thickness [mm]	A [mm ²]	E [N/mm ²]	L [mm]	K_x [kN/m/m]
400	400x1000	29333	20	$5.87 \cdot 10^8$
500	500x1000	29333	20	$7.33 \cdot 10^8$

The stiffness of the connection is based on a thickness of 20mm. The stiffness of the wall element is determined by AxisVM, based on the entered parameters (dimensions and material properties). But in AxisVM, the connection has no physical stiffness and therefore the stiffness of the wall element is based on a length of 3050 instead of 3030mm. As a result, the stiffness is slightly underestimated (by 0.65%). This can be explained by the following example.

The equation for serial springs is given by:

$$\frac{1}{k} = \frac{1}{k_1} + \frac{1}{k_2}$$

The three different values for the stiffness are:

$$k_1 = \frac{E \cdot A}{L} = \frac{29333 \cdot 500 \cdot 1000}{20} = 7.33 \cdot 10^8 \text{ [kN/m/m]}$$

$$k_2 = \frac{E \cdot A}{L} = \frac{29333 \cdot 500 \cdot 1000}{3030} = 4.84 \cdot 10^6 \text{ [kN/m/m]}$$

$$k_3 = \frac{E \cdot A}{L} = \frac{29333 \cdot 500 \cdot 1000}{3050} = 4.81 \cdot 10^6 \text{ [kN/m/m]}$$

$$\frac{1}{k_{\text{actual}}} = \frac{1}{k_1} + \frac{1}{k_2} = \frac{1}{7.33 \cdot 10^8} + \frac{1}{4.84 \cdot 10^6} = 2.08 \cdot 10^{-7} \text{ [1/kN/m/m]}$$

The total actual stiffness should be $k_{\text{actual}}=4.81 \cdot 10^6 \text{ kN/m/m}$ (equal to k_3), but in AxisVM the following is applied:

$$\frac{1}{k_{\text{AxisVM}}} = \frac{1}{k_1} + \frac{1}{k_3} = \frac{1}{7.33 \cdot 10^8} + \frac{1}{4.81 \cdot 10^6} = 2.09 \cdot 10^{-7} \text{ [1/kN/m/m]}$$

Resulting in $k_{\text{AxisVM}}=4.78 \cdot 10^6 \text{ kN/m/m}$, which is 0.65% smaller than the calculated stiffness. With an increasing connection thickness, this difference will become larger. This slightly lower value that is applied in AxisVM will not have a noticeable effect on the calculation results, since the stiffness is already considerably high. According to section 8.1.5, a high stiffness is insensitive to small changes. This conclusion is based on the shear stiffness, but it also holds for the normal stiffness.

C.3.3 Shear stiffness of the horizontal connection k_x

The shear stiffness is determined with the Eurocode NEN-EN 1992-1-1, section 6.2.5 and with a formula determined by Straman. First the shear resistance is calculated with the Eurocode:

$$V_{Rdi} = c f_{ctd} + \mu \sigma_n + \rho f_{yd} (\mu \sin(\alpha) + \cos(\alpha)) \leq 0,5 v f_{cd}$$

in which:

V_{Rdi}	is the design shear resistance at the interface
c and μ	are factors depending on the interface (for smooth: $c=0,2$ and $\mu=0,6$)
f_{ctd}	is the design tensile strength of the concrete
σ_n	is the minimum normal stress in the joint that can coincide with shear force, positive for pressure, whereby $\sigma_n < 0,6 f_{cd}$ and negative for tension. It's advised to use $c f_{ctd}=0$ when σ_n is in tension.
ρ	is the area of the protruding bars divided by the connection area: A_s/A_i
α	is the angle of the reinforcement (see Figure 54)
v	is the stiffness reduction factor:

$$v = 0,6 \left[1 - \frac{f_{ck}}{250} \right]$$

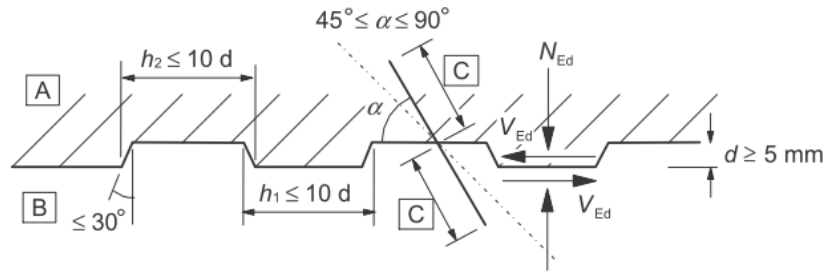


Figure 143 Shear resistance of a horizontal connection [NEN, 2011]

The first part of the shear resistance formula takes the adhesion into account. Because the concrete elements have a smooth surface, c^*f_{ctd} becomes equal to zero. The second part is responsible for the normal stress. In case the connection is loaded in tension, this value also becomes equal to zero. The third part is the contribution of the reinforcement.

When a connection is loaded in compression and contains starter bars at an angle of 90° , the formula can be rewritten as:

$$v_{Rdi} = \mu\sigma_n + \mu\rho f_{yd} \leq 0,5 v f_{cd}$$

The values that are still required are the normal stress, the reinforcement ratio, the steel quality and the design compression strength of the concrete. According to section 8.1, an iterative calculation isn't required for the variable normal force and a value of 20N/mm^2 may be applied. Two starter bars with a diameter of 25mm (B500B) are placed at a centre to centre distance of 400mm. Two starter bars are chosen because of the thickness of the walls. As a result, a reinforcement ratio of 0.49% is obtained. This value isn't very high since there is almost no tension in the cross-section (see section 9.2). With a concrete strength class of C90/105, a design compression strength of $f_{cd}=60\text{N/mm}^2$ is obtained. With these values the shear resistance is calculated:

$$v_{Rdi} = 0.6 \cdot 20 + 0.6 \cdot 0.0049 \cdot 435 = 12.00 + 1.28 = 13.28 < 0.5 \cdot 0.38 \cdot 60 = 11.52 \text{ [N/mm}^2\text{]}$$

The shear resistance is limited at 11.52N/mm^2 due to the shear limit. An interesting aspect is the ratio between reinforcement and compression: the reinforcement is less than 10% of the unlimited value. Now that the shear resistance is known, the shear stiffness can be calculated. The formula of Straman [Straman, 1988] states that there is a linear relation between the shear resistance and the deformation:

$$k_x = \frac{v_{R,di}}{\delta_x} \text{ [N/mm}^3\text{]}$$

In which:

- k_x is the shear stiffness
- $v_{R,di}$ is the shear resistance
- δ_x is the deformation, also known as slip.

Although this research was performed on vertical connections, the mechanism remains equal. Tests done in this research show that the connection will fail at a deformation of approximately 1mm. But according to Figure 144 the relation shouldn't be linear but bi-linear. At first, the mortar and concrete are still connected to each other and the stiffness is relatively high. At a certain deformation the connection is lost and the stiffness is reduced.

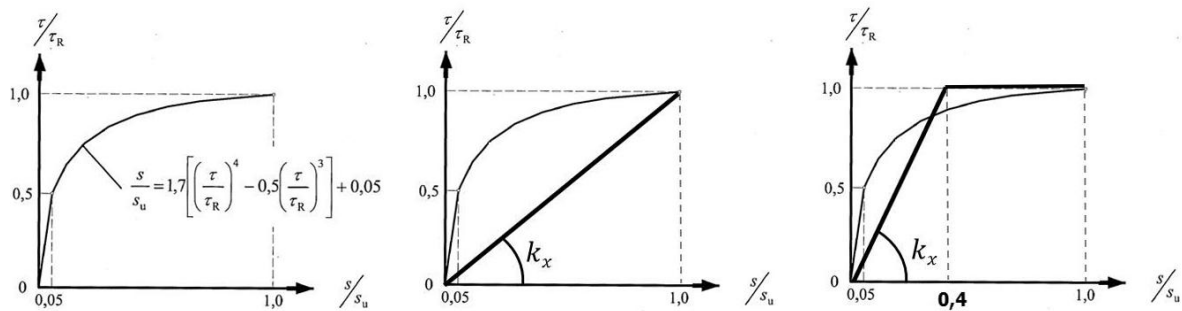


Figure 144 Relation between shear resistance and deformation [Keulen, 2012]

In consultation with two of the supervisors (Dr.ir.dr.s. C.R. Braam and Ir. D.C. van Keulen) this certain deformation is placed at $\delta_{x,1}=0.4\text{mm}$. At the moment there is no literature available that supports this assumption, but preliminary research shows that this assumption is reasonable.

The units of this shear stiffness are N/mm^3 . To go from N/mm^3 to kN/m/m , the stiffness has to be multiplied by the thickness to obtain N/mm^2 (or N/mm/mm). Subsequently the stiffness has to be multiplied by 10^3 to obtain kN/m/m . In Table 39 the results are shown for the two walls and the different slip value.

Table 39 Shear stiffness horizontal connection k_x

Wall thickness [mm]	Shear resistance V_{Rdi} [N/mm ²]	Shear stiffness k_x (s=1) [kN/m/m]	Shear stiffness k_x (s=0.4) [kN/m/m]
400	11.52	$4.61 \cdot 10^6$	$1.15 \cdot 10^7$
500	11.52	$5.76 \cdot 10^6$	$1.44 \cdot 10^7$

C.3.4 Normal stiffness of the connection between perpendicular walls

Just as the horizontal connection, the connection between perpendicular walls has a normal stiffness equal to the surrounding concrete under compression. In section 7.7 it is explained that the connection is modelled by a spring (kN/m). Therefore the values obtained in C.3.2 have to be multiplied by the connection length. The results are depicted in Table 40.

Table 40 Normal stiffness perpendicular connection under compression

Wall thickness [mm]	Normal stiffness k_y [kN/m/m]	Connection length [m]	Spring stiffness $k_{y,s,c}$ [kN/m]
400	$5.87 \cdot 10^8$	0.5	$2.93 \cdot 10^8$
500	$7.33 \cdot 10^8$	0.4	$2.93 \cdot 10^8$

When the connection is loaded by tension, which occurs only at the top of the perpendicular walls, the normal stiffness is reduced considerably. The distribution of forces is shown in Figure 145.

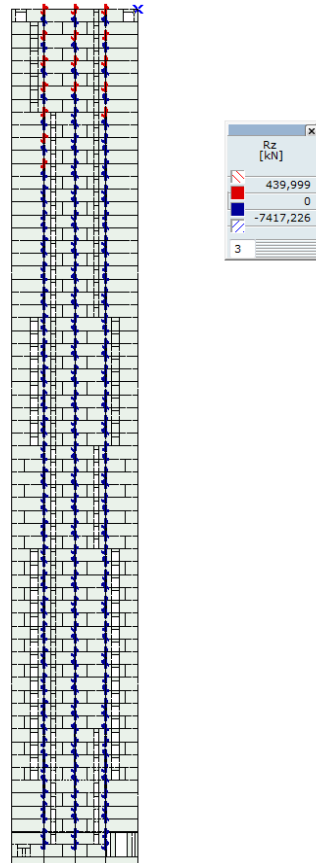


Figure 145 Distribution of forces in the perpendicular connections

To calculate the stiffness, fib Bulletin 43: "Structural connections for precast concrete buildings" is used. For this elaborate calculation, a calculation sheet of ingenieursstudio DCK is utilised which is slightly adapted, shown in Figure 146. According to this calculation, the stiffness is reduced to $k_{y,s,t}=4.01 \cdot 10^6 \text{ kN/m}$ (a reduction of 99%). This is noticeable lower than the values of Table 40. This tension stiffness is based on 16 bars with a diameter of 25mm.

Due to confidentiality, this figure cannot be displayed.

Figure 146 Calculation sheet tension stiffness [DCK, 2012]

C.3.5 Shear stiffness of the connection between perpendicular walls

Just as the normal stiffness of the previous section, the shear stiffness has to be multiplied by the connection length. For the shear stiffness under compression the results are shown in Table 41.

Table 41 Shear stiffness perpendicular connection under compression $k_{x,s,c}$

Wall thickness	Connection length	Wall shear stiffness $k_{x,w,c} (s=1)$	Wall shear stiffness $k_{x,w,c} (s=0.4)$	Spring shear stiffness $k_{x,s,c} (s=1)$	Spring shear stiffness $k_{x,s,c} (s=0.4)$
[mm]	[m]	[kN/m/m]	[kN/m/m]	[kN/m]	[kN/m]
400	0.5	$4.61 \cdot 10^6$	$1.15 \cdot 10^7$	$2.30 \cdot 10^6$	$5.76 \cdot 10^6$
500	0.4	$5.76 \cdot 10^6$	$1.44 \cdot 10^7$	$2.30 \cdot 10^6$	$5.76 \cdot 10^6$

When the connection between the perpendicular walls is loaded by tension, the shear stiffness is reduced. According to section C.3.3 only the reinforcement resistance remains. Due to the large reinforcement ratio (3.9%), the shear stiffness decreases only with 11%. The results of the calculation are shown in Table 42.

Table 42 Shear stiffness perpendicular connection under tension $k_{x,s,t}$

Wall thickness	Shear resistance V_{Rdi}	Wall shear stiffness $k_{x,s,t}$ (s=1)	Wall shear stiffness $k_{x,s,t}$ (s=0.4)	Spring shear stiffness $k_{x,s,t}$ (s=1)	Spring shear stiffness $k_{x,s,t}$ (s=0.4)
[mm]	[N/mm ²]	[kN/m/m]	[kN/m/m]	[kN/m]	[kN/m]
400	10.25	$4.10 \cdot 10^6$	$1.02 \cdot 10^7$	$2.05 \cdot 10^6$	$5.20 \cdot 10^6$
500	10.25	$5.12 \cdot 10^6$	$1.28 \cdot 10^7$	$2.05 \cdot 10^6$	$5.10 \cdot 10^6$

Appendix D: Influence of the connection properties

In chapter 8 the influence of the connection and element properties is discussed. The analysis of the horizontal and vertical connection are based on multiple models and the total analysis is provided in this appendix.

Section D.1 examines the influence of the shear stiffness of the horizontal connection and section D.2 considers the influence of the vertical connection.

D.1 The influence of the shear stiffness of the horizontal connection

The shear stiffness of the horizontal connection depends on the concrete strength class, reinforcement ratio and normal stress (see section 7.8.3). The first two aspects are considered constant over the building height, but the normal stress deviates over the building height and width. Since no variable stiffness can be entered in the FEM program, the values have to be entered manually with an iterative process. In this section it will be examined if this is required. However, first the influence of the shear stiffness on the total structure will be analysed by investigating five models with a different shear stiffness in part 1. The iterative method is examined in part 2.

D.1.1 Model scheme of the investigation part 1

The investigation starts with modelling five walls with a different constant shear stiffness value over the height. Based on these five walls, the preliminary influence of the stiffness can be determined. Consequently a sixth wall will be modelled with the actual shear stiffness values via an iterative process. The results of this wall will be compared with the other five walls.

For this investigation wall 4 is used with openings. To obtain accurate values, a small mesh size is required. In section 7.6 it's shown that a mesh size of 250mm in the first 81.3m (approximately 1/3rd of the building height) and 750mm in the remaining 120.95m results in accurate values while the calculation time remains acceptable.

The five structures are clamped at the foundation ($R_x=R_z=1*10^7$ kN/m/m and $R_y=0$ kN/m/m) and a 2D calculation with membrane elements is used in the X-Z plane. Concrete class C90/105 is used with $E_x=E_y=29333$ N/mm² (the concrete is uncracked due to the high dead load of the structure). For the lintels a Young's modulus of $E_x=E_y=14667$ N/mm² is used since it's very likely that the lintels are cracked.

The shear stiffness of the first wall is $k_x=6.41*10^5$ kN/m/m. This value is based on a normal stress of 0N/mm², a slip value of $s=1.0$ mm and a reinforcement ratio of $\rho=0.0049$ (two bars of $\Phi 25-400$). The second wall is modelled with a shear stiffness of $k_x=2.14*10^6$ kN/m/m, based on a normal stress of 5 N/mm². At the third wall a normal stress of 10N/mm² is used to obtain a stiffness of $k_x=3.64*10^6$ kN/m/m. The fourth structure has a stiffness of $5.76*10^6$ kN/m/m, induced by a normal stress of 20N/mm². Actually, a normal stress of 20N/mm² should result in a shear stiffness of $6.64*10^6$ kN/m/m, but the calculation value of the shear stiffness is limited at 11.52N/mm² ($0.5*v*f_{cd}$). The used stiffness of $5.76*10^6$ kN/m/m represents a normal stress of 17N/mm². For the normal stiffness of the four walls $k_y=7.33*10^8$ kN/m/m is used, representing the stiffness of the surrounding concrete. The fifth wall is modelled as a monolithic wall and has no interface elements. The stiffness values are combined in Table 43.

Table 43 Parameters for the shear stiffness investigation

Wall number	Shear stiffness	Normal stiffness	Young's modulus	Slip value	Representative normal stress
	[kN/m/m]	[kN/m/m]	[N/mm ²]	[mm]	[N/mm ²]
1 (low)	6.41*10 ⁵	7.33*10 ⁸	29333	1.0	0
2 (medium low)	2.14*10 ⁶	7.33*10 ⁸	29333	1.0	5
3 (medium high)	3.64*10 ⁶	7.33*10 ⁸	29333	1.0	10
4 (high)	5.76*10 ⁶	7.33*10 ⁸	29333	1.0	20*
5 (monolithic)	-	-	29333	-	-

* This value is limited at 17N/mm² due to a shear limit.

The section forces are calculated with a deformation value of 1mm. The top deflections are calculated with a deformation value of $\delta=0.4\text{mm}$, resulting in shear stiffness values that are a factor 2.5 higher than the values of Table 12 (see section 7.8.3).

The five structures are loaded by dead load and a non-uniform wind load (the wind load increases with the building height) as described in 5.2 and 5.3. The differences between the walls will be determined by three sections and the top deflection. The considered sections are shown in Figure 147 and they are located at the sixth floor. The sixth floor is chosen because of the intersections at the lower floors. It should be noted that there may be sections with higher forces and that the current three sections are only chosen for comparison purposes. In section I, the shear force and moments will be considered, in section II the normal force and in section III the moments. These three locations on the sixth floor are chosen because they often contain the largest forces at that level.



Figure 147 Location of the sections

D.1.2 Results of part 1

In Table 44 the results are shown of the different shear stiffnesses. The location of the three sections can be found in Figure 147. Besides the calculated values, the table also contains the relative difference with the previous calculated value.

Table 44 Section results of the investigation on different shear stiffnesses of part 1

Wall number	Top deflection U_{max}		Shear force at section 1		Moment at section 1		Normal force at section 2		Moment at section 3	
	[mm]	[%]	[kN]	[%]	[kN/m]	[%]	[kN]	[%]	[kN/m]	[%]
1 (low)	409.463	-	317.574	-	236,223	-	59196,370	-	26007,110	-
2 (medium low)	395.849	-3.3	322.450	1.5	221.497	-6.2	59128.640	-0.1	27045.870	4.0
3 (medium high)	393,238	-0.7	323,848	0.4	219,247	-1.0	59123,020	0.0	27298,610	0.9
4 (high)	391.521	-0.4	324.658	0.3	218,164	-0.5	59123.980	0.0	27438.370	0.5
5 (monolithic)	351.476	-10.2	274.209	-15.5	174.185	-20.2	58977.220	-0.2	27783.000	1.3

Besides the section forces, the maximum and minimum shear and normal stresses have been determined in Table 45. The stresses have been determined in the horizontal connection at the same level as section 2 and 3.

Table 45 Normal and shear stress results of the investigation on different shear stiffnesses of part 1

Wall number	Maximum normal stress* $\sigma_{hor,max}$		Minimum normal stress $\sigma_{hor,min}$		Maximum shear stress $T_{hor,max}$		Minimum shear stress $T_{hor,min}$	
	[N/mm ²]	[%]	[N/mm ²]	[%]	[N/mm ²]	[%]	[N/mm ²]	[%]
1 (low)	-5.66	-	-29.95	-	4.09	-	-4.48	-
2 (medium low)	-5.72	1.1	-29.15	-2.7	4.42	8.1	-4.55	1.6
3 (medium high)	-5.77	0.9	-28.93	-0.8	4.51	2.0	-4.64	2.0
4 (high)	-5.79	0.3	-28.79	-0.5	4.58	1.6	-4.73	1.9
5 (monolithic)	-6.27	8.3	-28.54	-0.9	5.49	19.9	-6.39	35.1

* At the lintels a small tension stress occurs, but this value is not taken into consideration because there is no vertical connection above the lintel.

From Table 12 it can be noticed that there is a large difference in stiffness between 0 and 5N/mm² of normal stress. This deviation results in a relative larger difference in Table 44 and Table 45 at wall 2. Besides this, a decreasing trend can be seen at all the values in Table 44 and Table 45: as the shear stiffness becomes higher, the results converge (wall 5 excluded). This phenomenon was also observed by Falger during his research on different connections [Falger, 2003, p86]. Increasing the shear stiffness of the horizontal connection has more effect when the current shear stiffness is relatively low.

Table 45 contains negative values at the minimum shear column. Normally there would only be positive shear values, but the openings in the wall create local negative areas. This phenomenon is discussed in more detail in section 9.1. In this table it can also be observed that a lower shear stiffness results in large values for the maximum normal stress and smaller values for the shear stress. This can be explained as following: due to the smaller shear resistance the bending resistance becomes more important and the bending forces increase, resulting in larger values for the normal stresses at the outer fibre.

Table 44 and Table 45 also show that there is a large difference between a precast wall with a high stiffness and a monolithic wall. In Table 44 the largest deviations can be found at the top deflection and at section 1 (the lintel). When wall 5 and 6 are compared on a larger scale, it can be concluded that generally the lintels endure larger forces in a precast structure than in a monolithic structure. When Table 45 is considered, the largest differences can be found at the shear stress.

Now that the walls have been modelled with a constant shear stiffness, it can be concluded that there is little difference between a medium low and high shear resistance of the horizontal connection. But what happens when the shear stiffness deviates over the building height and width?

D.1.3 Model scheme of the investigation part 2

To answer the question of the previous paragraph, the same model scheme will be used as in part 1, but now the shear stiffness will be related to the normal stress. To achieve this, the connection (one entire concrete element) will be placed in a class depending on the normal stress. Per wall element the average normal stress is determined and consequently placed in the associated class. The error that is made by placing the entire wall elements in a specific class is relatively small since the average normal stress is used (the higher normal stress resulting in a higher shear stiffness on one side of the element compensates the lower shear stiffness on the other side). The different normal stress classes can be found in Table 46. The interval between 0 and 10N/mm² is divided into two classes because the results change faster at low shear stiffness values.

Table 46 Normal classes for part 2

Average normal stress σ_{aver} [N/mm ²]	Calculation value normal stress σ_{calc} [N/mm ²]	Shear stiffness k_x [N/mm ²]
0-5	2.5	1.39*10 ⁶
>5-10	7.5	2.89*10 ⁶
>10-20	15	5.14*10 ⁶
>20-30	25*	5.76*10 ⁶ **

* This value is limited at 17N/mm² due to a shear limit.

** Maximum shear stiffness due to shear limit at 17N/mm².

D.1.4 Results of part 2

In Table 47 the results are shown of the different shear stiffnesses. Next to every result the relative difference with the previous calculated result is provided.

Table 47 Section results of the investigation on different shear stiffnesses at level 6, part 2

Wall number	Top deflection U_{max}		Shear force at section 1		Moment at section 1		Normal force at section 2		Moment at section 3	
	[mm]	[%]	[kN]	[%]	[kN/m]	[%]	[kN]	[%]	[kN/m]	[%]
1 (low)	409.463	-	317.574	-	236,223	-	59196,370	-	26007,110	-
2 (medium low)	395.849	-3.3	322.450	1.5	221.497	-6.2	59128.640	-0.1	27045.870	4.0
3 (medium high)	393,238	-0.7	323,848	0.4	219,247	-1.0	59123,020	0.0	27298,610	0.9
6 (depending on σ)	393,251	0.0	328,809	1.5	222,059	1.3	59139,710	0.0	27391,100	0.3
4 (high)	391.521	-0.4	324.658	-1.3	218,164	-1.8	59123.980	0.0	27438.370	0.2
5 (monolithic)	351.476	-10.2	274.209	-15.5	174.185	-20.2	58977.220	-0.2	27783.000	1.3

Besides the section forces, the maximum and minimum shear and normal stresses have been determined in Table 48. The stresses have been determined in the horizontal connection at the same level as section 2 and 3.

Table 48 Normal and shear stress results of the investigation on different shear stiffnesses at level 6, part 2

Wall number	Maximum normal stress* $\sigma_{hor,max}$		Minimum normal stress $\sigma_{hor,min}$		Maximum shear stress $T_{hor,max}$		Minimum shear stress $T_{hor,min}$	
	[N/mm ²]	[%]	[N/mm ²]	[%]	[N/mm ²]	[%]	[N/mm ²]	[%]
1 (low)	-5.66	-	-29.95	-	4.09	-	-4.48	-
2 (medium low)	-5.72	1.1	-29.15	-2.7	4.42	8.1	-4.55	1.6
3 (medium high)	-5.77	0.9	-28.93	-0.8	4.51	2.0	-4.64	2.0
6 (depending on σ)	-5.77	0.0	-28.84	-0.3	4.56	1.1	-4.69	1.1
4 (high)	-5.79	0.3	-28.79	-0.2	4.58	0.4	-4.73	0.9
5 (monolithic)	-6.27	8.3	-28.54	-0.9	5.49	19.9	-6.39	35.1

When Table 47 is studied in detail, it can be observed that the values of wall 6 with a stiffness that depends on the normal stress are nearly equal to wall 3 and 4. At the top deflection, section 2 and 3 the differences is always smaller than 0.4%. At section 1 (the

intel) the difference is slightly larger, but never bigger than 1.8% (local differences smaller than 2% are considered to be acceptable). In Table 48 the normal and shear stresses are depicted and here wall 6 always remains between the values of wall 3 and 4. The maximum error is 1.1 or 0.9%, depending on which wall it is compared with. A shear stiffness between that of wall 3 and 4 will probably approach results of wall 6.

The results of Table 47 and Table 48 are determined at the sixth floor. Are the values of wall 6 still located within that of wall 3 and 4 if a different location is examined? To answer this question the section forces, normal stress and shear stress have been determined again at the twenty-sixth floor (still within the mesh zone of 250mm). The results are shown in Table 49 and Table 50.

Table 49 Section results of the investigation on different shear stiffnesses at level 26, part 2

Wall number	Top deflection U_{max}		Shear force at section 1		Moment at section 1		Normal force at section 2		Moment at section 3	
	[mm]	[%]	[kN]	[%]	[kN/m]	[%]	[kN]	[%]	[kN/m]	[%]
3 (medium high)	393,238	-	442,262	-	353,492	-	44399,110	-	28511,820	-
6 (depending on σ)	393,251	0.0	439,926	-0,5	351,462	-0,6	44416,300	0,0	28428,400	-0,3
4 (high)	391.521	-0.4	441,153	0,3	352,703	0,4	44404,660	0,0	28324,060	-0,4

Table 50 Normal and shear stress results of the investigation on different shear stiffnesses at level 26, part 2

Wall number	Maximum normal stress* $\sigma_{hor,max}$		Minimum normal stress $\sigma_{hor,min}$		Maximum shear stress $\tau_{hor,max}$		Minimum shear stress $\tau_{hor,min}$	
	[N/mm ²]	[%]	[N/mm ²]	[%]	[N/mm ²]	[%]	[N/mm ²]	[%]
3 (medium high)	-7,16	-	-21,39	-	3,13	-	-2,56	-
6 (depending on σ)	-7,15	-0,1	-21,41	0,1	3,14	0,3	-2,51	-2,0
4 (high)	-7,17	0,3	-21,40	0,0	3,15	0,3	-2,48	-1,2

Compared to Table 47, the differences between the values have decreased in Table 49. The maximum difference is -0.6% between wall 3 and 6 at section 1. In Table 50 all the differences, except the minimum shear stress, have decreased compared to Table 48. The maximum difference is -2.0% between wall 3 and 6. It can be concluded that the location has nearly no influence on the difference between wall 3, 4 and 6. The differences have even become smaller. This can be explained by the fact that the tension and compression stresses are larger near the bottom of the structure. A large difference between tension and compression results in more different load classes, making it more susceptible to differences.

When all the result are considered, it can be concluded that there are differences between a wall with a constant shear stiffness and a wall with a shear stiffness that depends on the normal force. These differences are relatively small ($\leq 2.0\%$) and the results of a wall with a constant shear stiffness are acceptable. Therefore the elaborated iterative method to design a wall with a normal stress dependent shear stiffness is not required.

D.2 The influence of the vertical open joint

The vertical connection plays an important role in the stiffness of traditional precast buildings. Since a masonry configuration is utilised, the vertical connection may be left open, reducing the amount of connections which have to be made. But what is the effect of this vertical open joint with respect to the deflections and distribution of forces?

To answer this question, multiple models will be analysed. First three closed 2D walls will be examined to understand the distribution of forces:

1. a closed 2D wall with an open vertical joint,
2. a closed 2D wall containing a vertical connection with a high stiffness,
3. a closed 2D monolithic wall.

Consequently, the openings will be added to the three walls. Based on the results, it will be determined whether or not the open vertical joint will be used structurally.

D.2.1 Model scheme

For the first three models wall 4 is used without any openings (see section 4.3.1). By removing the openings, disruptions created by the openings are prevented, resulting in the actual behaviour of the vertical open joint. For the last three models also wall 4 is chosen and the openings are maintained to obtain the actual behaviour.

The mesh size for the six models is dependent on the building height: at the bottom a mesh size of 250mm will be used and at the top 750mm. In section 7.6 it was determined that this size provides accurate results with an acceptable calculation time.

The six structures are clamped at the foundation ($R_x=R_z=1*10^7$ kN/m/m and $R_y=0$ kN/m/m) and a 2D calculation with membrane elements is used in the X-Z plane (hence $R_y=0$ kN/m/m). Concrete class C90/105 is used with $E_x=E_y=29333$ N/mm² in the three closed models. This concrete class is also applied at the three models with openings, but due to the large forces in the lintels, the Young's modulus has been reduced in the lintels to $E_x=E_y=14667$ N/mm². The normal and shear stiffness is equal for all the models (except the monolithic model, which is modelled without interface elements, see section 7.5): $k_y=7.33*10^8$ kN/m and $k_x=5.76*10^6$ kN/m (see section 7.8.2 and 7.8.3). The stiffness of the vertical connection is discussed in the following section. All the models are loaded by a non-uniform wind load (the wind load increases with the building height) and dead load as described in 5.2 and 5.3.

To compare the models, local and global results will be examined. The top deflection and shear distribution provide the global results. Locally the moment, shear and normal force of several critical sections will be examined and compared. In Figure 148 the location of the sections in the closed wall are shown. The location of the sections in the wall with openings is identical to Figure 147.

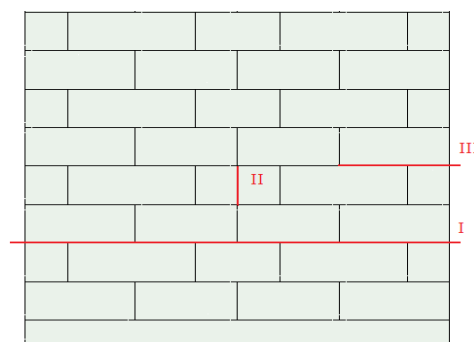


Figure 148 Location of the sections at the closed walls

D.2.2 Stiffness of the vertical connection

To determine the stiffness of the vertical connection, it must first be known if the connection is under compression or tension. One might expect that wind load on the facade will result in compression in all the vertical connections, but due to the load

introduction of the floors, a different phenomenon occurs. In the monolithic model of Figure 149, it can clearly be seen that the left hand side of the neutral axis is under compression while the right hand side is under tension. This is unexpected, but a 3D control model in which the floors are modelled shows approximately the same distribution, see Figure 150⁴⁵. In the precast model of Figure 149, the division between tension and compression is less easy to distinguish. Therefore it's very difficult to model the exact behaviour of all connections.



Figure 149 Load introduction of the floors in a precast (left) and monolithic (right) 2D model

⁴⁵ In this control model the neutral line is slightly shifted to the right because of the force coefficient of the wind load (wind pressure and suction).

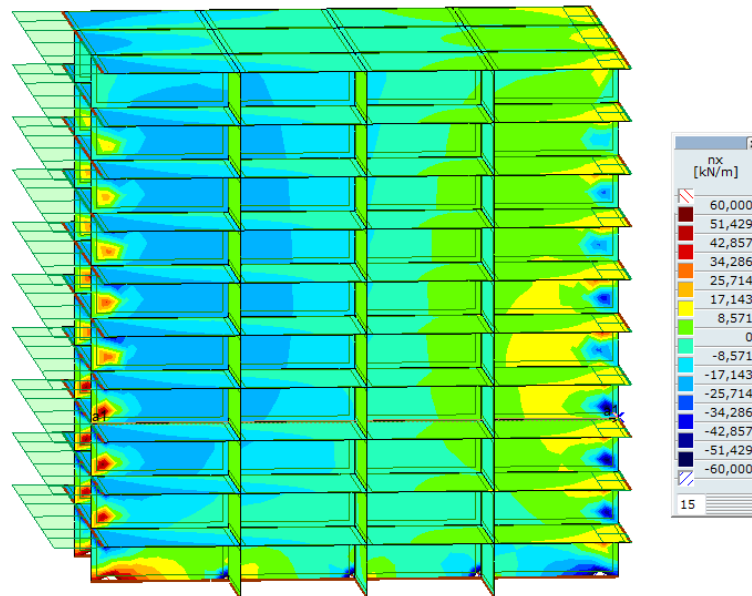


Figure 150 Load introduction of the floors in a 3D control model

To resolve this problem, an extreme case has been used for the stiffness of the vertical connections: it's assumed that all the vertical connections are loaded with a large compression force. According to the results of this extreme case, an upper boundary can be formed (under tension the stiffness will be lower). Therefore the actual behaviour will always be more moderate.

With a large compression force, the vertical connection obtains a normal stiffness equal to the surrounding concrete: $k_y = 7.33 \cdot 10^9 \text{ kN/m}$ and a shear stiffness of $k_x = 5.76 \cdot 10^6 \text{ kN/m}$ (see section 7.8.2 and 7.8.3).

D.2.3 Results of the closed 2D walls

In Table 51 the results are shown of three walls with a different stiffness for the vertical connection. The location of the three sections can be found in Figure 148. Besides the calculated values, the table also contains the relative difference with the previous calculated value.

Table 51 Global and local section results of different vertical connections at the closed wall

Properties vertical connection	Top deflection U_{\max}		Moment at section 1		shear force at section 2		Normal force at section 3	
	[mm]	[%]	[kNm]	[%]	[kN]	[%]	[kN]	[%]
1: Open joint	260.193		722119,6		1766,531		27488,21	
2: High stiffness	258.121	-0.80	721886,3	-0,03	1322,164	-25,15	27685,27	0,72
3: Monolithic	253.944	-1.62	722302,4	0,06	1106,522	-16,31	27820,56	0,49

Table 51 shows that the high stiffness of the second model only reduces the deflection slightly. Since this is an upper boundary value, the difference will be even smaller. The moments at section 1 and the normal force at section 3 also change very little. At section 2, a large reduction of shear force is visible. This can be explained by the fact that the second model and the monolithic model are capable of transporting shear force via the vertical connection. As a result, the shear force is reduced in the elements above and below the vertical connection. This phenomenon is depicted in Figure 151.

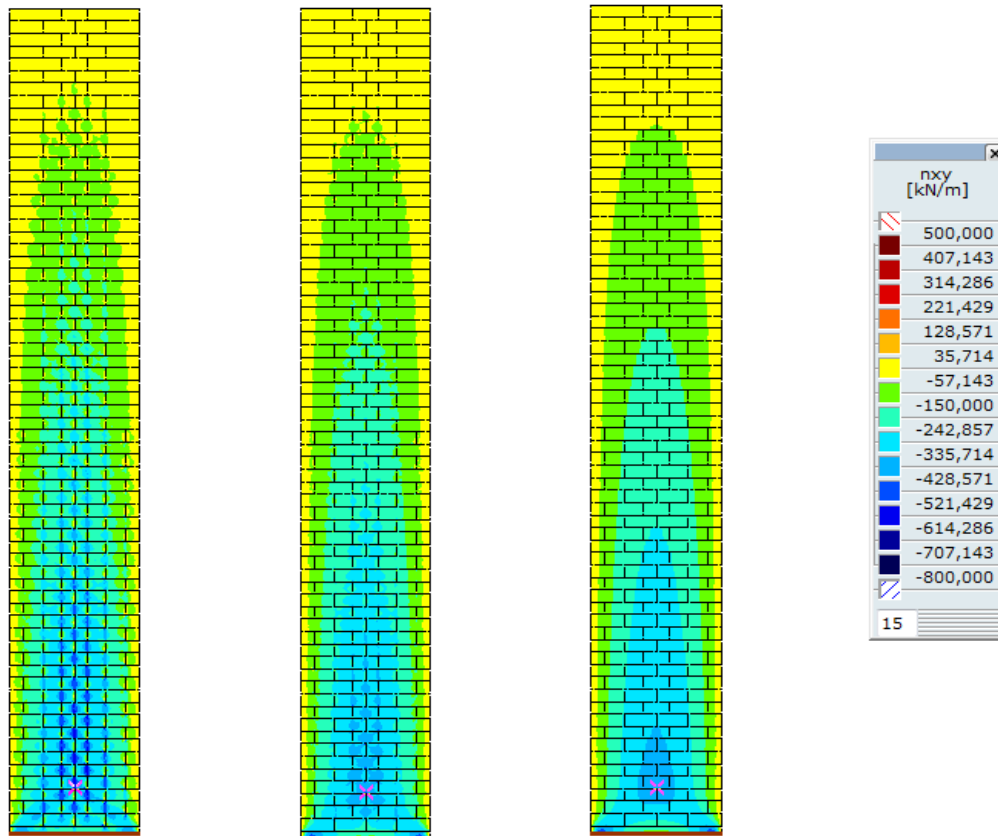


Figure 151 Distribution of shear force in model 1 (left), model 2 (centre) and model 3 (right)

The increase of shear force due to the vertical open joint is clearly visible in model 1 of Figure 151. The second model with a high stiffness still shows a slight increase around the vertical connections, but it's considerable less than the first model. Since this is an upper boundary limit, the reduction of shear force will be less in the actual model. In the third (monolithic) model, the distribution of shear force isn't affected by the vertical joint.

Based on the three models it can be concluded that the vertical connection has nearly no influence on the stiffness and the distribution of normal force and moments. Though, by using the connection structurally, the shear force may be reduced up to 25%.

An interesting aspect is the difference in top deflection between the three models without openings: the precast wall with open vertical joint only deflects 2.5% more than the monolithic wall (see Table 51). When the deflections of the wall with openings are considered (see Table 52), it can be observed that the deflection increases to 13%. This difference in deflection between the closed wall and wall with openings can be explained by the behaviour of the wall on the openings. By adding openings, the distribution between shear and bending and also the internal flow of forces changes (see section 9.1).

The results of the monolithic wall differ considerably from that of the two other models due to the monolithic properties. It can be stated that the monolithic schematisation will result in non-realistic results when used for a precast structure.

D.2.4 Results of the 2D walls with openings

In Table 52 the results are shown of three walls with openings and a different stiffness for the vertical connection. The location of the three sections can be found in Figure 147 Location of the sections.

Table 52 Global and local section results of different vertical connections at the wall with openings

Properties vertical connection	Top deflection U_{\max}		Shear force at section 1		Moment at section 1		Normal force at section 2		Moment at section 3	
	[mm]	[%]	[kN]	[%]	[kNm]	[%]	[kN]	[%]	[kNm]	[%]
Open joint	361,772		323,067		215,400		59213,09		29083,15	
High stiffness	359,158	-0,72	276,425	-14,44	185,871	-13,71	59140,56	-0,12	28963,06	-0,41
Monolithic	319,588	-11,02	274,209	-0,80	174,185	-6,29	59202,80	0,11	29279,67	1,09

The results in Table 52 show that when the openings are included, the small differences between model 1 and 2 encountered in the previous section remain. It can be stated that with or without openings the vertical connection has nearly no influence on the top deflection, normal force at section 2 and the moment at section 3. The shear force and moment in section 1 (the lintel) remain considerably high. This difference can be explained by the shear force distribution: the shear force has to be transported around the open vertical joint into the dowel elements. Because of the open vertical joint the structural area is locally reduced by 50% and the dowel elements absorb up to 25% more shear force. The distribution of shear forces is shown in Figure 152 and when compared to Figure 151 many disruptions can be distinguished. In section 9.1 the cause of these differences will be examined in more detail.

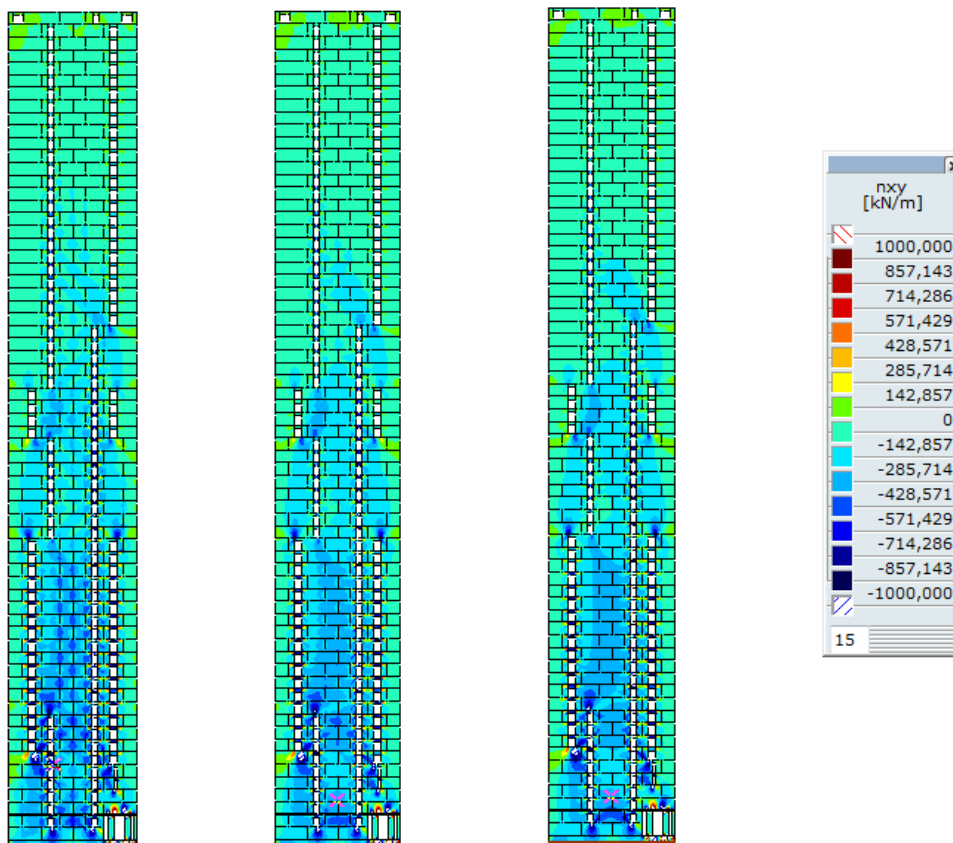


Figure 152 Distribution of shear force in model 1 (left), model 2 (centre) and model 3 (right) with openings

Based on the results it can be concluded that the behaviour of the vertical connection in the three walls with openings remains identical to the walls without openings. The vertical connection has nearly no influence on the stiffness, normal force and moments of the walls. The only aspect which is influenced is the distribution of shear force.

Appendix E: Results of the FEM analysis

In this appendix the complete results of the FEM analysis are provided, corresponding to chapter 9.

E.1 Distribution of forces

One of the main functions of the stability structure is to transport the present forces to the foundation. This can be live or dead load. But how do these forces flow through the structure? This section will start with a simplified 2D wall. This wall will then be extended with openings and re-examined. Finally, the 3D structure will be investigated. The level of detail is slowly increased to be able to understand the effects.

E.1.1 Model scheme

In Figure 153 normal (n_y) and shear (n_{xy}) force are shown due to wind load in the x-z plane. The normal force is calculated in the local y-direction and this corresponds with the global z-direction (vertical). The shear force is calculated in the local x-direction which corresponds with the global x-direction (horizontal). The layout of Figure 153 is based on wall 4 without any openings (wall 4 is discussed in section 4.3.2). Table 53 shows the parameters that are used for the connections of the precast structure.

Table 53 Connection parameters for the precast structure

Connection type	Shear stiffness K_x [kN/m/m]	Normal stiffness k_y [kN/m/m]
Horizontal connection	$5.76 \cdot 10^6$	$7.33 \cdot 10^8$
Vertical connection	0	0

The normal stiffness is equal to the surrounding concrete (C90/105) and the shear stiffness is based on a slip of 1mm and an average stress of 25N/mm^2 (see section 7.8 for more details on the stiffness calculations). The monolithic structure is based on the same wall, but the interface elements are removed. In section 7.5 it was determined that using multiple domains for a monolithic structure has nearly no influence on the results. The wind load is placed in the positive x-direction (from left to right) and the forces are equivalent to the values calculated in section 5.3. The dead load of the structure and the live floor load is obtained from section 5.2 and placed at every floor. In all the calculations a mesh size of 250mm is used for the bottom and 750mm for the top section (see section 7.6), unless a different size is specified.

To examine the distribution of forces, eight different models will be analysed. From the eight models, the first model contains a 2D precast wall without openings. The second model contains the same 2D precast wall, but now the openings are added. The third and fourth model are identical to the first two models, except that they're modelled in 3D. The remaining four models are identical to the first four models, but now monolithic properties have been applied (the interface elements are removed).

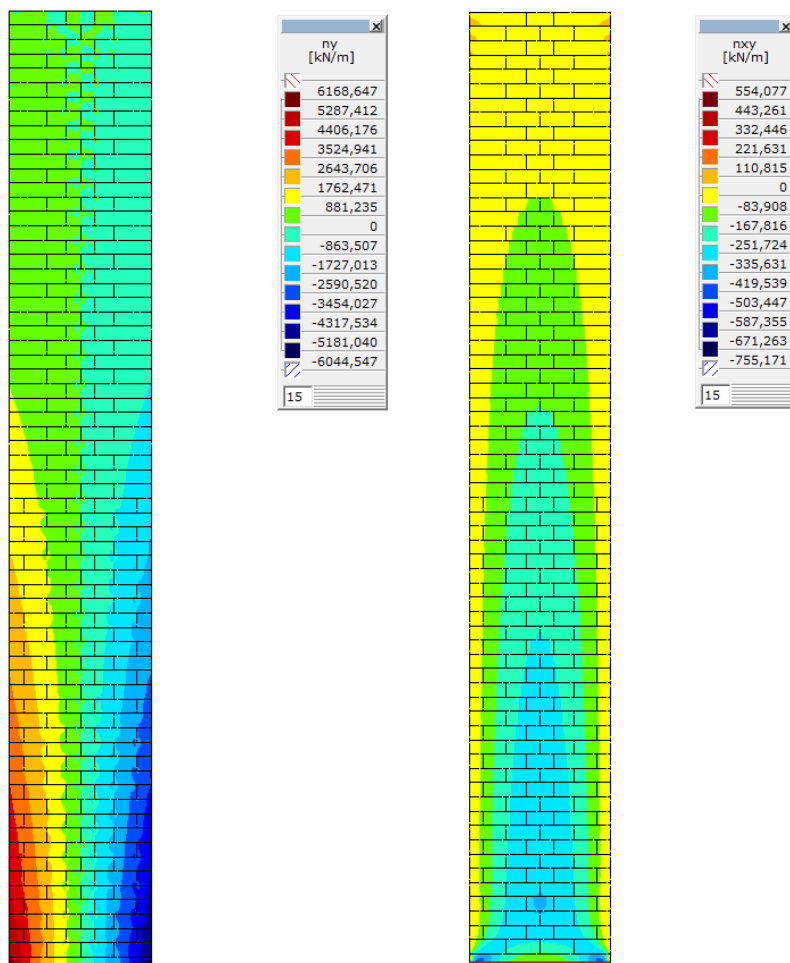


Figure 153 Normal (left) and shear (right) force due to wind load

E.1.2 Normal force in the simplified 2D wall

In Figure 154 the normal force in a precast and monolithic structure are depicted due to wind load. On a global scale, the normal force of a precast structure is comparable to a monolithic structure, but slight deviations can be seen at the bottom of the precast structure.

The monolithic structure still contains separate domains, but the interface elements are removed from the structure. A monolithic structure should actually be constructed out of one domain, but then it would be difficult to place the loads. In section 7.5 it was determined that multiple domains have a negligible effect on the results of a monolithic structure.

The red colour in Figure 154 represents tension and the blue colour compression. The distribution of forces is comparable to what one would expect when a clamped beam is loaded with a more or less uniform load (the wind load increases over the height). It should be noted that Figure 154 doesn't represent an actual load case since there is only wind load and no dead load. When tension does occur in a load case, the stiffness will decrease considerably.

When a smaller area is considered, the normal force for a precast structure slightly deviates from that of a monolithic structure, as can be seen in Figure 155.

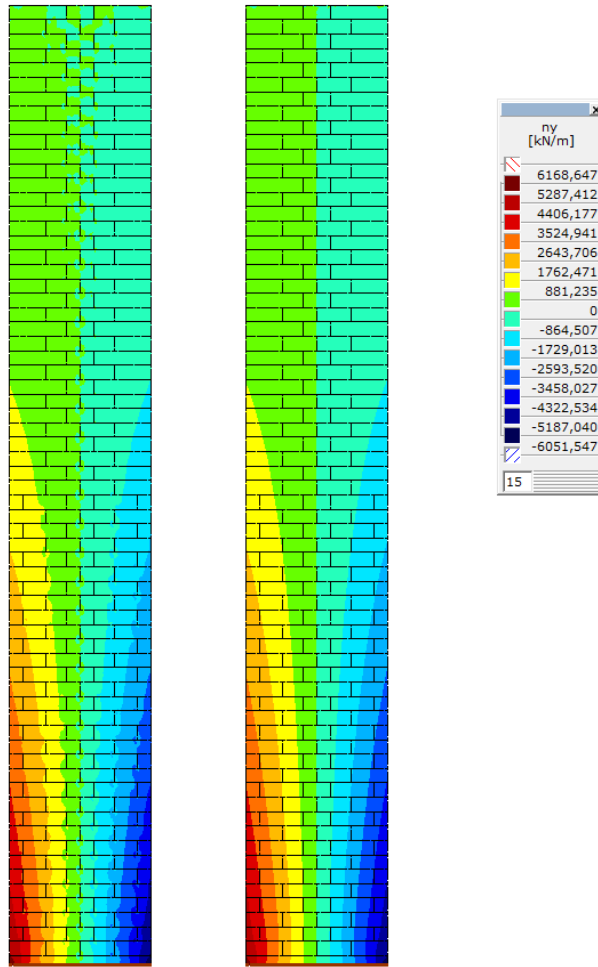


Figure 154 Normal force in the simplified precast (left) and monolithic (right) model

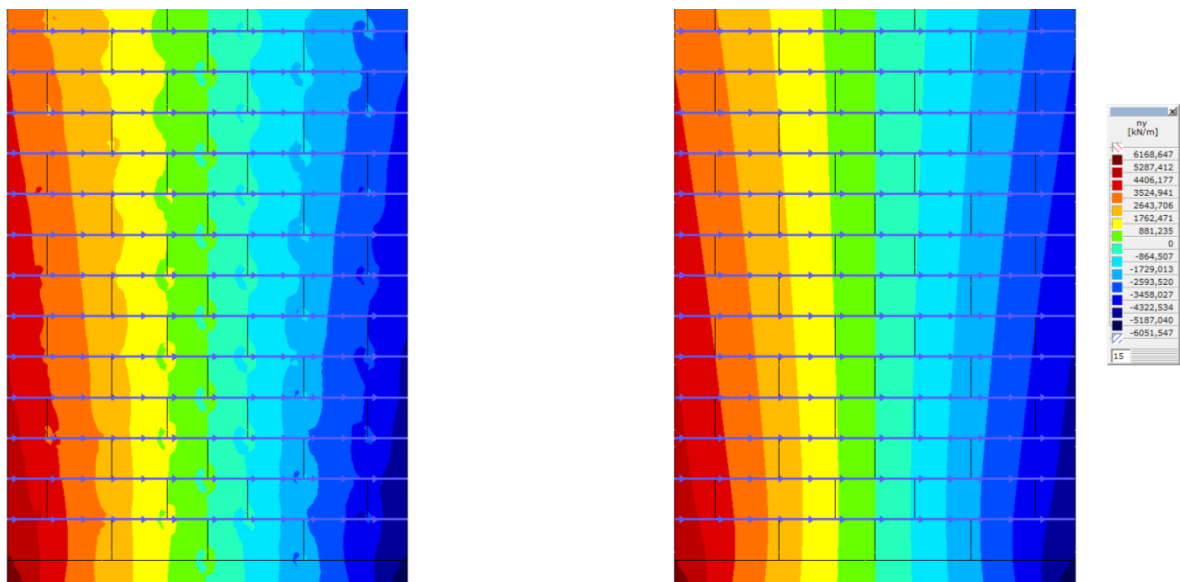


Figure 155 Detailed view of the normal force in the simplified precast (left) and monolithic (right) model

The deviations are concentrated at the bottom of the vertical connections, while there are only small interruptions at the top of the vertical connections visible. This observation is confirmed by a section line of the horizontal connection, depicted in Figure 156. When the mesh size is increased from 250mm to 1000mm, the small deviations at the top of the vertical connections disappear, but the large differences at the bottom remain (see Figure 157). A second observation which can be made in Figure 156 and Figure 157 is that the width of the deviations is reduced and the absolute peak values increase with a smaller mesh size: the deviations are constrained within one mesh element. This phenomenon is depicted in Figure 158 and Figure 159.

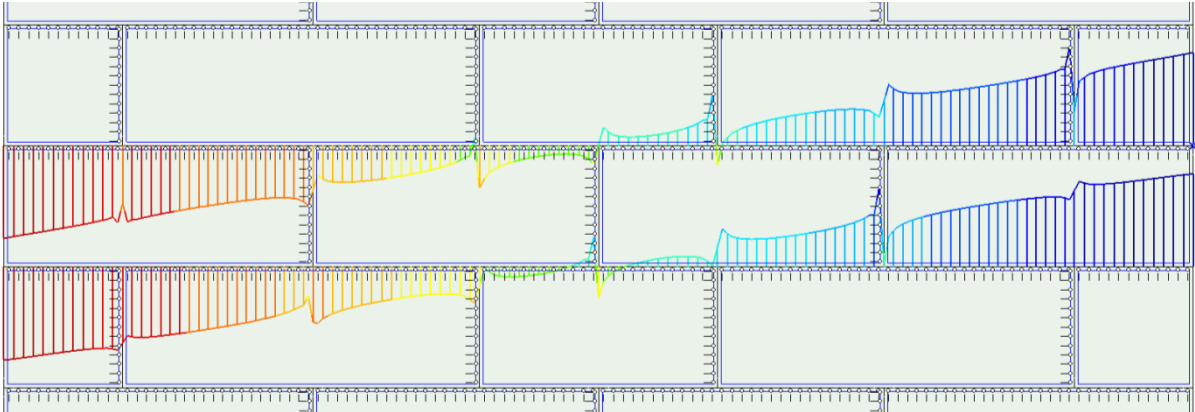


Figure 156 Normal force in the horizontal precast connection, mesh size is 250mm

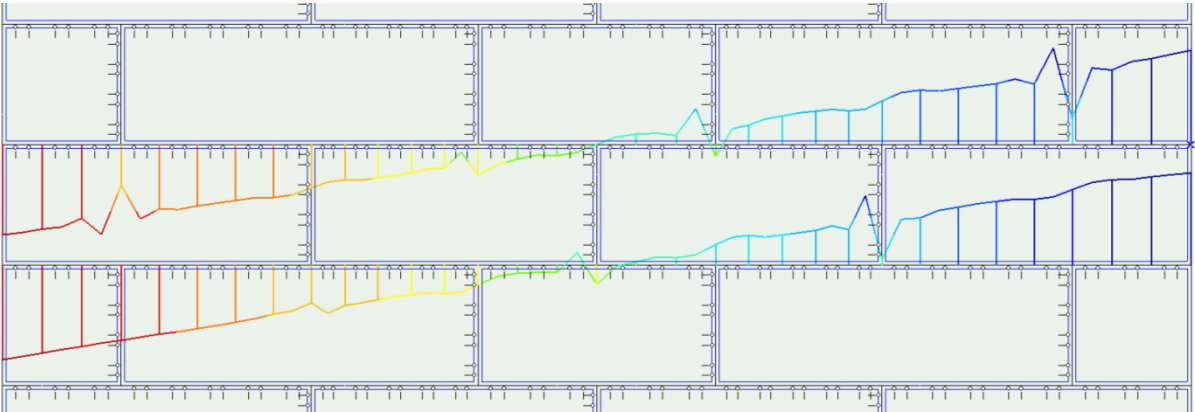


Figure 157 Normal force in the horizontal precast connection, mesh size is 1000mm

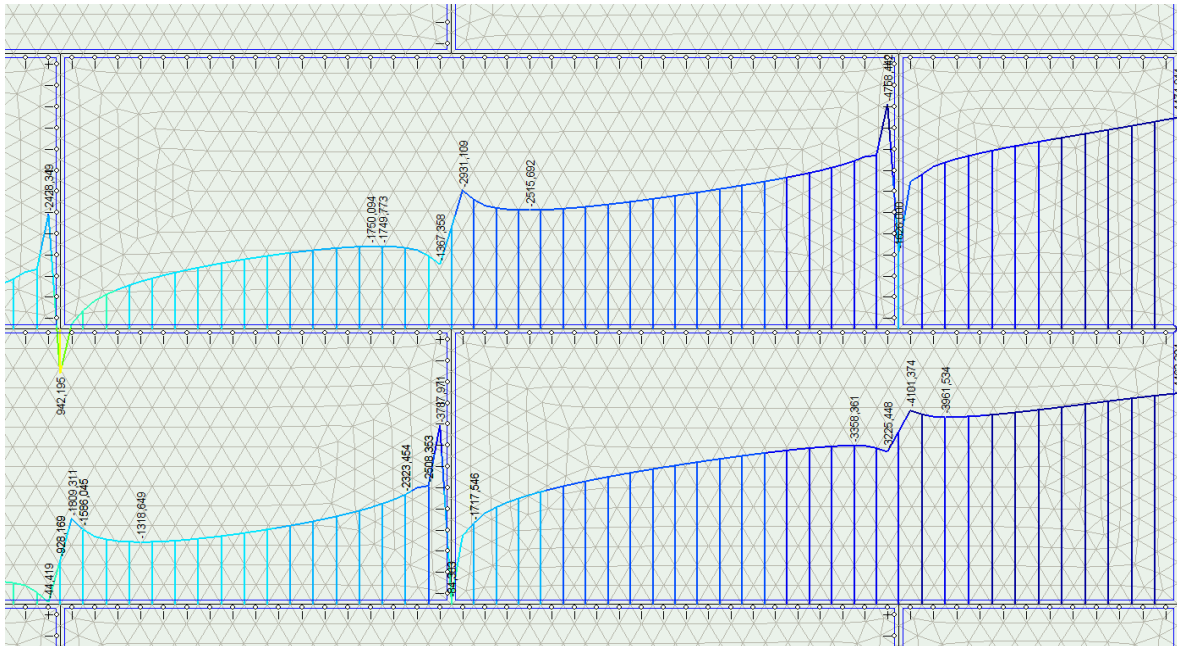


Figure 158 Detailed view of normal force in horizontal precast connection, mesh size is 250mm

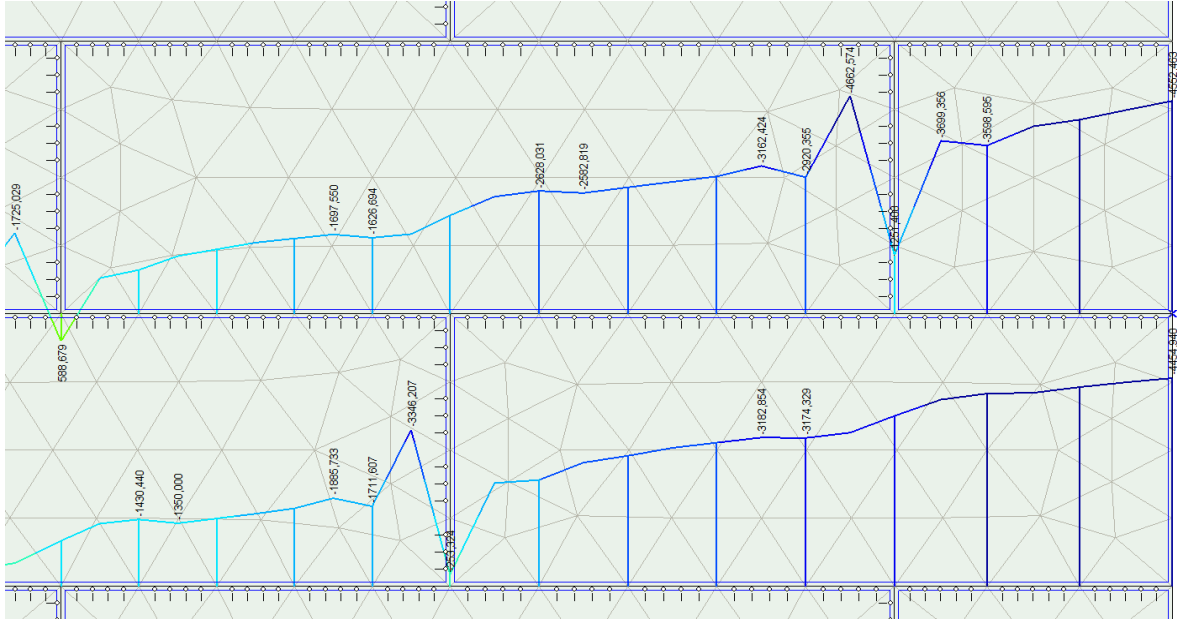


Figure 159 Detailed view of normal force in horizontal precast connection, mesh size is 1000mm

Local deviations at the vertical connections may be expected by a small rotation of the elements with respect to the surrounding elements and the compression force should be in the same order of magnitude as the tension force. This additional force is calculated at approximately 20kN/m for an element with the dimensions $w \times h = 3 \times 3,05 \text{ m}^2$. But when Figure 158 is inspected, it can be observed that the compression force is larger than the tension force: 780,6kN/m of tension versus 1645.6kN/m of compression, resulting in a difference of more than 50%⁴⁶ (this is at a mesh size of 250mm, a mesh size of 1000mm results in 63% difference). Because of this large difference and the high values, it's likely

⁴⁶ These values are obtained by first calculating the mean tension force at the connection: $(4474.911/15) \times 7.2 = 2148.0 \text{ kN/m}$ or $(4463.304/15) \times 7.2 = 2142.4 \text{ kN/m}$. Then the peak value is subtracted from the mean value to obtain the compression or tension force: $2148.0 - 1367.358 = 780.6 \text{ kN/m}$ or $2142.4 - 3787.971 = -1645.6 \text{ kN/m}$.

that the deviations are caused by a different phenomenon: the interface elements. The location of the interface elements and how AxisVM retrieves the results from the postprocessor (how the results are extrapolated from the calculation unit to the graphical unit) are the likely cause of this difference. In Figure 160 it can be seen that the interface elements are placed on the left side of the vertical black line: they are part of the left domain. When the interface elements are placed in the right domain, the peak values change. Furthermore, the location of the horizontal interface element also affects the peak values. The fact that the peak values always remain within one mesh element make it very plausible that the interface elements and the mesh elements are the cause of the variations.

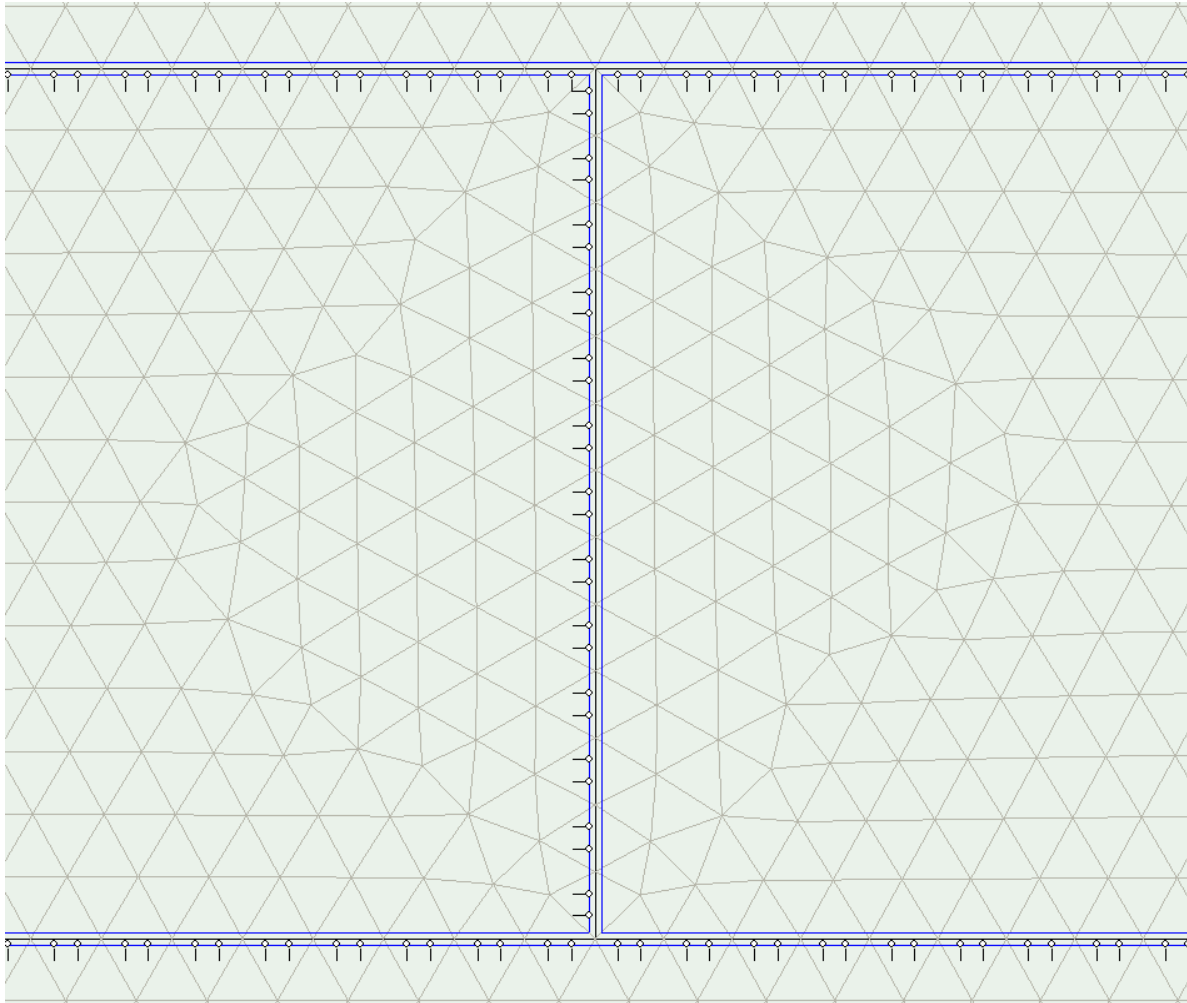


Figure 160 Location of the interface element

It can be concluded that the normal force diagram in the local y-direction (n_y) of a precast structure slightly deviates from a monolithic structure due to the location of the interface elements and how AxisVM retrieves the results from the postprocessor. The differences between a precast and a monolithic structure are only local and the global flow of forces remain comparable.

When the normal force due to dead load is observed, the same deviation as with the wind load can be seen in Figure 161. Figure 162 shows a detailed view of the connection and the peak values are always located within one mesh element. Furthermore, the peak value is always located at the side of the interface element. When the interface element is moved to the right domain, the compression peak also moves to the right. Therefore it can be assumed that the precast and the monolithic wall behave nearly identical when they are loaded by dead load. Besides the deviations, the models behave as expected.

The compression lines are horizontal and towards the bottom the forces increase. At the bottom also a compression arch becomes visible.

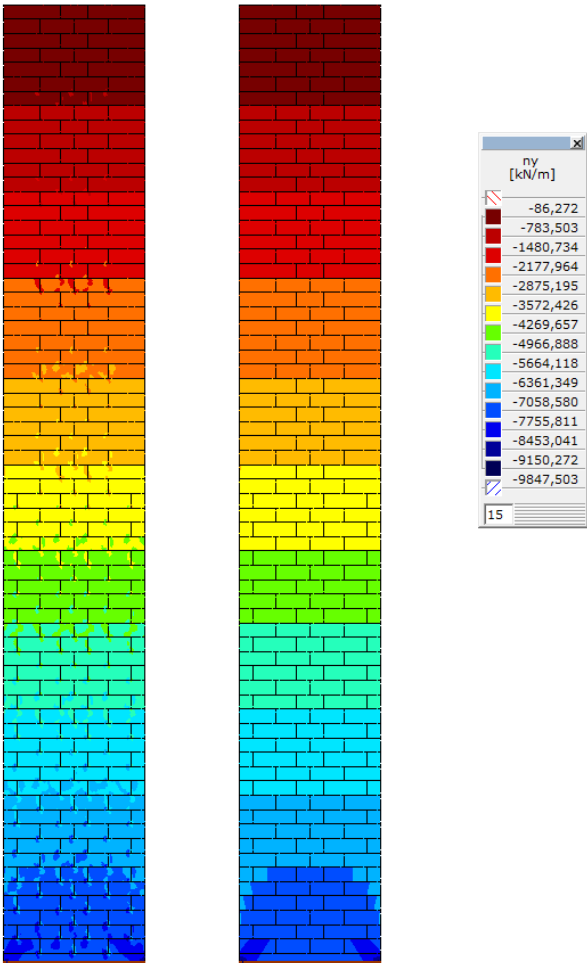


Figure 161 Normal force due to dead load in the simplified precast (left) and monolithic (right) model

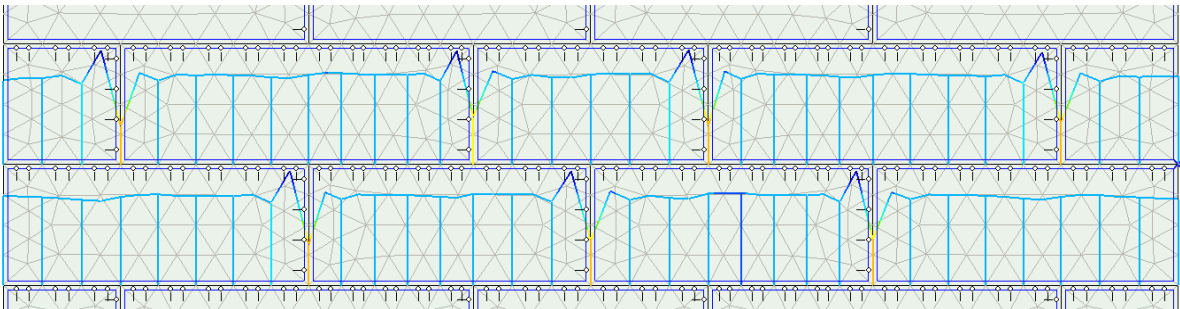


Figure 162 Detailed view of normal force in the horizontal connection due to dead load, mesh size is 1000mm

E.1.3 Shear force in the simplified 2D wall

When the shear force (n_{xy}) of a precast structure is compared with a monolithic structure, it can be observed in Figure 163 that they appear to be comparable on a global scale. Locally, small deviations occur due to the open vertical joints.

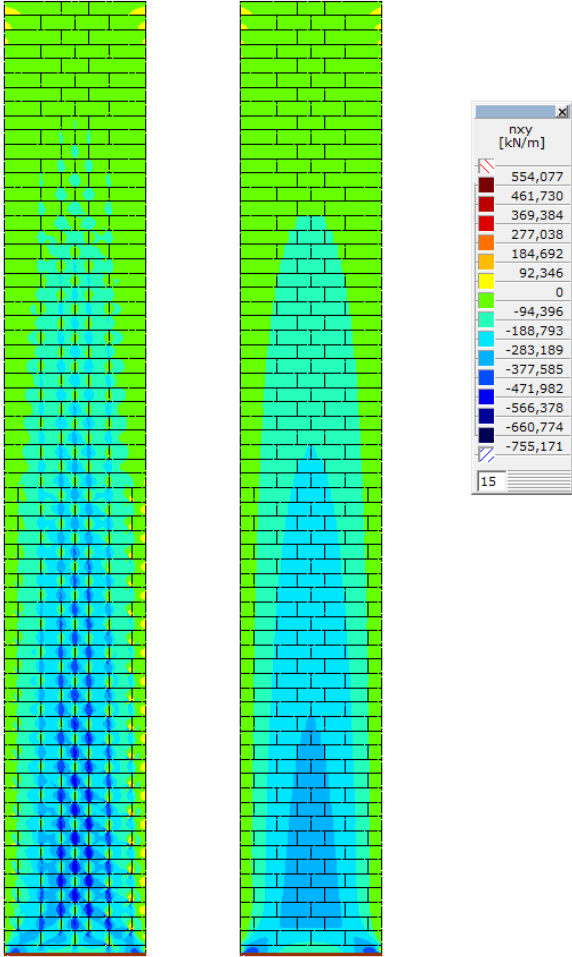


Figure 163 Shear force due to wind load in the simplified precast (left) and monolithic (right) model

The green and blue areas represent a negative shear force. The wind force is applied in the positive x-direction (from left to right) and the sign of the shear force corresponds to the opposite direction. At the edges and some vertical connections, small positive shear force areas can be found at the precast structure (yellow and red areas in Figure 164 and Figure 165). These areas are mainly located at the right hand side of the wall and are created by the direction of the forces and the lack of supporting elements.

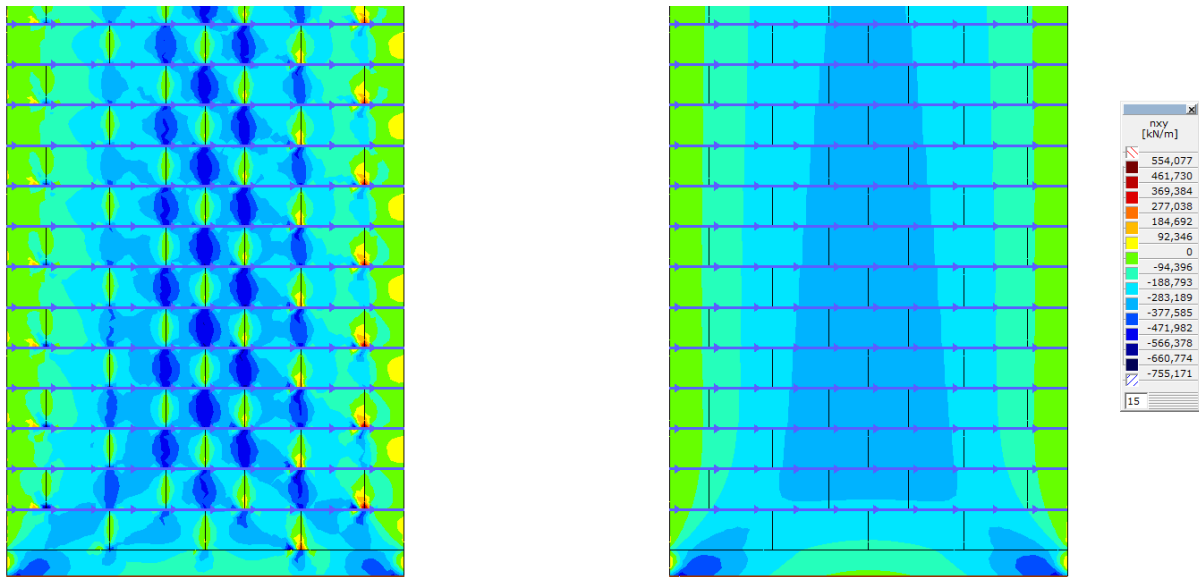


Figure 164 Detailed view of the shear force in the simplified precast (left) and monolithic (right) model

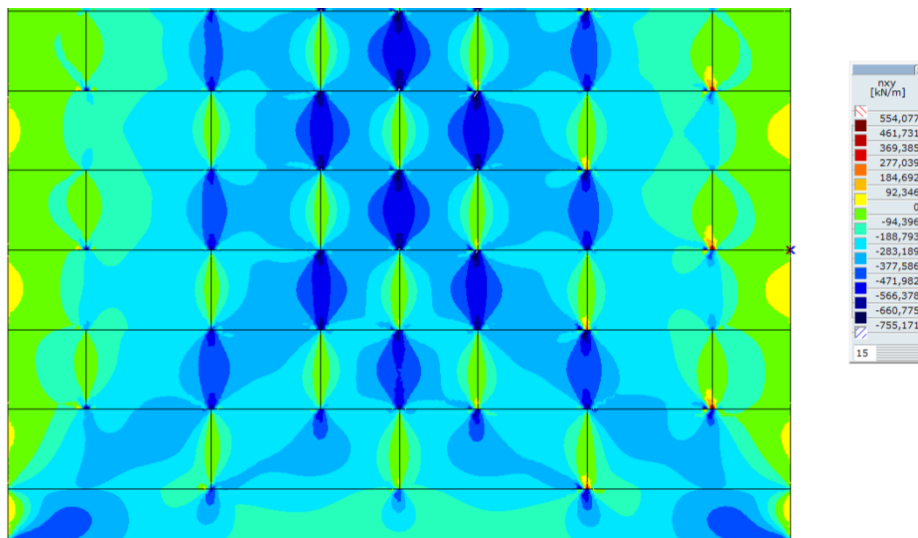


Figure 165 Detailed view of the shear force in the simplified precast model

When Figure 165 is studied in detail, it can be noticed that there are large compression zones between two vertical connections. This phenomenon can be explained by the lack of horizontal stiffness of the open vertical joint: the open joint cannot take up any horizontal forces and the shear force has to be directed to the surrounding elements. Furthermore, compression diagonals become visible in Figure 165. Since the forces are relative low compared with the vertical normal forces of Figure 154, the diagonals disappear when the two main forces are shown (n_1 and n_2).

Insight in the flow of forces can also be provided by sections. In Figure 166 the bottom section is made at the horizontal connection and the top section is made halfway the open vertical joint. In Figure 167 the two sections of the precast structure are shown on a larger scale.

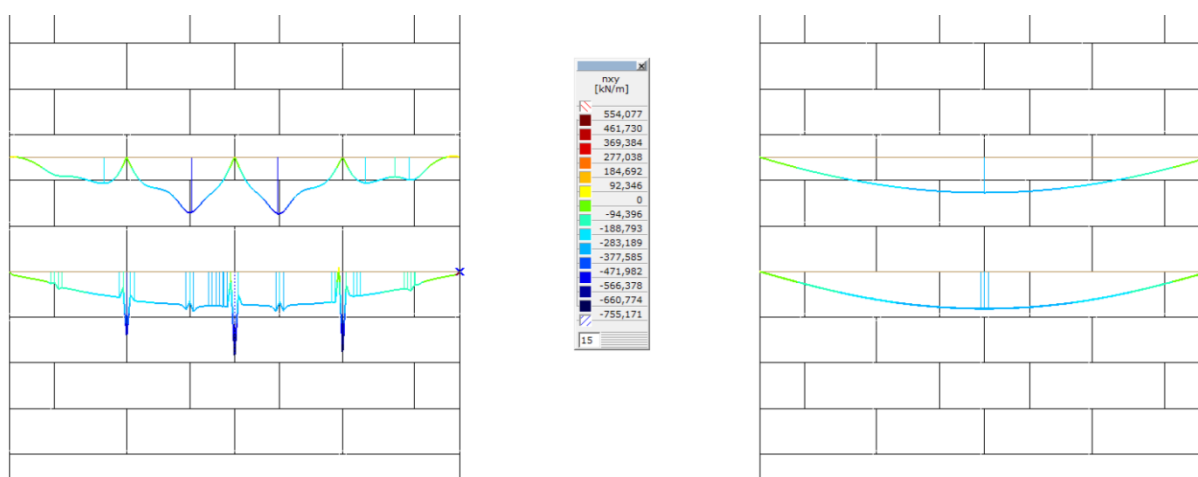


Figure 166 Shear force sections of the simplified precast (left) and monolithic (right) model

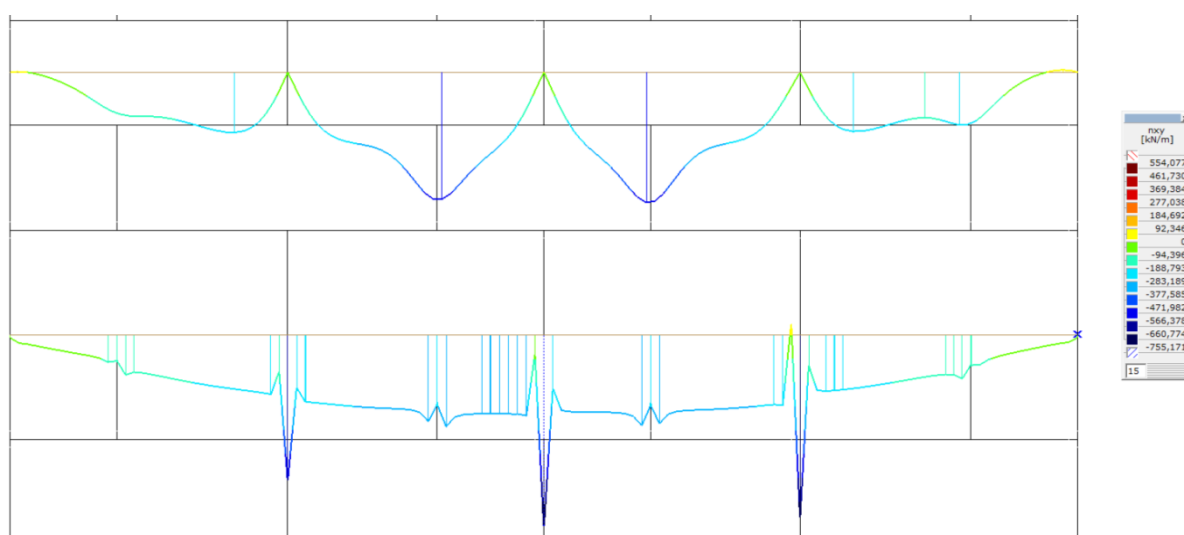


Figure 167 Detailed view of the shear force section in the simplified precast model

The bottom section of the precast structure shows a shear diagram that is comparable to the monolithic structure (the values are in the same order of magnitude), but there are three peak values located at the vertical open joint. At the top section made halfway the element the same diagram is slightly visible. The distribution clearly shows that the vertical open joint has no shear stiffness and the values at the dowel element are less severe (the peak values are more gradual). This distribution of shear force is also clearly visible in Figure 165: the blue area is very concentrated at the horizontal joint and diffuses to a larger area between the elements. The question arises: why does this distribution occur? To answer this question, the underlying behaviour is examined. In Figure 168 it's depicted how the two elements without a vertical connection introduce a shear force in the dowel element. Since a linear calculation is utilised, the distribution of forces isn't spread out. When this is combined with a smeared stiffness, which is able to take up tension forces, a considerable part of the forces will be transferred at the last possible point, i.e. the intersection of the two connections.

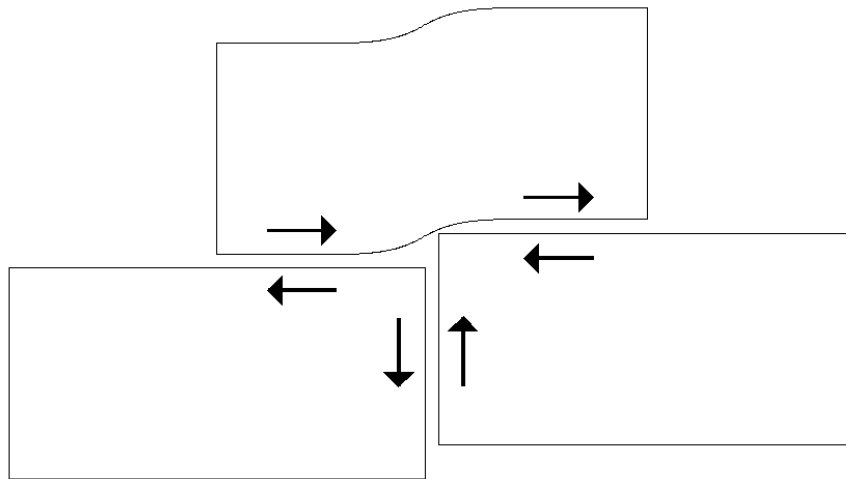


Figure 168 Behaviour of the elements

As a result of these two aspects, a very large peak force is created in this connection point, shown by the bottom section of Figure 167 (the high values are contained within one mesh element). Between the top and bottom horizontal connection the values spread out, creating the curved blue lines of Figure 165. When the values at the connection point are analysed in more detail, it can be concluded that in the last 5% of the horizontal connection, 11% of the shear force is contained.

When a non-linear calculation would be applied in combination with the actual connection behaviour (by using a smeared stiffness a lot of mechanism which play an important role in the actual behaviour of the connection are neglected, for example the distribution of tension forces by the nearest starter bar), the shear concentration would be less severe in the top and bottom connection point. Therefore these values may be smoothed, but these two connection points will always contain a higher shear force compared to the surroundings.

It can be concluded that on a global scale the shear force of a precast structure is comparable to that of a monolithic structure. When they are compared on a local scale, deviations can be seen due to the open vertical joint. As a result of the calculation, local peak values may be expected around the vertical joints. Since they are created by the calculation, the peak values may be smoothed.

E.1.4 Normal force in the actual 2D model

When the openings are added to the simplified 2D wall of the previous section, Figure 169 is obtained (loaded only by wind). Compared with Figure 154, the global flow of forces in both models remains equal. Because of the reduced structural area, the values of the normal force have slightly increased in Figure 169. Near the bottom of the wall, the largest differences can be found as a result of the large openings in the lobby area.

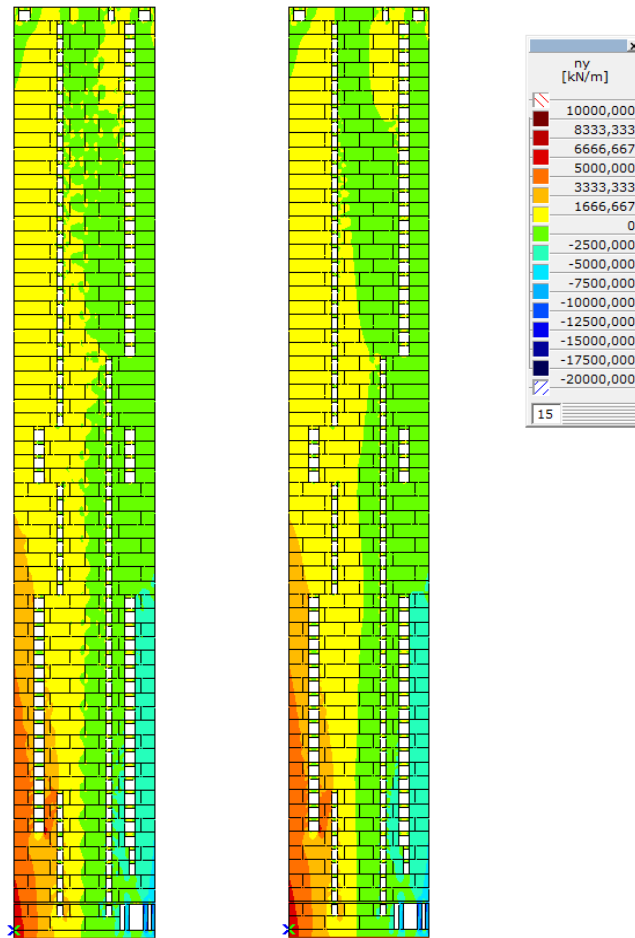


Figure 169 Normal force in the precast (left) and monolithic (right) model

To observe the flow of forces in more detail, a smaller section is depicted in Figure 170. In the top left corner of the both walls it can be seen how the tension force is concentrated between two rows of openings. In the right bottom corner it can be observed that the compression force is concentrated within the three columns. In Figure 170 it can also be noticed that the line between tension and compression isn't centred. This difference can be explained by the higher amount of openings at the right hand side of the wall (reduced structural area).

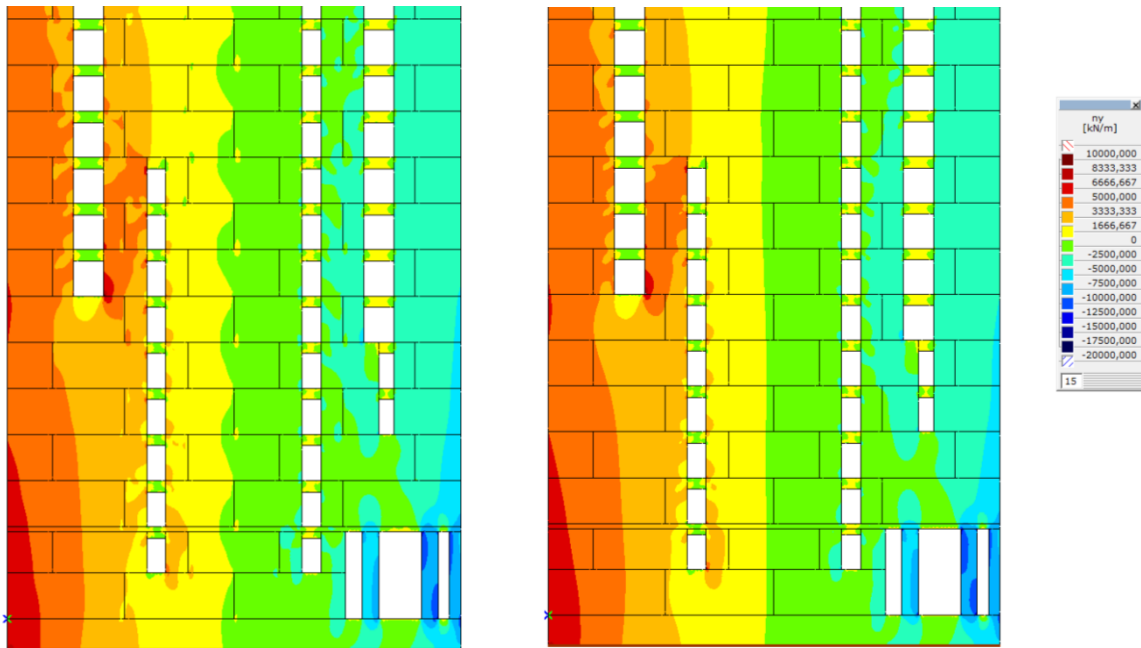


Figure 170 Detailed view of the normal force in the precast (left) and monolithic (right) model

When the precast wall is compared with the monolithic wall, small local differences can be seen around the open vertical joints. In section E.1.2 this difference was already encountered and this is most likely caused by the location of the interface elements and how AxisVM retrieves the results from the postprocessor. When Figure 170 is compared with Figure 155 it can be noted that the amount of deviations around the vertical open joints has decreased. This is most likely caused by wall openings, which create larger forces and therefore the deviations are more difficult to distinguish.

When the same scale as in Figure 154 is used, it can easily be seen where the forces have increased due to the reduced structural area. In Figure 171 three areas can be distinguished: near the lobby in the right bottom corner, at the left bottom corner and around several lintels. As a result of the openings, the amount of local peak values also increases compared with the simplified wall.

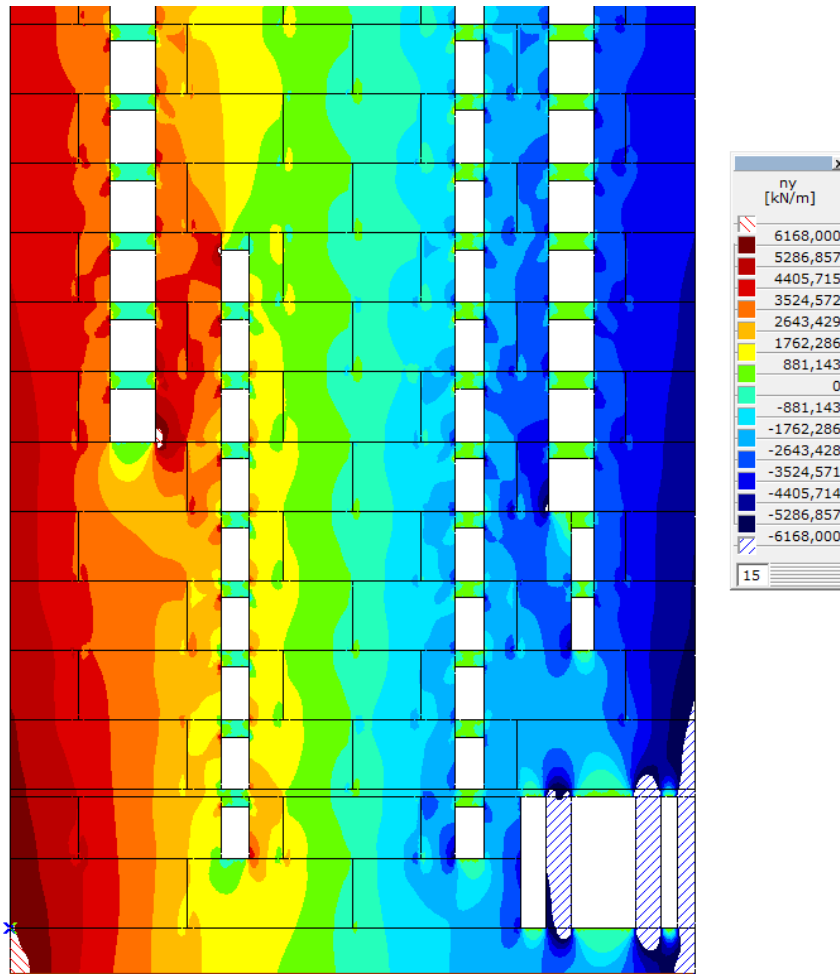


Figure 171 Detailed view of the normal force in the precast model

When the normal force from only wind load in a precast 2D wall is compared with a monolithic wall, it can be concluded that they are approximately identical on a global scale. Just as the simplified 2D wall there are small differences due to the location of the interface elements and how values are determined by the postprocessor.

If the structure is only loaded by dead load, a normal force diagram as depicted in Figure 172 may be expected. Just as the simplified wall, there are small differences between the precast and monolithic wall because of the postprocessor and the locations of the interface elements. When Figure 172 is compared with Figure 161, it can be observed that the values locally increase due to a reduced structural area. Above and underneath the openings a normal force reduction can be seen because these openings cannot transport any forces.

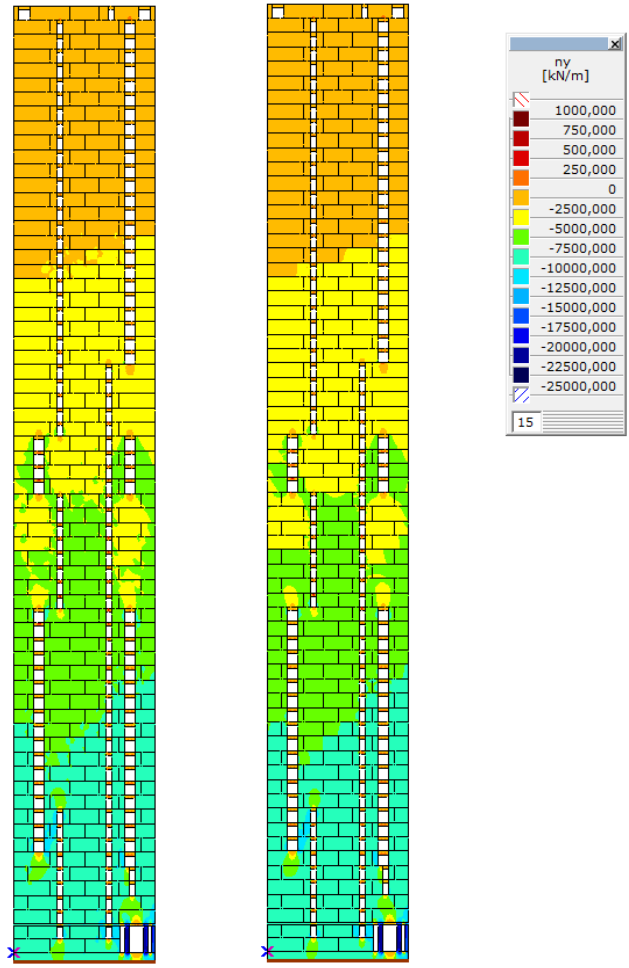


Figure 172 Normal force due to dead load in the precast (left) and monolithic (right) model

A second observation that can be made is that the lines (orange/yellow and green/blue) are not straight. Because of the large openings in the lobby, the stiffness is reduced and the forces have to flow around it. The stiffness reduction also provides an initial horizontal deformation. Actions have to be taken to provide a level structure when it's loaded by dead load, for example slightly longer columns or elements.

E.1.5 Shear force in the actual 2D model

In Figure 173 the shear force as a result of wind load is depicted. On a global scale it's difficult to find any differences between the precast and monolithic wall and the two diagrams are more or less comparable with the simplified walls (see Figure 163).

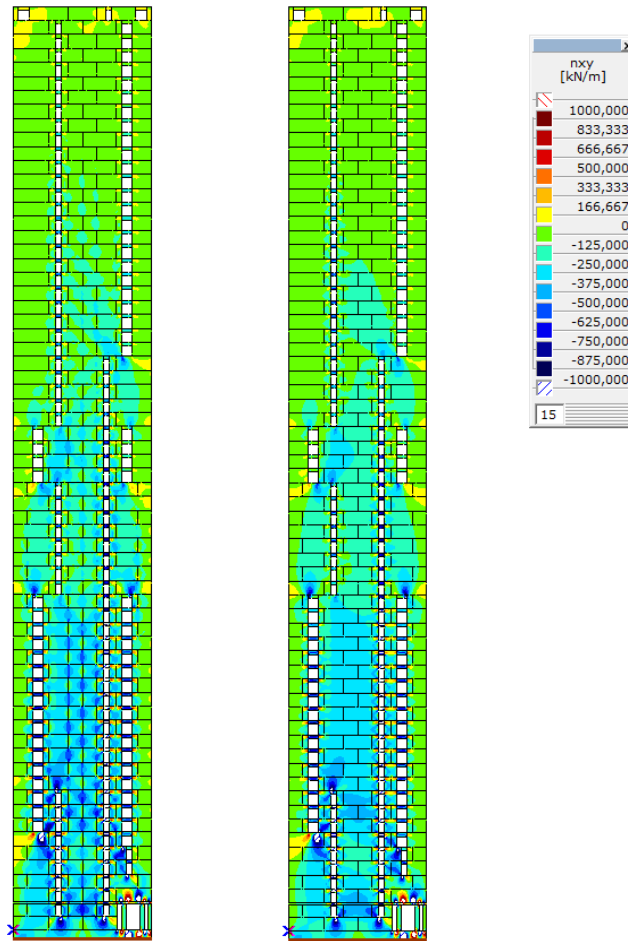


Figure 173 Shear force due to wind load in the precast (left) and monolithic (right) model

When a smaller area is considered, the differences between the precast and monolithic wall become more visible, see Figure 174. The vertical open joint is unable to take up any shear forces and the surrounding walls have to be activated. Just as with the simplified wall, large negative shear force areas can be found in the elements between the vertical joints.

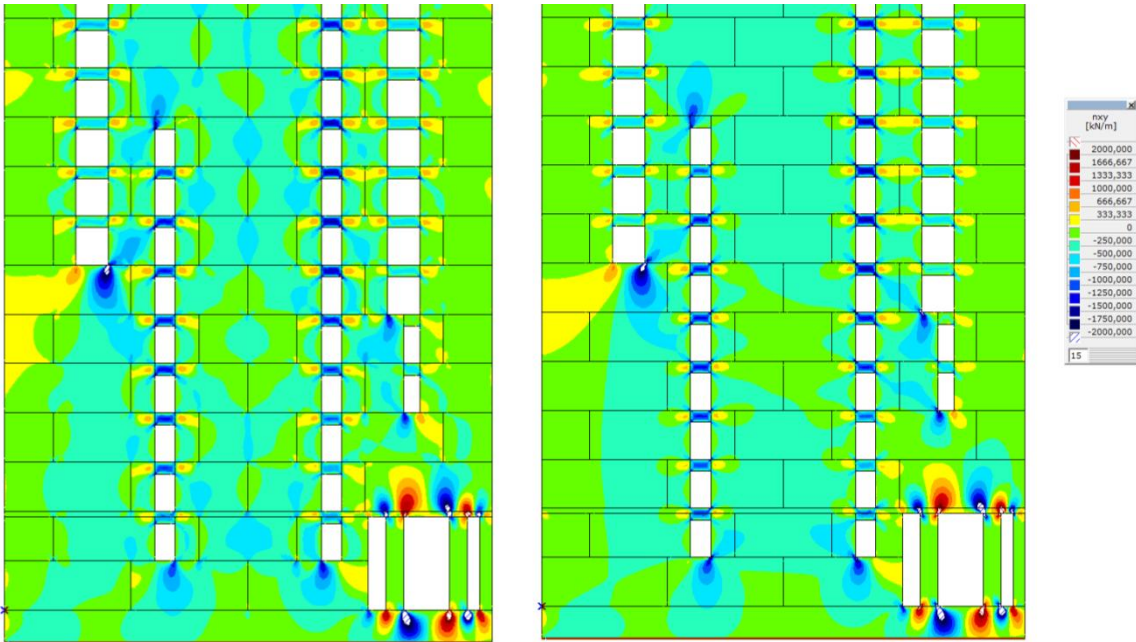


Figure 174 Detailed view of the shear force in the precast (left) and monolithic (right) model

In the simplified wall the entire element height is available to transport the shear force. In Figure 175 it can be seen that at some location there is only a lintel available. As a result, large negative shear areas are created in the lintel. Because of the direction of these forces around the lintels, small positive shear areas arise near the lintels (yellow areas).

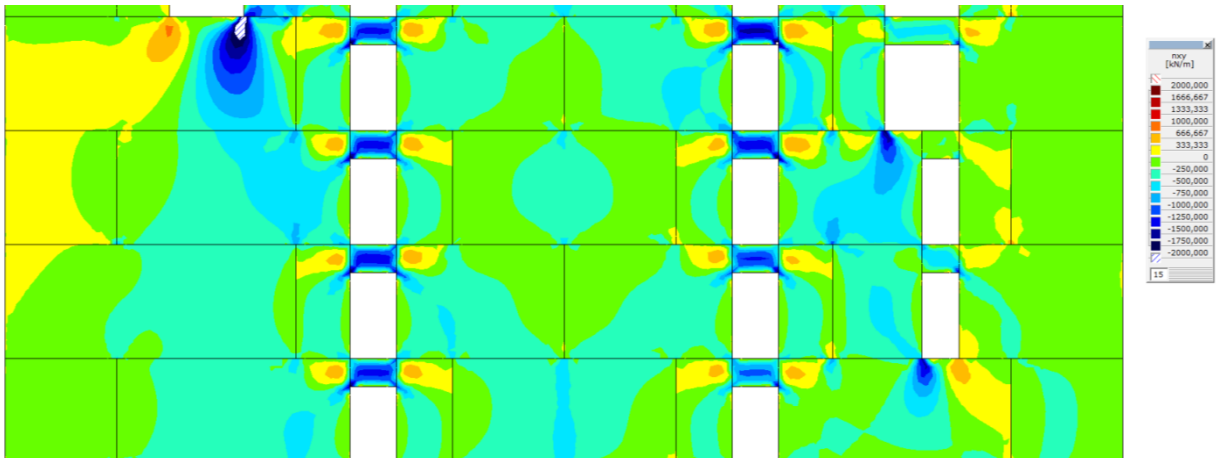


Figure 175 Detailed view of the shear force in the precast model

When the shear force is determined at a section, it can be noticed that the round shear shape of Figure 166 is not present anymore in the monolithic wall. The openings are the cause of the disruptions. When the precast wall is observed, even more disruptions can be distinguished, see Figure 176.

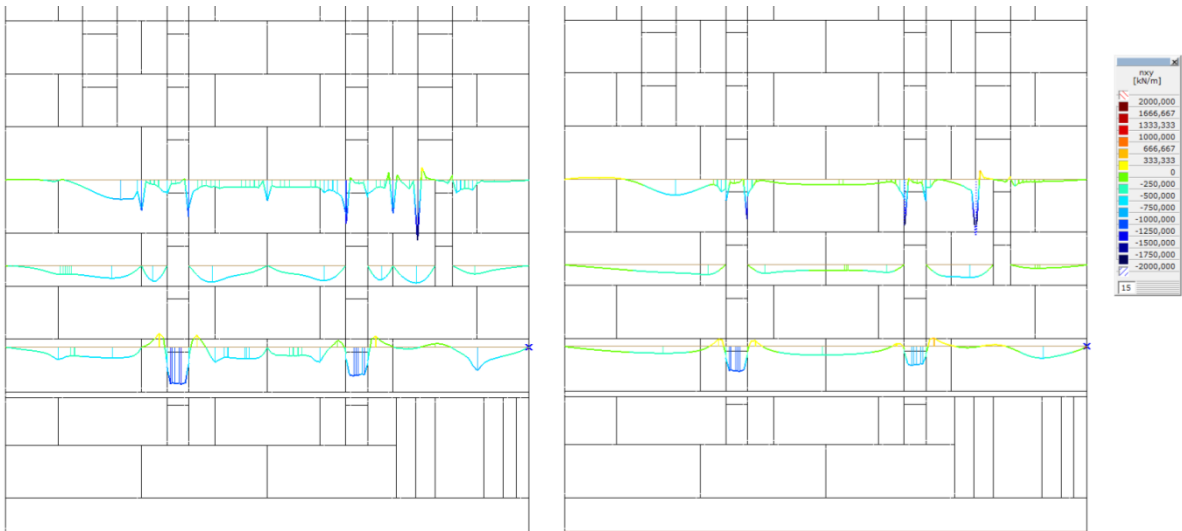


Figure 176 Shear force sections of the precast (left) and monolithic (right) model

In Figure 177 a more detailed section is depicted of the precast wall. The middle section shows that halfway the element, the vertical open joint transports no shear forces. When a section is made close to a horizontal connection (the lowest section line in Figure 177), the shear forces increase around the open joint. The open vertical joint still doesn't transfer any shear forces, but the element placed on top does and therefore the shear forces decrease rapidly near the open vertical joint. This can be seen in more detail in Figure 178.

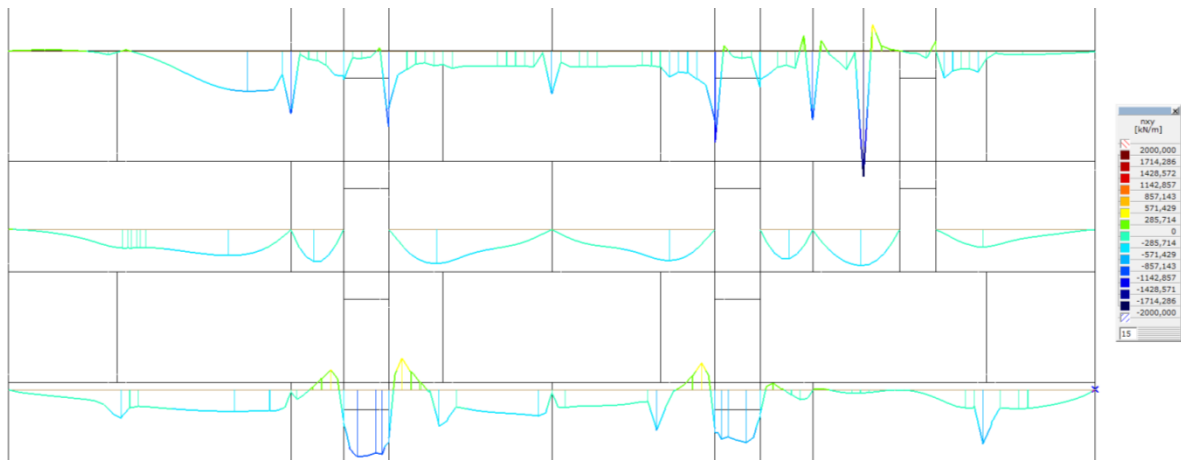


Figure 177 Detailed view of the shear force section in the precast model

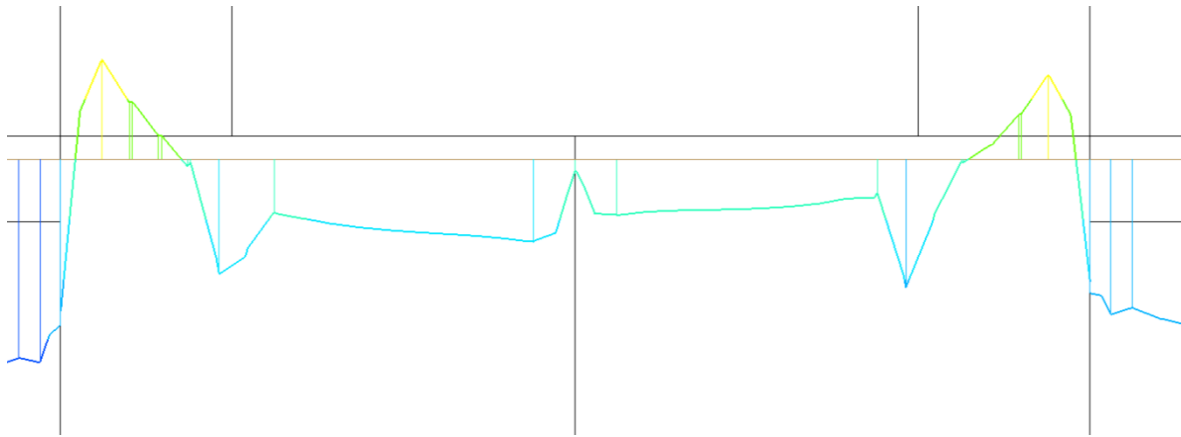


Figure 178 Shear force section near the horizontal connection in the precast model

From the previous observations it can be concluded that on a global scale the shear force of a precast structure is comparable to that of a monolithic structure. When they are compared on a local scale, deviations can be seen due to the open vertical joint. In section E.1.3 it was already discussed that these peak values are created by the calculation and that they may be smoothed for the reinforcement calculations. Compared with the simplified 2D wall, the lintels will also introduce negative and positive shear areas. The size of the overlap between the elements determines how large these peak values are.

E.1.6 Normal force in the simplified 3D model

The previous sections have shown that introducing openings in the structure has a considerable effect on the local scale. While the global forces only change slightly, locally peak force areas are created. To understand how the forces flow through a three dimensional building, first a simplified 3D model without openings will be examined. Subsequently, the openings are added, creating a model that approximates the actual structure.

In Figure 179 the normal force in the local y -direction is shown due to wind load. When the distribution of forces is compared with Figure 154 (2D wall without openings), it can be concluded that the simplified 3D model has lower tension and compression forces. This difference can be explained by the flanges of the 3D model, which take up a part of the normal force. Also small disturbances can be seen at the top of Figure 179. The values are relatively low (between -0.2 and 0.2 kN/m) and are probably caused by the calculation. Besides these two aspects, the figures are nearly identical.

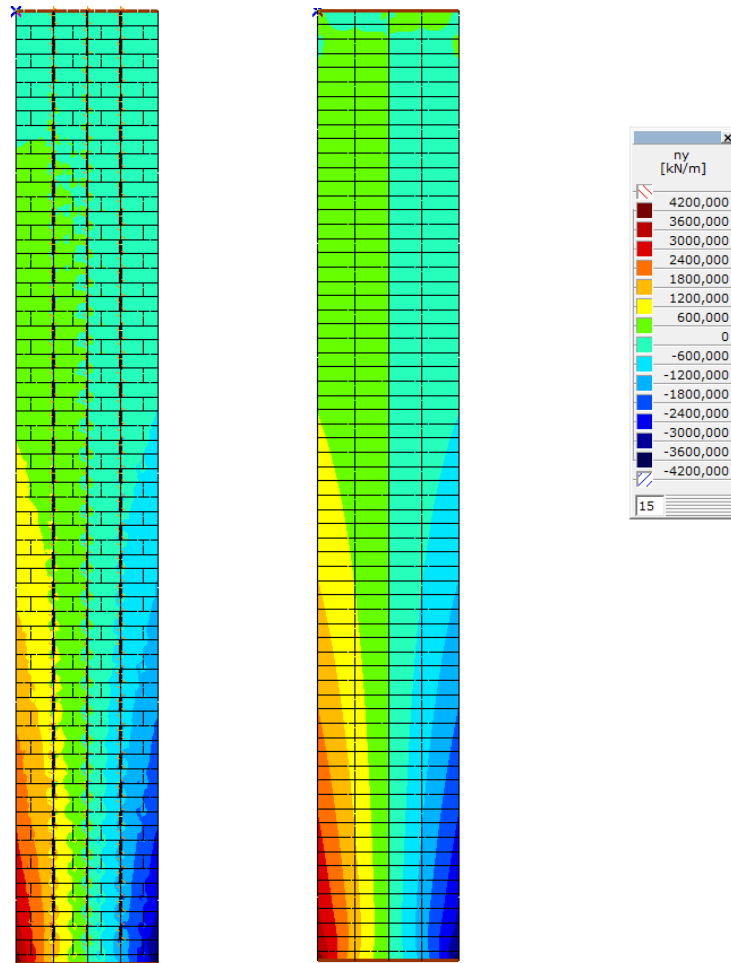


Figure 179 Normal force in the simplified precast (left) and monolithic (right) 3D model

In Figure 180 it's clearly visible that the flanges contribute to the distribution of forces.

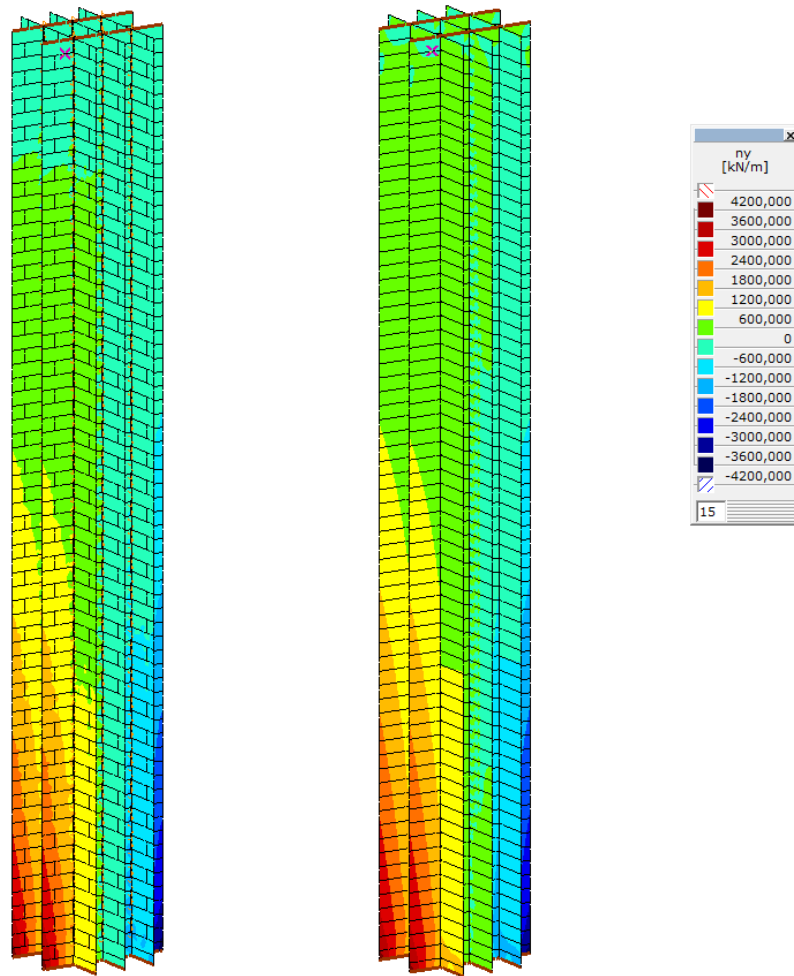


Figure 180 Side view of the normal force in the simplified precast (left) and monolithic (right) 3D model

In Figure 181 a more detailed view of the 3D model is depicted. This figure clearly shows how the left flange is under tension and the right flange under compression. The central flange is not activated due to the location of the flange. Just as with the simplified precast 2D model, the precast 3D model contains disruptions around the vertical connections. They are induced by the calculation and may be neglected (see section E.1.2).

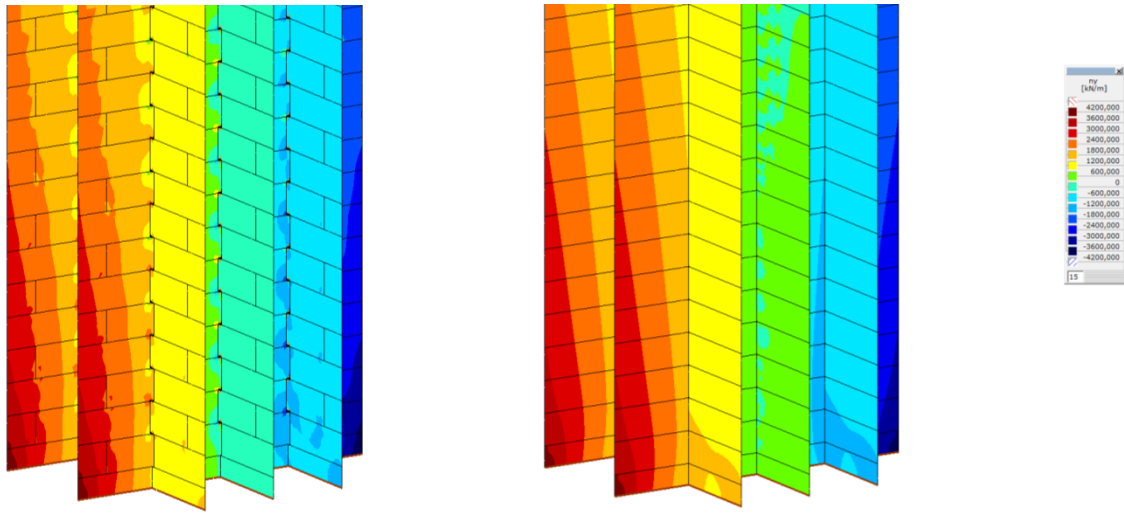


Figure 181 Detailed view of the normal force in the simplified precast (left) and monolithic (right) 3D model

When the normal force resulting from dead load is examined, the results of the precast and monolithic 3D model are nearly identical on a global scale. On a local scale small deviations can be observed at the precast structure in Figure 182. These deviations were also present at the simplified 2D model and they are likely caused by the interface elements. When the values of Figure 182 are compared with Figure 161 (the 2D model without openings), it can be stated that as a result of the larger structural area, the normal force values have decreased.

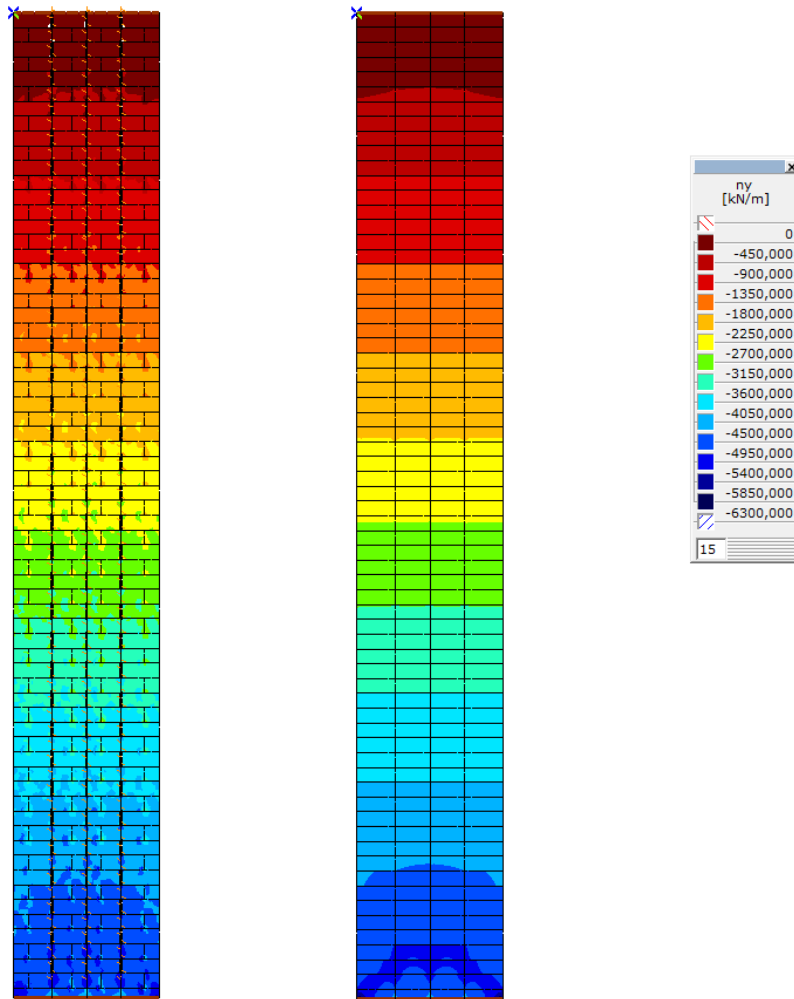


Figure 182 Normal force due to dead load in the simplified precast (left) and monolithic (right) 3D model

When in Figure 183 the normal force as a result of the dead load is examined in perspective an interesting aspect can be noticed: wall 4 and 5 receive a higher normal force than wall 1, 2 and 3. This is unexpected since the floors are supported by wall 1, 2 and 3. This phenomenon is probably caused by the larger thickness of wall 4 and 5 (500mm versus 400mm) and the fact that the stiffest elements attract the largest forces.

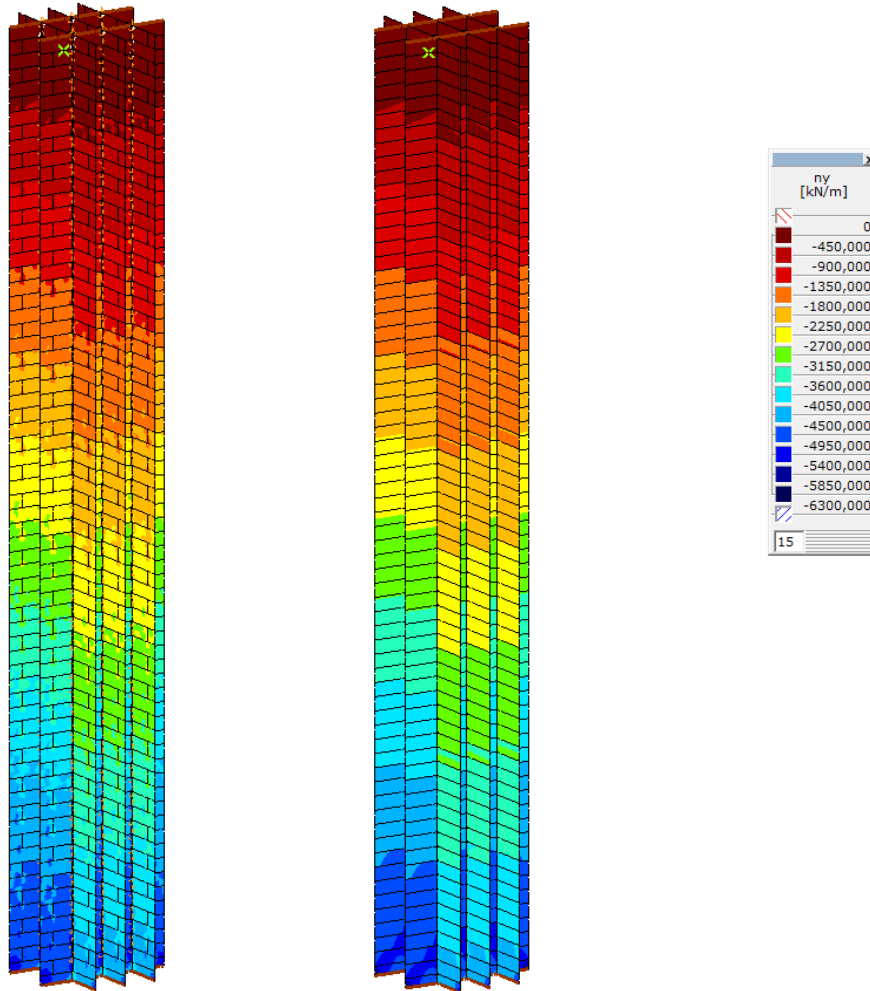


Figure 183 Side view of the normal force due to dead load in the simplified precast (left) and monolithic (right) 3D model

It can be concluded that the simplified precast and monolithic 3D model are nearly identical. Due to the interface elements small deviations occur in the precast model. The simplified 2D and 3D model also share many similarities, but due to the larger structural area of the 3D model, the absolute values decrease. The stiffest elements in the structure attract the largest forces and therefore wall 4 and 5 receive a large normal force when loaded with dead load.

E.1.7 Shear force in the simplified 3D model

In Figure 184 the shear force per meter as a result of wind load is shown. The distribution of forces between a precast and monolithic model is comparable on a global scale, but the precast model contains many deviations on a local scale. Just as with the simplified 2D model in Figure 163, these deviations are created by the open vertical joint. Therefore the under and overlaying dowel elements are activated, creating areas with larger forces.

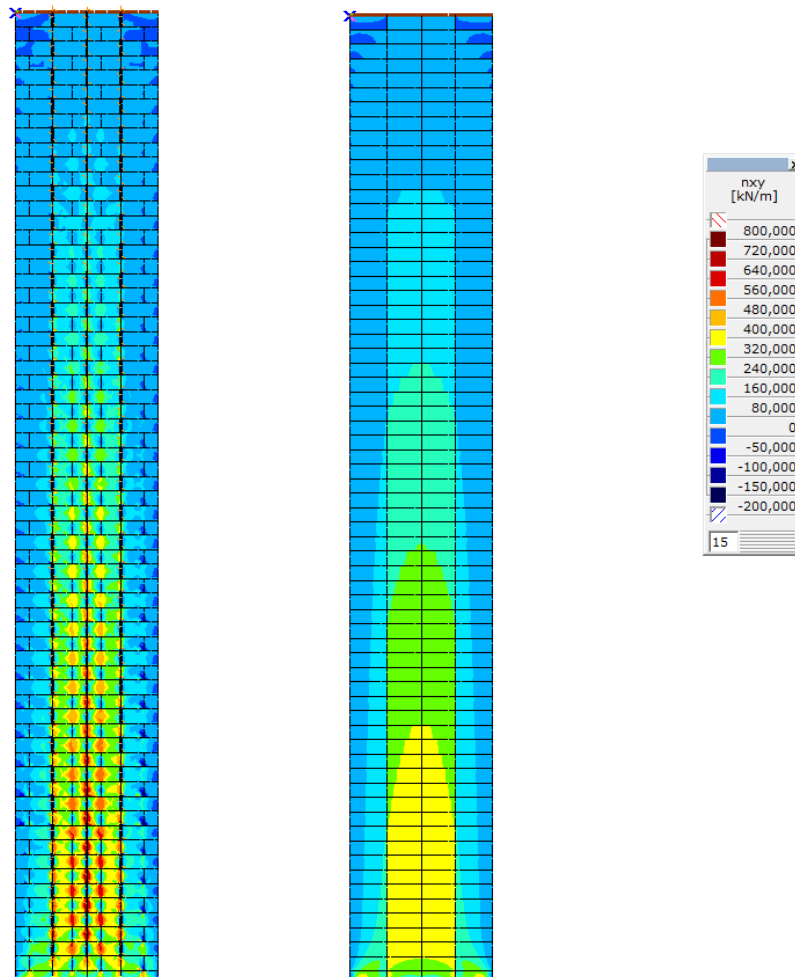


Figure 184 Shear force due to wind load in the simplified precast (left) and monolithic (right) 3D model

The amount of deviations is furthermore increased by how the 3D precast model is created. In Figure 185 open slots can be seen where wall 1, 2 and 3 intersect wall 5. These openings have a width of 400mm, increased with two times the joint thickness (30mm). The simplified 2D precast model had no physical openings; only an interface element with a stiffness equal to 0kN/m/m was modelled. Due to these differences, locally larger forces are encountered in the precast 3D model compared to the monolithic model. In Figure 185 also compression and tension diagonals become visible. Since the force values of diagonals are relatively low compared with the normal force in the local y-direction (previous section), the diagonals disappear when the two main forces (n1 and n2) are depicted.

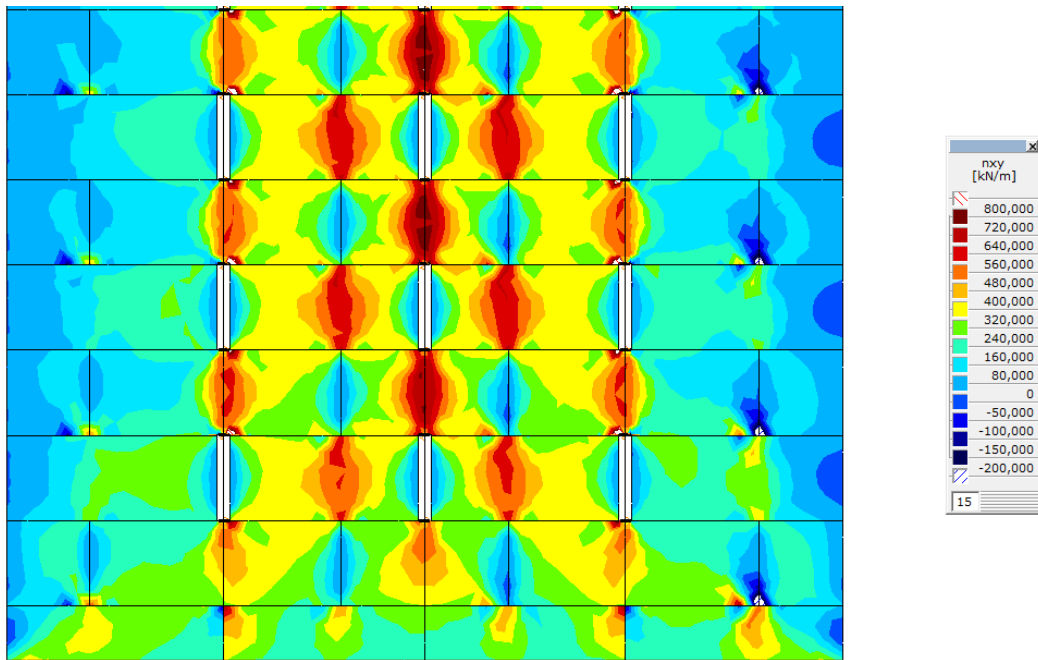


Figure 185 Detailed view of the shear force in the simplified precast 3D model

When the values of the simplified 3D model are compared with the simplified 2D model, a sign difference that can be distinguished. In Figure 184 the shear force has mainly positive values while in Figure 163 there are mainly negative values. This difference is created by a different local coordinate system relative to the global system. When the values of the monolithic 3D model are compared with the 2D model, they have approximately the same order of magnitude (the values of precast 3D model are slightly larger due to how it's modelled).

Because of the connection between the perpendicular walls, the flanges (wall 1, 2 and 3) also obtain a shear force. In Figure 186 the two 3D models are shown in perspective, but the distribution of forces is difficult to differentiate. Therefore several sections have been made.

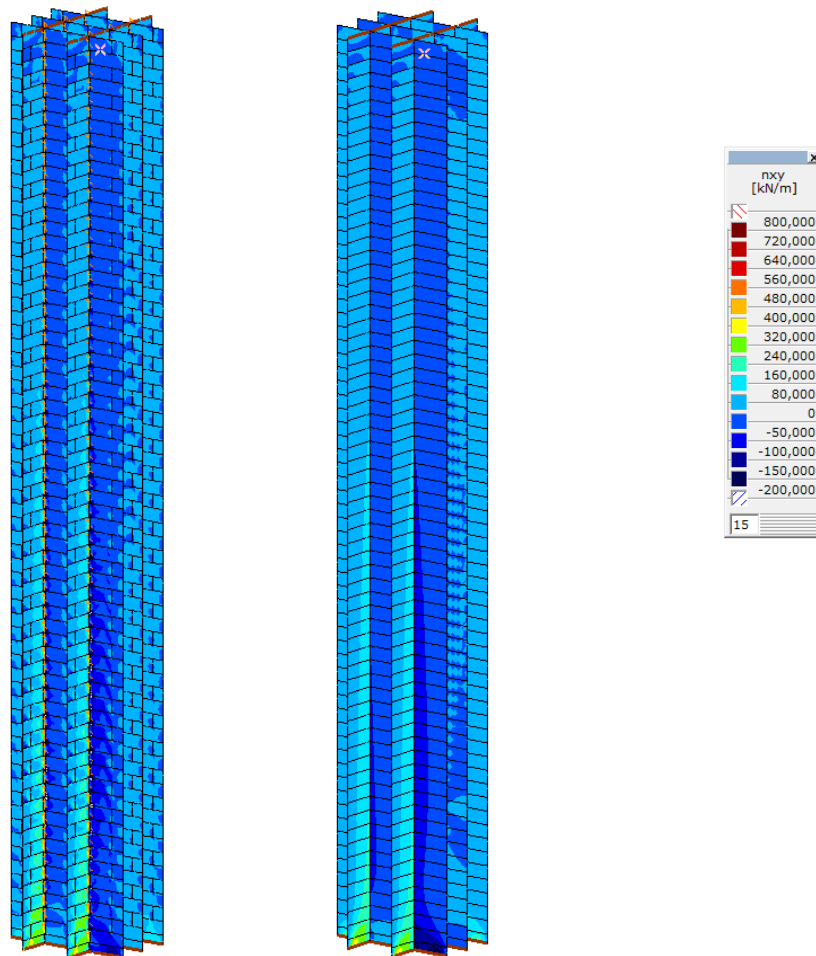


Figure 186 Side view of the shear force due to wind load in the simplified precast (left) and monolithic (right) 3D model

In Figure 187 two sections are made at wall 5. In the monolithic model a shear distribution is shown that is comparable to an I-profile beam. The following shear stress formula holds for in I-profile:

$$\tau_{Ed} = \frac{V_{Ed}S}{I_t} \quad [\text{N/mm}^2]$$

At the end of the wall, the shear stress will be 0N/mm^2 . Between the end and wall 1 or 3, the shear stress increases parabolically due to the increasing static moment of inertia. At wall 1 and 3, the shear stress reduces considerably because of the increasing wall thickness. Unfortunately, this isn't shown because the walls don't have a physical thickness in the model. Though, according to the shear stress formula, the reduction at the flanges should be there. Between wall 1 and 2 or 2 and 3, the shear stress continuous to increase in a parabolic shape. The difference between the value left and right of wall 1 (this also holds for wall 3) is caused by the static moment of inertia. Between the end and wall 1, wall 1 isn't included in the static moment, resulting in a lower shear stress. Wall 2 doesn't have any effect on the shear stress distribution since it's located at the neutral line.

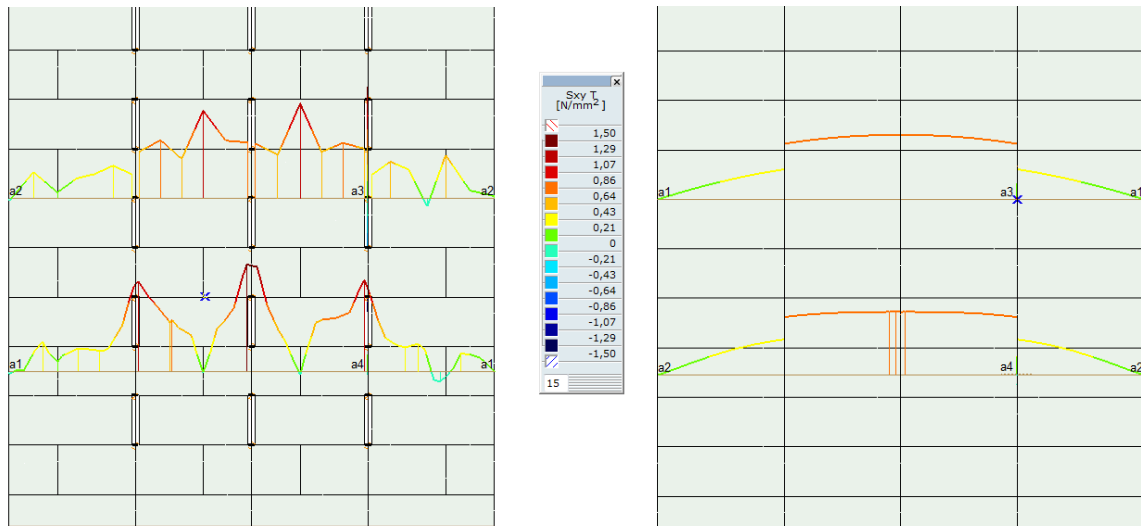


Figure 187 Shear stress section at wall 5 of the simplified precast (left) and monolithic (right) 3D model

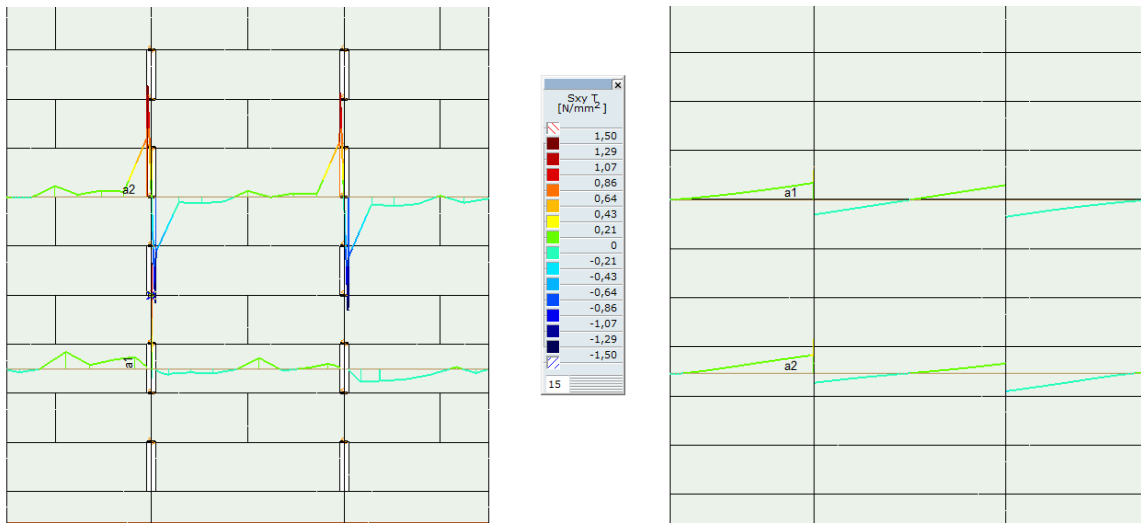


Figure 188 Shear force section at wall 3 of the simplified precast (left) and monolithic (right) 3D model

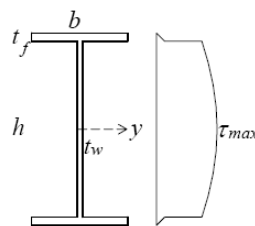


Figure 189 Shear stress distribution of an I-profile without rounded edges [Abspoel, 2008]

When the shear stress distribution of the precast model in Figure 187 and Figure 188 are examined, approximately the same lines can be distinguished. Though, as a result of the open vertical joints and how it's modelled, larger stresses occur at the precast model. An important difference between the precast and monolithic model can be observed in Figure 187: in the precast model there is almost no difference between left and right hand side of wall 1 (or 3). In the monolithic model all the perpendicular walls are

connected at every floor. At the precast structure this was impossible with the masonry configuration and at every even floor, wall 4 and 5 continue. At every uneven floor, wall 1, 2 and 3 continue. Therefore wall 4 and 5 are only connected to wall 1, 2 and 3 at a small cross-section. This reduces the static moment of inertia, creating a smaller difference between the left and right hand side of wall 1 and 3.

When the precast and monolithic simplified 3D models are examined, it can be concluded that they are comparable on a global scale. However, due to the open vertical joints and how the model is created, they differentiate considerably on a local scale.

On a global scale the shear force of a simplified monolithic 3D model is comparable to that of a simplified 2D model. This is because the flanges only have a small effect on the shear force. On a local scale the difference become more present. For example: near the flanges large differences occur due to the thickness of the wall and the static moment of inertia. This conclusion also holds for the precast 3D model, but due to how the model is created, the local differences between the 2D and 3D precast model increase.

E.1.8 Normal force in the 3D model

In Figure 190 the normal force due to wind load in the 3D model is shown. When this figure is compared with the normal force in the 2D model with openings (see Figure 169⁴⁷), it can be concluded that the distribution of forces is nearly identical. The only difference which can be observed very clearly is the location of the neutral line. In Figure 169 this line was located on the left side of the centre because of the large openings on the right hand side. In Figure 190 this line is located at the centre since wall 5 contains more openings on the left hand side. Furthermore, when the absolute normal force values of the 3D model and the 2D model are compared, it can be noted that the 3D model includes lower values. This difference is created by the flanges of the 3D model, which contribute in the force distribution.

⁴⁷ In Figure 169 wall 4 is displayed. Due to the location and orientation of this wall, it's impossible to use the same wall in the 3D model in this perspective. Therefore wall 5 is displayed in Figure 190. The difference between these two walls is marginal.

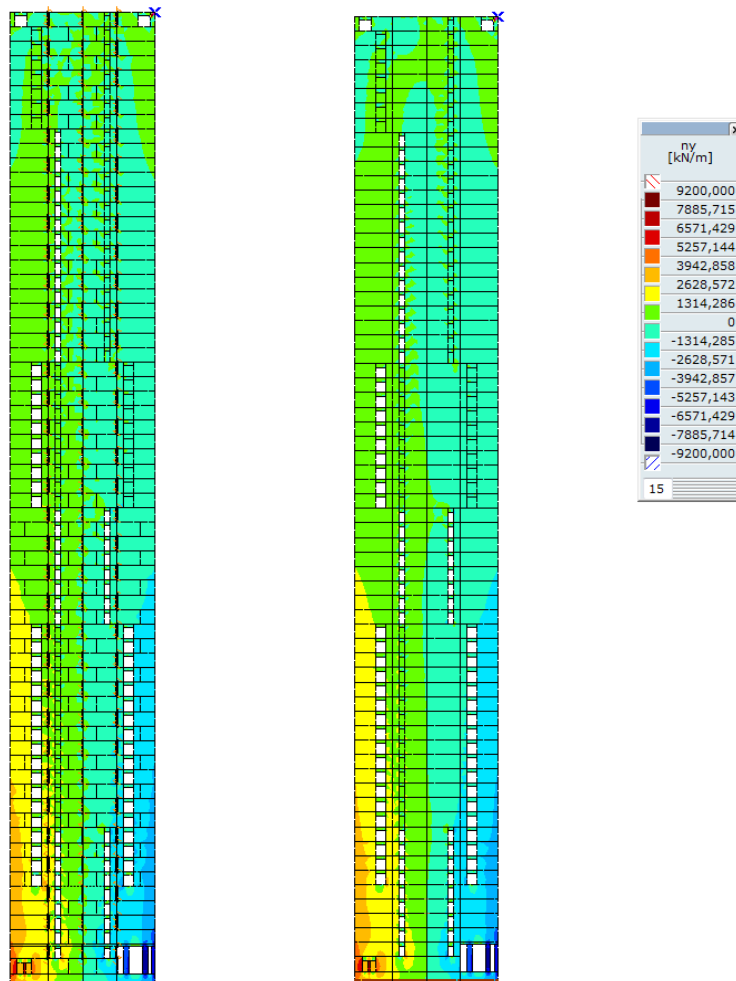


Figure 190 Normal force in the precast (left) and monolithic (right) 3D model

When the distribution of forces in the precast model is compared with monolithic model, only small differences can be distinguished. For example the edge disturbance around the open vertical joint. In section 8.1.5 this aspect was already discussed and may be neglected as it is created by the calculation.

In Figure 191 a more detailed view is depicted of the normal force. The precast and monolithic 3D models loaded by wind are shown in perspective in Figure 192.

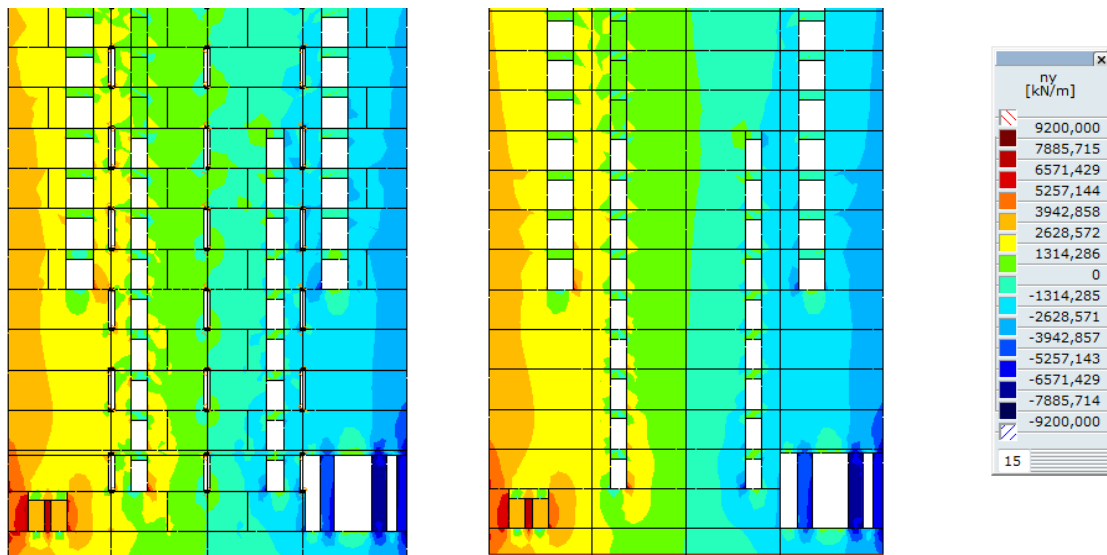


Figure 191 Detailed view of the normal force in the precast (left) and monolithic (right) 3D model

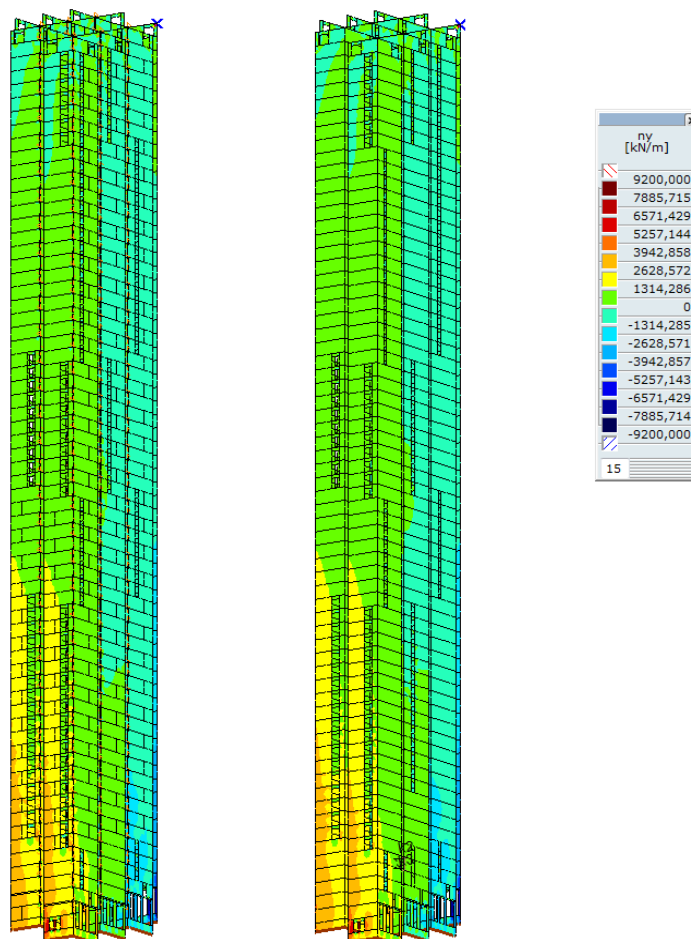


Figure 192 Side view of the normal force in the precast (left) and monolithic (right) 3D model

When the normal force as a result of dead load is examined, Figure 193 is obtained. Compared to Figure 182 (3D model without openings), the absolute values of the normal force have increased due to the reduced structural area. Another difference that can be

distinguished is the lack of visible deviations around the vertical open joint of the precast structure. This also occurred at the 2D precast wall with openings (Figure 169) and the openings are the likely cause of this difference.

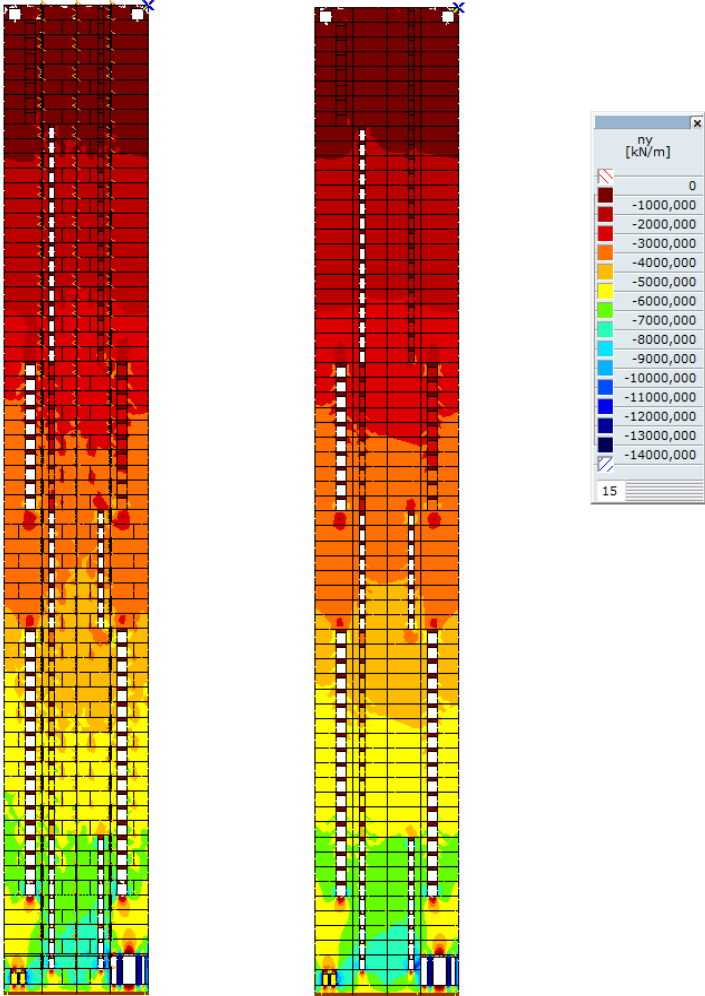


Figure 193 Normal force due to dead load in the precast (left) and monolithic (right) 3D model

When the normal force as a result of dead load is observed in perspective (Figure 194), it can be noted that also in the 3D model with openings the two walls in x-direction take up the largest forces. This was also encountered in 3D model without openings and the difference in stiffness of the walls (500mm versus 400mm) induces this behaviour.

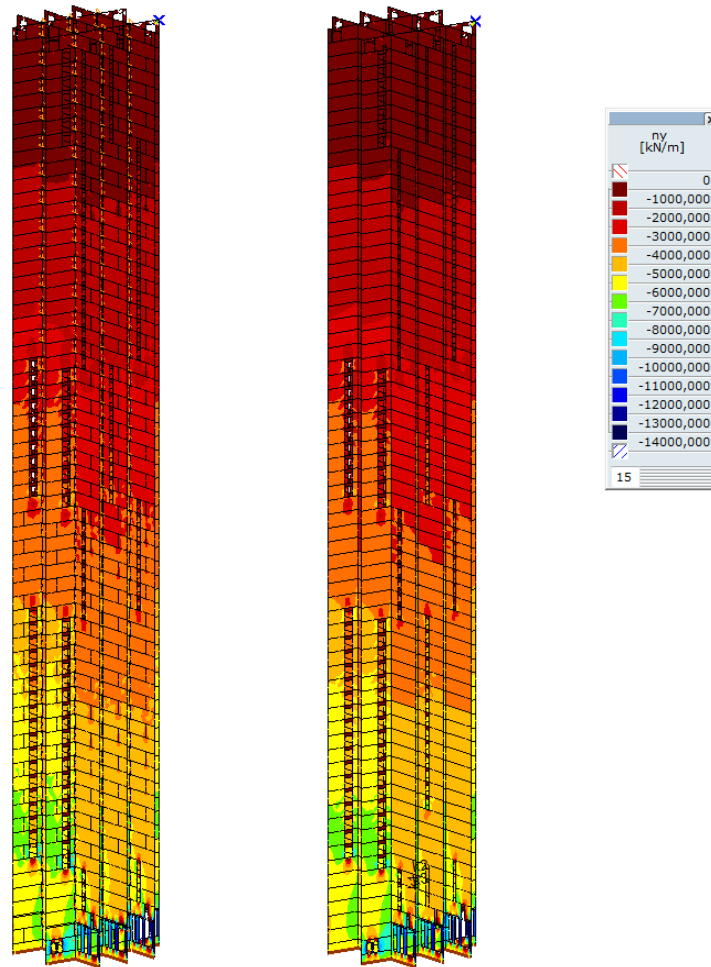


Figure 194 Side view of the normal force due to dead load in the precast (left) and monolithic (right) 3D model

When all the models are compared, it may be concluded that the results of the 3D model are a combination of the 2D wall with openings and the 3D simplified wall without openings. No new phenomena occur in the distribution of forces and the models behave as expected.

E.1.9 Shear force in the 3D model

In Figure 195 the shear force is depicted in a precast and monolithic 3D model. The precast and monolithic model are comparable on a global scale, but locally differences occur due to the open vertical joint and how the precast model is created (the staggered connection).

When both models are compared with the previous models, it can be observed that the 3D model shows a distribution based on a combination of the 2D model with openings and the simplified 3D model without openings.

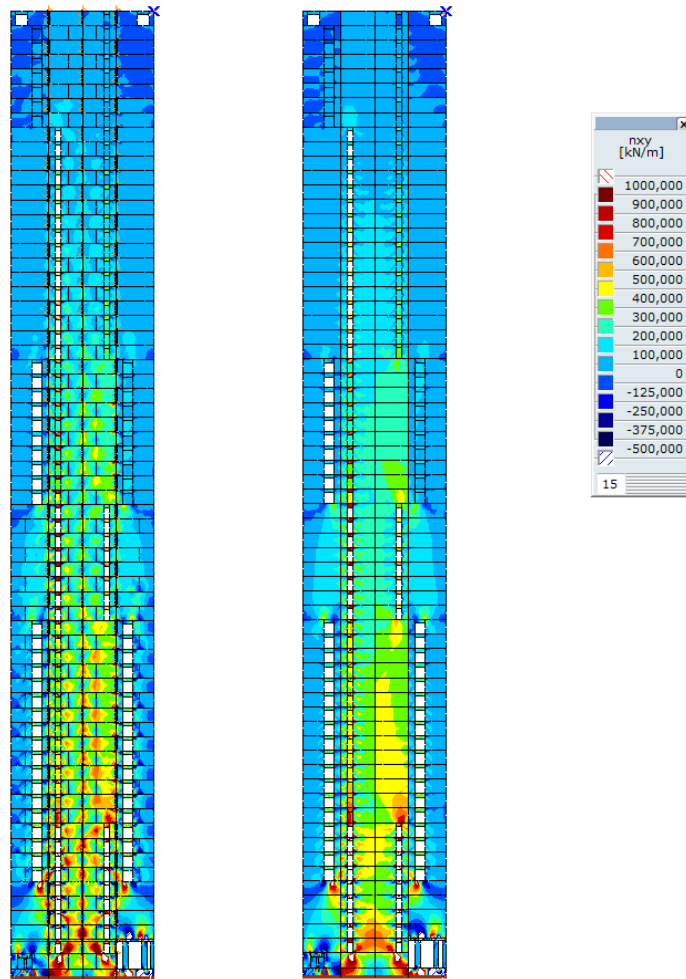


Figure 195 Shear force due to wind load in the precast (left) and monolithic (right) 3D model

In Figure 196 a more detailed view of the shear force in the precast wall is depicted. The compression and tension diagonals, already examined in section E.1.7, are clearly visible. It can also be observed that the shear force increases drastically around disruptions. At the lintels, the shear force is considerably higher because all the forces have to be transferred by a small area. Therefore reinforcement design of the lintels will be based on the high shear force (the disruptions aren't created by the calculation, but will also be present in the actual design). The other large red areas are often located at a turning point of the compression diagonals or above/beneath an opening. It's difficult to tell whether they are created by the simplified liner calculation or if they are the actual behaviour of the structure. Since the red areas are always located at a corner point of an element, there will likely be a relation between the linear calculation method⁴⁸ and the peak values. To provide a definitive answer, more research is required on the behaviour of the linear calculation method of AxisVM and precast elements.

⁴⁸ At a linear calculation, the forces are often transferred at the last possible location.

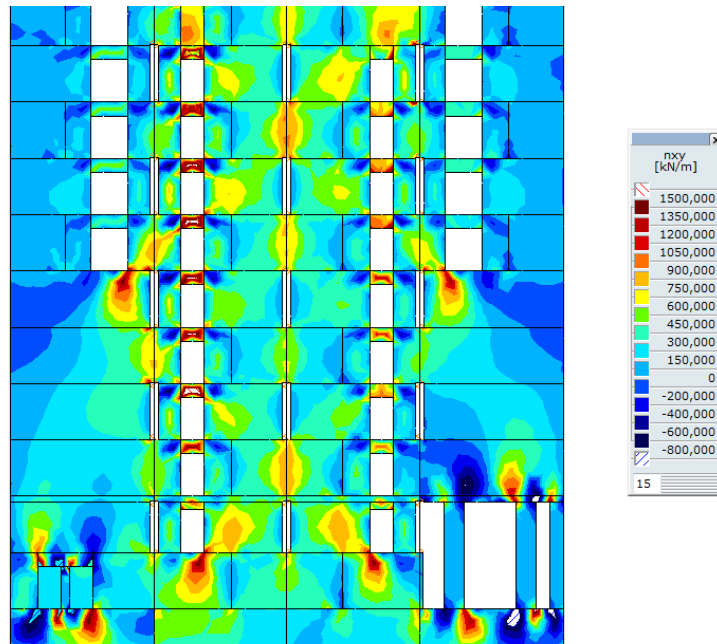


Figure 196 Detailed view of the shear force in the precast 3D model

E.1.10 Conclusion

With the 8 different models, insight is gained in the behaviour of the precast distribution of forces. By slowly increasing the level of detail, it was possible to analyse the effects of several properties of the model. Based on the results, several conclusions can be made:

- Due to the location of the interface elements and how AxisVM retrieves the results from the postprocessor, disruptions occur around the vertical open joint in the precast model. Since these disruptions are created by the calculation, they may be neglected in the design. By neglecting these disruptions, the simplified precast 2D wall has a similar distribution of forces compared with the simplified monolithic 2D wall.
- When the shear distribution of a precast wall with open vertical joints is compared with a monolithic wall, an interesting difference can be observed: due to the lack of stiffness of the vertical open joint, the over and underlying dowel elements are activated and receive a higher shear force than the elements in the monolithic wall. As a result of this higher shear force in the dowel elements, shear reinforcement is required in the lower section of the model.
- The introduction of shear force into the dowel elements isn't linear and a large peak force is located at the connection point between the horizontal and vertical open joint. In the last 5% of the connection length, the element transfers 11% of its shear force. Furthermore, this peak value is always contained within one mesh element and the shear force value increases when the size of the mesh element is reduced. Between the two horizontal connections, the shear force spreads out in the dowel element. This distribution of shear force originates in the underlying behaviour of the elements and is concentrated by the linear calculation and smeared stiffness. It's known of linear calculations that a large portion of the force is often transferred at the corner (last possible location without redistribution) and by neglecting important mechanisms of the connection (non-smeared stiffness and starter bars) the forces remain concentrated. Therefore this peak value may be smoothed in the actual design. A non-linear calculation in combination with the actual connection behaviour should determine the exact reduction of this peak value.
- By adding openings to the simplified wall, the structural area is reduced. Therefore the forces in the structure will increase. This phenomenon can clearly

be distinguished at the normal force in the local y-direction (n_y) and shear force (n_{xy}). For example: due to wall openings, all the shear force has to be transferred via the lintels to the other elements, resulting in high shear force values in the lintels.

- When the perpendicular walls (flanges) are added to the 2D model, a 3D model is obtained. The increased structural area ensures a reduction of the normal forces. The shear force isn't affected considerably by the perpendicular walls since most of the shear force is taken up by the 2D wall (web).
- In the shear force diagrams, locally high peak force areas can be distinguished. Since all these areas are located at an edge, they are most likely an edge disturbance created by the calculation. Therefore the peak force areas may be smoothed during the reinforcement design.
- The floors are supported by wall 1, 2 and 3 because this results in the shortest floor span. Nevertheless, the largest normal forces are encountered in wall 4 and 5. This can be explained by the different stiffness of the walls: wall 4 and 5 have a thickness of 500mm, which is 100mm more than wall 1, 2 and 3. The larger thickness provides a higher stiffness and the stiffest elements attract the largest forces.

Besides the conclusions, there also remains one aspect which acquires more attention: peak values. During the analysis of all the models, many disturbances have been encountered. For all the disturbances a likely cause has been identified, but it should be examined if they are the main reason for the peak value or if other aspects also contribute. Due to the limited time of this thesis, a more thorough analysis has not been performed, but for future examinations it's recommended to do so.

E.2 Calculation sheets of the natural frequency, structural factor, acceleration and reinforcement

In this appendix, the calculation sheets required for the first natural frequency, structural factor, acceleration and reinforcement are combined.

E.2.1 Calculation sheet for the first natural frequency

Due to confidentiality, this calculation sheet cannot be displayed.

E.2.2 Calculation sheet for the structural factor and acceleration

Due to confidentiality, this calculation sheet cannot be displayed.

This calculation uses the SLS basic wind velocity of 19.4m/s and may only be used to calculate the acceleration. To calculate the structural factor c_{s,c_d} , the ULS basic wind velocity of 27m/s should be applied, see section B.2.

E.2.3 Calculation sheet required reinforcement area

Due to confidentiality, this figure cannot be displayed.

Figure 197 Vertical reinforcement

Due to confidentiality, this figure cannot be displayed.

Figure 198 Horizontal reinforcement

In Figure 197 and Figure 198 the reinforcement area of the wall element of section 9.7 is determined. This is done with the help of a column program of Zonneveld ingenieurs. Since the reinforcement should be divided along the height of the column (see Figure 197 or Figure 198) and not at the edge, the reinforcement is placed manually in the program: 5 bars with a centre to centre distance of 200mm are placed along the height. In the actual design of section 9.7 the reinforcement is placed with a smaller centre to centre distance (for example 125mm), but this cannot be entered in the program. Nevertheless, the difference should be negligible due to the very small moment. The forces entered in the program work as shown in Figure 197 and Figure 198.

Appendix F: Dimensional control

This appendix provides the calculations sheet required to calculate at which level the tolerances of the Zalmhaven tower are exceeded. This appendix corresponds to section 10.3. It should be noted that all the deviations are calculated respectively to the bottom of the element. Because in this examination the elements are placed on top of each other without a joint, the deviations in height only occur at the top of the element.

Size of the element	Element deviation A ₁	Reduction factor	Adjustment deviation A ₂	Reduction factor	
height (z)= length (x)= thickness (y)=	z= x= y=	z= x= y=	z= x= y=	z= x= y=	
3,05 m 12 m 0,5 m	5,6 mm 4,4 mm 4,9 mm	0,7 0,4 0,7	2,5 mm 4 mm 3,5 mm	0,5 0,4 0,5	
Maximum dimensional deviation due to the element (A₁) and adjustments (A₂)					
Deviation due to element and adjustment on the gf	Deviation due to element and adjustment per floor				
height (z)= length (x)= thickness (y)=	gf	1 2 3	2 3 4	3 4 5 6 7 8 9 10 11	
0 6 6	0 6 6	6 8 9	9 10 10	11 12 13 14 15 16 17 18 19 20 21	
Deviation due to element warpage and curvature on the gf	Reduction factor				
squarness (x)= Warpage (y)=	0,4 0,7	Total deviation due to element and adjustment per floor			
4 mm/m= 12,2 mm	0,4 0,7	1 6 6	2 9 15	3 11 16 17 18 19 20 21 22	
Maximum dimensional deviation due to the placing of the measurement points (A₃)					
Distance A-B Distance A-1 Distance 1-2	21 m 12,9 m 7,2 m	Reduction factor			
Horizontal (x) and vertical (z) deviations	A _{B-A-1,hor} = A _{B-A-1,vert} =	Reduction factor			
Hor deviation A-1 Reduction factor	0 0	A _{1-2,z} = A _{1-2,hor} = A _{1-2,vert} =			
Vert deviation A-1 Reduction factor	0 0	3 mm 2 mm 2 mm			
Horizontal (x) and vertical (z) deviations due to height (oploeden in Dutch)					
Hor deviation due to oploeden B-A-A'	A _{B-A-A',hor} =	Deviations per floor due to height (oploeden)			
Reduction factor	0,4	gf	1 2 3	2 3 4 5 6 7 8 9 10 11	
Vertical deviation due to oploeden D-A-A'	A _{D-A-A',vert} =	x=	0 2	2 3 3 4 4 5 6 7 8 9 10 11	
Reduction factor	0,5	z=	0 2	2 3 3 4 4 5 6 7 8 9 10 11	
Height deviation due to oploeden A-A'	A _{A-A,height} =	y=	0 2	2 3 3 4 4 5 6 7 8 9 10 11	
Reduction factor	0,5	Total deviation per floor due to placing of the measurement points			
gf					
1 2 3 4 5 6 7 8 9 10 11					
x= z= y=					
2 2 0					
3 3 2					
3 3 3					
4 4 3					
4 5 3					
5 6 3					
6 7 4					
7 8 4					
8 9 4					
9 10 4					
10 11 5					

Figure 199 Dimensional deviations

Total maximum dimensional deviation due to the element (Ai), adjustments (As) and placing of the measurement points (Au)

	gf	1	2	3	4	5	6	7	8	9	10	11
Height (z) [mm]	0	7	9	11	13	14	15	17	18	19	20	21
Length (x) [mm]	6	15	16	17	19	20	21	22	23	24	25	26
Thickness (y) [mm]	6	11	12	14	15	16	18	19	20	21	22	23

Maximum allowable dimensional deviation for buildings

Maximum allowable dimensional deviation on the gf												
A _{z,1-2} =	26 mm											
A _{x,1-2} =	23 mm											
A _{y,1-2} =	35 mm											
Maximum allowable dimensional deviation per floor												
	gf	1	2	3	4	5	6	7	8	9	10	11
Height (z) [mm]	26	26	26	26	27	27	27	27	27	27	27	27
Length (x) [mm]	23	23	24	24	24	24	24	24	24	24	24	25
Thickness (y) [mm]	35	35	35	35	35	35	35	35	35	35	36	36

Figure 200 Division of deviations and tolerances

Appendix G: Cycle time

In this appendix an overview is provided of the transported elements and the resulting vertical cycle time. This appendix corresponds to section 11.1.

Even floors-6-26	Element type	Number of elements per floor [-]	Area [m ²]	Mass [10 ³ kg]	Transport speed [m/min]	Time per floor [min]	New number	Transport mass [10 ³ kg]	Transport speed [m/min]	Time per floor [min]	Total mass [10 ³ kg]	Total time per floor [min]	Return time [min]	Total mass per transport movement [10 ³ kg]	Mass per transport movement walls [10 ³ kg]
Wall 1/2/3-1	6	27.45	27.98	17.32	0.18	6	27.98	17.32	0.18	167.88	1.06	0.61			
Wall 1/2/3-2	3	33.73	34.38	15.34	0.20	3	34.38	15.34	0.20	103.14	0.60	0.31			
Wall 4/5-1	4	9.15	11.60	23.65	0.13	4	11.60	23.65	0.13	46.40	0.52	0.41			
Wall 4/5-2	4	24.58	16.29	16.29	0.19	4	31.22	16.29	0.19	124.88	0.75	0.41			
Wall 4/5-3	2	18.30	23.32	18.93	0.16	2	23.32	18.93	0.16	46.64	0.32	0.20			
Floor 1	20	20.40	16.64	21.49	0.14	20	16.64	21.49	0.14	332.72	2.84	2.03			
Floor 2	20	21.90	17.86	20.99	0.15	20	17.86	20.99	0.15	357.19	2.91	2.03			
Facade 1	4	21.96	7.83	25.40	0.12	4	7.83	25.40	0.12	31.32	0.48	0.41			
Facade 2	4	23.79	8.49	25.08	0.12	4	8.49	25.08	0.12	33.96	0.49	0.41			
Facade 3	4	27.45	14.00	22.59	0.14	4	14.00	22.59	0.14	56.00	0.54	0.41			
Facade 4	4	18.30	9.33	24.69	0.12	4	9.33	24.69	0.12	37.32	0.49	0.41			
Bathroom	6	1.25	28.78	0.11	6	1.25	28.78	0.11	7.50	0.64	0.61				
Scissor stairs	1	16.00	21.75	0.14	1	16.00	21.75	0.14	16.00	0.14	0.10				
Equipment/mat.	1	2.00	28.38	0.11	1	2.00	28.38	0.11	2.00	0.11	0.10				
Concrete blocks	6	1.15	28.84	0.11	6	1.15	28.84	0.11	6.90	0.63	0.61				
Total	89	1369.85	12.50	9.05	15.39	19.98	1348.77	12.55	9.15	14.99	19.30				

Average amount of elements: 89.5
Average time per floor: 25.05

Figure 201 Vertical cycle time of level 6-26

Even floors 27-44	Element type	Number of elements per floor [-]	Area [m ²]	Mass [10 ³ kg]	Transport speed [m/min]	Time per floor [min]	New number	Transport mass [10 ³ kg]	Transport speed [m/min]	Time per floor [min]	Total mass [10 ³ kg]	Total time per floor [min]	Return time [min]	Total mass per transport movement [10 ³ kg]	Mass per transport movement walls [10 ³ kg]
Even floors 27-44	Wall 1/2/3-1	6	27,45	20,99	19,78	0,15	6	20,99	19,78	0,15	125,94	0,93	0,61	14,81	19,42
	Wall 1/2/3-2	3	33,73	25,79	18,06	0,17	3	25,79	18,06	0,17	77,37	0,51	0,31	14,81	19,42
	Wall 4/5-1	4	33,73	34,38	15,34	0,20	4	34,38	15,34	0,20	137,52	0,80	0,41	14,81	19,42
	Wall 4/5-2	2	18,30	18,65	20,68	0,15	2	18,65	20,68	0,15	37,30	0,29	0,20	14,81	19,42
	Floor 1	20	20,40	16,64	21,49	0,14	20	16,64	21,49	0,14	332,72	2,84	2,03	14,81	19,42
	Floor 2	20	21,90	17,86	20,99	0,15	20	17,86	20,99	0,15	357,19	2,91	2,03	14,81	19,42
	Facade 1	4	21,96	7,83	25,40	0,12	4	7,83	25,40	0,12	31,32	0,48	0,41	14,81	19,42
	Facade 2	4	23,79	8,49	25,08	0,12	4	8,49	25,08	0,12	33,96	0,49	0,41	14,81	19,42
	Facade 3	4	27,45	14,00	22,59	0,14	4	14,00	22,59	0,14	56,00	0,54	0,41	14,81	19,42
	Facade 4	4	18,30	9,33	24,69	0,12	4	9,33	24,69	0,12	37,32	0,49	0,41	14,81	19,42
	Bathroom	6	1,25	28,78	0,11	6	1,25	28,78	0,11	7,50	0,64	0,61	14,81	19,42	
	Scissor stairs	1	16,00	21,75	0,14	1	16,00	21,75	0,14	16,00	0,14	0,10	14,81	19,42	
	Equipment/mat.	1	2,00	28,38	0,11	1	2,00	28,38	0,11	2,00	0,11	0,10	14,81	19,42	
	Concrete blocks	6	1,15	28,84	0,11	6	1,15	28,84	0,11	6,90	0,63	0,61	14,81	19,42	
Total							85				1259,04	11,79	8,64	14,81	19,42
Unrevenue floors 27-44	Element type	Number of elements per floor [-]	Area [m ²]	Mass [10 ³ kg]	Transport speed [m/min]	Time per floor [min]	New number	Transport mass [10 ³ kg]	Transport speed [m/min]	Time per floor [min]	Total mass [10 ³ kg]	Total time per floor [min]	Return time [min]	Total mass per transport movement [10 ³ kg]	Mass per transport movement walls [10 ³ kg]
Unrevenue floors 27-44	Wall 1/2/3-1	6	9,15	7,00	25,81	0,12	6	7,00	25,81	0,12	42,00	0,71	0,61	14,81	19,42
	Wall 1/2/3-2	6	33,71	25,77	18,06	0,17	6	25,77	18,06	0,17	154,62	1,01	0,61	14,81	19,42
	Wall 4/5-1	4	19,19	19,56	20,33	0,15	4	19,56	20,33	0,15	78,24	0,60	0,41	14,81	19,42
	Wall 4/5-2	4	21,96	22,39	19,26	0,16	4	22,39	19,26	0,16	89,56	0,63	0,41	14,81	19,42
	Floor 1	20	20,40	16,64	21,49	0,14	20	16,64	21,49	0,14	332,72	2,84	2,03	14,81	19,42
	Floor 2	20	21,90	17,86	20,99	0,15	20	17,86	20,99	0,15	357,19	2,91	2,03	14,81	19,42
	Facade 1	4	21,96	7,83	25,40	0,12	4	7,83	25,40	0,12	31,32	0,48	0,41	14,81	19,42
	Facade 2	4	23,79	8,49	25,08	0,12	4	8,49	25,08	0,12	33,96	0,49	0,41	14,81	19,42
	Facade 3	4	27,45	14,00	22,59	0,14	4	14,00	22,59	0,14	56,00	0,54	0,41	14,81	19,42
	Facade 4	4	18,30	9,33	24,69	0,12	4	9,33	24,69	0,12	37,32	0,49	0,41	14,81	19,42
	Bathroom	6	1,25	28,78	0,11	6	1,25	28,78	0,11	7,50	0,64	0,61	14,81	19,42	
	Scissor stairs	1	16,00	21,75	0,14	1	16,00	21,75	0,14	16,00	0,14	0,10	14,81	19,42	
	Equipment/mat.	1	2,00	28,38	0,11	1	2,00	28,38	0,11	2,00	0,11	0,10	14,81	19,42	
	Concrete blocks	6	1,15	28,84	0,11	6	1,15	28,84	0,11	6,90	0,63	0,61	14,81	19,42	
Total							90				1245,33	12,22	9,15	13,84	17,57
Average amount of elements: 87,5															
Average time per floor: 24,00															

Figure 202 Vertical cycle time of level 27-44

Even floors 45-		Number of elements per floor	Area [m ²]	Mass [10 ³ kg]	Transport speed [m/min]	Time per floor [min]	New number	Transport mass [10 ³ kg]	Transport speed [m/min]	Time per floor [min]	Total mass [10 ³ kg]	Total time per floor [min]	Return time [min]	Total mass per transport movement [10 ³ kg]	Mass per transport movement walls [10 ³ kg]
65	Wall 1/2/3-1	6	27,45	20,99	19,78	0,15	6	20,99	19,78	0,15	125,94	0,93	0,61		
	Wall 1/2/3-2	3	33,73	25,79	18,06	0,17	3	25,79	18,06	0,17	77,37	0,51	0,31		
	Wall 4/5-1	4	33,73	25,79	18,06	0,17	4	25,79	18,06	0,17	103,16	0,68	0,41		
	Wall 4/5-2	2	18,30	13,99	22,60	0,13	2	13,99	22,60	0,13	27,98	0,27	0,20		
	Floor 1	20	20,40	16,64	21,49	0,14	20	16,64	21,49	0,14	332,72	2,84	2,03		
	Floor 2	20	21,90	17,86	20,99	0,15	20	17,86	20,99	0,15	357,19	2,91	2,03		
	Facade 1	4	21,96	7,83	25,40	0,12	4	7,83	25,40	0,12	31,32	0,48	0,41		
	Facade 2	4	23,79	8,49	25,08	0,12	4	8,49	25,08	0,12	33,96	0,49	0,41		
	Facade 3	4	27,45	14,00	22,59	0,14	4	14,00	22,59	0,14	56,00	0,54	0,41		
	Facade 4	4	18,30	9,33	24,69	0,12	4	9,33	24,69	0,12	37,32	0,49	0,41		
	Bathroom	6	1,25	28,78	0,11	6	1,25	28,78	0,11	7,50	0,64	0,61			
	Scissor stairs	1	16,00	21,75	0,14	1	16,00	21,75	0,14	16,00	0,14	0,10			
	Equipment/mat.	0	2,00	28,38	0,11	0	2,00	28,38	0,11	0,00	0,00	0,00			
	Concrete blocks	0	1,15	28,84	0,11	0	1,15	28,84	0,11	0,00	0,00	0,00			
Total		78					78				1206,46	10,90	7,93	15,47	16,62
Uneven floors 45-		Number of elements per floor	Area [m ²]	Mass [10 ³ kg]	Transport speed [m/min]	Time per floor [min]	New number	Transport mass [10 ³ kg]	Transport speed [m/min]	Time per floor [min]	Total mass [10 ³ kg]	Total time per floor [min]	Return time [min]	Total mass per transport movement [10 ³ kg]	Mass per transport movement walls [10 ³ kg]
65	Wall 1/2/3-1	6	9,15	7,00	25,81	0,12	6	7,00	25,81	0,12	42,00	0,71	0,61		
	Wall 1/2/3-2	6	33,71	25,77	18,06	0,17	6	25,77	18,06	0,17	154,62	1,01	0,61		
	Wall 4/5-1	4	19,19	14,67	22,31	0,14	4	14,67	22,31	0,14	58,68	0,55	0,41		
	Wall 4/5-2	4	21,96	16,79	21,43	0,14	4	16,79	21,43	0,14	67,16	0,57	0,41		
	Floor 1	20	20,40	16,64	21,49	0,14	20	16,64	21,49	0,14	332,72	2,84	2,03		
	Floor 2	20	21,90	17,86	20,99	0,15	20	17,86	20,99	0,15	357,19	2,91	2,03		
	Facade 1	4	21,96	7,83	25,40	0,12	4	7,83	25,40	0,12	31,32	0,48	0,41		
	Facade 2	4	23,79	8,49	25,08	0,12	4	8,49	25,08	0,12	33,96	0,49	0,41		
	Facade 3	4	27,45	14,00	22,59	0,14	4	14,00	22,59	0,14	56,00	0,54	0,41		
	Facade 4	4	18,30	9,33	24,69	0,12	4	9,33	24,69	0,12	37,32	0,49	0,41		
	Bathroom	6	1,25	28,78	0,11	6	1,25	28,78	0,11	7,50	0,64	0,61			
	Scissor stairs	1	16,00	21,75	0,14	1	16,00	21,75	0,14	16,00	0,14	0,10			
	Equipment/mat.	0	2,00	28,38	0,11	0	2,00	28,38	0,11	0,00	0,00	0,00			
	Concrete blocks	0	1,15	28,84	0,11	0	1,15	28,84	0,11	0,00	0,00	0,00			
Total		83					83				1194,47	11,36	8,44	14,39	16,87

Average amount of elements: 80,5
Average time per floor: 22,26

Figure 203 Vertical cycle time of level 45-65

Appendix H: Construction time

In section 11.2 a short overview is provided of the construction time. The determination of the total construction time is provided in this appendix.

The following aspects have to be considered when the total construction time is determined of the Zalmhaven tower:

- construction of the diaphragm walls,
- creating a 1m thick foundation slab,
- constructing the first 6 levels with the crawler crane,
- erecting the hoisting shed,
- construction of level 6 to 65 with the hoisting shed,
- climbing back of the hoisting shed,
- disassembling of the hoisting shed,
- execution of the finishing stage.

The diaphragm walls are the first step of the construction process. Elements with a length of 63.2m, a thickness of 1.5m and a width of 3.3m are applied (see section 4.4). A diaphragm rig is able to construct one element every 2 days⁴⁹. After these 2 days, a 3rd day is required to finish the diaphragm wall (placing reinforcement and pouring concrete), but the diaphragm rig can already start with the next wall element. In total 70 diaphragm elements are required. Since creating half a diaphragm wall provides problems (the diaphragm wall filled with bentonite has to stay open during the night) this process will continue 16 hours per day. Creating diaphragm walls is a relative low noise process and creating diaphragm walls during the evening isn't uncommon. Creating 70 diaphragm walls requires 70 days or approximately 12 weeks of 6 days.

The 1m thick foundation slab is constructed after the diaphragm walls are finished. Constructing the formwork and reinforcement requires approximately 2.5 weeks. This process can't be executed simultaneous with the construction of the diaphragm walls because the area is too small, the diaphragm process isn't very clean and the freedom to move around the rig is limited considerably because the rig may topple over. At Friday the entire slab is casted in a continuous process and during the weekend the slab hardens.

Simultaneous with the construction of the slab, the crawler crane for the first 5 levels (ground floor until level 5) and the hoisting shed is assembled. When the construction process is up to speed, 2 floors per week can be created with the hoisting shed. Since the first 5 levels are constructed by the crawler crane and there are several disruptions, a construction speed of 1 level per week is maintained.

At level 5 the hoisting shed is assembled. Within two weeks the load bearing structure of the hoisting shed is assembled. The load bearing structure exists of many smaller truss sections, which are already combined to several larger sections at ground. To finish the hoisting shed, an additional week is required. Since double shifts are applied, 6 days per week, the total amount of hours is equal to 6 normal working weeks. At the Erasmus MC tower, the construction of the hoisting shed started at 26th of October 2010 and the hoisting shed was finished at 11 December 2011 (approximately 6 weeks of 36 hours).

Depending on the time of year the previous actions are executed, delays have to be incorporated. Since a considerable amount of concrete has to be poured it's not advised to perform these actions during the winter. Unfortunately, it's not always possible to choose the desired starting date and delays have to be incorporated. Per year 25 days are lost due to frost and high wind speeds (low construction height). The entire

⁴⁹ These values are obtained in a consult with Robert Schippers from MOS Grondmechanica in Rhoon.

construction process until the completion of the hoisting shed requires 24 weeks (46% of 52 weeks), resulting in 12 lost days due to the weather. Within the previous mentioned processes, one week can be absorbed. The buffers within the processes are too small for a second week and this week is added to the construction time.

When the hoisting shed is finished, the construction of level 6 to 65 will start. Because the construction workers have to become familiar with the process, the efficiency isn't optimal at the lower levels. When the vertical gantry crane assists the horizontal gantry crane, only 69% of the cycle time is required (see section 11.1.1.4). Therefore $0.31 \cdot 2160 = 670$ minutes or 11 hours remain to absorb possible delays. Therefore no additional time is included in the construction process for the first few levels: the 60 levels are constructed in 30 weeks.

After the hoisting shed has reached and constructed level 65, the roof of the hoisting shed is removed, which takes approximately 4 days. Then the hoisting shed starts to climb back and the remaining facade elements are placed over jacking anchors. When the hoisting shed travels 8 floors per day, the hoisting shed will be at level 5 in 8 days. Combined with the 4 days of the roof, 2 weeks are required to climb down. Travelling 8 layers in 12 hours results in 1.5 hours per level. Of this time 30 minutes is reserved to remove the jacking anchors (see section 4.5.4) and to place the remaining facade elements. As a result, the hoisting shed will travel 3.05m/hour or 5.1cm/minute on average. Since the automated climbing systems of Peri GmbH are capable of reaching a stroke speed of 50cm/minute, the average speed of 5.1cm/minute should be no problem. The climbing system should be especially designed to climb back since most systems contain safety measures preventing the system to move downwards (for example if the hydraulic pressure is lost, the automatic climbing system may not fall down). Peri GmbH provides systems which are capable of climbing down.

At the ground level again 3 weeks are required to disassemble the hoisting shed. The total process of assembling, disassembling and climbing back requires 8 weeks, which is 27% of the time required to construct level 6 to 65. This value is considerably high because a special system (hoisting shed) is required to reach the short cycle times. A tower crane requires a shorter assemble and disassemble time and in combination with a longer construction time of the building, this value is significantly reduced.

Simultaneous with the construction of the levels by the hoisting shed, the completed floors are finished by multiple finishing crews (afbouwploegen in Dutch). The finishing stage starts when the hoisting shed is assembled at level 5. The finishing stage has to wait on the hoisting shed because it provides a weather tight occlusion at the top floor. By using massive floors with integrated ducts and reinforcement for the diaphragm action, sandwich elements and prefabricated bathroom units, it's estimated that 6 levels under the hoisting shed the finishing stage is completed. To reach these high speeds, multiple finishing crews are required. 6 levels equals 3 weeks, but in Figure 204 5 weeks are incorporated. These two additional weeks are required to install the elevators and installations. Since these actions only take place at certain levels, these two weeks can also be used as buffer for the finishing of the floor levels.

With the previous examination of the construction time, no (national) holidays are included. Since a cycle time of 6 days is used, the Sunday has to be used in case the construction stops at the national holiday. Otherwise this delay will accumulate to the next week.

The total construction time is shown in Figure 204. It can be observed that it requires 60 weeks to construct the Zalmhaven tower, which is incredible short. For example, Het Strijkijzer with a height of 132m was completed in 2 years. Figure 204 also shows that the finishing stage isn't leading: the finishing stage is completed at the same time the hoisting shed is dismantled.

Appendix I: Feasibility check of the hoisting shed

The structural design is based on large precast elements with a mass up to 34.7 ton. To transport these heavy elements to the construction floor, a hoisting shed is used. By utilising the hoisting shed, a separated transport system is created which isn't dependant on the building height. Furthermore, the weather dependency is reduced considerably. But are the boundary conditions on which the design of the hoisting shed is based feasible and realistic? To asses this question the boundary conditions have been re-examined:

- Large steel trusses were used at the Erasmus MC tower hoisting shed because a distance of 38m had to be spanned. At the Zalmhaven tower the distance between the supports is only 7.8m, reducing the weight of the supporting structure significantly. The dimensions of the steel structure aren't determined, but with the reduced span, the dimensions will decrease.
- With the reduced span, the hoisting shed has an estimated weight of 300 ton. During the construction a large part of the live floor load will not be present, compensating the weight of the hoisting shed. Within six floor levels, the live load is already larger than the weight of the hoisting shed.
- As a result of the hoisting shed the building area increases with 3%. Therefore more wind load will be endured by the structure. Since the wind load is non-linear distributed over the building height, the total horizontal force on the structure increases with 6 instead of 3% when the highest floor is constructed. Because of the larger load, the deflections will increase with approximately 6%, resulting in a total deflection of 341mm in the x-direction. This value remains within the limit of $u_{\max}=h/500=405\text{mm}$. Also the forces on the structure increase due to the larger area: the moment at the foundation increases with 6%. To prevent a higher reinforcement ratio as a result of the execution phase there are two solutions: reduce the safety factors or reduce the wind load. Since the Zalmhaven tower is located in an urban environment it's not advised to reduce the safety factor. A better solution is to reduce the wind load because the higher loads are only governing when the top floors are constructed (time span of 2 weeks). According to the NEN 6702⁵⁰ the wind load may be multiplied by $\psi_t=0.57$ ($t=1$ year and $\psi=0.0$). This reduction is larger than the 6% higher moment and the construction phase isn't governing.
- The hoisting shed is supported at ten locations. When the load is equally distributed, every support obtains a dead load of 30 ton. Due to the wind load, this value will increase. Since the anchors have a maximum load capacity of 10 ton, multiple anchors have to be used, possibly distributed over several floor levels. This requires a high amount of accuracy because if one of the anchors is located slightly lower than designed, it will not bear any load. It's possible to use a different support system, for example the special notches used at the Delftse Poort. With this system, the hoisting shed was supported on one level at the four corners. Every support had a load capacity of 100 ton, which would be more than sufficient for the Zalmhaven tower. The final hoisting shed design has to indicate which method is preferred.
- The transport load capacity and speed of the Zalmhaven tower hoisting shed are derived from the Erasmus MC hoisting shed. Therefore the obtained values can be considered as realistic and feasible.
- After the top floor has been constructed, the hoisting shed climbs back via the end faces of the structural walls. In order to climb back, the roof has to be removed. This method was also considered at the Erasmus MC tower hoisting shed. Because

⁵⁰ At this moment there is no national annex available of NEN-EN 1991-1-6 specifying reduction factors during the construction phase. Therefore section 5.5.2 of NEN 6702 is used instead.

the surrounding low-rise buildings were completed at an earlier stage, the hoisting shed couldn't be dismantled at the bottom and was eventually dismantled at the top floor. The process of climbing back is almost identical to climbing upwards and shouldn't provide any problems. When climbing back the final facade elements can be placed over the end faces and the facade can be cleaned thoroughly.

The previous boundary conditions do not provide any problems because they are mainly based on reference projects from the Netherlands and Japan. Therefore the boundary conditions and the resulting hoisting shed design should be realistic and feasible. Nevertheless, the final design has yet to be made and many aspects have to be considered and designed. The economical feasibility of this design has to determine whether or not the hoisting shed will be applied at the Zalmhaven tower.